Assessment of magnetic particles for neural stem cell-based therapies

Christopher Francis Adams

Thesis submitted for Doctor of Philosophy in Biomedical Engineering

October 2015

Keele University

Keele University

Declaration Part 1. To be bound in the thesis

SUBMISSION OF THESIS FOR A RESEARCH DEGREE

Part I. DECLARATION by the candidate for a research degree. To be bound in the thesis

Degree for which thesis being submitted: **Doctor of Philosophy in Biomedical engineering**

Title of thesis: **Assessment of magnetic particles for neural stem cell-based therapies**

This thesis contains confidential information and is subject to the protocol set down for the submission and examination of such a thesis. NO

Date of submission **July 2015** Original registration date: **3rd October 2011**
(Date of submission must comply with Regulation 2D)

Name of candidate: **Christopher Francis Adams**

Research Institute: **ISTM**

Name of Lead Supervisor: **Professor Divya Chari**

I certify that:

(a) The thesis being submitted for examination is my own account of my own research
(b) My research has been conducted ethically. Where relevant a letter from the approving body confirming that ethical approval has been given has been bound in the thesis as an Annex
(c) The data and results presented are the genuine data and results actually obtained by me during the conduct of the research
(d) Where I have drawn on the work, ideas and results of others this has been appropriately acknowledged in the thesis
(e) Where any collaboration has taken place with one or more other researchers, I have included within an 'Acknowledgments' section in the thesis a clear statement of their contributions, in line with the relevant statement in the Code of Practice (see Note overleaf).
(f) The greater portion of the work described in the thesis has been undertaken subsequent to my registration for the higher degree for which I am submitting for examination
(g) Where part of the work described in the thesis has previously been incorporated in another thesis submitted by me for a higher degree (if any), this has been identified and acknowledged in the thesis
(h) The thesis submitted is within the required word limit as specified in the Regulations

Total words in submitted thesis (including text and footnotes, but excluding references and appendices) ……**47408**

Signature of candidate ……Date ……

Achievements during PhD

Publications:

1. Adams, C.F., Pickard, M. R., & Chari, D. M. Magnetic nanoparticle mediated transfection of neural stem cell suspension cultures is enhanced by applied oscillating magnetic fields. *Nanomedicine:NBM;* **9**, 737–41 (2013).
2. Adams, C. F., Rai A., Sneddon G., Yiu H. H. P., Polyak B. & Chari D. M. Increasing magnetite contents of polymeric magnetic particles dramatically improves labelling of neural stem cell transplant populations. *Nanomedicine:NBM*; **11**, 19-29 (2014).
3. Fernandes, A.*, Adams, C. F.*, Jenkins, S. I., Furness, D. N. & Chari, D. M. Early membrane responses to magnetic particles are predictors of particle uptake in neural stem cells. *Particle and Particle Systems Characterization.* **In Press,** (2015).

   **Joint first author.*

Prizes:

1. ***Royal Society of Chemistry Journal of Materials Chemistry B Prize for 'Best Presentation on a Translational Topic'***

   DTC Joint Conference, July 2013, University of Sheffield
2. ***Awarded joint first prize for the poster entitled 'Attempts to enhance genesis of transfected neurons following MNP mediated gene transfer to NSCs'***

   Joint DTC Conference, July 2011, University of Leeds

Grants:

1. Awarded EPSRC funded ETERM (Engineering: Tissue Engineering and Regenerative Medicine) fellowship to complete a research project entitled "***Engineering neural 'bridges' to promote repair in spinal cord injury***", Keele University, January 2015.

Abstract

Transplantation of genetically engineered neural stem cells (NSCs) into sites of central nervous system (CNS) disease/injury is a promising strategy to promote repair of damaged tissue. However, translating this strategy into the clinic requires several challenges to be overcome including facilitating '*combinatorial therapy*' (achieving multiple therapeutic goals – essential in CNS injury/disease). Nanotechnologies are emerging as multifunctional platforms capable of meeting this requirement. For example, magnetic particles (MPs) and implantable hydrogels offer several biomedical advantages for transplant populations, including: safe genetic manipulation; non-invasive cell tracking, via MRI; and safe and efficient accumulation of cells at sites of injury. However, the use of these nanotechnologies remains to be explored in detail for NSC transplantation therapies.

In this thesis, it is shown that MPs can mediate gene delivery to NSCs grown as neurospheres and monolayers with the most efficient transfection efficiencies achieved using oscillating magnetofection protocols (9.4% and 32.2% respectively). In both culture systems, developed protocols had no effect on key regenerative properties of NSCs such as cell viability, proliferation, stemness and differentiation. Further, '*magnetofected*' monolayer NSCs were shown to have survived and differentiated in a cerebellum slice model acting as host tissue, indicating safety of the procedures. It was also shown that assessing procedural safety and extent of transfection of magnetofection protocols may be feasible by employing mass spectrometry and proteomics analysis.

It was also found that tailored enhancement of particle magnetite content offers a means to efficiently label NSCs, up to a maximum of 95.8%. Labelling procedures had no effect on cell viability, proliferation, stemness or differentiation. In addition, labelled cells could survive and differentiate in a slice model of spinal cord injury indicating safety of the labelling procedures.

Functional labelling was also demonstrated by magnetic capture of labelled cells in an *in vitro* flow system.

Hydrogels offer major advantages for delivery of transplant populations into injury sites. Here it was shown that an intraconstruct genetic engineering approach was feasible for NSCs cultured with a clinically translatable, collagen hydrogel system. Magnetofection protocols safely increased MP mediated transfection of NSCs grown in '2-D' and '3-D' hydrogel cultures.

Contents

List of figures and tables

Abbreviations

4-OHT	4-hydroxy-tamoxifen
AAS	Atomic absorption spectroscopy
ALS	Amyotrophic lateral sclerosis
ANOVA	Analysis of variance
BBB	Blood brain barrier
BMSC	Bone marrow stem cells
CAM	Carbamidomethylation
CHN	Carbon, hydrogen, nitrogen (elemental analysis)
CMV	Cytomegalovirus
CNS	Central nervous system
CPP	Cell penetrating peptide
CSF	Cerebrospinal fluid
CSPG	Chondroitin sulphate proteoglycans
Cy-3	Cyanine-3
DAPI	4,6-diamidino-2-phenylindole
DMEM	Dulbecco's modified eagle medium
DTT	Dithiothreitol
EBSS	Earle's balanced salt solution
ECM	Extracellular matrix
EDTA	Ethylenediaminetetraacetic acid
EGF	Epidermal growth factor
FESEM	Field emission scanning electron microscopy
FGF-2	Basic fibroblast growth factor
FITC	Fluorescein isothiocyanate
FTIR	Fourier transform infrared
GALC	ß- galactocerebrosidase
GDNF	Glial derived neurotrophic factor
GFAP	Glial fibrillary acidic protein
GFP	Green fluorescent protein
GSH	Glutathionine
HPLC	High performance liquid chromatography
IPA	Ingenuity Pathway Analysis
iPSC	Induced pluripotent stem cell
LC-MS/MS	Liquid chromatography tandem mass spectrometry
LSD	Lysosomal storage disorder
MAPK	Mitogen-activated protein kinase
MBP	Myelin basic protein
MCT	Multiple comparison test
ML-M	Monolayer medium
MP	Magnetic nano or micro particle
MPTP	1-methyl-4-phenyl-1,2,3,6-tetrahydropyridine
MTS	3-(4,5-Dimethylthiazol-2-yl)-5- (3-carboxymethoxyphenyl)-2-(4-sulfophenyl) 2H-tetrazolium
MTT	Methylthiazolyldiphenyl-tetrazolium bromide
NCL	Neuronal ceroid lipofuscinoses
NGF	Nerve growth factor
NMR	Nuclear magnetic resonance
NSC	Neural stem cell
NS-M	Neurosphere medium

NT-3	Neurotrophin-3
OEC	Olfactory ensheathing cell
OPC	Oligodendrocyte precursor cell
OTOTO	Sequential osmium (O) and thiocarbohydrazide (T)
PDGF-α	Platelet derived growth factor-α
pDRE2	pCMV-DsRed-Express2
PEI	Polyethylenimine
PLA	Poly(D,L-lactic acid)
PLGA	Poly(lactic-co-glycolic acid)
PLL	Poly-L-lysine
pmaxGFP	pmaxGFP plasmid
RFP	Red fluorescent protein
ROS	Reactive oxygen species
RT	Room temperature
SCB	Sodium cacodylate buffer
SCI	Spinal cord injury
SDS	Sodium dodecyl sulphate
TBI	Traumatic brain injury
TEM	Transmission electron microscopy
TH	Tyrosine hydroxylase
Tuj-1	β-tubulin
VEGF	Vascular endothelial growth factor
WST-1	Water soluble tetrazolium salts
XRD	X-ray diffraction

Acknowledgements

First and foremost I am indebted to my Supervisor, Professor Divya Chari, who has provided me with expert supervision and guidance. She has taught me how science should be conducted and reported and any development in myself as a scientist I owe largely to her. I have had an incredible amount of help during my PhD from her and for that I am very grateful.

I have also been lucky enough to have had excellent guidance on experimental technique and data analysis and presentation and from Drs Mark Pickard and Stuart Jenkins who also provided expert advice and intelligent discussion of scientific ideas. A special thanks to Dr Pickard who taught me the protocols for neural stem cell culture which underpin this whole thesis.

For Chapter 3, Dr Boris Polyak (Drexel University, Philadelphia, USA) kindly formulated magnetic particles for me to test in neural stem cells and has also provided details for the formulation and characterisation of the MPs used. In addition Dr Humphrey Yiu (Heriot-Watt University, Edinburgh, UK) has generously added extra characterisation in the form of the XRD and FTIR analysis. Where this has been performed by them, this is indicated by BP (Dr Boris Polyak) or HY (Dr Humphrey Yiu). Both also greatly assisted discussions of the scientific merits of the project. Also, in this Chapter Dr Alan Weightman provided expert assistance, both technically and scientifically with regards to the organotypic slice model of spinal cord injury.

I have also been aided and advised my numerous people during my PhD without whose help the work could not have been achieved. In this regard, I owe thanks to Dr Sarah Hart, for teaching and explaining proteomics to me, Dr Paul Horrocks, Dr Rosemary Fricker, Dr Paul Roach and Dr Richard Emes.

For the electron microscopy work I owe a huge thanks to Professor David Furness and Karen Walker, whose expertise with sample preparation and imaging are extraordinary and incredibly helpful.

Dave Bosworth, Dr Stefanie Jones, Zoe Bosworth and Debbie Adams always made me feel welcome and were incredibly helpful with any procedures I was performing to generate cells. Also, to staff of the Life Sciences building I extend thanks including Phil and Chris for keeping the lab spotless and Jayne Bromley, Chris Bain, Nigel Bowers, Ian Wright and Ron Knapper for enabling the research to proceed smoothly.

My research was funded by the EPSRC through the DTC in Regenerative medicine who have supported me scientifically and professionally and through which I have made many lifelong friends.

Crucially, I could not have survived the process without scientific input from, and (perhaps more importantly) in depth discussion about a wide range of subjects with, Sile Griffin, Josh Price, Jackie Tickle, Dr Alinda Fernandes, Dr James Edwards-Smallbone, Tim Hinchcliff, Dr Andrew Morris, Lyndsey Wheeldon, Daniel Weinberg, Emma Parr and Dr Amy Holmes.

Finally, I would like to thank my family for their support and belief that I could finish this PhD. Also, a special mention to my Dad who proof read a chapter for me.

Chapter 1: General Introduction

1.1 Introduction summary

This thesis covers a broad range of materials and methods for improving neural stem cell (NSC) transplantation therapy by utilising various nanotechnology strategies. For clarity, this section provides an overview of the areas to be covered by the introduction. Initially, it provides a brief description of central nervous system (CNS; brain and spinal cord) disease/injury and why repair is difficult to achieve. This is followed by a discussion of the benefits of NSC transplantation for repairing the CNS after insult. As CNS disease is highly complex, achieving multiple clinical goals is desirable for effective regeneration. In this context, genetically engineering NSCs can enhance their therapeutic potential by enabling them to replace lost or damaged cells and deliver therapeutic biomolecules, a strategy which will be expanded in **Section 1.5**. However, there are major barriers to the clinical transplantation of genetically engineered NSCs which will be expanded in **Section 1.6**. The key research aims of this thesis are to take steps towards addressing these barriers by exploring the potential of combining the rapidly emerging field of nanotechnology with NSC transplantation therapy. Therefore, the subsequent sections will outline two nanotechnologies, magnetic (nano)particles (MPs) and implantable hydrogels, and discuss how these materials can be used as novel tools to benefit NSC transplantation. Within these sections, gaps in the literature for applying nanotechnology to NSC transplantation will be highlighted and these will serve as the basis for the aims of each of the experimental chapters. Finally, the use of primary cells and organotypic slice culture will be introduced as tools for assessing the safety and efficacy of nanotechnological interventions.

1.2 Central nervous system injury and disease currently has poor prognosis

No treatment is currently able to reverse damage caused and restore function of the tissue after CNS injury and disease. These conditions can cause severe human disability and frequently culminate in premature death (stroke, neurodegenerative disorders and depression are all in the

top 20 causes of death worldwide).[1] As well as the negative impact on the quality of life of patients and their support network, there is also huge cost to healthcare systems as initial therapies are expensive and often substantial palliative care is required for the remainder of the patient's life. For example, in the USA, spinal cord injury (SCI) resulting in paraplegia costs about $500 000 in the first year then $67 000 for each subsequent year.[2] In addition, due to increasing life expectancies, the prevalence of neurodegenerative diseases are predicted to increase and become one of the leading causes of disability and death by 2030.[1] As a result, efforts to find therapies which can restore function to the damaged CNS are vital both for human well-being and to alleviate the cost-burden for global healthcare services. However, this constitutes a major challenge as CNS tissue has a complex cytoarchitecture and a poor regenerative capacity, posing considerable obstacles to the development of neuroregenerative strategies.

In terms of its cytoarchitecture, the CNS consists of two major classes of cells: the neurons and their supporting glia. Neurons transmit electrical signals and reside in groups forming multiple connections with other neurons to make up neural circuits which perform a common function, for example, vision or movement.[3] Neurons extend axons which are highly specialised structures unique to neuronal cells adapted to relay information within the body.[3] Axons are ensheathed by layers of an insulating and supporting fatty deposit called myelin. CNS myelin is made and maintained by the oligodendrocytes which can myelinate multiple axons.[4] Astrocytes are the major supporting cell type within the CNS and research is still ongoing into their specific roles within this remit. Their currently accepted functions include: maintaining CNS homeostasis; intake and potential release of glutamate (a neurotransmitter) to control signal intensity and prevent excitotoxicity; providing metabolic support to neurons and roles in synapse formation and maintenance.[4,5]

Other important CNS glial subtypes include the microglia which are the resident immune cells (involved in phagocytosis and cell recruitment to sites of injury)[6] and precursor cells – both neural

stem cells (NSCs) and oligodendrocyte progenitor cells (OPCs). NSCs will be described in greater detail in **Section 1.4**. OPCs produce their daughter cells the oligodendrocytes throughout development but are also present as slowly dividing populations in adulthood and are reported to be recruited to sites of injury.[5,7] Finally, a mixture of astrocytes and endothelial cells forming tight junctions make up the blood brain barrier (BBB) which strictly controls the entry of molecules to the CNS. In this manner, it functions to maintain the specific molecular environment (e.g. optimal ion concentrations for signal transduction) crucial for the function of the above cell types and overall CNS function.[3,4]

Unsurprisingly, insult to the CNS affects all these cell types. However, each has their individual influence on the poor regenerative capacity of the CNS resulting in a complex, multifactorial pathology. Insult generally results in three stages of response: (1) Extensive cell death and breakdown of the BBB – involving a wave of neuronal cell death followed by the death of oligodendrocytes (which normally receive pro-survival signalling from the neurons). Cell death coupled with breakdown of the BBB produces an incredibly hostile environment consisting of inflammatory and other cell signalling molecules which act on the surrounding CNS cells. (2) '*Reactive gliosis*' – where glia cells are mobilised in response to this environment. This includes recruitment of microglia and precursor cells where the former will attempt to clear debris from the infarct site. The role of precursor cell migration to sites of injury is yet to be fully understood but they may play a part in replacing lost cells. Local astrocytes also respond to the injury and display an increase in proliferation. (3) Tissue remodelling – which involves formation of a so called '*astrocyte scar*' – a combination of hypertrophied astrocytes and secreted extracellular matrix (ECM) molecules including chondroitin sulphate proteoglycans (CSPGs).[5,6,8]

Regeneration of CNS axons in this environment is inhibited in two ways. Firstly, by extrinsic cues which include the physical barrier of the astrocyte scar and chemical signals – myelin associated proteins released by dying oligodendrocytes and CSPGs have both been shown to be potent axon

growth inhibitors.[5] Secondly, intrinsic signalling pathways have been shown to sensitise the neuron to the extracellular milieu and prevent axon outgrowth. For example, intracellular activation of RhoA by myelin fragments causes destabilisation of the neuronal cytoskeleton, rendering axon protrusion unfavourable.[5] In terms of cell replacement from endogenous sources, there is some evidence for neurogenesis in areas of stroke arising from NSCs that have migrated from germinal regions within the brain.[9] However, there is speculation over the contribution of endogenous neurogenesis to functional improvements as only a small percentage of migrating NSCs differentiate into mature neurons. In addition, this effect is reported to be lower in older animals (an important observation as stroke is most prevalent in the elderly population) and sites of severe injury.[9] Ultimately, endogenous tissue replacement does not have the capacity to restore the original function of the lost tissue. Given the complexity of pathology and the multiple parameters that contribute to regenerative processes, there are a number of avenues which could be explored for therapeutic interventions, including the use of combinatorial therapies which aim to address more than one target. Disrupting the astrocyte scar, removing inhibitory signalling molecules, promoting intrinsic neuronal growth and replacing lost neurons are all exciting therapeutic avenues which if targeted simultaneously could promote repair in the CNS.

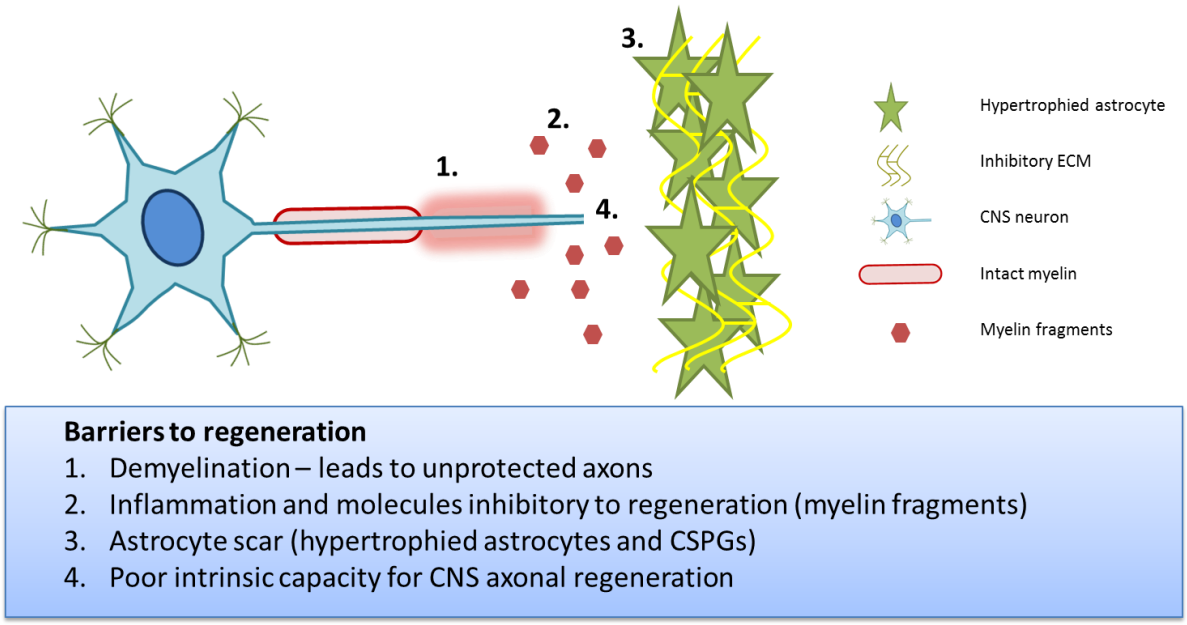

Figure 1.1. Schematic highlighting the multiple barriers to regeneration present in sites of neurological injury.

Current clinical treatments for neurological injury do not generally promote regeneration and aim to reduce symptoms and slow disease progression, for example, by administering drugs to modulate inflammation, in SCI,[10] or reduce blood clotting in stroke.[11] Physiotherapy to improve neurological function has shown benefits for patients experiencing stroke, traumatic brain injury (TBI) and SCI.[12] It is generally used for rehabilitation and to slow disease progression after neurological injury. In severe circumstances, surgery may be required to remove blood-clots or attempt to reduce bleeding. These treatments offer some relief, and may result in an environment which is favourable for regeneration, for example, by reducing inflammation based inhibition of axon growth.[8,13] However, there is some controversy about the administration of anti-inflammatory agents to treat neurological injury as some aspects of neuro-inflammation may be beneficial for regenerative processes.[10] Ultimately, therapies widely used in the clinic do not restore function of the CNS. Some promising alternatives to promote axon regrowth are close to clinical use, including drugs which breakdown or antagonise molecules inhibitory to axonal

regeneration, for example, Nogo-A inhibitors.[14] However, these drugs only address one factor within the complex nature of neurological injury. Current research efforts in the field of neuro-regeneration are therefore focussed on truly regenerative therapies for CNS disease and injury – to enhance the repair processes within the CNS and functionally replace lost or damaged cells.

1.3 Cell transplantation shows benefits for neurological injury

In the context of replacing lost tissue and restoring neurological function, cell transplantation is a promising therapeutic strategy. The scientific rationale for cell transplantation involves two main objectives: (1) to replace lost or damaged cells and (2) to release molecules to promote repair, such as neurotrophic factors. In terms of candidates for cell therapy, many different cell types are being investigated for the treatment of neurological injury. Stem cells, owing to their self-renewal capacity, offer an attractive source for cell transplantation as they can be expanded to clinically required numbers through *ex vivo* cell culture. Embryonic stem cells (ESCs), generated from aborted foetuses, have the capacity to generate any cell in the body. However, in their undifferentiated form, they have the potential to generate teratomas after transplantation. Consequently, they need to be pre-differentiated prior to transplantation and care is needed to ensure no teratoma forming cells remain within the transplant population.[15] Mesenchymal stem cells (MSCs) have also been used for neurological applications and can be derived autologously, from blood or bone-marrow samples, potentially avoiding immune rejection issues surrounding cell transplantation. MSCs are not thought to be tumorigenic and demonstrate functional recovery in models of neurological injury; believed to be the result of paracrine signalling and release of neurotrophic factors which promote the survival of host axons.[16] Although MSCs are multipotent, doubts remain over the ability of MSCs to effectively replace neural cells.[17] A relatively new technology has also seen the ability to reprogram terminally differentiated cells into stem cells termed induced pluripotent stem cells (iPSCs). These cells have similar properties

to ESCs with the advantage of being able to derive them from the patient's own cells using relatively non-invasive procedures. However, engineering cells in this manner is currently achieved using viruses which (as expanded later in **Section 1.6**) are not suitable for clinical translation. Further, the efficiency of transformation into stem cells is low (ca. 1%), meaning a large number of cells have to be taken from the patient, and doubts remain about iPSC tumorigenicity.[18,19] Olfactory ensheathing cells (OECs) have also been transplanted into areas of spinal cord injury (SCI) and shown to promote functional recovery.[20] These cells can be generated from autologous mucosal biopsies and propagated in culture. After transplantation into sites of SCI they appear to have an innate ability to guide long distance axonal regeneration and recovery of locomotion. Although these cells may have considerable promise for SCI therapy their application in other neurological deficits is less proven and their inability to produce cells of the CNS may hamper their clinical translation for cell replacement therapies. Neural stem cells (NSCs) are another cell type widely used in clinical trials for neurological disorders[17] and have unique properties which may allow them to address the multifactorial nature of CNS injury, as will be described in the following section.

1.4 NSCs as promising candidates to promote repair in CNS disease and injury

NSCs are defined as multipotent precursor cells to the major cell types of the CNS (neurons, oligodendrocytes and astrocytes) with the capacity to self-renew.[21] They exist in the developing nervous system but also reside in specialised niches within the adult CNS. In the brain, these are the subventricular zone (SVZ) in the forebrain, which continuously supplies neurons to the olfactory bulb, and the subgranular zone which generates new neurons in the granular layer of the dentate gyrus.[22] NSCs have also been derived from the periventricular tissue region of the spinal cord.[23,24] NSCs from the different areas have been reported to generate region specific neurons or differentiate primarily into oligodendrocytes when taken from the spinal cord,[24] which

could have an important bearing on choosing a cell source for transplantation as different sources could have benefits for different CNS pathologies.[25] Primary NSCs can be derived from each of these regions using embryonic or adult tissue and are cultured by neuroscience laboratories worldwide as monolayers (adherent, 2-dimensional cultures) or neurospheres (3-dimensional, floating cell aggregates). NSCs are also routinely derived from ESCs and there are reports of iPSC-derived NSCs[19] involving the reprogramming of post-mitotic cells into stem cells using key transcription factors: *Oct4*, *Sox2*, *c-Myc* and *Klf4*.

NSCs offer an attractive alternative to commonly used transplant cell populations for several reasons. NSCs have been shown to secrete numerous trophic and immunomodulatory factors which are thought to be among the main mechanisms by which NSC transplantation slows disease progression and imparts functional benefits after transplantation into models of CNS disease/injury.[26] Molecules such as neutrophin-3 (NT-3), nerve growth factor (NGF) and glial derived neurotrophic factor (GDNF) have been shown to be secreted from NSCs with some evidence that their release has neuroprotective effects.[26] For example, NSCs were transplanted into a rat model of Parkinson's Disease, generated by injecting rats with MPTP (1-methyl-4-phenyl-1,2,3,6-tetrahydropyridine) which renders dopaminergic neurons tyrosine hydroxylase (TH) deficient but avoids cell death.[27] Transplanted NSCs appeared to migrate to the diseased neurons and it was shown that a large proportion of the transplant cells express high-levels of GDNF. GDNF has been shown to be neuroprotective of dopaminergic neurons *in vitro* and in this study rescue of TH activity *in vivo* was observed along with behavioural improvements in rats receiving an NSC transplant.

NSCs also have the ability to cross the BBB[28] and display high migration and integration within host CNS[28,29] exhibiting a phenomenon termed '*pathotropism*' – the homing of cells towards sites of pathology.[28,29] Aboody *et al.* were among the first to demonstrate the pathotropism of NSCs by transplantation into rodents with brain tumours, established using highly aggressive glioblastoma

cell lines.[29] Tumours were always established in the right frontal lobe of the brain. NSCs were transplanted into various areas within the brain and in one instance into the vasculature, through the tail vein. In all cases, NSC juxtaposition to the tumour was observed, sometimes as rapidly as two days after NSC transplantation. In addition, when NSCs were injected directly into the tumour bed they could be seen to track single, migratory tumour cells – potentially of considerable benefit if attempting to deliver targeted chemotherapy to invasive cancers. This ability to cross the BBB and their homing capacity allows NSCs to be administered via systemic routes without direct transplantation into the CNS which could mitigate the risk of secondary pathology; potentially a critical safety feature of this cell type. Further, extensive NSC migration within the CNS could enable treatment of large or multi-focal areas of disease, of particular relevance to global disease pathologies such as Alzheimer 's disease, brain cancer and lysosomal storage diseases (LSDs).

NSCs can differentiate into all three cell types of the CNS lineage[21,30] and there is evidence for their differentiation into neurons, which form synapses with the host circuitry,[31] and myelinating oligodendrocytes[28,31] after transplantation into CNS models of disease/injury. Pluchino *et al.* demonstrated that tail vein injection of NSCs into a mouse model of multiple sclerosis resulted in donor NSCs surrounding areas of myelin loss.[28] The majority of donor cells expressed platelet-derived growth factor-α (PDGF-α, an oligodendrocyte precursor marker) as assessed by immunohistochemistry, and were actively involved in remyelination, observed using electron microscopy. However, the extent to which functional recovery is due to cell replacement and functional integration into the CNS, or trophic support for surrounding neural tissue supplied by transplanted NSCs, is currently difficult to confirm.

NSCs can be isolated from embryonic and adult tissue, allowing the possibility of allogeneic and autologous treatment, and can be expanded and genetically manipulated *in vitro*. The former is of clinical relevance as the required quantity of cells for a cell therapy can be generated in culture.

To highlight this particular problem, it has been suggested that 8-12 foetuses are required for cell transplantation into the brains of Parkinson's Disease patients.[15] *In vitro* genetic manipulation of transplant cell populations can be used to introduce genes which encode therapeutic biomolecules. The transplanted cells can then act as '*vehicular biopumps*' to deliver therapeutic factors to sites of injury or disease.[32]

NSC transplantation has also overwhelmingly been shown to be safe, with little evidence of tumour formation and indeed NSCs are thought to be non-tumorigenic.[33] The advantages described in this section have led to numerous pre-clinical studies demonstrating promotion of neurological recovery after NSC transplantation into sites of injury/disease and their potential as therapeutic agents is evidenced by the fact that NSCs are currently utilised in several clinical trials. Neuralstem (USA) are currently in phase I clinical trials for transplantation of NSCs into the spinal cords of patients suffering from amyotrophic lateral sclerosis (ALS). The NSCs are hypothesised to protect surviving motor neurons and prolong the life of ALS patients. Phase I was successfully completed with no adverse reactions to the transplantation and phase II trials (NCT01730716) are to be initiated.[34] Reneuron Group plc (a UK-based stem cell company) have also completed phase I clinical trials with their NSC cell line product designed to ameliorate the effects of ischaemic stroke. Phase II trials have since been initiated in 10 UK centres (NCT02117635). Phase I clinical trials are also ongoing to examine the safety of transplanting NSCs into multiple sites within the brain in patients with neuronal ceroid lipofuscinoses (NCL), a form of LSD. Transplanted NSCs are thought to migrate within the brain and supply replacement enzyme for cross correction therapy of deficient cells. This enzyme acts to reduce build-up of lipofuscin in neurons which is the major pathological contributor to NCL.[35]

1.5 Genetically engineering NSCs could provide combinatorial therapy

Although NSCs possess numerous advantages for transplantation into the CNS, addressing one factor by utilising cell replacement (or gene delivery) is unlikely to be sufficient to restore the function of the CNS. To promote effective neural repair several factors need to be addressed in the context of the complex biological processes in neural disease/injury. '*Combinatorial*' therapies, which have the ability to achieve concurrent goals such as cell replacement coupled with therapeutic gene delivery, are thought to be the most realistic approach to achieve functional repair. Several studies have demonstrated enhanced benefits when transplanting genetically manipulated NSCs compared to transplantation of NSCs alone. Strategies to improve clinical outcomes after transplantation of genetically engineered NSCs vary, but some examples are highlighted in the following section and in **Table 1.1**.

Some groups introduce genes designed to enhance the survival of NSCs (such as Akt-1 or vascular endothelial growth factor, VEGF) to address the well-known problem of abundant cell death post transplantation.[36,37] Akt-1 is a mediator of the P13K-Akt signalling pathway which is involved in pro-survival and anti-apoptotic signalling. Lee *et al.* introduced this gene into NSCs via retroviral transduction and selection by hygromycin resistance. Akt-1 modified NSCs displayed enhanced survival when transplanted into areas of stroke induced in mice and improved behavioural outcomes in comparison to NSCs alone.[36] In this scenario, enhanced neuroprotective effects and improved functional outcomes, compared to the non-engineered NSCs, are thought to be the result of increased survival of the engineered transplant population allowing more cells to deliver a therapeutic effect. Whether introducing genes such as Akt-1 will be applicable in the clinic remains to be seen, however, as immortalising cells could lead to potential tumour formation. Reneuron have ongoing clinical trials for stroke therapy with their NSC cell line (Phase I: NCT01151124 and Phase II: NCT02117635) which has been conditionally immortalised by retroviral introduction of c-mycER(TAM). Using this system, expression of the growth promoting c-myc can only occur in the presence of a hormone, 4-hydroxy-tamoxifen (4-OHT). With the

inclusion of growth factors and 4-OHT in the culture medium, stable clonal expansion of NSCs can be achieved for production without chromosomal aberrations (a common risk in late passage cell-lines),[38] up to at least passage 16.[39] So far no adverse safety effects have been associated with transplantation of NSCs expanded in this manner into areas of stroke, suggesting that introducing genes which control cell proliferation could be a viable clinical strategy. Rigorous safety testing will have to be performed to ensure the absence of teratoma formation or abnormal cell divisions when using this approach.

A more regenerative strategy involves engineering NSCs to release repair promoting factors such as NT-3, GDNF or VEGF.[40–43] Transplanted NSCs engineered to release NT-3 and GDNF have shown enhanced neurite extension of host axons into lesion sites and greater evidence of neurogenesis from the transplanted NSCs when compared to non-engineered controls.[40,42,43] For example, in one study NSCs were retrovirally modified to secrete NT-3. After transplantation into rat spinal cord lesions, both engineered and non-engineered NSCs promoted axon growth into the lesion. However, a marked increase in axonal density was observed in the lesion receiving NT-3 expressing NSCs. Analysis of mRNA levels in the lesion site demonstrated that NT-3 mRNA was indeed greatly enhanced after transplantation of engineered NSCs in comparison to non-engineered NSCs which provides a reasonable explanation for the observations.[40]

Along with enhancing axonal outgrowth, a key goal in regenerative medicine is to improve vasculature of regenerating tissue in order to supply nutrients to the newly formed tissue. To address this, VEGF was introduced into NSCs for transplantation into rat brain in two studies. Although increased blood vessel formation was not noted in either study, both studies demonstrated enhanced numbers of endothelial cells, which form blood vessels, in the vicinity of the NSCs.[37,41] In the case of VEGF overexpressing NSC transplantation into a rat stroke model, functional improvements occurred at an earlier stage in the study (two weeks post-transplantation) compared to transplantation of non-engineered NSCs (eight weeks post-

transplantation) – although by the end of the study functional improvements were broadly similar between the two groups.[41] The results could suggest that gene expression was not sustained for a long enough time period to mediate further functional improvement, highlighting the need to consider time-course of gene expression and transfection efficiency when developing an optimal clinical strategy for genetically engineering a transplant population.

NSC mediated delivery of molecules which target underlying disease pathologies have also been developed. Two recent studies have demonstrated the neurological benefits of transplanting NSCs in models of Alzheimer 's disease and LSDs. The first showed that NSCs can increase synaptic connectivity and neuronal survival and consequently cognitive function in a rat model. Subsequent engineering of the NSCs to release neprilysin was shown to further address the underlying pathology of Alzheimer's Disease by breaking down amyloid plaques in diseased areas.[44] In the model of LSD, NSCs were engineered to release ß- galactocerebrosidase (GALC), the enzyme responsible for controlling lysosomal storage which is otherwise deficient in the disease. Here, NSCs showed immunomodulatory and neuroprotective effects which slowed down disease progression. Overexpression of GALC resulted in widespread delivery through the cerebrospinal fluid (CSF) and more cells which were corrected to normal storage phenotypes compared to transplantation of non-engineered NSCs.[45] Both these studies show the great potential in combining neuroprotective efficacy of NSCs with biomolecule delivery to address several therapeutic goals in one step. Whilst all the studies described in this section have shown some benefits of genetically engineering NSCs prior to transplantation (summarised in **Figure 1.2**), it is overwhelmingly the case that genetic manipulation has been achieved using viral vectors (**Table 1.1**). As discussed in **Section 1.6** viruses are associated with several disadvantages and currently pose a major barrier to the clinical translation of this therapeutic strategy.

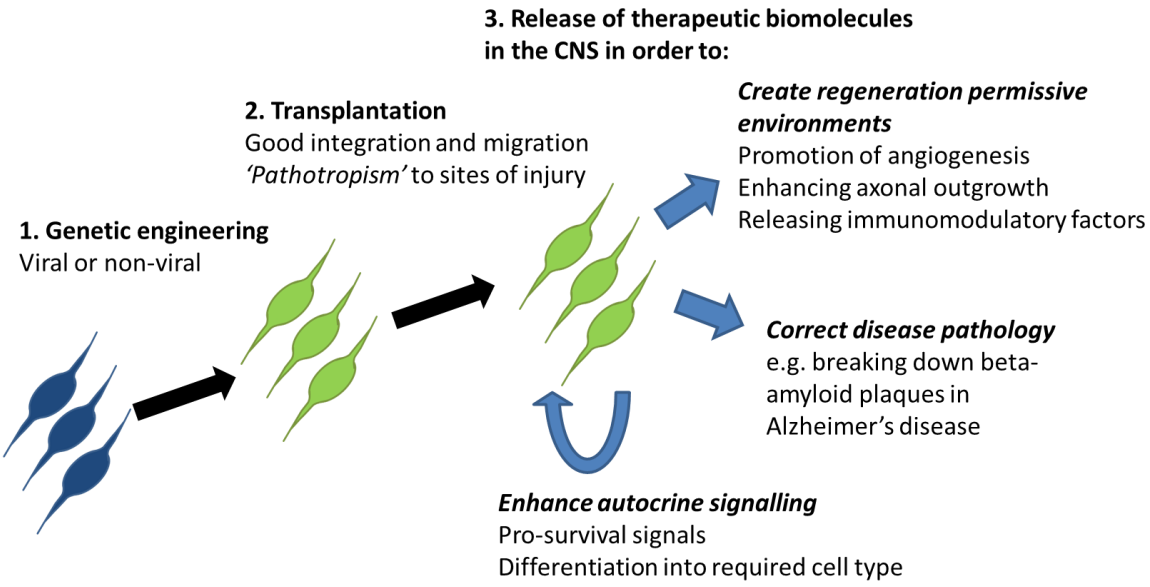

Figure 1.2. Schematic detailing how genetically engineering NSCs for transplantation offers several clinical advantages.

Disease model	*Strategy*	*Genetic engineering method*	*Outcome*	*Reference*
Alzheimer's Disease in transgenic mice	NSCs overexpressing neprylsin enzyme (breaks down beta-amyloid plaques). NSCs also shown to improve synaptic connectivity and neuronal survival	Nucleofection followed by stable transfection selection (6 weeks) and lentiviral transduction	Reductions in beta-amyloid plaques and increased synaptic density	[44]
Mouse intracerebral haemorrhage stroke model	NSCs modified to survive through introduction of Akt1	Retrovirus	Greater NSC survival and improved behavioural outcomes	[36]
Intact rat brain	NSCs overexpress VEGF to induce angiogenesis	Adenoviral vector. Transfection efficiency of 20-30%	Increased NSC survival and enhanced number of endothelial cells after 11 days	[37]
Rat spinal cord lesion	NSCs transfected with NT-3	Retroviral system	Enhanced axonal growth into lesion compared with non-transfected NSCs	[40]
Middle cerebral artery occlusion ischemic brain model in rat	NSCs transfected with VEGF to improve neuroprotection and angiogenesis	Lipofection resulting in VEGF expression for at least 2 weeks	Earlier improvement in behavioural scores after transplantation of transfected NSCs	[41]
Hypoxic-ischemic model in mice	NSCs transduced with NT-3 to promote neurogenesis	Retroviral transduction and antibiotic selection with G418	Higher numbers of NSC derived neurons in the infarct site compared to a previous study of non-engineered NSCs	[42]
Middle cerebral artery occlusion ischemic brain model in rat	NSCs modified to secrete GDNF which enhances progenitor proliferation and exerts neuroprotective effects	Fibre-mutant Arg-Gly-Asp adenovirus vector system (50% transfection efficiency with reporter plasmid)	Modified NSC transplantation reduced infarct size and resulted in better behavioural outcomes than controls	[43]
Compression SCI in mice	NSCs modified to produce noggin, a BMP inhibitor – BMP signalling is up-regulated in SCI and causes NSC differentiation into astrocytes when neurons may be more appropriate	Retroviral system	Improved differentiation of NSCs into neurons and oligodendrocytes compared to non-engineered NSCs and enhanced functional improvement	[46]
Intracranial brain tumour induced by transplanting glioma cells	NSCs genetically engineered to release cytosine deaminase. NSCs home towards tumours and release therapeutic molecule	Retrovirus transduction with antibiotic selection	Cytosine deaminase activity metabolises pro-drug into its active form and caused 80% reduction in tumour volume	[29]
Contusive SCI in common marmosets	NSCs engineered to overexpress galectin-1 – shown to enhance NSC proliferation and axonal regeneration	Lentiviral system. Over 80% transfection efficiency	Reduced myelination loss and lesion size and improved behavioural outcomes compared to non-engineered NSCs	[47]
Murine model of globoid cell leukodystrophy (LSD)	NSCs engineered to overexpress GALC to replace the deficient enzyme	Lentivirus (70-90% transfection efficiency)	NSC transplantation provided neuroprotective effects with GALC overexpression resulting in more correction than non-engineered NSCs	[45]
Mouse model of Type-A Niemann-Pick disease (LSD)	NSCs engineered to release acid sphingomyelinase which corrects disease pathology	Retrovirus and antibiotic selection	Marked reduction to lysosomal pathology in genetically manipulated NSC transplanted mice compared to non-engineered NSC transplantation	[48]

Table 1.1. Examples of genetically engineering NSCs for transplantation into the CNS. *NSC – neural stem cell; VEGF – vascular endothelial growth factor; NT-3 – neurothrophic factor 3; GDNF – glial derived neurotrophic factor; BMP – bone morphogenetic protein; SCI – spinal cord injury; LSD – lysosomal storage disease; GALC* – ß- galactocerebrosidase.

1.6 Barriers to translation of genetically engineered NSC transplantation

Despite the benefits shown in models of neurological disease/injury of transplanting genetically engineered NSCs, many barriers to their translation into the clinic exist (summarised in **Figure 1.3**). Overcoming these barriers is therefore a key research goal and one that this thesis aims to start to address through the use of nanotechnology. This section will outline four major obstacles and the reasons they exist, whilst subsequent sections will highlight the potential of using nanotechnologies to address them.

1) *Safe and efficient genetic engineering*: For clinical use, the most desirable transfection agent to introduce therapeutic genes into NSCs would: combine high transfection efficiency; provide minimal toxicity to target cells and host tissue; be amenable to scale-up and have the versatility to enable delivery of a range of DNA and RNAi molecules. Currently, the most popular method of genetic manipulation of NSCs is achieved using viral vectors (used almost exclusively when engineering NSCs for combinatorial therapy [**Table 1.1**]) which offer high transduction efficiencies. However, viruses have several drawbacks including: safety issues, associated with toxicity to the target cells and oncogenicity of the transduced population due to insertional mutagenesis (especially relevant when using stem cells which have a capacity to self-renew); a limit to plasmid size in the most versatile vectors; and a complex, time-consuming method of application.[49,50] Additionally, genes introduced by retroviral transduction have been shown to undergo down-regulation over time.[51] All of these disadvantages pose a considerable barrier to clinical and commercial adoption of stem cells transduced with viruses. Although considered safer than viruses, non-viral transfection is generally associated with low transfection efficiencies, especially in the case of lipofection and electroporation,[52,53] or high cell death, in the case of nucleofection.[53] In the latter case, although nucleofection results in high transfection efficiencies (ca. 50%),[53] losing valuable cells is costly and transplantation of cellular debris resulting from cell death could lead to adverse reactions at the site of transplantation.

2) *Safe and efficient delivery of cells to injury sites*: Accumulation of cells at the desired site is a key requirement of successful cell therapy. However, current cell delivery techniques to the injured CNS are associated with considerable disadvantages. Direct transplantation of cells generally results in a larger accumulation of cells than systemic injection. However, this approach is associated with significant risks in the CNS including secondary pathology, breakdown of the BBB and embolism.[54] Systemic injection, either intra-arterially or intravenously, can alleviate these risks so has a higher translational potential, however, cells can be cleared by the tissue macrophage system, often ending up in the lung, spleen or liver so that few cells are retained at the desired site.[55,56] Ramifications of this include the need to inject more cells (which will be costly to produce) to compensate for cell loss together with the possible need for multiple injections therefore further increasing risk to the patient. A further problem, common to both systemic and direct injection, arises from transplanting large concentrations of cells within the injected solution (ca. 1 x 10^5 cells/µL). This leads to high viscosity and cell clumping within the injected solution resulting in poor distribution of the cellular suspension throughout the lesion site. In addition, direct injection can cause damage to the cells and extensive cell death resulting in low numbers of viable cells delivered into the lesion (e.g. <5% OECs survived direct transplantation into a SCI site)[57] – an issue known as '*low stability*'.

3) *Cell tracking post-transplantation*

    a) *Non-invasive imaging*: Cell transplant populations need to be monitored in order to correlate cell behaviour with functional outcome and assess integration upon transplantation. This applies *in vitro*, for example, in monitoring cell transplantation in slice models of injury, and *in vivo*, for pre-clinical and clinical work. Real-time, non-invasive imaging of transplant populations *in vivo* is essential to monitor correct engraftment, both position and viability of the graft, cell migration and ideally cell

differentiation. This is commonly achieved by using several techniques such as: magnetic resonance imaging (MRI) where the cells are labelled with a contrast agent; bioluminescence imaging (BLI) where cells express photon producing enzymes; single photon emission computed tomography (SPECT) and positron emission tomography (PET), which both detect radioactive labels; or near infrared fluorescence (NIRF) microscopy which detects fluorophore labelled cells.[58] Each technique has its own advantages and disadvantages, for example, MRI has high spatial resolution and tissue penetration whereas BLI and PET have a high sensitivity (the ability to detect lower numbers of cells) and BLI has the possibility of providing information on differentiation by detecting luciferase expression that is under the control of cell specific promoters.[59]

b) *Histological examination*: Ultimately, the tissue has to be analysed post-mortem for thorough histopathological examination of integration, migration and differentiation of the transplanted cells and also, the effect of the transplant on the host tissue. This means that the transplanted population needs to be distinguished from the host cells. This can be accomplished by using cells from another species which can be detected with antibodies against that species, using cells from mutant animals which express GFP, labelling cells with lipophilic fluorescent dyes[60], or genetically modifying cells to express a detectable marker.[42] The first two techniques, although useful in a laboratory setting, are not readily translatable. Labelling cells with dyes can result in non-specificity due to 'leaky' dyes[61] and virally transducing a cell population to express a detectable gene is undesirable from a translational perspective as discussed above.

4) *Functional integration*: The therapeutic efficacy of NSCs is often ascribed to their bystander effect – the release of neurotrophic and immunomodulatory factors.[26] However, a key goal of NSC transplantation is to replace lost or damaged cells. Although there are many reports of NSCs differentiating into useful cells for the disease pathology,[24] NSC differentiation after transplantation depends on many factors such as source of NSCs (age of donor, tissue derived

from) and injury site environment. Controlling NSC differentiation into required cell types is therefore an important area of research to enhance successful function of the transplanted cells. In addition, undesirable differentiation of NSCs into astrocytes has been observed in rat models of SCI[46] and associated with mechanical allodynia[24] highlighting the importance of careful control over NSC differentiation.

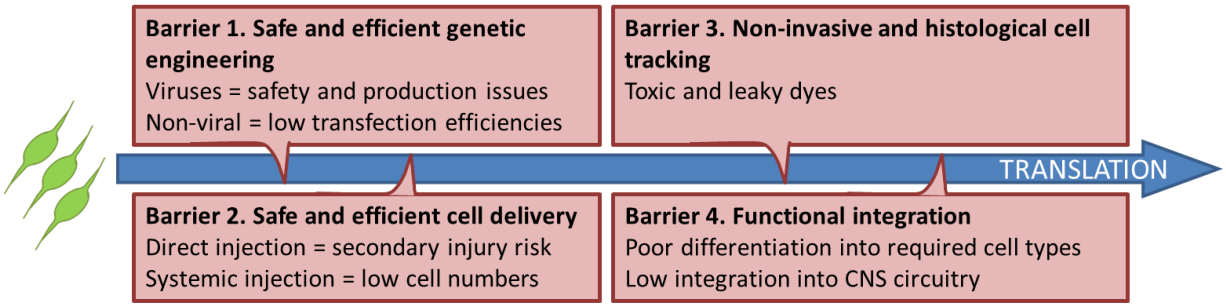

Figure 1.3. Schematic highlighting barriers to translation facing genetically engineered NSC transplantation therapy.

1.7 Investigating nanotechnologies in order to address translational barriers

In order to overcome the described obstacles, alternative strategies need to be developed. With the field of nanomedicine advancing at a rapid pace, nanotechnology platforms such as nano and micro sized particles and engineered hydrogels now offer a wealth of biomedical functions that can aid in overcoming the translational barriers identified in **Section 1.6**. Detailed discussion of the properties of MPs and hydrogels and how these relate to their biomedical function will be provided in following sections. However, this section briefly summarises how specialised nanomaterials may overcome the outlined barriers to translation. Safe genetic manipulation (***Barrier 1***) of neural cells has been demonstrated by using MPs with gene transfer efficiency improved by application of oscillating magnetic fields below the culture plate.[62,63] Key regenerative properties such as cell proliferation, survival and differentiation are unaffected by

such protocols – of high importance for clinical application (expanded in **Section 1.9** and **Chapter 2**). Nanomaterial strategies for safe and efficient delivery of cells to injury sites (***Barrier 2***) are two-fold. Firstly, MP labelled cells have been shown to be amenable to magnetic cell targeting where systemically delivered cells can be localised to required sites by external magnets, avoiding cell clearance through the tissue macrophage system (expanded in **Section 1.11** and **Chapter 3**).[64,65] Secondly, cells can be evenly distributed in protective, implantable hydrogel matrices. This second strategy addresses the issue of low transplant stability and potentially facilitates the delivery of a highly viable cell graft (expanded in **Section 1.12** and **Chapter 4**). Post-transplantation, MP labelled cells have also been tracked (***Barrier 3***) non-invasively by MRI and in fixed tissue using histopathological detection of iron.[66] Finally, as will be expanded in **Section 1.12** and **Chapter 4** the issue of functional integration (***Barrier 4***) may be addressed by engineering sophisticated hydrogels that can control stem cell differentiation, through tuneable stiffness, and potentially provide topographical cues for regenerating tissue.

Initially, combinatorial therapy was expected to involve cell delivery in conjunction with drug delivery. However, through advent of these nanotechnologies combinatorial therapy is being redefined as several important biomedical functions could be achieved simultaneously. For example, MPs have been separately shown to mediate gene delivery and MP labelled cell targeting and tracking through MRI. Engineering a multifunctional MP capable of all these features would therefore provide a one-step approach to addressing several barriers to translation. In addition, fusion of technology could further broaden the scope of what is achievable. In this regard, combinations of MP and hydrogel technology could address all of the barriers to cell transplantation outlined in **Section 1.6**.

Therefore, given the potential of these technologies for cell transplantation, this thesis aims to explore key concepts of utilising nanotechnology for NSC transplantation in more detail. The following sections will describe MPs and hydrogels, how they might influence future therapeutic

strategies (by addressing the barriers to NSC transplantation therapy and providing platforms for the next generation of combinatorial therapies to enhance repair in the CNS) and the gaps in the literature which require further research.

1.8 MP composition and properties

MPs are a class of materials that interact with a magnetic field and can be functionalised to perform different tasks. They are used for *in vivo* imaging as MRI contrast agents,[67] drug and gene delivery[68] and cell or biomolecule separation[69] amongst other uses. In general they possess a magnetic core surrounded by a biocompatible layer and they can range in size from about 10 nm to 1 µm. Functional molecules, such as fluorophores or small targeting molecules, can be added to the particle and, recently, due to improvements in the synthesis of these particles, multifunctional MPs capable of achieving several goals in one system have been developed (**Figure 1.4 and Table 1.2**).[68,70,71] MP labelling has been shown not to affect NSC survival and differentiation after transplantation *in vivo*[61] indicating these are an attractive technology to explore for clinical application. This overview will give a brief discussion of the chemistry of the particles and how they can achieve multi-functionality, while subsequent sections will examine the biomedical applications of these particles.

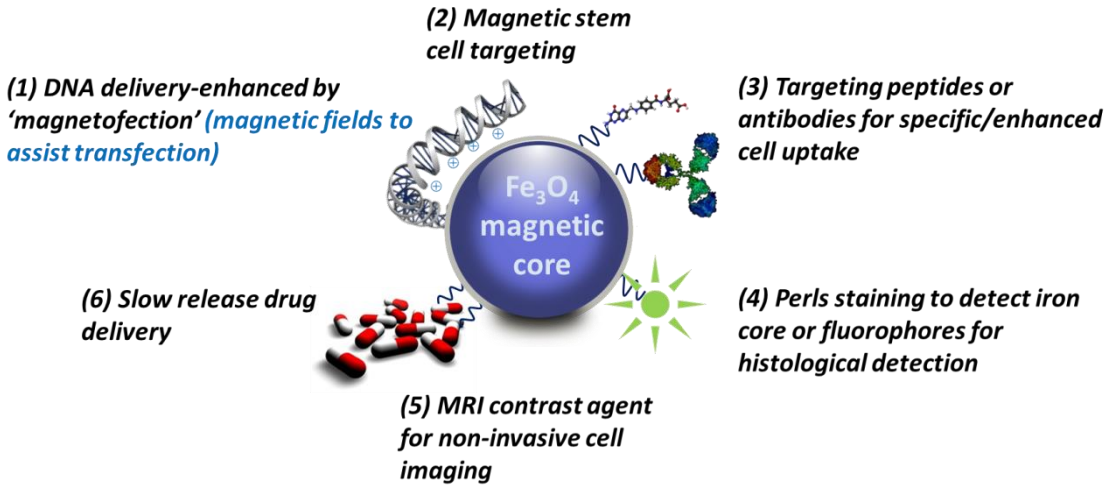

Figure 1.4. Schematic detailing multiple biomedical applications of MPs.

The core material of an MP dictates how the particle will interact with a magnetic field and total core size, crystal size, and iron content all impact on this, reviewed by Laurent *et al*.[72] The most popular core material for *in vivo* use is iron oxide, as magnetite (Fe_30_4) or maghemite (y-Fe_2O_3), which can be metabolised by cells and appears to be non-toxic.[73,74] A key property of the core is superparamagnetism which occurs when iron-oxide core size reduces to below 30 nm. Iron-oxide is normally ferromagnetic which means that it displays strong attraction to a magnetic field and remains magnetised after a magnetic field has been removed. Paramagnetic materials display a weak attraction to a magnetic field and lose their magnetism once the field has been withdrawn. Superparamagnetism is a combination of both characteristics and occurs in the nanoscale dimensions of MPs whereby particles display high susceptibility to a magnetic field but do not retain magnetism after the magnetic field has been removed.[75] Contrast enhancement from MPs, in MRI images, is due to the fact that the superparamagnetic particles display high magnetic moments which act to shorten proton relaxivity times in the immediate surroundings, leading to loss of signal in both T_1 and T_2 MRI images.[70,76] As the particles do not retain any residual magnetism after the field has been removed, aggregation is avoided. This characteristic is important for the safety of the particles application *in vivo* to reduce the risk of aggregate

mediated embolization of capillaries. Along with acting as a contrast enhancer, it should also be noted that the iron core can be detected histologically using Perls' stain for identification of labelled cells.[77]

To coat the particle, natural and synthetic polymers are generally used for their biocompatibility (i.e. the ability to interact within a biological system without causing adverse toxicity) and their amenability to further functionalisation. Coating materials can be physically associated with the core by creating a dense network of cross-linked polymer around the core or can be covalently attached through linker molecules.[71] The former can degrade over time so any long term functionality required of the particles will likely utilise polymers covalently linked to the iron oxide core. The functional groups which are available on the coating polymers (e.g. primary amines or carboxylic acids) allow for addition of functionalising molecules, such as fluorophores or targeting molecules, alone or in combination. Some polymers can also be used to bind drugs or nucleic acids[68] while leaving their functional groups available for further manipulation. Careful design, therefore, could lead to a single nanoparticle with multiple functionalities and therefore multiple capabilities. In this respect, 'multimodal' particles have been designed which offer: complementary imaging techniques, such as MRI coupled with fluorescence (near infra-red);[84] cell targeting and imaging capability;[85] and the capacity for gene delivery and cellular imaging.[83]

Uses	Name (if applicable)	Core	Coating	Reference
MRI	Feridex	Superparamagnetic Iron Oxide	Dextran or poly-l-lysine	[67]
Magnetofection for neuronal cells	Neuromag	Iron Oxide	+vely charged Complexes with DNA or RNA	[30,62,63]
Magnetofection	PEI-Mag2	Iron Oxide	PEI (+vely charged polymer)	[78]
Magnetofection	LS-Mag-PEI	Iron Oxide	PEI and lauroyl sarcosinate – amphiphilic molecule	[78]
Hyperthermia Ligands allow uptake by NSCs		Cores of Iron oxide	Aminosiloxane Stealth L1 Tetra-4-carboxy-phenyl porphyrin	[79]
Magnetic cell targeting		Styrene acryl polymers	Magnetic ferrite with outer layer of peptides	[80]
Examining particle uptake	Spherofluor	Polystyrene with embedded fluorophore	Iron oxide crystals	[81]
MRI/PET contrast agents	Multimodal imaging particle	Iron-oxide	Poly aspartic acid, RGD targeting ligand, DOTA – radiolabel for PET imaging	[82]
MRI contrast agent Histological labelling Transfection	Multimodal imaging/transfection particle	Iron-oxide	PEI Conjugated to RITC	[83]

Table 1.2. Examples of MPs and their biomedical applications.

The most widely used coating polymer for transfection is PEI,[86] a highly positively charged, synthetic polymer which has been used as a transfection reagent in its own right.[87] PEI is thought to display high transfection efficiency for several reasons: firstly, it can condense DNA and act as a carrier; secondly, due to its positive charge it can interact with cell membranes and; thirdly, once inside endosomes, PEI buffers the internal environment causing proton and concomitant chloride ion and water influx resulting in endosome lysis, releasing the DNA which can be transported to the nucleus.[88] PEI displays dose dependent toxicity probably due to its interaction with cell membranes and also lysosome rupturing capabilities. Chitosan, a natural polymer, which displays lower toxicity than PEI, has also been studied[89,90] but is not as effective a transfection agent as PEI, possibly because it has lower buffering capability and therefore less chance of rupturing endosomes. However, Kievit *et al.*[90] combined chitosan with low molecular weight PEI to improve transfection efficiency of a human umbilical vein endothelial cell line and also make use of chitosan's biocompatibility to reduce toxicity.

The coating material also has an impact on the capability of the particle to act as a contrast agent for MRI. It has been shown that exchanging a hydrophobic coating for a hydrophilic coating increases contrast in T_2-weighted MRI scans.[91] This is because water molecules can diffuse close to the core so the protons experience greater relaxivity. Also, materials closest to the core affect the superparamagnetism property of the iron-oxide and ultimately the particles proton relaxivity.[91] Both these observations are critical to multi-functional nanoparticles as any alterations to the particle surface, for example, to enhance drug or DNA binding, will have an effect on the *in vivo* imaging capability of the particle.

1.9 Application and mechanism of MP mediated gene delivery

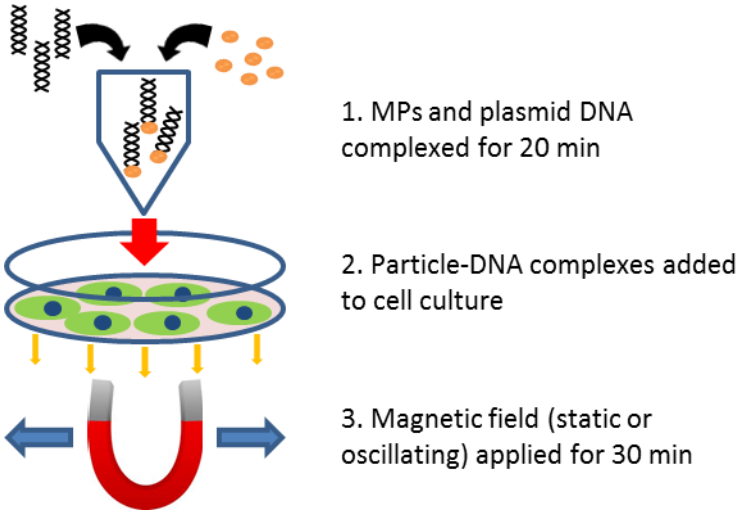

Figure 1.5. Schematic of typical magnetofection protocol.

'*Magnetofection*' is the process of delivering genetic material complexed to MPs into cells under the influence of magnetic force. The most widely used protocol for magnetofection is the application of a static magnetic field, placed beneath the cell culture surface during transfection, which draws the particles towards the magnet concentrating them at the cell surface (**Figure 1.5**). It appears that increased cellular interaction with the particles is the mechanism by which transfection efficiency is increased by magnetofection rather than the field enhancing uptake or forcing the particles inside the cells. Huth *et al.*[92] demonstrated this by applying MPs onto the cell surface by centrifugation then performing transfection in the presence or absence of a magnetic field. As the concentration of particles is now the same at the cell surface at the start of transfection in both protocols, if the magnetic field acts to increase cellular uptake through enhanced endocytosis or forcing the particles into the cells, then applying a magnetic field during this transfection should see an increase in transfection efficiency. There was no significant difference in transfection efficiencies between the two protocols suggesting that the static field solely acts to concentrate the particles at the cell surface.

The Dobson group has recently been advancing magnetofection technology and have shown the addition of an oscillating component (the magnetic plate physically oscillates in an x-y plane beneath the culture plate [**Figure 1.5**]) to the magnetic field can further enhance MP mediated gene delivery over and above that of static field transfection.[93] The mechanism for the enhanced transfection efficiency observed when using oscillating magnetic fields remains to be elucidated but there are two theories: (1) the particles are more disperse in solution due to their lateral motion and therefore are able to contact more cells; (2) the oscillation of the particles actually stimulates membrane uptake of the particles. This stimulation could cause a general increase in endocytosis, promote a more specific uptake pathway which leads to nucleic acid transport to the nucleus or be a physical shearing effect. The latter seems unlikely as cell viability, proliferation and differentiation appear to be unaffected.[62,63,93] Despite the advantages of genetically manipulating transplant cells using MPs, magnetofection protocols, in particular the application of oscillating fields, have not been tested in NSCs. This is an important area of study as these cells constitute a population with high clinical impact but data regarding the use of magnetofection protocols in other cell types cannot be extrapolated to this cell population.

1.10 MPs for cell tracking

There is a large body of basic research concerning the use of iron nanoparticles to label transplant cells which can be imaged non-invasively by MRI in real time.[67,70] Feridex, a dextran coated iron-oxide nanoparticle, was approved by the FDA to act as a contrast agent in the clinic, highlighting these particles' safety.[67] Feridex was originally designed as a liver contrast agent as it accumulates there, but has since been used to label various stem cell populations.[73] NSCs have been labelled with MPs and tracked using MRI in various rat and mouse models of disease[67] and also in a canine model of LSD.[94] Using a detailed analysis, Cohen *et al.* have shown that neurospheres isolated

from GFP^+ mice and labelled with Feridex can be tracked *in vivo* using MRI.[66] In this study, labelled NSCs were transplanted into the cerebral ventricles of mice with an induced form of multiple sclerosis (experimental autoimmune encephalomyelitis). Using *in vivo* MRI, a hypointense region where the cells had been injected was observed on day one and was followed by progressive migration of the cells into the corpus callosum over 7 days, thought to result from NSC pathotropism towards lesion sites. After sacrificing the animal, *ex vivo* MRI confirmed the widespread hypointense signal which correlated well with both GFP fluorescence and Perl's staining, indicating that the signal was derived from the labelled transplant population. One study has also examined the feasibility of labelling NSCs with MPs and tracking them using MRI in the clinic.[95] A hypointense region in the T_2-weighted MRI image was observed which was attributed to the transplanted and labelled NSCs. However, the study also highlighted some limitations. For example, the signal reduces over time (after 7 weeks the signal was no longer detectable) either due to migration of stem cells or their proliferation, which dilutes the MP concentration within daughter cells. Long term monitoring *in vivo* has been shown, with MRI signal persisting for 58 days, although convincing evidence that the signal originates from just the transplant population is not available.[96] One study has demonstrated that particles released by dead cells are taken up by immune cells or microglia leading to a false signal where the labelled NSCs were injected, as this is where most transplanted cells die.[97] Caution will therefore be required when labelling NSCs with MPs for long term tracking purposes as establishing whether MPs have been taken up by host cells could be difficult. However, a useful application which does not rely on long term retention of the signal, is observing the cells immediately after transplantation using MRI. Transplanted cells are often injected using ultrasound observation to guide the surgeon to the required site. Ultrasound images do not have the soft-tissue resolution of MRI and it has been shown that cell transplants have been injected into the wrong position using ultrasound.[98]

Therefore MRI could be used to check that the correct localisation of the transplanted cells has been achieved.

Although a powerful tool to track transplanted cells non-invasively, MRI does have some drawbacks. Signal dilution and particle uptake by host cells has already been mentioned. In addition, some conditions that may respond to stem cell therapy, such as traumatic injury, result in similar hypointense regions in the MRI signal as those resulting from MP labelled cells. Different imaging modalities can provide complementary information to MRI. For example, PET has a high sensitivity and the ability to detect low numbers of cells, which could be useful when tracking NSCs involved in widespread migration.[59] However, PET does not contain anatomical information. For real time imaging, fluorescence microscopy can obtain the greatest resolution but does not have good tissue penetration.[59] MRI contrast enhancing iron-oxide nanoparticles conjugated with radiotracers, which can be tracked using PET or fluorophores have been synthesised, which allow a combination of imaging modalities to be used. Lee *et al.*[82] have synthesised iron oxide nanoparticles for tumour imaging. These are functionalised with a PET radiotracer and an RGD targeting peptide which binds integrin $\alpha_v\beta_3$, expressed on cancer cells. The particles collect at the tumour site and allow MRI and PET visualisation of the affected area and the authors speculate that these might be used in early cancer detection as the integrin expression is switched on very early in tumorigenesis. Similar multifunctional imaging tools may be able to provide complex information on stem cell localisation, viability and differentiation.

1.11 Localising MP loaded cells to sites of injury and disease using magnetic force

To address the need for safe and efficient delivery methods of cells to the CNS, localising magnetically labelled cells using magnetic force may be a promising strategy. This approach could be especially beneficial for indirect methods of cell transplantation such as systemic injection or

lumbar puncture (into the CSF) in the spinal cord. Non-invasive delivery of cells is important in the CNS due to the risks of secondary pathology when cells are administered by direct injection, however, it is generally associated with low cell retention at the desired site due to cell removal through the tissue macrophage system or cell dispersal by the CSF which is produced and cleared in humans at rates of about 0.35 mL/min.[99] Applying external magnets after transplantation of MP labelled cells by both intravenous and lumbar puncture delivery has been shown to enhance cell retention post-transplantation in the brain and spinal cord. In one study, GFP^+, bone marrow stromal cells (BMSCs) were labelled with Feridex complexed to poly-L-lysine (PLL) and transplanted into a rat contusion model of SCI via lumbar puncture into the CSF. When transplanted in the presence of a magnet over the lesion, the area occupied by the MP labelled BMSCs was measured as being 20 times that of non-labelled cells. Localisation of MP labelled cells appeared to reduce cavity formation at the site of injury and improved hind-limb function.[100] Cells transplanted under magnetic field application have also been monitored via MRI, demonstrating the potential multifunctionality of MP labelling for clinical applications referred to in **Section 1.7 and 1.8**.[101,102]

Despite the advantages of using MPs for both non-invasive tracking and targeting of transplanted NSCs, clinical use of such protocols is hampered by the lack of available neurocompatible particles and the various strategies used to initiate uptake of MPs. As will be expanded in Chapter 3 these include use of high iron concentrations in the media, lengthy incubation times, transfection agents and cell penetrating peptides (CPPs). All of these strategies are associated with considerable drawbacks including toxicity and time-consuming protocols. Novel designs of MPs which can display functional efficacy in imaging and magnetic targeting could provide an alternative approach to achieving high uptake, however, very few neurocompatible particles are described in the literature.

1.12 Hydrogels as novel cell delivery devices

Hydrogels are used for *in vitro* research and have been used for several applications in regenerative medicine including in bone, cartilage and cardiac repair.[103,104] They have a jelly like appearance but are actually fibrous cross-linked polymers which can mimic ECM. Water molecules disperse in-between the pores of the fibres which lends the hydrogel a translucent appearance and, as a result of their high water content, biocompatibility. This confers the ability to support cell growth including in 3-D structures with cells dispersed through the matrix. They can be made up of a variety of materials both natural, for example collagen and hyaluronic acid (a spinal cord ECM molecule) which are biocompatible and mimic the native cell environment, and synthetic, which can be more readily predefined in terms of binding sites and fibre diameters.[105] In addition to materials, there are numerous features of the hydrogel which can be modified to suit the application, such as fibre diameter and spacing which influences porosity, amount of crosslinking and availability of cell binding sites. Altering these parameters affects the cells' interaction with and ability to migrate through the construct, the ease at which molecules diffuse through the fibres and mechanical properties such as stiffness and biodegradability.[105] These tuneable features allow for a range of versatile applications for hydrogel technology including for neural applications where hydrogels have several attractive features for their use in regenerative neurology (**Figure 1.6**). This section briefly outlines some of the tuneable features of hydrogels and how they are useful for cell delivery.

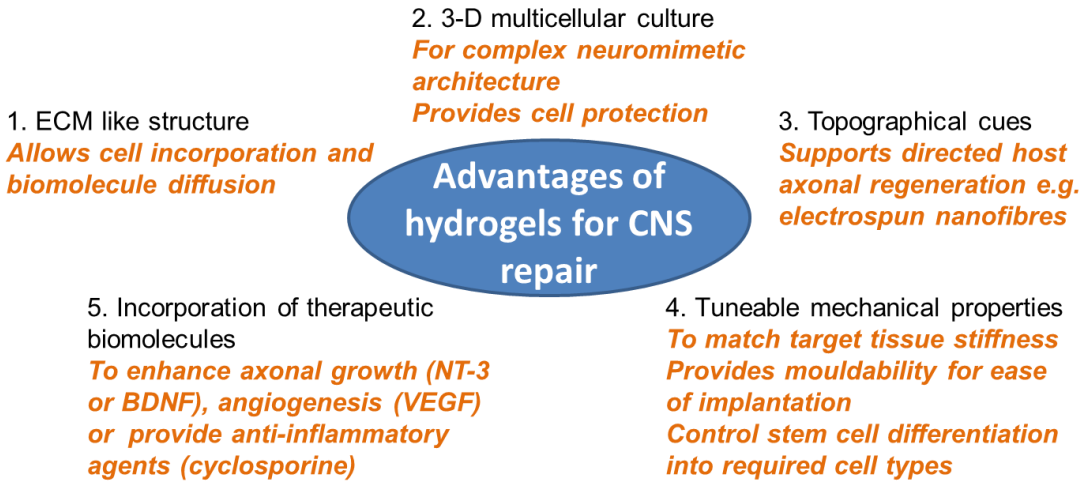

Figure 1.6. Schematic depicting advantages of hydrogels for repairing the CNS.

Hydrogel systems provide 3-D support for cells which in terms of cell transplantation provides the cells with a pre-formed substrate. This avoids problems such as cell death, dispersal or clumping outlined in **Section 1.6**, which result in a transplant of low stability. Some of the first instances of combining cells with hydrogel systems show improved survival of the transplant population compared to cells transplanted alone.[106] For example, Jin *et al.* combined NSCs with Matrigel™ and cultured the cells for one week before transplanting into an area of ischemic brain in rats.[107] After eight weeks rats were sacrificed to examine the fate of the cells. Compared to a cell only group, NSCs transplanted in combination with Matrigel™ displayed higher numbers within the cavity site (300 cells/mm^2 compared to negligible numbers in the cell only group – judged by image of the cavity) and a resultant reduction in cavity size. Some of the surviving cells displayed evidence of differentiation into astrocytes and neurons and behaviour outcomes were improved in the Matrigel™ compared to the cell only group. However, this study used an NSC cell line (which may not be physiologically relevant to primary NSCs, **Section 1.13**) and as Matrigel™ is derived from xenogenic sources it is not suitable for translation.

It has also been shown that implanting cells with hydrogels can improve their biodistribution. Ballios *et al.* mixed retinal stem cells (RSCs) with HAMC (a mixture of hyaluronan and methycellulose) before injection into the sub-retinal space in mouse eyes.[108] Cellular coverage of the retinal pigmented epithelial membrane (the tissue targeted for regeneration in therapies for age related macular degeneration) was assessed and found to be greater in hydrogel transplanted RSCs compared to RSCs transplanted in saline alone. The authors also noted continuous banding of RSCs on the membrane when transplanted with HAMC compared to aggregations of cells, in non-continuous banding patterns, when cells were transplanted in saline. This study, therefore, provides evidence that distribution of a transplant cell population can be improved by using hydrogels which could be of benefit when promoting regeneration over large lesion sites.

Generally hydrogels can be formulated using biocompatible materials that are non-toxic to both incorporated cells and host tissue – essential for clinical application – and are biodegradable. Using different polymers it is also possible to control the rate of matrix degradation. This is important to provide initial support for the growing cell population within the matrix – so as the cells grow they can slowly integrate into the lesion site and ensure that further tissue regeneration is not inhibited by the construct.[105] For additional consideration when delivering hydrogels to the CNS, Mahoney *et al.* showed that neurite extension into hydrogels is dependent on matrix degradation rate.[109] In that study, NSCs were incorporated into polyethylene glycol matrices formulated with different macromers which display different rates of degradation. NSCs seeded into the scaffolds formed neurospheres that extended processes on a time-frame which correlated with the degradation profile of the hydrogel. This characteristic of an implantable hydrogel is an important consideration when they are destined for transplantation into the CNS where the aim will be to improve axonal regeneration.

In terms of the physical properties of hydrogels, stiffness can be adjusted in a multitude of ways such as varying polymers or polymer concentration and increasing the amount of crosslinking within the gel. Mechanical properties of the gel can have a profound effect on gel acceptance and biocompatibility within host tissue and also on the encapsulated cells.[110] For example, Banerjee *et al.* incorporated NSCs into alginate scaffolds of various stiffness (ranging from ca. 180 – 20000 Pa).[111] From initially seeding 4000 cells a much higher number of cells was obtained after one week in culture in the softest gel (ca. 65000) compared to the stiffest gel (ca. 10000). In addition, higher expression levels of ß-tubulin (a neuronal marker) mRNA were found after the seven days in culture in the softest gel. The data suggest hydrogel stiffness could have an effect on cell response especially in proliferation and differentiation; two key regenerative properties of transplanted cells.

Various techniques also exist for incorporating guidance cues into the hydrogel formulations. These can include imparting a directional mechanical strain on the gel or inclusion of micro or nanofibres. For the first approach, East *et al.* incorporated astrocytes into a collagen scaffold which is tethered at two ends.[112] As the astrocytes attach to the collagen and contract it the strain imparted onto the collagen appears to align the astrocytes (and presumably the collagen fibrils) parallel to the direction of force. In this manner, a gel which is tethered at two ends creates areas of alignment within it, most notably along the edges of the gel. When dorsal root ganglia cells were also incorporated into this construct, their neurites could be seen to extend alongside the aligned astrocytes and had a greater length compared to those seeded in areas of unaligned astrocytes. For the alternative approach, Weightman *et al.* seeded astrocytes onto aligned nanofibres and then embedded these in a collagen hydrogel.[113] By building up layers of PLA fibres within collagen the authors demonstrated that spatial control of aligned astrocytes could be achieved in three-dimensions. This is particularly important for transplantation into 3-D lesions so that repair can be mediated throughout the depth of the injury.

Although advances in the field of hydrogel technology for cell transplantation are occurring at a rapid pace, several aspects have the potential for improvement which include: (1) The fact that most transplanted constructs contain one cell type, which can only address one issue within the complex nature of CNS injury. Alternatively, the construct may contain stem cells, which rely on correct differentiation to replace a certain cell type. (2) A lack of ability to monitor implants after transplantation to assess engraftment and survival and (3) the absence of genetically engineered cells within matrices. This is despite the fact that the technology could improve the survival and biodistribution of genetically engineered cells to enhance their therapeutic effect. Combinations of hydrogel systems with MP technologies could address these issues with the MP platform providing the ability to monitor the graft and a means of safe genetic engineering. Enhancing the complexity of implantable hydrogels by inclusion of multiple cell types and application of MP technology could facilitate the next steps in CNS therapy by promoting repair through biomolecule release (from the incorporated cells) and subsequently providing support and guidance for regenerating tissue.

1.13 Using cell lines in neuro-nanotechnology research

Many of the studies investigating the use of MPs for clinical application in NSCs rely on the use of cell lines. While these studies can provide useful proof of principle data in the field of nanotechnology, especially regarding the transplantation and monitoring of MP labelled cells non-invasively using MRI, there are questions surrounding the suitability of cell lines as accurate predictors of cellular uptake and toxicity of MPs in primary cells. Cell lines are designed to be passaged multiple times for ease of study however due to genetic drift and selective pressure (fastest growing cells dominate cultures) over time these cells start to lose key functions and traits of the cellular source they are supposed to represent.[38] Concerns over cell line provenance are

widespread with a number of studies potentially reporting erroneous data generated from contaminated or misidentified cell line stocks.[114] It is estimated that as many as 20% of cell lines in use are contaminated and 18% of human cell lines investigated displayed cross-contamination.[38] These findings suggest that data generated with respect to the application of nanotechnologies in cell lines might not accurately represent the behaviour of primary cells. An example of this was shown recently where PC-12 cells, a cell line widely used as a neuronal model, displayed six-times the amount of particle uptake when compared to primary neurons.[115]

Further, in terms of clinical application, cell lines are unlikely to be utilised due to high survival and proliferation rates and resistance to cell death signals increasing the risk of tumour formation post-transplantation. Primary cell sources for NSCs include cells from aborted foetuses, ESC derived NSCs and adult NSCs. These populations are generally heterogeneous containing different cellular subtypes, cells in different stages of the cell cycle and diverse differentiation states.[116] Cell lines on the other hand are often homogenous in composition as they have been expanded from a relatively small original cell source through multiple passages with the aforementioned selection pressures. Therefore, it is preferable to test novel nanomaterials *in vitro* using primary cells to more closely represent clinical application. In the context of nanomedicine, addressing the safety of nanomaterials for medical application is critical for the safety of the patient. Concerns surrounding cell lines also indicate that these models may not provide accurate data on toxicity of nanomaterials to NSCs. This is especially pertinent given the impact the field could have on global health which could be stalled with poor safety data.

1.14 Testing novel therapies whilst reducing reliance on live animal models

The gold standard for testing novel regenerative neurology strategies is to use animal models. These are no doubt crucial as pre-clinical models and are often the next steps following promising *in vitro* studies. However, animal models have several drawbacks for neural applications, including: cost, associated with animal husbandry and the requirement for specialist personnel to perform the experiments; significant experimental variability, meaning large numbers of animals are required to achieve statistically significant results; and ethical concerns, especially pertinent for CNS injury and disease which involve considerable suffering for the animal. Therefore, in accordance with the 3R's principle (to replace, reduce and refine animal usage)[117] novel techniques are required to test the next generation of regenerative strategies in an efficient, high throughput, cost effective and ultimately predictive manner.

In this context, the use of organotypic slice cultures could be one viable option to precede animal studies. Organotypic slice culture involves taking slices of target tissue and culturing at an air-medium interface and has been demonstrated for neural tissue for many years.[118,119] These slices can be cultured for several weeks[118] allowing long-term analysis of experimental manipulations. In terms of their predictive utility, they mimic the cellular composition and cytoarchitecture of the tissue they have been derived from and have been shown to follow regenerative events similar to those seen *in vivo*. For example, a slice model of SCI exhibited limited axonal outgrowth, astrocyte scarring and microglial infiltration into the lesion site[120] – all hallmark traits of SCI *in vivo*. As several slices can be derived from one animal (control and test slices can be derived from the same animal) the number of animals for an experiment is reduced but also there is limited suffering endured by the animal.

Slices are easier to monitor post manipulation compared with *in vivo* models, facilitating detailed single cell observation and time-lapse studies for the therapeutic time-course. The utility of

organotypic slice cultures for testing nanotechnologies has been demonstrated in several areas including investigating the regenerative capacity of aligned nanofibres to promote directed axonal outgrowth in a slice model of SCI,[120] studying the feasibility of magnetic stem cell targeting using MP loaded NSCs,[80] MRI tracking of MP labelled NSCs in spinal cord slices[121] and also examining the survival and differentiation of neural cells post-transplantation after they have been genetically manipulated using MPs and magnetofection protocols.[30,62,63] However, despite the advantages of this system as a useful indicator of the regenerative potential of nanotechnological strategies it is often overlooked as a research tool.

1.15 Aims of experimental chapters

This thesis aims to investigate the potential of using a range of tissue engineering approaches in order to address the barriers to translation of genetically manipulated NSCs outlined in **Section 1.6**. Given the advantages of MPs for safe and efficient gene delivery and facilitation of non-invasive cell targeting and tracking this is an especially exciting platform for investigation for use with NSCs. Several gaps in the literature have been identified with respect to utilising the MP platform in conjunction with NSCs. Firstly, the application of oscillating magnetofection protocols has been shown to greatly enhance MP mediated gene delivery in other neural cells, however, establishing the optimal transfection protocol by detailed investigation of oscillating field magnetofection has not been attempted in NSCs. Further, a comparison of the efficiency of magnetofection protocols between NSCs grown as monolayers and neurospheres has never been performed. Secondly, although successful non-invasive imaging of labelled NSCs has been demonstrated, there is a lack of translatable strategies to achieve high MP labelling in NSCs. As most studies in this area use Feridex, there also appears to be a substantial lack of neurocompatible particles which can facilitate non-invasive cell tracking and magnetic cell

localisation. Lastly, cell delivery strategies using hydrogels have been developed, however, an extra level of complexity can be added to these cell-hydrogel composites by developing protocols to potentially facilitate multiple cell delivery and genetic manipulation of intraconstruct cells. In this regard, developing protocols to culture and differentiate NSCs incorporated in hydrogels and combining this with MP mediated genetically manipulation using MPs offers an enticing strategy to achieve this. Given the potential for these nanotechnologies to address the described barriers to translation and the gaps in the literature present in this area the broad and specific aims of the experimental chapters are as follows:

Chapter 2: Safe and efficient gene delivery to NSCs grown as monolayers and neurospheres using magnetofection protocols

The broad aim of this chapter is to address '*barrier 1 – safe and efficient gene delivery to NSCs*'. This will be achieved by investigating the feasibility of delivering genes into the NSC population using MPs and whether this can be improved by application of oscillating fields. Of significant novelty in terms of genetically engineering a transplant cell population a comparison will also be performed to examine differences in magnetofection outcomes between NSCs cultured in two systems: monolayers and neurospheres. The safety of the developed protocols will be investigated using standard techniques for both systems. Owing to the transfection efficiency obtained in monolayers this culture format will be taken forward to assess the feasibility of revealing subtle changes in cellular biology after magnetofection by mass spectrometry and bioinformatics analysis. Further, magnetofected monolayer NSCs will be transplanted onto cerebellar slices as an additional safety assessment to investigate their survival and differentiation in host tissue. An examination of the utility of using the cerebellar slice as a model to test functional capacity of the cells after magnetofection will also be made.

Chapter 3: Developing high iron content particles for the efficient labelling of NSC transplant populations

The broad aim of this chapter is to address '*barrier 2 – safe and efficient delivery of transplant cell populations'* and '*barrier 3 – cell tracking (both non-invasive and post-mortem)*'. In an attempt to address the lack of neurocompatible particles in the literature, Dr Boris Polyak has kindly synthesised PLA based MPs and the tests in NSCs of these are described in this chapter. These particles vary in iron content and, as will be expanded in the introduction for this chapter, enhancing iron content within MPs in conjunction with magnetic field application may increase their uptake in NSCs. Therefore, the aim is to investigate the effects on MP uptake in NSCs of systematically modulating iron content of polymeric MPs in conjunction with the applied static and oscillating fields used in Chapter 2. The safety and compatibility with NSCs of these procedures will also be investigated by utilising standard histological methods and transplantation of the labelled NSCs into a slice model of SCI. Further, a preliminary assessment of the functional capacity of the particles and labelling protocols will be examined by investigating magnetic capture of MP labelled cells in an *in vitro* flow system.

Chapter 4: Magnetofection of intraconstruct neural cells

The broad aim of this chapter is to also address '*barrier 2 – safe and efficient delivery of transplant cell populations'* with added complexity in terms of generating a multicellular construct for transplantation. In this regard, this chapter aims to take steps towards addressing '*barrier 4 – successful functional integration*' as transplanting cells as part of a hydrogel formulation can enhance their survival in the lesion area and potentially provide guidance for directed restoration of axonal circuitry. As this is the first time that NSCs have been cultured in the hydrogel format in

our laboratory, the first aim of this chapter is to establish successful NSC culture using collagen hydrogels. Subsequently, protocols to genetically engineer the intraconstruct NSCs will be investigated using MPs in conjunction with magnetic fields. Safety of the culture procedures and the protocols developed to engineer the NSCs will also be examined.

Chapter 2: Safe and efficient gene delivery to NSCs grown as monolayers and neurospheres using magnetofection protocols

2.1 Introduction

In the General Introduction the multifactorial nature of CNS disorders was discussed along with the general opinion that, to address these multiple challenges, combinatorial therapy (for example replacement of lost or damaged cells and concomitant therapeutic biomolecule delivery) is necessary to achieve successful repair (**Sections 1.2 and 1.5**). Genetically engineering transplant cell populations so that they produce and release therapeutic biomolecules into transplant sites may be one strategy to achieve this.[32] NSCs are an especially attractive target for such genetic manipulation as they integrate into endogenous tissue and display considerable migratory behaviour post-transplantation into the CNS, potentially allowing biomolecule delivery to a wide variety of pathologies (including lesions of different sizes and shapes and diseases with multiple lesion sites).[28,29,32] Further, they differentiate into the three major cell types of the CNS, generating cells useful for repair e.g. oligodendrocytes for supporting and protecting axons.[28] Although the potential clinical utility of this approach has been shown in several animal studies, researchers have overwhelmingly relied on viral vectors to introduce genetic material into the NSC transplant population[36,42,44] and, as discussed in **Section 1.6**, this strategy cannot yet be translated into the clinic, primarily for safety reasons.[50] Therefore, there has been a major drive to find non-viral alternatives; however, the most widely used techniques for non-viral gene delivery to NSCs also have significant drawbacks for their potential use in the clinic including low transfection efficiency and low post-transfection cell viability.[52,53] A promising alternative in this regard is to use MPs – a novel class of transfection agent with multiple clinical applications (expanded in the General Introduction, **Section 1.8**) – to bind and condense DNA for cellular delivery. There are many instances of neural cell transfection achieved using MPs *in vitro*.[86] This technique is increasingly being adopted due to its simplicity, well-established and good safety profile and the potential for gene delivery to '*hard to transfect*' cell types, such as mature neurons and primary cells.[86,122] All these features are also applicable to a potential clinical grade

transfection protocol, although as far as I am aware, no study has utilised magnetofection as a procedure to introduce genetic material into a transplant cell population for therapeutic application (in humans or animal models).

Our laboratory has shown that transfection of several neural transplant cell populations is achievable using MPs.[30,62,63] In both astrocytes[62] and OPCs[63] transfection efficiency could be enhanced to a similar order to viral transfection by utilising oscillating magnetofection protocols (e.g. in the astrocyte population, transfection efficiencies using magnetofection were 54% compared to wide-ranging viral transfection efficiencies of 14-100%). The developed protocols did not demonstrate adverse effects on cell viability or morphology, and did not diminish key regenerative properties of the cells such as proliferation or stemness (*in vitro*). Further, magnetofection did not adversely impact transplant cell survival or differentiation post-transplantation onto an organotypic slice model acting as host tissue. The data from these studies suggest magnetofection is a technique with significant translational potential. Therefore, this chapter aims to investigate the use of oscillating magnetic fields to enhance MP-mediated transfection efficiency of NSCs when grown in two distinct culture systems, both commonly used worldwide to propagate NSCs – neurospheres and monolayers (described in the General Introduction, **Section 1.4**).

Magnetofection using a *static* magnetic field has been attempted with NSCs expanded as both neurospheres[30] and monolayers.[123] In neurospheres, no benefit was derived from applying a static field during transfection procedures; although a repeat transfection step (the following day) was utilised to achieve a final transfection efficiency of 22%.[30] In monolayers, a transfection efficiency of 15% was achieved under static field magnetofection,[123] however, no comparison was made to the absence of a magnetic field during transfection, necessitating further study to determine whether magnetofection provides enhanced transfection efficiency in NSCs grown as monolayers.

In both studies, the novel step of performing transfection in the presence of an *oscillating* magnetic field was not tested, yet reports from other cell types suggest that this could confer a substantial increase in transfection efficiency.[62,63] Further, in previous studies, protocols to obtain enhanced transfection differed between cell types. The most effective transfection levels in astrocytes[62] and OPCs[63] were achieved in fields oscillating at 1 Hz and 4 Hz respectively, suggesting the most effective magnetofection frequency needs to be established for each unique cell type. Additionally, significant differences have been observed in particle handling and uptake between various neural cell types in both monocultures and co-cultures.[124] These observations mean it is imperative that novel particles and magnetofection protocols are investigated and optimised for each neural transplant cell population.

2.1.1 Why does magnetofection need to be studied in NSCs cultured as neurospheres and monolayers?

NSCs are routinely cultured in neuroscience laboratories worldwide using two culture systems: as 3-D cell aggregates in suspension, termed neurospheres, and as 2-D adherent cells termed monolayers. Both culture systems are also used when expanding NSCs (including human NSCs) for pre-clinical and clinical cell transplantation[25,125–128] and have associated advantages and disadvantages for this purpose (**Table 2.1**).

Clinical consideration	*Neurospheres*	*Monolayers*
Neurogenic potential	✓	✓✓✓
Survival after transplantation	✓✓✓ *enhanced by maintenance of cell-cell contacts*	✓✓
Scalable expansion	✓✓✓ *via suspension bioreactor*	✓
Automation of culture	✓✓	✓✓✓
Online monitoring of cell characteristics	✓	✓✓ *allows observation of individual cells*

Table 2.1. Clinical advantages of expanding NSCs as neurospheres vs monolayers

For example, NSCs maintained as monolayers are thought to develop as a relatively homogenous population of cells which largely retain their ability to generate neurons.[116] In contrast, neurospheres are a relatively mixed population of cells, with some differentiation occurring within the sphere, and reports showing reduced ability of NSCs to generate neurons post-transplantation, following prolonged expansion as spheres.[125] This may impact the choice of culture system when expanding NSCs to be transplanted in order to replace lost or damaged neurons, particularly in diseases such as Parkinson's or Alzheimer's, where efficient generation of neurons from the NSC grafts would be highly desirable. However, transplantation of NSCs as neurospheres is thought to result in higher levels of cell survival post-transplantation when compared with dissociated cells, although direct comparisons are rare in the literature.[129] The reasons for these post-transplantation differences could be two-fold. Firstly, transplanting NSCs as neurospheres avoids cell death and toxicity associated with enzymatic and mechanical dissociation into single cells. Secondly, neurospheres have complex ECM and physical cell-cell interactions which are thought to promote NSC survival and, at least *in vitro*, enhance the response of the NSCs to growth factors (namely EGF and FGF-2) which stimulate proliferation and cell survival.[130]

One major issue in the cell therapy field is the production of large numbers of cells to satisfy the requirements of treating multiple patients (for example 8-12 foetuses are required per patient for a cell graft to treat Parkinson's).[15] Growing NSCs as neurospheres has the advantage of propagation in suspension which allows more cells to be produced using a smaller surface area than 2-D culture. The scalability of suspension culture makes this possible with estimates suggesting that, using bioreactors with similar footprints, cells propagated in suspension can generate 100-fold more cells when compared to adherent culture.[131]

In terms of generating the large cell numbers required for the global regenerative medicine market it is widely accepted that automation of culturing procedures will be essential for manufacturing cell therapies.[132] In this regard, both suspension and adherent automated cell culture systems are available, although adherent cultures provide a more technically simple platform, as routine media changes are much simpler (without the need to collect cells in suspension). In addition, novel imaging systems coupled with state of the art image analysis software can provide online information on adherent cell proliferation and differentiation.[133] These systems rely on the propagation of cells in 2-D so as to distinguish individual cells and also to determine cellular morphology, which would not be feasible in 3-D cell aggregates. This will be important for quality control purposes, including demonstrating cellular identity and health to regulators.

The differences described here between monolayers and neurospheres, in terms of constituent cell-types and cytoarchitecture, offer distinct advantages and disadvantages to their clinical use but could also lead to significant differences between the two culture systems in terms of particle handling and response to magnetofection protocols. Given the potential for both culture systems to be used for clinical cell transplantation, it is crucial to investigate protocols designed to manipulate NSCs in both monolayer and neurosphere cultures.

2.1.2 The need for rigorous, high throughput safety testing of nanotechnology protocols to genetically engineer NSCs

Nanomaterials for translational applications are made from a variety of materials and have wide-ranging physicochemical properties including size, shape and surface charge. How each of these parameters relates to nanomaterial cellular toxicity is poorly understood, with further levels of complexity arising from synergistic effects between the parameters, meaning the toxicity of novel nanomaterials is difficult to predict.[134] As the field rapidly expands, protocols for quick and accurate assessment of the effects of novel materials on cell health will need to be developed to facilitate testing of large numbers of different materials.

Currently, cellular toxicity of nanoparticles is assessed *in vitro* with numerous tests, for example, the MTT (Methylthiazolyldiphenyl-tetrazolium bromide) assay, LIVE/DEAD staining, viability testing and cell marker expression (**Table 2.2**). Although these tests are useful for determining the overall acute toxicity of a nanomaterial, it has been reported that MTT assays and other fluorimetric readouts can experience interference from adsorption of the dye to the nanomaterial, resulting in inaccurate absorbance readings.[135] In addition, these tests may mask more subtle molecular changes within the cells which could lead to aberrant cell behaviour – of particular concern to manipulated cell transplant populations. For example, some studies utilise assays to measure reactive oxygen species (ROS) generation which is thought to be one of the main mechanisms behind nanomaterial toxicity.[136] ROS generation has been observed in one study without obvious effects on cell health as measured by the MTT assay[101] indicating that underlying molecular changes in cells exposed to nanomaterials may be missed by commonly used safety assays.

A further point to note is that not all cellular effects of nanomaterials result in membrane rupture or mitochondrial malfunction (for example effects on cell migration or proliferation) and may

have other underlying molecular features not exposed by routine toxicity tests. In addition, knowledge of the mechanism of toxicity is becoming increasingly important in the nanotoxicology field to provide a systematic evaluation of specific biological effects of particular materials and formulations at the nanoscale. Such detailed information on molecular changes would require more thorough examination of cellular biology which could be provided by either genomic or proteomic approaches. There are many examples of the wealth of data which can be generated from both genomic and proteomic analyses of cells labelled with nanoparticles,[137–139] however, most studies of this nature have been performed using non-neural cells – commonly macrophage cell lines as these are the cell types expected to encounter nanoparticles after human exposure. One study has used global gene expression profiling to identify differentially expressed genes in NSCs after labelling with a clinically approved MP, Feridex – proposed as a possible cell tracking agent for non-invasive imaging by MRI.[140] The authors found that the overwhelming majority of genes were expressed at similar levels in labelled and control cells and these included genes involved in programmed cell death, regulation of cell metabolism and neural differentiation, suggesting the labelling procedures are largely safe. Changes in gene expression were noted at early time-points (1-2 days post-labelling) for proteins involved in iron metabolism (an observation also reported by others in mesenchymal stem cells[141] and not shown to affect cell viability) and later time-points (4-7 days) for proteins involved in controlling cell stress (such as ceruloplasmin, a protein responsible for converting Fe^{2+} to the less oxidative form, Fe^{3+}). The findings highlight the power of this technique for examining specific molecular pathways but also reveal some potential stress responses in MP-treated cells. Although a useful study in terms of a detailed investigation into the effect on cell biology of labelling with MPs, the results were generated using an NSC cell line and no protein expression analysis was performed. Cell lines might not be representative of primary cells in terms of their response to nanoparticles (**Section 1.13**) and it is known that increases in gene expression may not correlate to increases in protein

expression,[142] therefore detailed analysis of protein expression in NSCs after labelling with MPs is desirable. In addition, with the benefits of magnetofection protocols to enhance labelling of neural cell populations becoming apparent, detailed proteomic analysis is required to test the safety of these procedures prior to clinical translation. The feasibility of this approach for examining molecular changes in primary NSCs after manipulation with MPs in conjunction with magnetic fields has never been demonstrated.

	Test	Description
Cell viability	Morphological assessment	*Microscopic evaluation of nanomaterial effect on normal cell morphology and adherence.*
	MTT, MTS and WST-1 assay	*Tetrazolium based solution added to cells. Active mitochondria break down tetrazolium leading to an absorbance change proportional to mitochondrial activity.*
	LIVE/DEAD assay	*Consists of calcein AM which can diffuse across intact cell membranes but will only fluoresce in live cells and ethidium homodimer-1 which can only cross disrupted membranes.*
	Trypan blue exclusion	*Trypan blue only crosses damaged membranes therefore only labels compromised cells.*
Molecular changes	Cell marker expression	*Evaluation of characteristic cell marker expression*
	ROS production	*The level of GSH is determined colorimetrically which is proportional to the levels of ROS.*
	Genomics or proteomics	*Either assesses mRNA transcription or protein expression to determine pathways which have been up or down regulated in response to nanomaterials*.
Functional assays	Stem cell differentiation	*Following cell differentiation after cell labelling/manipulation with nanomaterials.*
	Organotypic slices	*Effects of nanomaterials on cellular survival, integration and some function can be determined by transplanting into host tissue and monitoring microscopically, live and post-fixation.*
	Animal models	*Large numbers of live animals are required for statistically relevant data, and large quantities of tissue will need to be processed. This process is expensive and low-throughput.*

Table 2.2. Safety and functional assays for nanotechnology platforms. *MTT - Methylthiazolyldiphenyl-tetrazolium bromide; MTS – 3-(4,5-Dimethylthiazol-2-yl)-5- (3-carboxymethoxyphenyl)-2-(4-sulfophenyl) 2H-tetrazolium; WST-1 – Water soluble tetrazolium salts; ROS – Reactive oxygen species; GSH – Glutathionine.*

The next step in nanomaterial testing is to evaluate safety and function *in vivo* and is often performed in animal models. Although testing novel nanomaterials in animals is vital to precede their use in humans, these are low-throughput and costly experiments with associated ethical concerns as described in the General Introduction (**Section 1.14**). Therefore, there is a requirement for rapid screening techniques to reliably predict *in vivo* function without heavy reliance on animal experimentation. Our laboratory has been developing and characterising organotypic slice models for use as host tissue for transplantation studies and potentially to assess the functionality of novel nanotechnologies. Specifically, we have recently developed and characterised cerebellar slice models which might be useful to test the transplantation of magnetofected NSCs. We have shown that cerebellar slices after 8-10 days *in vitro* display retention of cytoarchitecture, with defined white matter tracts apparent, and astrocytes, OPCs and Purkinje cells all present in the slices.[143] Therefore these slices provide a good representation of the cerebellum *in vivo*; however, their utility for testing genetically engineered NSCs has not been investigated.

2.1.3 Objectives

Given the lack of knowledge of how NSCs will respond to oscillating magnetic field magnetofection protocols especially grown in the two widely different culture systems the objectives of this chapter are:

(i) To determine optimal magnetofection protocols in NSCs grown as monolayers and neurospheres and compare transfection efficiencies in each culture system.

(ii) To assess the safety of magnetofection procedures using standard microscopic analyses in both monolayers and neurospheres.

(iii) To perform several routinely used safety assays and examine the feasibility of using a mass spectrometry approach to assess molecular changes in monolayer NSCs after magnetofection.

(iv) To investigate the utility of using the cerebellar slice model to assess post-transplantation survival and differentiation of NSCs magnetofected as monolayers.

2.2 Methods

Although the methods described in the individual chapters have similarities, they are sufficiently different that a separate methods section has been provided within each chapter for clarity. However, an expanded methods section appears in this chapter which will be referred to when necessary in the subsequent chapters. Some of the methods have been adapted from publications in which the work features and these have been indicated as footnotes in the text.

2.2.1 Reagents

Cell and slice culture: Cell culture reagents were from Invitrogen (Paisley, Scotland, UK) and Sigma (Poole, Dorset, UK). Basic fibroblast growth factor (FGF-2) was from Peprotech (Rocky Hill, NJ, USA) and epidermal growth factor (EGF) was from R&D systems Ltd (Abingdon, UK). Penicillin and streptomycin were from Fisher (Loughborough, UK). Accutase was from Sigma and DNase I was from Roche (Welwyn, UK). Nunc T25 cell culture flasks, Nunc 24 well plates, 24 well suspension culture plates and other cell culture grade plastics were purchased from Fisher Scientific, UK. Millicell culture inserts, Omnipore membrane and the Immobilon-P membrane were from Millipore (Watford, UK).

Viability analysis: 3-(4,5-Dimethylthiazol-2-yl)-5- (3-carboxymethoxyphenyl)-2-(4-sulfophenyl)-2H-tetrazolium, inner salt (MTS) assay reagent (CellTiter 96 AQueous One Solution Reagent) was from Promega UK (Southampton, UK). The LIVE/DEAD Viability/Cytotoxicity Assay Kit was from Invitrogen (Paisley, UK).

Antibodies: Primary antibodies were rabbit anti-β-tubulin (Tuj-1) from Covance (Princeton, NJ), rat anti-myelin basic protein (MBP) from Serotec (Kidlington, UK), rabbit anti-glial fibrillary acidic protein (GFAP) from DakoCytomation (Ely, UK), mouse anti-nestin from BD Biosciences (Oxford, UK) and rabbit anti-SOX-2 from Millipore (Watford, UK). A summary of antibody targets is given in **Table 2.3**. Cy-3 and Fluorescein isothiocyanate (FITC) conjugated secondary antibodies were from Jackson Immunoresearch Laboratories Ltd (Westgrove, PA, USA). Vectashield mounting medium with 4,6-diamidino-2-phenylindole (DAPI) was from Vector Laboratories (Peterborough, UK).

Antigen	Description
Nestin	**NSC** cytoskeletal protein
SOX-2	Transcription factor expressed in **NSCs**
GFAP	Cytoskeletal protein in **astrocytes**
Tuj-1	Major constituent of microtubules in **neurons**
MBP	Main component of myelin produced by **oligodendrocytes**

Table 2.3. Targets for the antibodies routinely used for immunocytochemistry

Animals: The care and use of all animals used for cell culture were in accordance with the Animals (Scientific Procedures) Act of 1986 (UK) with approval by the local ethics committee.

Plasmids: Plasmid maps are shown in **Figure 2.1**. The pmaxGFP plasmid (size 3.5 kb; encodes green fluorescent protein [GFP]) was from Amaxa Biosciences (Cologne, Germany) chosen for brightness to ensure transfection efficiency levels could be accurately determined. Clontech (Saint-Germain-en-Laye, France) supplied the pCMV-DsRed-Express2 plasmid (herein termed pDRE2; size 4.6 kb; encodes red fluorescent protein [RFP]) used for transfection of NSCs before transplantation into cerebellar slices – pDRE2 has low phototoxicity so is suited for *in vivo* tracking applications but is a different size to pmaxGFP so results in slightly lower transfection efficiencies.[143]

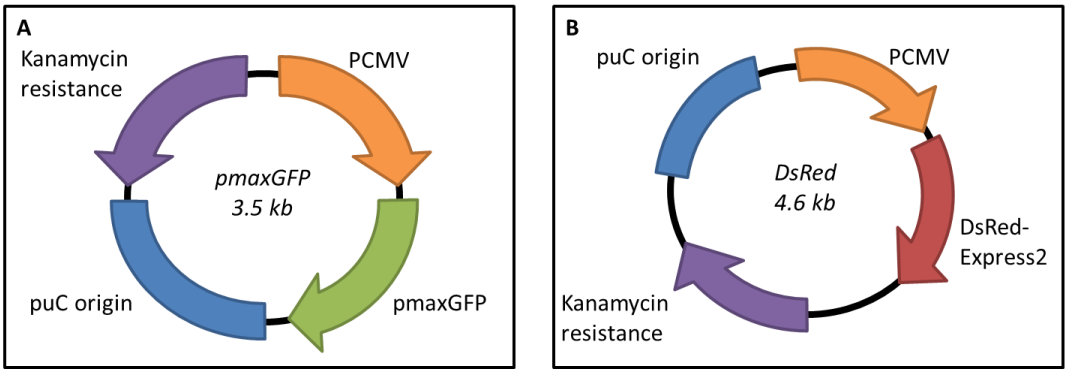

Figure 2.1. Schematics of plasmids used in experiments. *Plasmid maps of (A) pmaxGFP and (B) pDRE2. CMV – cytomegalovirus promoter for constitutive expression in most mammalian cells.*

2.2.2 Primary NSC derivation and maintenance

Primary NSCs were used for all experimental studies performed. These were derived by mechanically dissociating the subventricular zone of CD1 mice using previously established procedures[30] and seeding cells in a 5 mL suspension at 1 x 10^5 cells/mL in T25 flasks. By using appropriate seeding densities and growth factor stimulation, selective propagation of NSCs from

an initial mixed population of cells can be achieved. NSCs were maintained in suspension at 37°C/5% CO_2 in complete medium (referred to herein as NS-M, **Table 2.4**) and as the NSCs proliferate they remain attached to each other to form so called 'neurospheres' – a well-established culture system for NSCs (**Figure 2.2**). For routine maintenance, neurospheres were fed every 2-3 days and passaged weekly by dissociation using a 0.1X solution of DNase I in Accutase and re-seeded at 0.2-1 x 10^5 cells/mL in T25 flasks. For experiments, dissociated cells were plated/seeded as required. Cells from passages one to three were used for experiments.

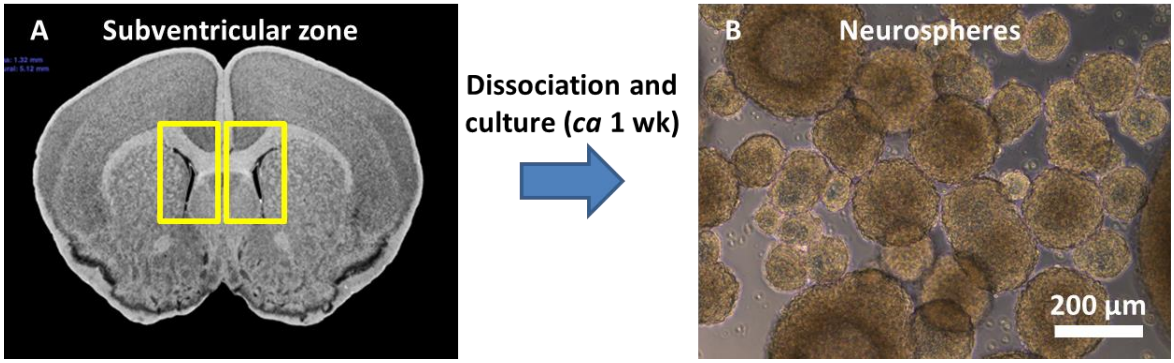

Figure 2.2. NSC derivation from the SVZ and propagation as neurospheres. *(A) Diagram depicting the localisation of the SVZ from which all NSCs described in this thesis were derived. (B) After 1 week in defined culture conditions, dissociated cells from the SVZ form neurospheres.*

2.2.3 Coverslip washing and coating

It has been observed in our laboratory that NSCs more reliably adhere to nitric acid washed coverslips than non-washed glass. Therefore coverslips for all adherent NSC culture were washed in 1% nitric acid overnight. The nitric acid was removed by six washes in deionised H_2O (dH_2O) and sonication in 70% ethanol. The washed coverslips were stored in 70% ethanol. To coat coverslips

(or any culture surface) for adherent NSC culture, sequential incubation with poly-ornithine (MW 30-70 000 Da, 0.002%, 1 h, 37^{o}C) and laminin (5 µg/mL, 1 h, 37^{o}C) was performed followed by three sterile water washes. Coated coverslips were used immediately.

2.2.4 Neurosphere and monolayer culture for transfection experiments

To investigate and compare magnetofection protocols in NSCs grown as monolayers and neurospheres, single cell suspensions of NSCs were generated from NSC maintenance cultures as above (**Section 2.2.2**). To generate experimental neurosphere cultures, these were resuspended in NS-M at 1 x 10^5 cells/mL and 500 µL was added to each well of a suspension 24 well plate. To generate monolayer cultures, single cells were resuspended in monolayer medium (herein referred to as ML-M, **Table 2.4**) at 3 x 10^5 cells/mL then 400 µL was added to wells containing coated coverslips in 24 well plates. Cells were cultured for 24 hours (37^{o}C/5% CO_2) before particle addition.

Media	***Composition***
Complete medium (NS-M)	*DMEM:F12 (3:1), 2% B27 supplement, 50 U/mL penicillin, 50 µg/mL streptomycin, 4 ng/mL heparin, 20 ng/mL of EGF and FGF-2*
Monolayer medium (ML-M)	*DMEM:F12, in a 1:1 mix, 1% N2 supplement, 50 U/mL penicillin, 50 µg/mL streptomycin, 4 ng/mL heparin, 20 ng/mL FGF-2 and EGF*
Differentiation medium	*Complete medium minus growth factors, supplemented with 1% FBS*
Slicing medium	*Earle's balanced salt solution (EBSS) buffered with 25mM HEPES*
Slice culture medium (cerebellum slices)	*50% minimum essential medium, 25% EBSS and 25% horse serum; supplemented with 1mM glutaMAX-I, 36mMD-glucose, 50 U/mL penicillin and 50 mg/mL streptomycin*
Slice culture medium (spinal cord slices)	*As for cerebellum slice culture medium but with addition of 250 ng/mL amphotericin B*

Table 2.4. Composition of media used in experiments throughout thesis

2.2.5 Magnetic array details

The desired magnetic fields were applied using the magnefect-nano oscillating magnetic array system, with a 24-magnet array (NdFeB, grade N42; field strength of 421 ± 20 mT)[63] supplied by nanoTherics Ltd (Stoke-On-Trent, UK). The array is adapted to fit a 24 well culture plate and either remains static (also referred to as F = 0), or can be programmed to move in the (horizontal) x-axis with oscillation frequency (F) and amplitude controlled via a computerised motor (**Figure 2.3**). Amplitude in all experiments was set to 0.2 mm as this has been previously observed to be more effective than other amplitudes for transfection in various neural cell types.[144]

Figure 2.3. Image depicting the magnefect-nano system and important features.

2.2.6 MP mediated transfection

To assess the efficiency of transfection protocols, a reporter plasmid was used: pmaxGFP (**Figure 2.1**). All transfections were carried out with a commercial transfection-grade magnetic particle: Neuromag. These particles are designed to transfect primary neurons but have been shown to transfect a range of neural cells in our lab including astrocytes,[62] OPCs,[63] oligodendrocytes[143] and NSCs.[30] They have an average diameter of 160 nm (range: 140-200 nm),[123] ca. 0.5% iron content and a positive surface charge (actual value undisclosed by manufacturer). It has been previously established that the optimal Neuromag:DNA binding is 3.5 µL/µg[62] which was used for all experiments. Field application was restricted to 30 min as heating effects were observed in pilot experiments using oscillating fields for longer time periods, and static fields applied for 24 h resulted in significant particle aggregation (especially using MP-5X particle formulation, **Chapter 4**).

2.2.7 Monolayer transfection

At 24 h post-plating, medium was replaced with fresh ML-M (0.225 mL) before addition of transfection complexes. To prepare complexes, 176 ng pmaxGFP plasmid was diluted with 75 µL base medium (DMEM:F12 mixed in 1:1 ratio) and added to 0.62 µL Neuromag before mixing by trituration and subsequent incubation for 20 min (RT). The complexes were added drop-wise to cells whilst gently swirling the plate to ensure even particle distribution. Controls were treated with an identical concentration of plasmid without particles in base medium. Plates were returned to the incubator, and exposed to the desired magnetic field for 30 min. Magnetic field conditions were: no-field, F = 0 Hz and a range of oscillating fields from F = 0.5 Hz to F = 4 Hz. Monolayer transfection efficiency and NSC marker expression were assessed using fixed cells at 48 h post-transfection. Some cultures were enzymatically detached for estimation of cell number

and viability (**Section 2.2.20**), then re-plated in 8 well chamber slides (4.8 x 10^4 cells per well; differentiation medium) for assessment of differentiation potential, or lysed for protein extraction in order to assess the effect of magnetofection on protein expression of the samples (**Section 2.2.15**).

2.2.8 Neurosphere transfection

After NSCs had been allowed to form neurospheres for 24 hours, 0.44 µL Neuromag and 125 ng pmaxGFP were mixed in 50 µL base medium (DMEM:F12 mixed in a 3:1 ratio). Plasmid-MP complexes were allowed to form for 20 minutes (RT) then added to the neurospheres while gently swirling the culture plate. It is worth noting that movement was kept to a minimum as this appeared to cause sphere aggregation which could result in reduced transfection due to fewer cells being exposed to transfecting complexes. Controls consisted of plasmid addition alone, without Neuromag. In pilot experiments, a trend for increased transfection was observed up to a frequency of 4 Hz. A frequency of 5 Hz displayed a reduction in transfection efficiency compared to 4 Hz so this was not studied further. The plates were returned to the incubator and exposed to the desired magnetic field for 30 min with post-transfection incubation for either 10 or 48 h. Four field conditions were tested: no-field, F = 0 Hz, F = 1 Hz and F = 4 Hz oscillating fields. At 10 or 48 h post-transfection, spheres were dissociated and estimates of transfection efficiency (**Section 2.2.19**), cell number (48 h time-points only) and viability were made (**Section 2.2.20**). From spheres dissociated at 48 h, cells were plated in 8 well chamber slides (4.8 x 10^4 cells per well) in either ML-M for 24 h (for assessments of NSC marker expression and pyknotic nuclei) or differentiation medium for 7 days (for assessing differentiation potential, **Section 2.2.9**).

2.2.9 NSC differentiation

In order to assess the influence of magnetofection protocols on the differentiation profile of NSCs, both neurosphere and monolayer cultures were dissociated 48 h post-transfection and resuspended in differentiation medium (**Table 2.4**) at 3 x 10^5 cells/mL. 160 µL of each solution was added to coated wells of an 8 well chamber slide then cultured for seven days (37^{o}C/5% CO_2), which produces a mixed cell population typically containing ca. 85% astrocytes, 10% neurons and 5% oligodendrocytes. Cultures were fed every 2-3 days with a 50% medium change.

2.2.10 Organotypic cerebellar slice derivation and culture

For an assessment of the transplantation potential of transfected NSCs, organotypic cerebellar slice cultures were used as an *in vitro* 'host tissue' system. The cerebellum was dissected from the brains of CD1 mice at postnatal day 10 and transferred to slicing medium (**Table 2.4**). Meninges were removed by rolling on paper tissue then 350 µm parasagittal slices were cut using a McIlwain tissue chopper and collected in ice cold slice medium. Slices were incubated on ice for 30 min before transfer to pieces of Omnipore membrane (which allows manipulation of individual slices) sitting on the membrane of Millicell culture inserts in six well plates. Slices were cultured at an air-medium interface with cerebellum slice culture medium (**Table 2.4**).

2.2.11 Transplantation of magnetofected NSCs onto slices

To examine the functional capacity of NSCs transfected as monolayers, these were transfected with pDRE2 which encodes RFP using the same protocol as used for pmaxGFP. RFP was used as the reporter plasmid as GFP has been observed to form rod-like crystals several days post-

transfection. Cell viability does not appear to be affected by rod formation (as judged by examining cellular and nuclear morphology); however, their presence confounds analysis of transfected cells. RFP was not observed to display this crystallisation so was chosen as the reporter plasmid for transplantation studies. After 24 h, half of all transfected cultures were detached and transferred to 24 well suspension plates (500 µL, 1 x10^5 cells/mL) for 24 h to produce neurospheres. This method was chosen due to the higher survival of NSCs transplanted as neurospheres *in vivo*.[129] 48 h post-transfection, monolayers were detached or neurospheres were collected and 0.5 µL was focally transplanted onto cerebellar slices at a concentration of 50 x 10^6 cells/mL. Success and localisation of transplantation was judged 30 min post-transplantation. Survival and differentiation of transplanted NSCs were judged in fixed slices 72 h post-transplantation as this time-point coincides with robust RFP expression (occurs across 24-120 h).[145] Where applicable, immunostaining was performed on fixed samples against the neural markers outlined in **Section 2.2.1**.

2.2.12 LIVE/DEAD staining

To assess slice and NSC (48 h post-transfection) viability, cells or slices were washed with PBS, incubated for 15 min with 4 µM calcein AM (produces green fluorescence in live cells) and 6 µM ethidium homodimer-1 (produces red fluorescence in dead cells), washed again with PBS, then mounted for fluorescence microscopy.

2.2.13 MTS assay

For an additional safety measure of magnetofection protocols on monolayer NSCs, an MTS assay was performed. Cells were plated and transfected by the described protocols in triplicate wells.

Blanks consisted of medium alone. MTS reagent was added to each well 48 h post-magnetofection and incubated for 3 hours at 37°C/5% CO_2. 200 µL medium was then taken from each well and added to a 96 well plate for absorbance measurements at 490 nm. Absorbance measurements were adjusted by subtracting blank readings from the test readings. The adjusted absorbance was then expressed as a percentage of the control readings.

2.2.14 Fixation

Cells and slices were washed once in PBS before fixation using 4% paraformaldehyde (PFA; 15 min, RT) for immunocytochemistry. Samples fixed in PFA were washed three times in PBS before further processing.

2.2.15 Preparation of peptides from magnetofected monolayer NSCs for mass spectrometry analysis

In parallel with the histological safety assessments, a proteomics based analysis was performed on one set of samples (n = 1). This was to assess the feasibility of using mass spectrometry for detailed examination as to whether there are any alterations in protein expression or specific signalling pathways when NSCs are exposed to MPs and magnetic fields. Four conditions were tested utilising the developed protocols for monolayer transfection: no-field without particles (control), plus no-field, F = 0 Hz and the 4 Hz oscillating field conditions (all with particles). Protein was extracted from cells at 48 h as this correlates with peak GFP expression as observed previously[30,63] and with the time-points used for the other safety analyses (cell number, cell viability and stem cell marker expression) to allow for a comparison between histological and molecular readouts.

Protein extraction from NSCs: Initial experiments, using either Triton-X or RIPA buffer to lyse the cells, failed to yield sufficient protein content from the collected cells. Therefore, a protocol was developed which used the following extraction buffer: 50 mM Tris (to buffer the solution), 150 mM NaCl, 200 µM Ethylenediaminetetraacetic acid (EDTA, prevents cell adherence), 10% glycerol, 0.5% NP40 (detergent/cell lysing agent), 0.2% protease inhibitors and 1% DNAse (prevents aggregates of DNA and cell fragments which hamper gel separation step). One million cells were lysed with extraction buffer (100 µL, 60 min, 4°C) with periodic vortexing to break cell membranes and aggregates in order to release proteins. The protein content of each sample was then normalised before gel electrophoresis using Bradford assay.

Polyacrylamide gel electrophoresis: To initially separate the proteins within the sample polyacrylamide gel electrophoresis was performed. Here, 100 µg of protein from each experimental sample were denatured using 5x Laemmli buffer [0.3 M Tris, 50% glycerol, 10% (w/v) sodium dodecyl sulphate (SDS), 8% (w/v) dithiothreitol (DTT), 0.1% bromophenol blue; 5 min, 95°C]. The denatured samples were added to pre-cast gels and run using approx. 200 V, whilst maintaining current between 35 and 50 mA. Upon run completion, gels were stained with InstantBlue (Expedion, Cambridge, UK), then destained in high performance liquid chromatography (HPLC)-grade water and imaged using a FluorChem™ M (ProteinSimple, San Jose, California). This image was used to annotate and dissect the gel into suitable pieces for digestion – assessed semi-quantitatively by observing the protein staining density in different regions of the gel.

In-gel protein digestion and extraction: In order to identify proteins from gel pieces by tandem mass spectrometry, proteins typically need to be digested into peptides, which are then extracted from the gel. This is achieved following removal of Coomasie (from the InstantBlue staining) from stained gel bands (25 mM ammonium bicarbonate, 50 % acetonitrile), then preparing the proteins

for trypsin digest by reduction (10 mM DTT, 45 min, 56°C) and alkylation (55 mM Iodoacetamide, RT, 1 h in the dark). In gel trypsin digestion was performed with 200 ng of trypsin per excised gel piece (25 mM ammonium bicarbonate 37 °C, 16 h). Residual trypsin activity was stopped and peptides extracted using extraction buffer (50% acetonitrile, 0.1% trifluoroacetic acid). Extracts were dried and dissolved in HPLC-grade water with 0.1% formic acid. Depending on analytical technique, these could be desalted using Zip-Tip® (Millipore) pipette tips according to the manufacturer's instructions.

2.2.16 LC-MS/MS peptide identification

Peptides were identified using a Liquid chromatography tandem mass spectrometry (LC-MS/MS), which sequentially eluted samples through a 5-95% acetonitrile gradient using a Quadrupole time-of-flight mass spectrometer premier (Waters Corporation, Manchester, UK). An initial MS survey mode identified abundant peptides with ≥ 2^+ charge. These are then selected for MS/MS to produce a product ion spectrum (averaged from multiple scans, depending upon product ion intensity). The gathered spectra (from individual peptides) are processed through Distiller 2.5.1.0 (Matrix Scientific, Colombia, SC) to enable Mascot 2.5.0 (Matrix Scientific) searching against a custom, GFP-*Mus musculus* concatenated database (GFP from *Pontellina plumata* and Uniprot mouse database, downloaded 01/02/2013). Search settings were as follow: mass tolerances 200 ppm (precursor), 0.6 Da (products), 1 missed tryptic cleavage per peptide, with fixed modification by Cys-CAM (carbamidomethylation of cysteine residues by iodoacetamide in the alkylation step) and variable methionine oxidation states. Identified peptides were then analysed by Scaffold Q+ 4.3.3 (Proteome Software, Toronto, ON) software, using 95% confidence interval and ≥ 2 peptides per protein filtering parameters, for output to Ingenuity Pathway Analysis (IPA, Qiagen, Limburg, Netherlands). IPA generates files for clustering analysis which was performed using R (Foundation

for Statistical Computing, Vienna, Austria). Relative protein abundances are then displayed within a heatmap.

2.2.17 Immunocytochemistry

Fixed cells and slices were immunostained to detect markers of neural cells. Samples were blocked (5% normal donkey serum in PBS supplemented with 0.3% Triton X 100; RT; 30 min), then incubated with primary antibody (4°C; overnight); antibody dilutions (in blocking buffer) were: 1:200 for nestin and MBP, 1:500 for GFAP and 1:1000 for SOX2 and β-tubulin. After washing, samples were incubated with blocking solution (RT; 30 min), then with Cy3- or FITC-labelled secondary antibody (1:200 in blocking solution; RT; 2 h). Samples were washed and mounted using Vectashield mounting medium with or without DAPI.

2.2.18 Imaging

Fluorescence and light microscopy: Fluorescence microscopy of monolayers and tissue slices was performed using an AxioScope A1 microscope equipped with an Axio Cam ICc1 digital camera and AxioVision software (release 4.7.1, Carl Zeiss MicroImaging GmbH, Goettingen, Germany). Phase-contrast and fluorescence microscopy of live cells was performed using a Leica DM IL LED inverted microscope equipped with a FC420C digital camera and Leica Applications Suite software version 3.4.0 (Leica Microsystems, Wetzlar, Germany). Images were merged using Adobe Photoshop CS3 (version 10.0.1) prior to quantification.

2.2.19 Assessment of transfection efficiency

Microscopic analysis was used to analyse transfection in monolayer NSCs. This approach was chosen as simultaneous assessment of GFP expression can be conducted in parallel with features of cell health, such as adherence and morphology. Although a useful and robust methodology for quantifying transfection efficiency or particle uptake and several parameters of cell health (e.g. apoptosis and cell cycle analysis), flow cytometry was not used here as the number of cells required for flow cytometric analysis were not routinely produced.

Maximum GFP expression occurs in NSCs at 48 h after MNP mediated transfection therefore this was chosen as the time-point at which GFP expression was analysed.[30] Transfection efficiency of fixed monolayer samples was determined from double merges of DAPI and GFP images; a minimum of 200 cells at X200 magnification were scored. Transfection efficiency in neurospheres was assessed after dissociation into single cells, adding a small sample to a haemocytometer and counting numbers of the live cells which expressed GFP (>150 cells scored at X200 magnification). In both cases, care was taken to assess the GFP exposure level using controls (no transfection) to rule out background fluorescence, with exposure levels kept constant for each individual experiment.

2.2.20 Assessment of cell number and viability

To examine procedural effects on NSCs grown as neurospheres and monolayers, they were dissociated and a small proportion of cells were mixed with trypan blue which stains non-viable cells. Using a haemocytometer, an estimate of cell number per well and cell viability were made for each condition.

Counts were also made of pyknotic nuclei (an indicator of cell death evidenced by nuclear shrinkage, fragmentation or DNA condensation) in cells dissociated from both culture systems and plated as monolayers for 24 h, to evaluate effects of the developed protocols on cell viability. Three fields were assessed, with at least 100 nuclei assessed for each condition.

Cellular viability as measured by the LIVE/DEAD assay was quantified by counting green (LIVE) and red (DEAD) cells and expressing the number of LIVE cells as a percentage of total cells (green + red) from a total of three images taken at X400 magnification.

2.2.21 NSC stemness and differentiation potential

Stem cell marker expression was assessed in monolayers from double merged images of DAPI and nestin/SOX2 stained cells; a minimum of 100 cells at X400 magnification were scored. The expression of neural cell markers after differentiation was also determined from double-merged images; a minimum of 200 cells at X400 magnification were scored.

2.2.22 Statistical analysis

All comparable groups were analysed by one-way ANOVA and Bonferroni's multiple comparison test (MCT) using Prism software (version 4.03; Graphpad, USA). Data are expressed as mean ± SEM with 'n' referring to the number of cultures, each derived from a separate mouse litter.

2.3 Results

2.3.1 Culture purity

Monolayer cultures displayed elongated and bipolar morphologies typical of NSCs and were of high purity as judged by immunostaining for the NSC markers nestin and SOX2 (96.0 ± 2.0% and 95.0 ± 2.0% positive respectively; **Figure 2.4A-C**). NSCs seeded in suspension formed small clusters of cells over 24 h consistent with normal formation of neurospheres (**Figure 2.4D**). When these spheres were dissociated they yielded high purity populations of NSCs with 94.5 ± 2.0% and 97.3 ± 0.7% cells positive for nestin and SOX2 respectively.

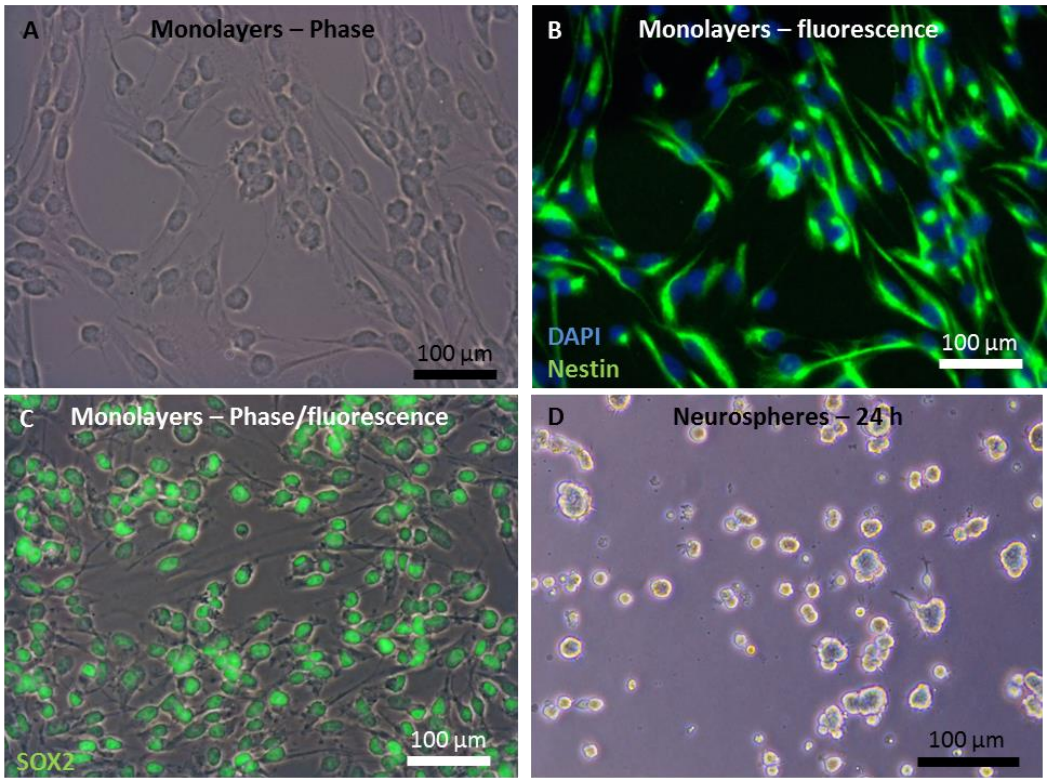

Figure 2.4. NSC culture characterisation. *(A) Phase contrast micrograph depicting typical bipolar morphology of NSCs with (B) fluorescence counterpart indicating high proportions of NSCs are nestin positive (94.5 ± 2.0%). (C) Merged phase and fluorescence micrographs of monolayer cultures showing bipolar NSCs positive for NSC specific marker SOX2, also present in a high*

proportion of cells (97.3± 0.7%). (D) Small clusters of cells forming in suspension after 24 h, indicative of neurosphere formation.

2.3.2 Influence of magnetic fields on transfection efficiency in monolayer and neurosphere cultures

Monolayers: GFP expression was observed in all transfection conditions (and was absent in plasmid only controls) in healthy, morphologically normal (adherent and bipolar) NSCs. Basal transfection efficiency (no magnetic field) was 9.4%, with efficiency approximately doubled when transfection was performed in the presence of a static magnetic field (18.4%). Several oscillating magnetic field conditions were tested, all of which resulted in enhanced transfection efficiency over basal levels. There was a frequency-dependent trend of increasing transfection efficiency up to a maximum of 32.2% when using an oscillating magnetic field of 4 Hz (**Figure 2.5A-B and 6A**). Notably, the most effective oscillating field condition significantly outperformed the static field condition.

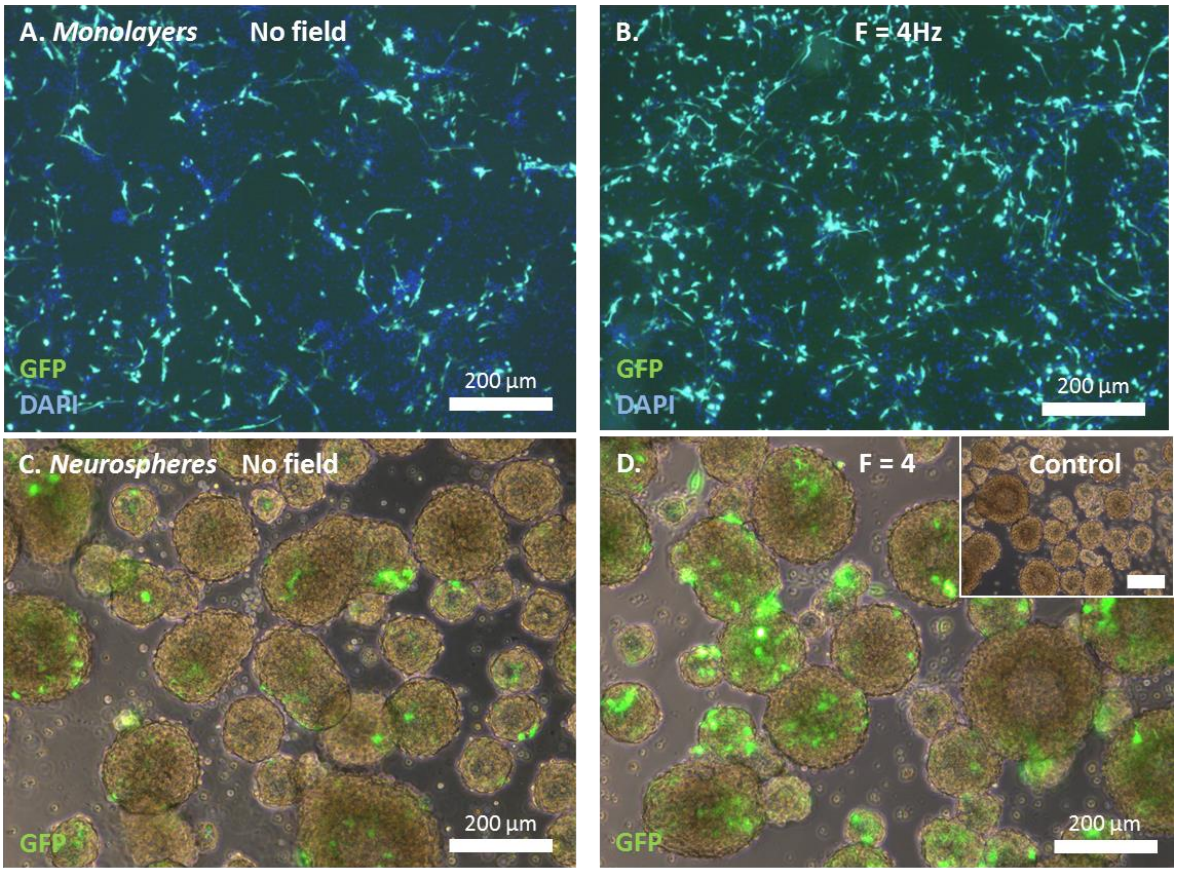

Figure 2.5. Magnetofection enhances transfection efficiency in NSCs cultured as monolayers and neurospheres. *Representative micrographs of monolayers 48 h post-transfection under (A) no-field and (B) F = 4 Hz conditions. Representative images of neurospheres 48 h after transfection performed under (C) no-field or (D) an oscillating field of 4 Hz. (D – inset) Control culture with plasmid addition only. Scale bar in the inset is also 200 µm. Note that in both culture systems GFP expression appears to be increased in the F = 4 Hz conditions. These effects have been quantified in* ***Figure 2.6****.*

Neurospheres: An optimal Neuromag dose (previously established in our laboratory) was used to investigate the effect of applying oscillating magnetic fields on transfection in neurosphere cultures. Similar to that observed in monolayers, NSCs appeared healthy post-transfection with

phase bright cells forming neurospheres similar in size and number to controls (**Figure 2.5C-D**). Transfected spheres were intact and GFP expressing cells appeared throughout the sphere. In this instance, basal transfection efficiency (no-field) was 4.2 ± 0.4% (**Figure 2.6B**). A similar frequency-dependent trend in transfection efficiency was observed to that in monolayers, however only F = 4 Hz produced a statistically significant enhancement of transfection above basal levels (**Figure 2.5D and 2.6B**). Here, transfection efficiency was doubled to 9.9 ± 1.7%. No transfected cells were observed in the plasmid only control samples. GFP expression was also observed to occur at earlier time-points when transfection was performed using the oscillating magnetic fields. The proportion of GFP expressing cells 10 h post-transfection was 3.3 ± 1.0% in the F = 4 Hz condition compared to almost no transfection observed in the no-field condition (0.2 ± 0.2%), although this difference was not found to be significant ($p = 0.07$, one-way ANOVA, Bonferroni's MCT). Cells from both groups also displayed high viability (>90%), as judged by trypan blue staining, suggesting there is no short term toxicity associated with these procedures.

Comparing transfection levels between culture systems: A clear difference in transfection efficiency between culture systems is evident (**Figure 2.6A-B**). The greatest transfection efficiency achieved in monolayers is over three times that in neurospheres. Further, applying the oscillating field during transfection yields a three-fold increase in transfection efficiency over basal levels in monolayers; compared to double the basal level in neurospheres. As both systems are important for clinical application, it was decided to perform basic safety analyses using both culture systems. However, only monolayers were taken forward for more rigorous safety analysis in the form of a proteomics-based assessment of the potential molecular changes incurred by magnetofection as well as functional assessments following transplantation onto cerebellar slices.

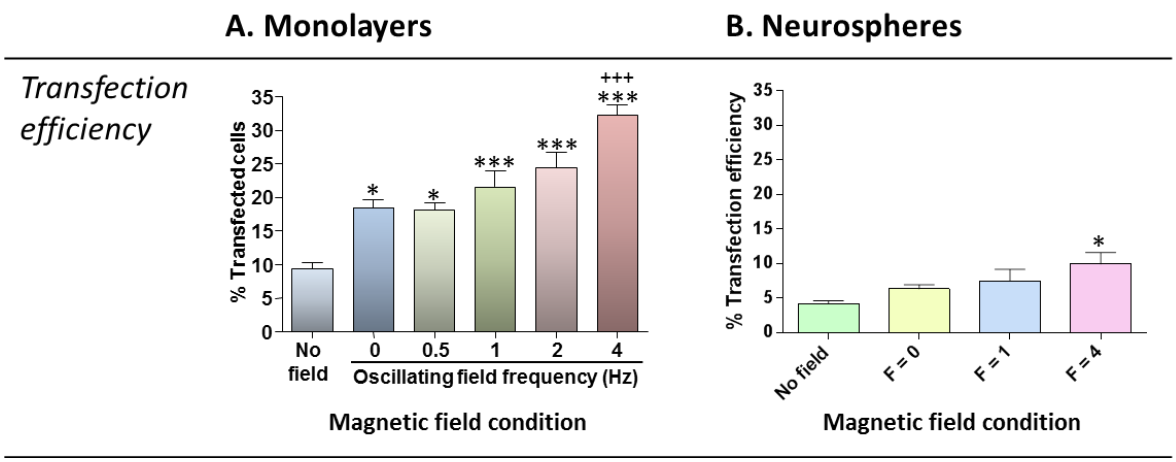

Figure 2.6. Quantification and comparison of transfection efficiency in monolayers and neurospheres. *(A) Bar chart displaying quantification of the percentage of GFP expressing cells in monolayers for each transfection condition. Significant differences are: *p<0.05, ***p<0.001 vs no-field transfection and $^{+++}$p<0.001 vs static (F =0 Hz) field transfection (one-way ANOVA and Bonferroni's MCT, n = 4). (B) Bar chart displaying quantification of the number of GFP positive cells following dissociation of neurospheres transfected under different conditions. The 4 Hz oscillating field condition significantly improved transfection efficiency over the no-field condition (*p<0.05, one-way ANOVA and Bonferroni's MCT, n = 6).*

2.3.3 Magnetofection has no effect on NSC proliferation and viability

Assessment of the safety of magnetofection protocols in monolayers was conducted in three conditions: no-field, static field and F = 4 Hz and all experimental conditions were assessed in neurospheres. Across all conditions, no effect was seen on total cell number or cell viability (**Figure 2.7**). Numbers of pyknotic nuclei were also assessed in re-plated, transfected neurospheres and counts were low (ca. 2%) and similar across all conditions (**Figure 2.7**).

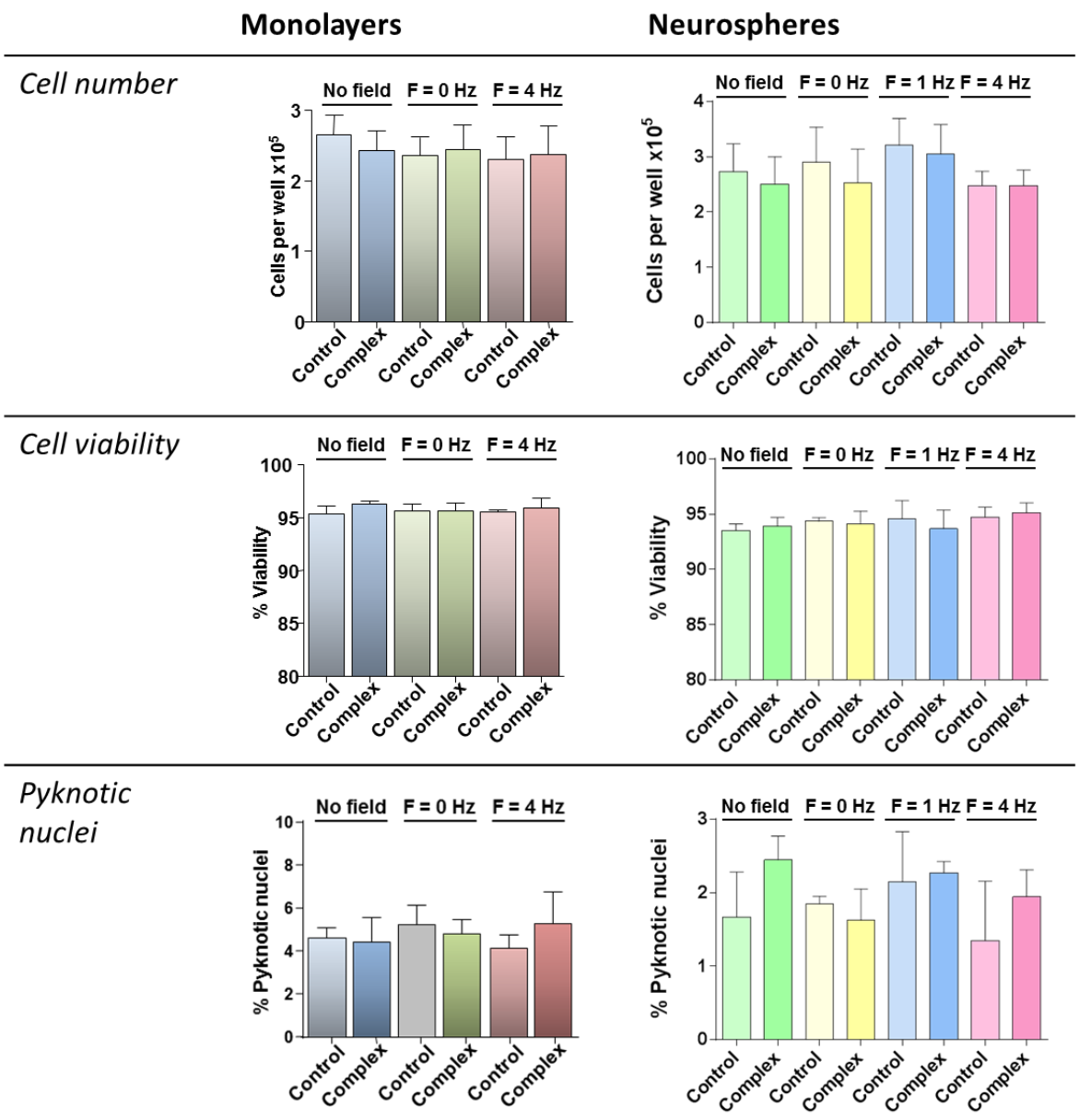

Figure 2.7. Magnetofection has no effect on NSC numbers or viability in either neurosphere or monolayer cultures. *Bar charts displaying quantification of cell number and viability as indicated in the figure across the selected magnetic field conditions. Numbers reported for the different assays in this panel are similar (and not statistically different) across conditions suggesting the protocols are not having an effect on these measures of cell health.*

2.3.4 Magnetofection has no effect on 'stemness' of NSCs

Highly pure populations of NSCs were generated from both transfected monolayer and neurosphere cultures with the majority of cells displaying the NSC specific markers nestin and SOX2. Importantly, cells expressing GFP also displayed normal patterns of NSC marker staining and regular circular nuclei as judged by DAPI staining (**Figure 2.8A and B**). GFP expression was found throughout the cytoplasm of these transfected NSCs (**Figure 2.8A and B**). There was also no difference between the proportions of cells expressing these markers in any condition (**Figure 2.8C-F**).

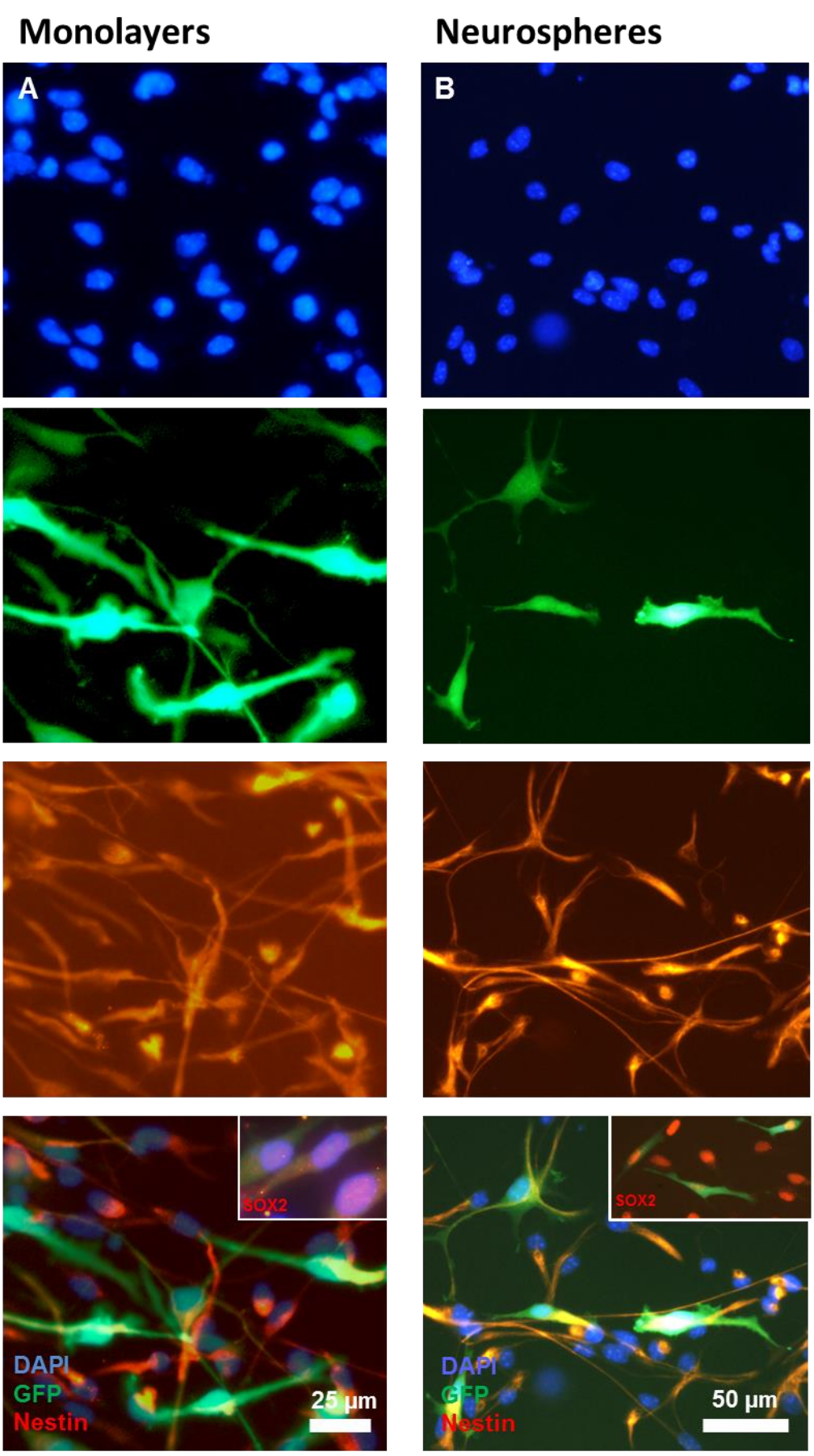
Monolayers
Neurospheres
A
B
SOX2
SOX2
DAPI
GFP
Nestin
25 µm
DAPI
GFP
Nestin
50 µm

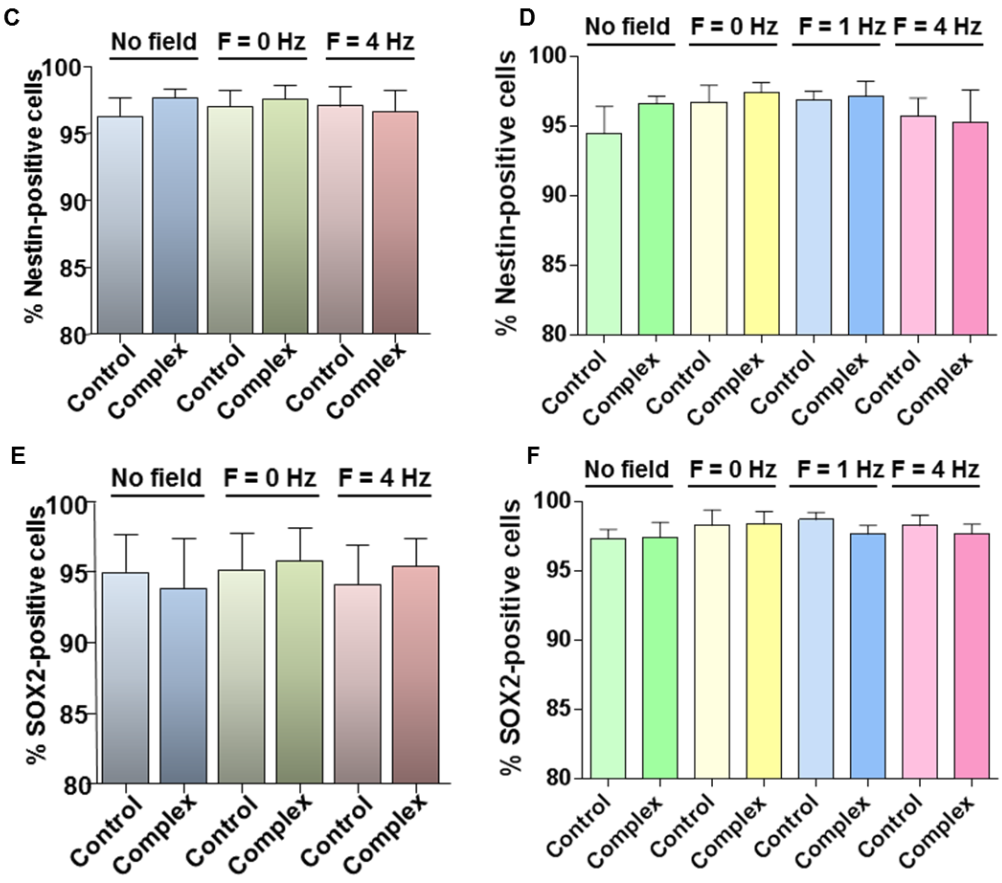

Figure 2.8. Stemness of magnetofected NSCs is unaffected. *Representative images of cells positive for stem cell markers nestin (main images) and SOX2 (insets) from NSCs transfected as (A) monolayers or (B) neurospheres with each individual channel shown from the nestin images. Note that GFP expressing cells also express the NSC specific markers. Bar charts displaying quantification of the proportions of cells positive for NSC marker nestin after transfection as (C) monolayers or (D) neurospheres across selected magnetic field conditions. Bar charts displaying quantification of the proportions of cells positive for NSC marker SOX2 after transfection as (E) monolayers or (F) neurospheres across the selected magnetic field conditions. Proportions of NSCs expressing both the quantified markers are similar across all conditions suggesting the magnetofection protocols are not having an effect on the stemness of the NSC population.*

2.3.5 LIVE/DEAD staining and MTS assays reveal no effects on cellular viability of selected magnetofection conditions on NSCs grown as monolayers

Some additional safety tests, routinely used in nanoparticle toxicity studies, were performed following monolayer transfection. After LIVE/DEAD staining, the majority of cells had normal bipolar NSC morphologies and were seen to stain green (LIVE) with small numbers of rounded cells appearing red (DEAD) in all conditions (**Figure 2.9A**). Using this assay, cell viability in magnetofected samples was observed to be high (>90%) and similar to controls (**Figure 2.9A-B**). The results of an MTS assay also showed no cytotoxicity following magnetofection procedures, with absorbance readings indicating comparable levels of mitochondrial function similar across all conditions (**Table 2.5**).

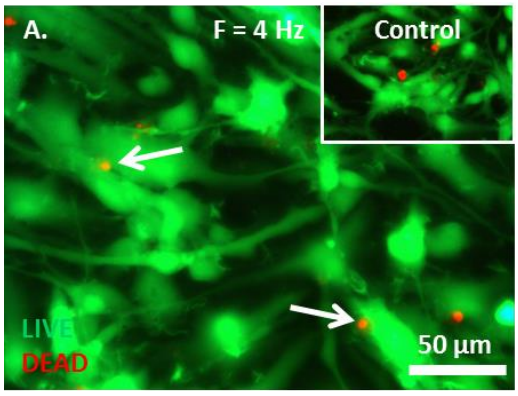

B. LIVE/DEAD

Experimental condition		*Viability, %*
No field	*Control*	91.4 ± 2.1
	Complex	93.8 ± 1.5
F = 0	*Complex*	91.1 ± 0.9
F = 4	*Complex*	91.9 ± 3.8

Figure 2.9. LIVE/DEAD staining of magnetofected NSCs grown as monolayers. *(A) Representative fluorescence micrographs showing LIVE cells appearing green and DEAD cells appearing red (arrows) 48 h after 4 Hz oscillating field magnetofection and (inset) no manipulation. (B) Table showing quantification of LIVE cells as a percentage of total cells. No significant differences were noted between groups (n = 3).*

Experimental condition		*Viability (% of control)*
No field	*Control*	100.0 ± 0.6
	Complex	95.4 ± 3.7
F = 0	*Control*	99.5 ± 1.4
	Complex	98.9 ± 1.5
F = 4	*Control*	99.4 ± 1.7
	Complex	97.2 ± 2.8

Table 2.5. MTS assay results from magnetofected monolayer NSCs. *Absorbance readings are given as percentage of control. No significant differences were observed between any conditions (n = 3).*

2.3.6 Differentiation profile of NSCs is unaffected by magnetofection

Astrocytes, neurons and oligodendrocytes were all produced from transfected NSC cultures in similar proportions across all conditions similar to the proportions generated in control cultures (**Figure 2.10**). Further, these cells displayed normal morphologies with broad, multipolar star-like astrocytes, immature neurons with generally one or two short processes and highly processed oligodendrocytes (**Figure 2.11A-C**). GFP expression in these mixed cultures was predominately confined to the astrocytic progeny (of normal morphology) with no GFP expressing neurons or oligodendrocytes observed in cultures derived from transfected neurospheres, and GFP expressing neurons were rarely observed (< 1% Tuj-1 positive cells) in cultures derived from transfected monolayer cultures (**Figure 2.11D**).

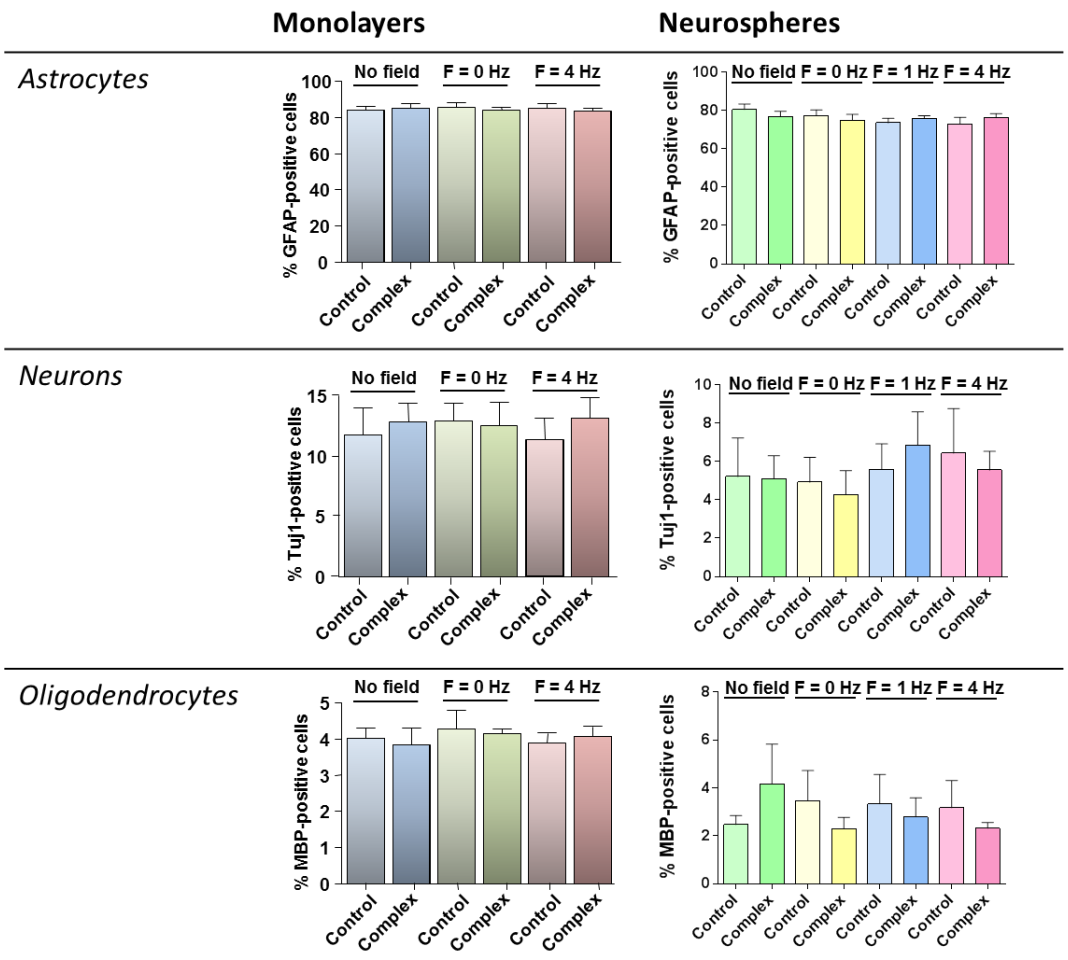

Figure 2.10. The relative proportions of NSC-derived daughter cell types are unaffected by magnetofection. *Bar charts depicting the proportions of each cell type (indicated in table) in mixed cultures generated from NSCs treated under different conditions.*

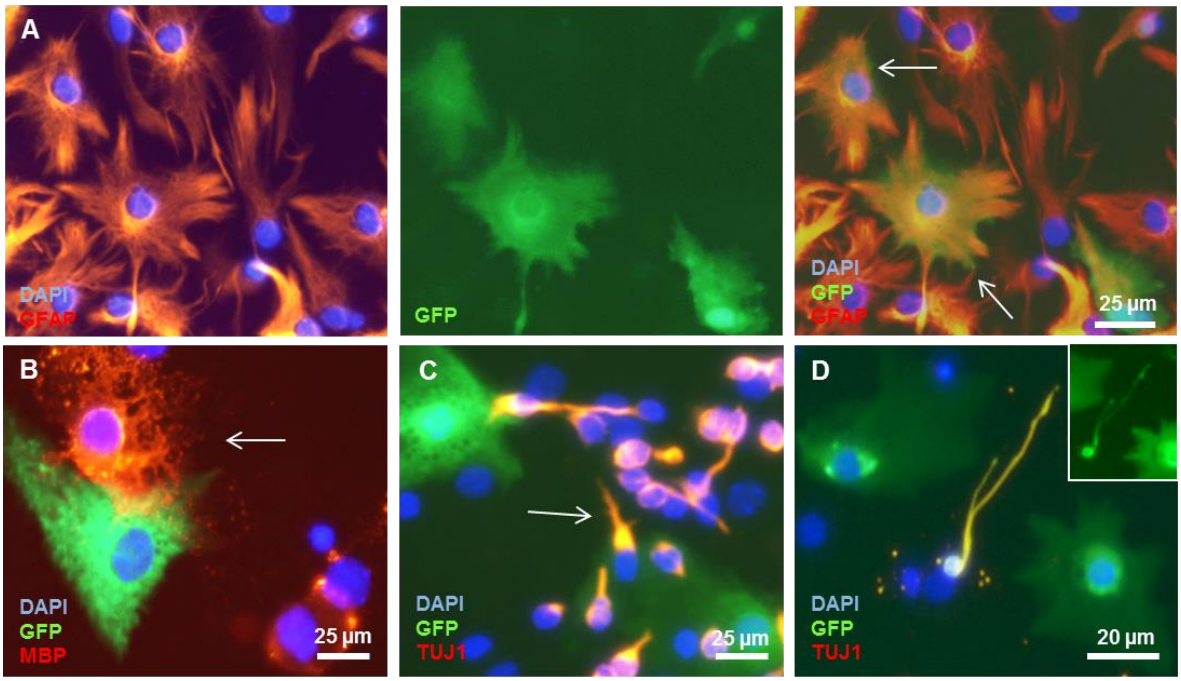

Figure 2.11. Magnetofected NSC cultures can generate the three major cell types of the CNS. *Representative images of cells positive for the neural cell markers (A) GFAP for astrocytes – fluorophore channels split to highlight overlap of GFP expression and GFAP staining – (B) MBP for oligodendrocytes and (C) Tuj-1 for neurons derived from magnetofected NSC monolayers. White arrows point to the named cell type in each image. Note that in (A) GFP expressing cells positive for GFAP staining are present (white arrows) and in (B) and (C) GFP expressing cells have the morphological appearance of astrocytes. (D) Rare example of a GFP expressing neuron, with the inset clearly showing the GFP expression throughout the neuronal processes.*

2.3.7 Proteomic analysis of magnetofected monolayer NSCs

To assess the feasibility of characterising the effect of magnetofection on protein expression and specific signalling pathways, a proteomics based analysis was performed. Cultures that were detached for the analysis had similar numbers of cells (ca. 3 x 10^5 cells per well) and high cell viability (> 95%). The subsequent banding pattern after gel electrophoresis of the extracted proteins was similar between each group, suggesting similar protein expression (**Figure 2.12**). LC-MS/MS of the excised protein bands and subsequent database searching identified >450 proteins in each group. The samples were similar in terms of the proteins that were identified and relative expression of these can be semi-quantified, represented in this case by a heatmap (**Figure 2.13** – judged by colour coding of individual bands). Clustering analysis revealed that, although the relationships between samples were close, similarity decreased so that relation to control followed the pattern: no-field > F = 0 Hz > F = 4 Hz. Specific cellular pathways could also be interrogated by this method. The example shown here is the Mitogen-activated protein kinase (MAPK) pathway which is involved in NSC proliferation and maintenance of phenotype.[146] As shown, the expression levels of the proteins within this pathway can be evaluated, however, some differences are apparent in the banding between samples (**Figure 2.14**). As expected, GFP could be identified within the transfected samples but was absent from the control. Two GFP peptides were detected (**Figure 2.15A**) and the mass spectrum produced was matched to the GFP peptide as shown in **Figure 2.15B and C**. Lowering the threshold of confidence of identity also revealed that more peptides were identified for GFP in the 4 Hz oscillating group than the other transfection groups, which is suggestive of more protein being present although this method of analysis cannot be considered conclusive.

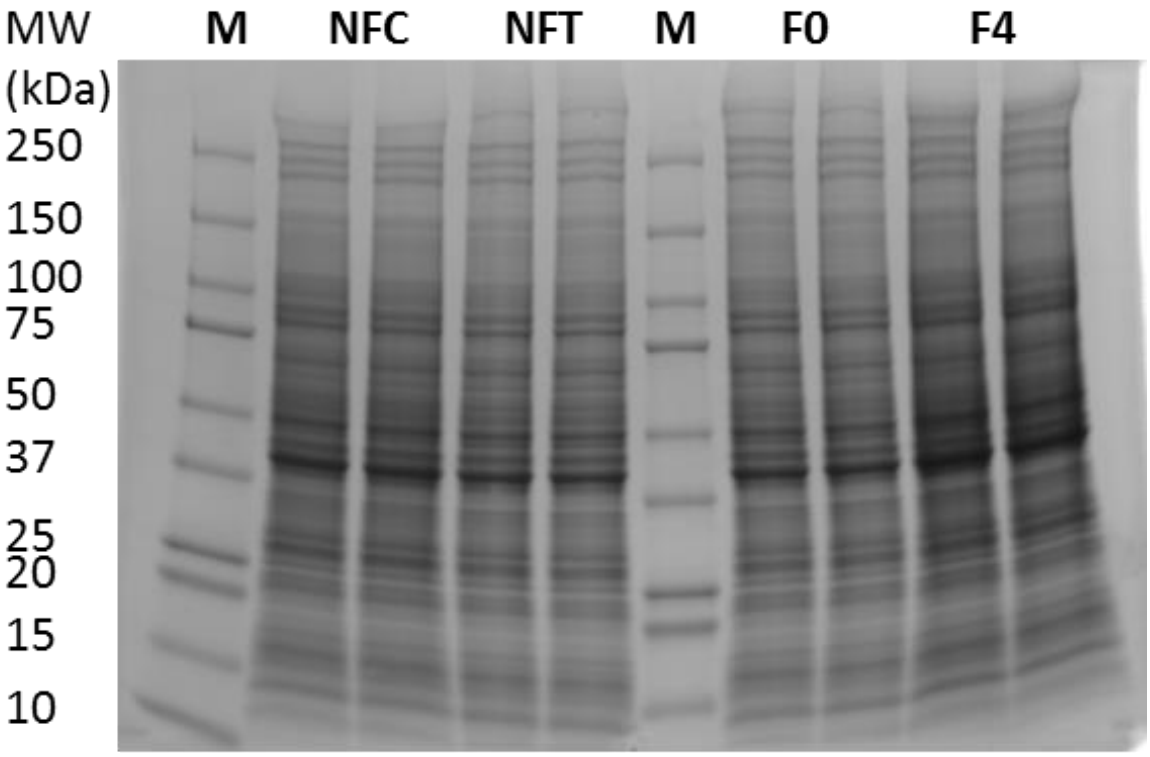

Figure 2.12. Gel electrophoresis of proteins extracted from magnetofected NSCs. *Densitometer image of the gel resulting from gel electrophoresis of control and magnetofected NSCs from selected conditions. Overall banding intensity and pattern appears similar between samples. MW – molecular weight; M – molecular weight markers; NFC – no-field, no particles; NFT – no-field, particles; F0 – static field, particles; F4 – 4 Hz oscillating magnetic field, particles.*

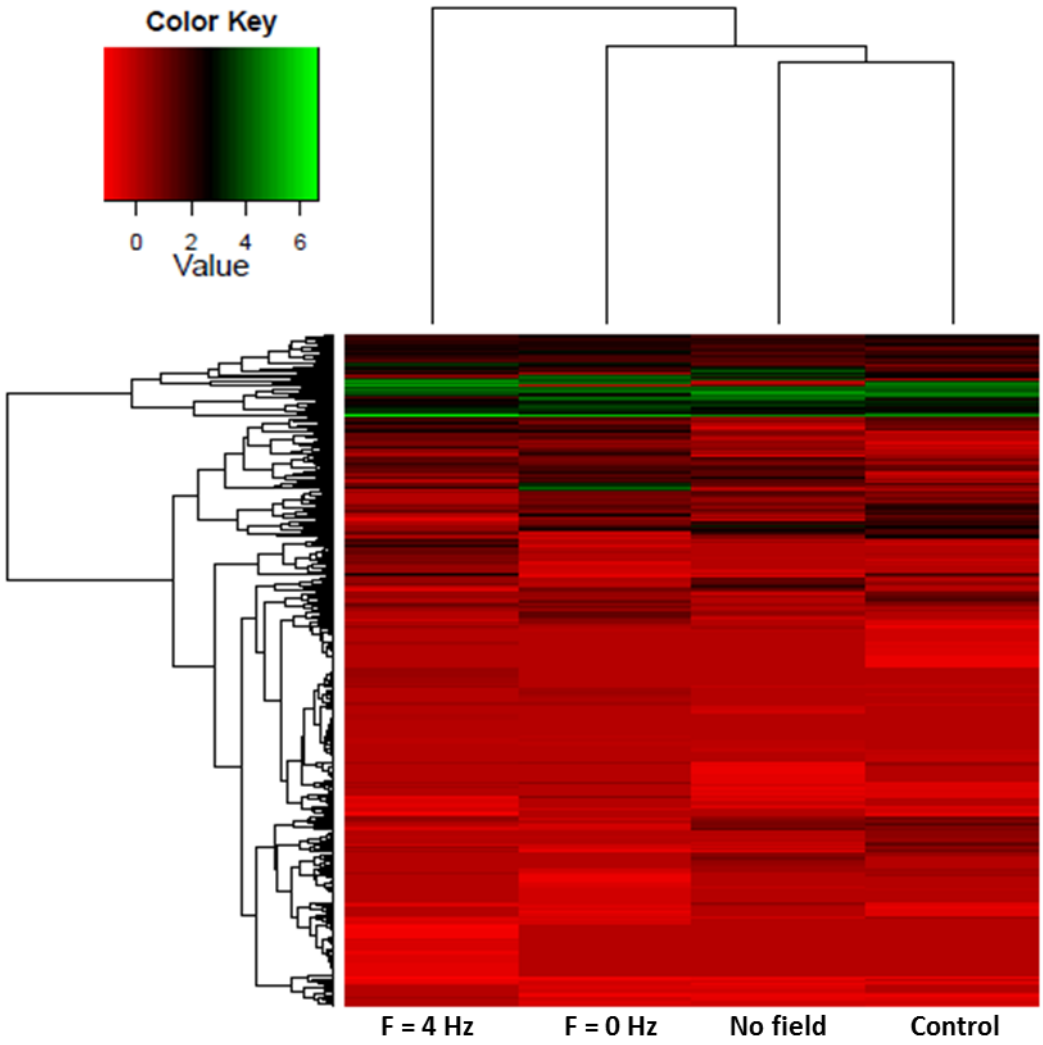

Figure 2.13. Overall comparison of expression levels for identified proteins. *Clustering analysis indicates that similar proteins were identified in each sample. Clustering of proteins by similarity of expression level is displayed in the family tree on the left of the heatmap. The number of peptides identified for each separate protein provides a semi-quantitative assessment of the amount of each protein in each sample which is represented by colour (green indicates greater protein levels). The clustering of the samples indicates that all conditions are similar, but F = 4 Hz exhibits more differences compared to control than either F = 0 Hz or the no-field conditions.*

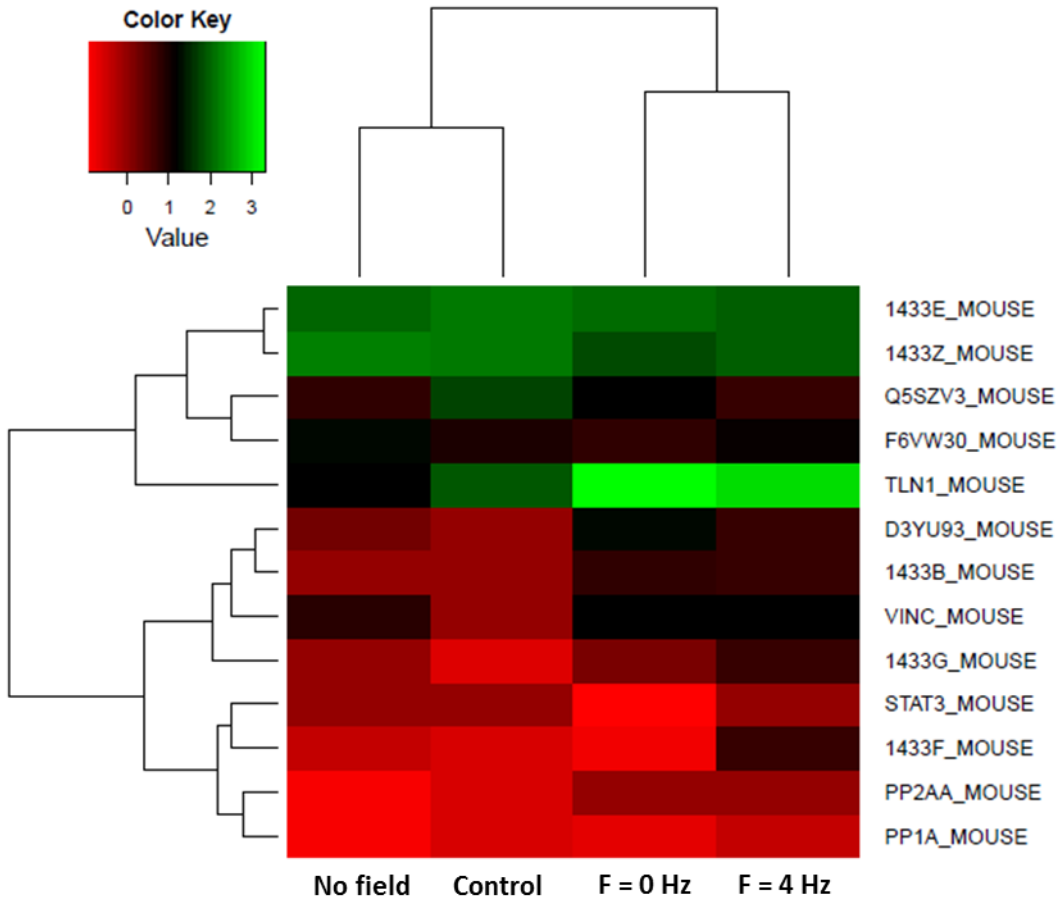

Figure 2.14. Heatmap of identified proteins from the MAPK pathway. *Individual cellular signalling pathways can be interrogated as in Figure 2.13. Here the MAPK pathway (involved in proliferation of NSCs) has been highlighted and displays no major difference in proteins identified.*

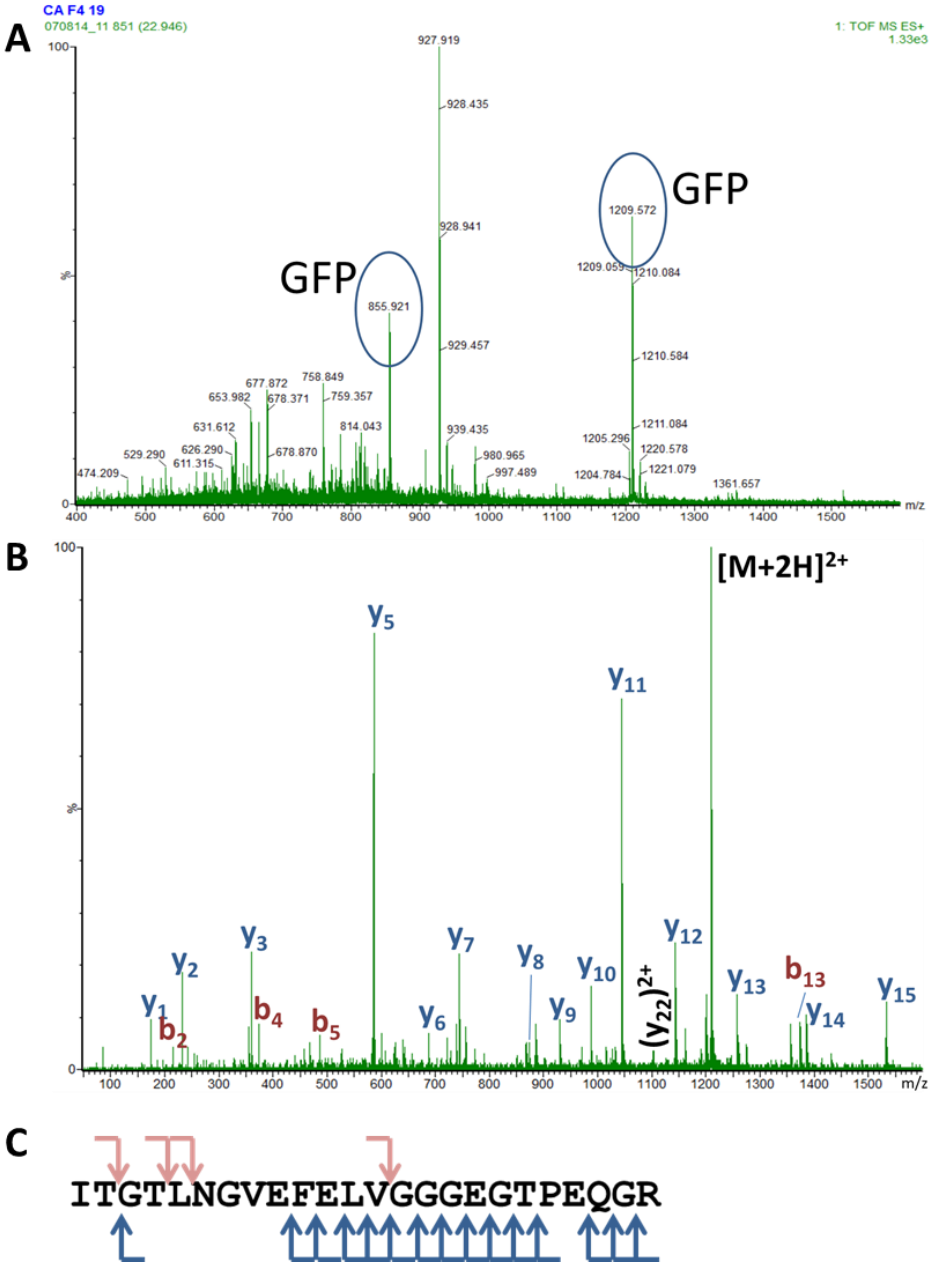

Figure 2.15. GFP can be identified in magnetofected samples. *(A) Survey spectrum from the MS/MS analysis indicating two peaks which were attributed to GFP. (B) Product ion spectrum of one of the tryptic fragments showing the b- and y-ions identified by MASCOT and matched to a peptide from GFP. (C) Peptide sequence displaying the various b- and y-ion fragments.*

2.3.8 Transplantation of monolayer magnetofected NSCs into organotypic slice models

To investigate the transplantation of magnetofected NSCs, transfected cells were transplanted onto organotypic cerebellar slices. These slices have been previously characterised in our laboratory[143] and contain multiple neural cell types with similar cytoarchitecture to that observed *in vivo*, therefore representing a pre-animal, test-bed for cell transplantation studies. Here, these were successfully derived and could be maintained for at least 30 days with high viability as judged by LIVE/DEAD staining (**Figure 2.16A**). Focal transplantation of transfected NSCs was achieved, using both re-formed neurospheres (**Figure 2.16B** – inset depicts re-formed neurosphere with RFP expressing cells within the structure) and dissociated monolayers (**Figure 2.16C**). Cell aggregates expressing RFP (20-50 µm in diameter) were observed on the slice following neurosphere transplantation, in contrast to the disparate (red) cells apparent after transplantation of detached monolayers (**Figure 2.16B and C**). At 72 h post-transplantation, RFP positive cells in both groups were seen displaying multiple processes indicating cell survival (**Figure 2.16D and E**). RFP positive cells predominately expressed GFAP signifying their differentiation into astrocytes, which is similar to NSC differentiation profiles on glass where the astrocytes are also the dominant daughter cell type generated (**Section 2.3.6**). Some RFP positive cells also retained expression of the NSC transcription factor SOX2 (**Figure 2.16F**).

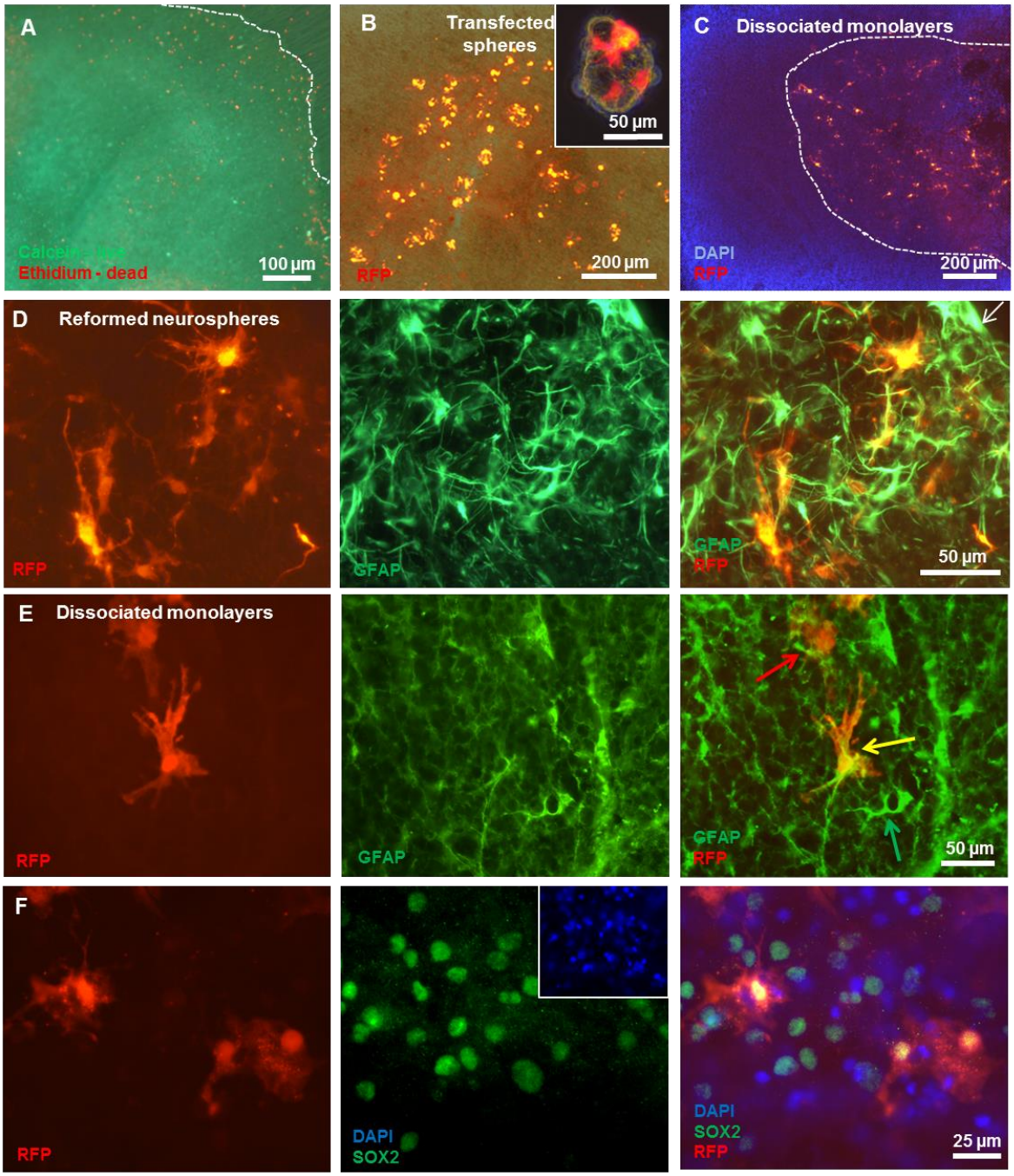

Figure 2.16. Transplantation of transfected NSCs onto cerebellar slices. *(A) LIVE/DEAD staining of cerebellar slice after 30 days in culture. Live cells take up calcein so appear green and dead cells take up ethidium homodimer-1 so have a red appearance. Dead cells mostly appear towards the slice margins. (B) Focal transplantation of transfected neurospheres (magnetofected NSC monolayers were re-formed into neurospheres), with transfected cells retaining cell-cell*

associations typical of neurospheres (B - inset). (C) Focal transplantation of single cells after monolayer dissociation with an absence of sphere morphology. Following transplantation of both (D) neurospheres and (E) dissociated monolayers, there is evidence of transfected cells integrating into the 'host' tissue, extending processes and differentiating into astrocytes, as indicated by expression of GFAP. (F) Some transfected cells were also found to retain the NSC specific marker SOX2. Where applicable, channels have been shown separately so that co-localisation of fluorophores can be observed.

2.4 Discussion

As far as I am aware this is the first report of utilising oscillating magnetic fields to enhance MP mediated transfection in primary NSCs, a highly clinically relevant cell population. Crucially, oscillating fields were shown to safely enhance transfection in NSCs propagated as both monolayers and neurospheres. The finding in neurospheres is of particular interest as it is the first time oscillating magnetofection protocols have been successfully demonstrated in a suspension culture. A number of safety analyses have also been performed including histological, molecular and functional tests encompassing a broad spectrum of cell behaviour. This is novel in the field of testing nanotechnologies and the assays described here could provide a benchmark for future testing of novel multifunctional MPs.

2.4.1 The utility of magnetofection protocols for NSC transplantation therapy

In terms of genetic manipulation strategies of transplant cell populations, viral transduction generally results in the highest levels of transduced cells; however, use of viruses may be

undesirable for clinical application for a number of reasons. Viral delivery is a complex procedure – involving transfecting a carrier cell type with up to three plasmids, collecting viral particles, and determining the amount of virus in the supernatant before transduction, which is often repeated several times to ensure high levels of target cell infection.[147] In combination with the necessity to house all viral preparation in biosafety level II containment facilities, viral transduction is not readily scaled up to clinical levels of production. Use of viruses to transduce transplant cells is also associated with significant safety risks, including insertional mutagenesis and oncogenicity,[49,50] of particular concern when transducing stem cell populations which already have the capacity to self-renew and proliferate. This drawback was exposed in a recent clinical trial where autologous $CD34^+$ cells (haematopoietic stem cells) were retrovirally transduced to produce a replacement enzyme to treat a form of human severe combined immunodeficiency.[148] After transplantation, although the enzyme was successfully produced, with resultant correction of disease pathology, 4 out of 20 patients treated developed leukemia which was traced to the genetically engineered stem cells.[148]

Nucleofection performs well as a non-viral transfection process (80% transfection efficiency in NSCs),[149] but results in substantial loss of cell viability post-transfection. From a translational viewpoint, this would increase production costs associated with generating more cells, to replace those lost during the nucleofection protocol, and could also lead to transplantation of a large number of dead cells – unfavourable for transplant survival and potentially detrimental to the host. Other non-viral strategies generally result in low levels of transfection and some systems have been shown to be toxic (through membrane rupture) to NSCs.[52] **Table 2.6** summarises some of the key properties of gene delivery strategies and their advantages or disadvantages for clinical application.

The data presented in this chapter suggests that using oscillating magnetic fields in combination with MP mediated transfection could provide an alternative strategy to genetically modify transplant NSC populations and address the problems encountered with other techniques, as outlined above. The MPs used in this study were shown to be non-toxic to NSCs and magnetofection protocols to enhance MP mediated transfection efficiency were also shown to be safe with regards to key regenerative properties of NSCs including proliferation, stem cell marker expression, differentiation and survival after transplantation into host cerebellar slices. In addition to the good safety profile of magnetofection, the highest transfection levels in NSCs achieved in this study (ca. 32% in monolayer NSCs with application of a 4 Hz oscillating magnetic field) are comparable to some viral systems and compare favourably to other non-viral gene delivery techniques (**Table 2.6**). Studies on transplanting genetically engineered NSCs which have seen benefits in pre-clinical models of neurological injury report transfection efficiencies of 20-80% (General Introduction, **Section 1.5**). This suggests magnetofection protocols could be utilised for this application whilst avoiding the safety issues associated with viral gene delivery. Finally, MPs can be routinely produced in large quantities, and are already used in the clinic,[70] and plasmid DNA production can also be scaled up to meet clinical requirements.[150] Combined with the simplicity of the technique, scale-up of magnetofection protocols seems feasible for both manual and automated operation. As discussed in **Section 2.1.1**, automation is thought to be a key requirement of scaling up cell therapies to clinical levels. The simplicity of the technique could allow for the adaption of existing automated cell culture systems, such as the CompacT SelecT, to magnetofection protocols – a strategy already being investigated for scale-up of non-viral transfection of HEK 293T cells using PEI.[151]

In terms of therapeutic delivery, plasmid transfection generally results in transient gene expression in the target cells. In our laboratory we have seen GFP expression persist for ca. 21 days in NSCs propagated as neurospheres; although a low proportion of spheres are GFP positive

by this point (<1%). Neurological injury and regeneration, as stated in the General Introduction (**Section 1.2**), is a highly complex process with temporally controlled gene expression precisely controlling cell recruitment and tissue remodelling. Therefore, in terms of therapeutic delivery, transient gene expression could be considerably advantageous when delivering therapeutic factors to promote repair in sites of CNS injury and disease. For example, factors could be released to recruit and drive proliferation of local progenitor cells for combined neuroprotection and cell replacement over a short period of time during an identified window of opportunity, then cease, avoiding transgene interference with subsequent stages of repair. Indeed, long term expression of factors involved in this process is likely to be detrimental to progenitor cell maturation and therefore functional cell replacement. Overexpression of FGF-2, which can promote NSC survival and angiogenesis has also been shown to stimulate astrogliosis (a process which can contribute to the astrocyte scar) and can disrupt myelin production in mature oligodendrocytes.[152]

Even greater levels of magnetofection efficiency may be required for clinical applications, and there are several strategies through which this may be achieved. Increasing particle size (from 187 nm to 375 nm) has been shown to enhance MP mediated gene delivery into smooth muscle cells and bovine aortic endothelial cells.[153] This could be the result of an enhanced capacity for binding DNA allowing the particle to deliver more plasmid copies to the cell. However, the authors also noted that the large particles avoided lysosomes and delivered DNA to the cytosol (although the comparison with smaller particles was absent) potentially resulting in low rates of DNA degradation. Several reports show that modifying particle chemistries through use of different polymers or combinations of polymers and use of CPPs can enhance uptake in various cell types,[154] however, few neurocompatible particles have been described. Optimising particle design to either enhance particle uptake or promote endocytosis routes more favourable for transfection could therefore represent a novel, if complex, route to improving MP mediated transfection in

NSCs. A simpler approach to enhance transfection levels could be to employ a repeat transfection procedure. Multifection has been shown to safely enhance gene delivery into NSCs grown as neurospheres[30] and findings from our laboratory suggest that the same is true for astrocytes grown as adherent monolayers (unpublished data, Jacqueline Tickle, Keele University). As the transfection efficiency was almost doubled in the neurosphere model, this suggests that combining magnetofection with multifection could be a potent strategy to enhance gene delivery to NSCs grown either as neurospheres or monolayers. Although promising strategies, optimising particle design and delivery will most probably need to be undertaken for each individual cell type, as results from one cell type cannot reliably be extrapolated to another. This further highlights the requirement for high-throughput analyses of novel particle function and safety in order to assess numerous particle formulations potentially in multiple cell populations and culture systems.

The findings are also of clinical relevance with respect to the potential for MPs to provide a multi-functional platform for regenerative medicine applications, including cell tracking through MRI, gene or drug delivery and magnetic stem cell targeting. In this regard, a recent study proved a high iron content particle coated with fluorescent PEI could act as a contrast agent for MRI and be used to label primary astrocytes.[83] From a clinical perspective this particle could potentially be used to detect transplant cells by MRI (for non-invasive imaging), and fluorescence microscopy (for post-mortem evaluation of cell fate). The particle was also shown to be able to bind DNA and deliver this to astrocytes, albeit with relatively low levels of transfection (<1%).[83] An oscillating magnetic field was not used in this study; therefore it may be of value to test whether the protocols developed in this chapter could be useful for enhancing uptake and transfection when using this and other novel multimodal particles.

Transfection method	Transfection efficiency	Capacity	Scalable production?	Safety	Comments
Retrovirus[49,155]	High (>80%)	8 kb	Large scale production of moderately pure vector	Initial exposure toxic Risk of insertional mutagenesis	Some viral genes left in construct which could result in immune system clearance or homologous replication with WT replication competent virus
Lentivirus[156]	High (>80%)	4.7 kb – possibly extendable to 10 kb	Scalable production available	Risk of insertional mutagenesis	Similar to retrovirus.
AAV[49,157]	Low – utilising different coat proteins may increase this	4.7 kb – stringent	Scalable production in use	Low pathogenesis Low immunogenicity	Preferred method of *in vivo* transduction due to safety profile Common vectors inefficient at transducing NSCs
Amplicon[158]	No data available	Theoretically – 150 kb	No method to produce large, contamination free stocks	Non-pathogenic Non-toxic	Not investigated in neural stem cells
Nucleofection[53,149]	Up to 80%	Large capacity	Potentially scalable	No effect on cell behaviour	Low cell viability post-transfection (40%)
Lipofection[52]	Low (11-16%)	Large capacity	Potentially scalable	Can be toxic	Diffusion limited transfection rate
Magnetofection	Medium (ca. 32%)	3.5 kb plasmid delivered here	Large scale production of MPs and plasmid DNA available	Non-toxic No effect on cell behaviour	Comparable transfection efficiency to viruses

Table 2.6. Comparison of transfection efficiencies and clinical considerations for different strategies to genetically engineer NSCs.

2.4.2 The advantages of a proteomics analysis of magnetofected NSCs

In the preliminary analysis of the ability of a mass spectrometry approach to compare the proteome of treated and untreated NSCs, a large number of proteins were identified (>450) and compared across conditions. Replicates will need to be performed in order to indicate any significant differences that might be present in protein expression between the magnetofected samples. As several proteins from a specific pathway could also be identified, alterations in global NSC function could be interrogated in more detail in the future. Quantification of all the proteins in the pathway could provide information on whether multiple proteins from the pathway are differentially expressed between samples which would be a strong indicator of the loss or gain of the function of that pathway.

One previous report has used genomic analysis to assess the effect of labelling NSCs with a clinical grade MP (Feridex), finding little evidence of an up-regulation of genes associated with cell death and stress.[140] However, no magnetic field was applied in these studies, which could be a key clinical uptake enhancing strategy. In addition, although the preliminary data presented here is semi-quantitative, it demonstrates the ability to map the proteome of magnetofected cells, which could facilitate the detection of functional changes within a cell, which examination of mRNA expression cannot stringently provide (i.e. mRNA presence does not automatically infer protein presence).

Future work will concentrate on developing proteomics analyses with greater quantitative power; however the approach described here does already provide several advantages over commonly used safety assays. As the field of nanoparticle design is rapidly advancing, novel particle designs will potentially have widely varying molecular effects on cells. Therefore it might be necessary to test for a number of pathways known to be associated with toxicity, for example, production of ROS or mitochondrial dysfunction. Using a proteomics approach could therefore allow a range of

different pathways to be interrogated for evidence of cellular toxicity. In addition, this approach could provide an unbiased and standardised protocol for the assessment of toxicity of novel nanomaterials in stem cell populations. Of particular interest to nanotechnology approaches to genetically engineering transplant populations, GFP was reliably detected in the magnetofected samples. Therefore, using a relatively simple and rapid one-step technique, pathways involved in cellular toxicity and gene delivery success could be assessed simultaneously. Further, by using advanced quantitative mass spectrometry analysis, transfection efficiency could be compared between different delivery strategies, such as the use of different oscillation frequency parameters in magnetofection protocols.

2.4.3 Advantages of assessing the safety of magnetofection protocols using cerebellar slices

Transplantation of genetically engineered NSCs onto cerebellar slices demonstrated survival of magnetofected cells, with some maintaining SOX-2 expression and some differentiating; only astrocytes exhibited transgene expression in this study. Survival, stemness and differentiation are key regenerative properties of the NSCs suggesting that the developed magnetofection procedures are safe for genetically engineering cell transplant populations. The data also highlight the utility of the slice model to act as a further safety assessment of genetic manipulation approaches by transplantation of the engineered cells into host tissue representing an *in vivo* environment. To further enhance the clinical relevance of the model, neurological injury can be simulated in cerebellar slices using, for example, demyelinating agents. NSCs have been previously shown to generate oligodendrocytes which subsequently myelinate axons in a model of multiple sclerosis.[28] Therefore, the slice could also be used to test the functional outcome of genetically engineering cells and transplanting them into sites of disease. In combination with the proteomics analysis of magnetofected cells detailed data could be readily obtained on the safety

and functional nature of genetically engineering transplant cell populations with nanoparticles. A hierarchical analysis such as this could dramatically reduce the reliance on animal models to provide such data and circumvent cost and animal suffering associated with these studies. In addition, results generated from proteomics analysis and slice work could inform animal studies allowing for more focussed data acquisition and reduced animal usage, all in accordance with the 3Rs principle to reduce, refine and replace animals used in experiments.

2.4.4 There are differences in magnetofection efficiency between NSCs cultured as monolayers and neurospheres

The data presented in this chapter reveal distinct differences between monolayer and neurosphere cultures in terms of their responses to magnetofection protocols. Primarily, it was observed that MP mediated transfection is higher in monolayers under all field conditions. In addition, application of a static magnetic field enhanced MP mediated transfection efficiency in monolayers above that of a no field condition, but this was not found with neurospheres – in agreement with previously published reports.[30] Oscillating magnetic fields significantly increased transfection efficiency over basal levels in both culture systems, with the greatest transfection efficiency being observed at the same frequency of oscillation (F = 4 Hz). However, the ability of the oscillating field to enhance transfection, above the no field condition, was not as great in the neurosphere culture system, producing a doubling of transfection efficiency (from *ca* 5 to 10%) compared to a tripling of transfection efficiency (from *ca* 10 to 30%) observed in monolayers. The physical characteristics of neurospheres and monolayers are very different which could account for the striking differences in transfection efficiency when utilising magnetofection protocols. The 3-D nature of neurospheres means that cells are both 'hidden' from the transfecting particles and also, cells at the top of the neurosphere are further from the magnet, which could have an effect

on how much influence the field has at that point. In contrast, monolayer cells are all exposed to particles in the media, are the same distance from the magnet and therefore uniformly experience the benefit of the field. In addition, cells within a neurosphere generally have a rounded appearance compared to monolayer NSCs which generally have two long processes. It has also been suggested that rounded cells are in more of a 'resting state' potentially therefore being less endocytotically active than adherent cells which can be highly processed. Differences in membrane activity could therefore be a mechanism for the lower transfection efficiencies observed in neurospheres compared to monolayers. It may be possible to assess membrane activity of NSCs grown in the two culture systems by stimulation with MPs then visualisation using electron microscopy – in particular in conjunction with OTOTO staining which allows for high resolution membrane imaging. OTOTO involves staining cell membranes with osmium (O) and then increasing the staining density, and therefore electron conductivity, through sequential staining with a high affinity osmium binding agent, thiocarbohydrazide (T) and osmium. This technique removes the need for gold coating of samples which can obscure membrane features and particles on the membrane surface; therefore is ideally suited to observing particle-membrane interactions in high resolution. In addition the stained samples are visualised by field emission scanning electron microscopy (together termed OTOTO-FESEM) facilitating observation of numerous cells at once. Therefore it also represents a higher throughput microscopy technique compared to transmission electron microscopy (TEM) where only thin (*ca* 250 nm) sections of a few cells can be visualised at one time.

Although the mechanism by which the oscillating magnetic field enhances transfection efficiency is not yet known, the proposed mechanisms for the enhanced uptake when using oscillating magnetic fields are: (i) increased dispersion of the particles, (ii) a physical stimulation of the cell membrane or (iii) a combination of both. In neurospheres there may be an additional element whereby magnetically labelled spheres are pulled down by the field, and then experience

subsequent membrane stimulation by the oscillating field (**Figure 2.17**). For both culture systems, elucidating the mechanisms behind the enhanced transfection efficiency observed when using oscillating magnetic fields needs to be determined to inform future particle design and delivery strategies to NSCs. This may be investigated by the OTOTO-FESEM method for examining membrane activity as described above. Potentially, time-lapse microscopy could also be utilised to visualise fluorescent particles and examine their interaction with the membrane in real time during exposure to an oscillating magnetic field to determine differences in particle dispersion or activity on the membrane.

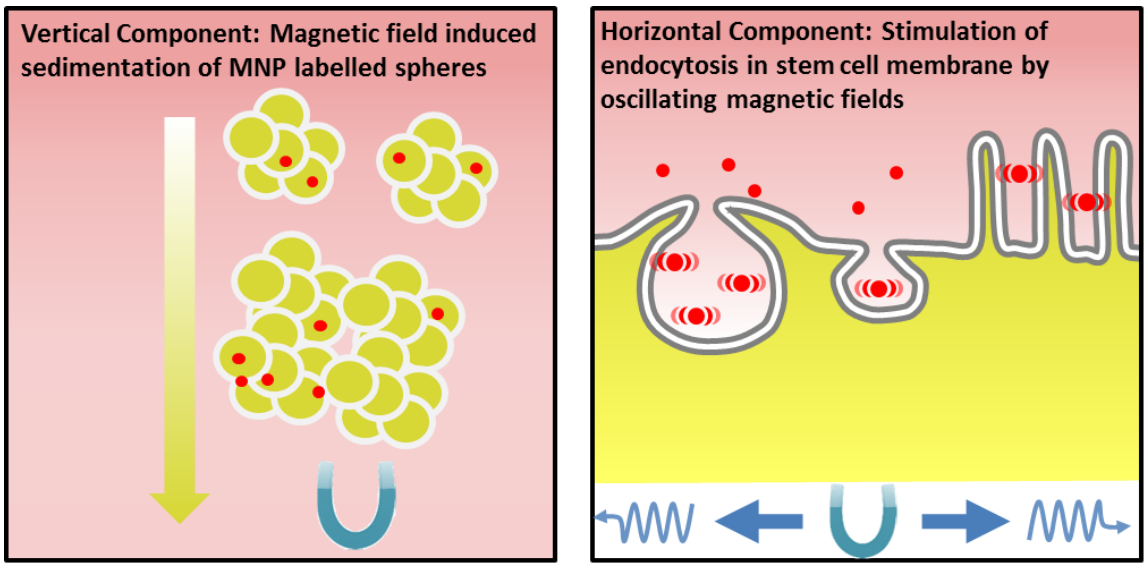

Figure 2.17. Schematic depicting possible mechanisms for enhanced MP mediated transfection efficiency in neurospheres when oscillating magnetic fields are applied during transfection.

2.4.5 GFP expression was largely confined to astrocytes

As has been described, no differences in NSC differentiation profiles were noted under any culture or magnetofection conditions, in terms of ratios of astrocytes, neurons and oligodendrocytes. However, following differentiation of transfected monolayer and neurosphere cultures, GFP^+ progeny were largely identified as astrocytes (%GFP^+ cells expressing GFAP; *ca* 100%), in proportions greater than would be expected given the differentiation profile of NSCs (% astrocytes derived from NSCs is 80-85%). This phenomenon has been reported previously by our laboratory when investigating MP mediated transfection of neurospheres.[30] In the present study, differentiation of NSCs transfected as neurosphere cultures produced no transfected neurons, and transfected neurons were rarely observed following differentiation of transfected NSC monolayer cultures. This observation could partly be explained by the fact that there appear to be fewer neurosphere derived neurons in this study (**Section 2.3.6**), a finding shown in other studies,[116] therefore leading to a lower percentage chance observing transfected neurons. Generation of transfected oligodendrocytes was never observed from either culture system. It remains to be seen whether this will be an issue for clinical application. Post-transplantation, NSC *in vivo* differentiation appears to depend on local environment and therefore it could be that transfected NSCs do differentiate into transfected neurons in a certain environment or injury pathology. In addition, there are reports that populations of transplanted NSCs can remain in a stem cell state and in that way mediate their neuroprotective effects. If this is the case, therapeutic proteins will be delivered by the engineered NSC population and not their daughter cells. Finally, even if NSCs mostly differentiate into astrocytes the data presented here indicate that these cells will still be able to express the transgene and deliver the desired therapeutic factor to sites of transplantation. However, in some disease states it may be beneficial to produce transfected neurons in particular, for example to promote neuronal survival. Cell specific peptides and antibodies have been conjugated to nanoparticles for cell targeting in human dendritic[159] and

macrophage cells.[160] Investigating peptides for targeting neuronal or oligodendroglial pre-cursors may provide a strategy to increase particle uptake, and therefore transfection, in these sub-populations, however, neural specific targeting peptides are currently rare in the literature. Alternatively, transfecting NSCs from different sources or developmental stages may provide a greater yield of transfected neurons. Preliminary results from our laboratory indicate that a greater proportion of transfected neurons could be generated when NSCs were taken from embryonic rats and magnetofected, compared with the post-natal NSC derivation protocol used here. However, these results have yet to be quantified and are from a different rodent model so will need to be validated.

2.4.6 Conclusions and future work

The data presented in this chapter demonstrate that oscillating field magnetofection can be used to enhance MP mediated gene delivery to NSCs without affecting key regenerative properties of the cells. The current work was performed with a commercially available transfection grade MP which may not be clinically translatable (the formulation is undisclosed by the manufacturer). In addition, the particle used is single function, being designed exclusively for gene delivery and, although comparable levels of transfection to those of viruses were observed, it may be required to increase transfection levels for clinical application. Further work in improving transfection levels, through particle and plasmid design, and investigating the application of magnetofection protocols to novel neurocompatible multifunctional particles (e.g. capable of gene delivery and MRI tracking) will broaden the applicability of magnetofection as a clinically relevant technique to enhance particle uptake.

Safety of the developed protocols was evaluated with a hierarchical microscopical, molecular and functional assessment of cellular toxicity. Further refinement to the proteomics analysis used here will need to be investigated to develop quantitative protocols for measuring protein expression which will aid in defining mechanisms of cellular toxicity and potentially provide information on gene delivery success. Combined with developing the clinical utility of the slice model (by introducing disease pathologies) the steps outlined in this chapter could be used by nanoparticle researchers as a key battery of tests to assess the safety and function of gene delivery mediated by MPs.[a]

[a] Most of the data relating to transfection of neurospheres has been published in Nanomedicine:NBM. The paper is attached as Appendix 1 and has been licensed for use in this Thesis by Elsevier.

Chapter 3: Developing high iron content particles for the efficient labelling of NSC transplant populations

3.1 Introduction

As discussed in the General Introduction (**Section 1.6**), safe delivery of transplant cells to sites of injury and disease is a major barrier to the clinical translation of NSC transplant populations. In recent years, a novel and minimally invasive approach to accumulate transplant cells at the desired site is to localise magnetically labelled cells using external magnetic fields. A description of this strategy and the physical principles underlying the technique is provided in the General Introduction (**Section 1.11**). The feasibility of this approach has been shown *in vitro*[80,161,162] and also *in vivo* for cardiac stem cell localisation to sites of myocardial infarction,[163] endothelial cell localisation to the surface of magnetised stents[65,164] and for some neurological applications, including sites within the spinal cord[100,102] and brain,[101] albeit with non-neural cell populations. Both studies combining magnetic capture with cell transplantation into the spinal cord utilised lumbar puncture to deliver the cells into the CSF, a less invasive procedure than direct injection. Both demonstrated that more cells accumulated at the lesion site when transplanted under external magnetic field application.[100,102] This demonstrates the spinal cord is an especially attractive neurological target for magnetic localisation strategies given the potential proximity to external magnets, due to its limited depth, facilitating efficient magnetic capture of labelled cells.

Two studies have been performed utilising magnetic localisation of MP labelled NSCs and are, as far as I am aware, the only studies of magnetic targeting of neural cell populations. In the first study, NSCs were associated with modified MPs designed to attach to the cell membrane (and not be internalised) by addition of an RGDS peptide to the surface of the particle. In this study labelled NSCs were transplanted, with and without magnetic targeting, into an organotypic slice model of axonal regeneration. Here, spinal cord slices are placed adjacent to cortex slices and axons projecting from the cortex to the spinal cord are counted to provide an assessment of the regenerative capacity of NSCs transplanted onto the spinal cord slice. A greater extent of axonal outgrowth was observed when labelled NSCs were transplanted in the presence of a magnet

compared to the non-magnet group. The authors attributed this effect to localisation of NSCs and therefore a more concentrated effect on stimulation of axon growth by the magnetically targeted NSCs compared with more 'scattered' NSCs in the no magnet group; although accumulation of NSCs was not quantified.[80]

In the second study, Song *et al.* labelled an NSC cell line with Feridex, using poly-L-lysine (PLL) as a transfection agent. Cerebral focal ischaemia was induced in rats who then received tail vein injection of the magnetically labelled NSCs with or without a magnet applied to the skull above the infarct site. Greater numbers of labelled NSCs were observed, in the infarct, in the magnet group compared to the no magnet group as judged by an examination of the area of Prussian blue staining (detects iron) and quantification of the amount of iron in the tissue surrounding the infarct by spectrometry. Further, transplantation of labelled NSCs in the presence of a magnet significantly reduced the infarct volume compared to controls and non-magnet treated groups, demonstrating a functional improvement when utilising this strategy.[64] This latter study is particularly exciting in terms of translating magnetic stem cell targeting to the clinic as the labelled cells were injected intravenously, a considerably safer means of cell administration than direct transplantation into the CNS, and still observed to accumulate at the desired site and exert a functional effect.

Although these two studies are promising from a mechanistic point of view, the first utilised MPs which labelled the exterior cell membrane of NSCs. This strategy may show utility in an organotypic slice model, but the MPs may have an increased likelihood of removal *in vivo* (e.g. through enzymatic cleavage of the linkers attaching the particles to the cell) – which would result in loss of their functional capacity and the potential for toxicity to surrounding tissue. The second study utilised a transfection agent to enhance uptake in NSCs. Transfection agents have been shown to demonstrate toxicity[165] and therefore, may not be a clinically translatable strategy for

cell labelling (expanded in **Section 3.1.1**). This study was also performed with an immortalised cell line, which as discussed in the General Introduction (**Section 1.13**) may not be a reliable indicator of particle uptake and toxicity in primary NSCs – a more physiologically relevant cell population. Therefore, there is a current requirement to develop neuro-compatible particles, with the capacity to mediate magnetic targeting, and protocols to efficiently label primary NSCs without affecting key regenerative properties.

3.1.1 The need for a clinically applicable approach to improve MP labelling in NSCs

In studies where magnetic localisation strategies have worked previously, cells have been highly loaded with MPs resulting in high intracellular iron concentrations (24.7 pg/cell in endothelial cells[101] and 225 pg/cell in MSCs[161]). This improves the responsiveness of the cells to a magnetic field and therefore enables their manipulation by magnetic force. Some cells appear to inherently take particles up to a large extent, including endothelial cells[101] and MSCs[161] (both demonstrated to be amenable to magnetic localisation approaches) without the use of particle uptake enhancing strategies. However, non-phagocytic cells, including stem cells, are generally thought to be difficult to label with MPs alone.[166] For example, Neri *et al.* studied labelling of NSCs with two clinical contrast agents: Sinerem and Endorem. Sinerem (incubated for 48 h) labelled ca. 50% of NSCs and Endorem (incubated for 24 h) ca. 60%. For both particles, only small accumulations of MPs (<50% of the nuclear area estimated from images in this paper) were observed in the NSCs as judged by Perl's staining.[167] Confirming this finding, we have observed in our laboratory that primary NSCs display low accumulation of several MPs, including, two commercially available fluorescent MPs, Spherofluor™ and nano-screenMAG/P-CMX (both formulations labelling ca. 40% cells), and a clinical MP used as a contrast agent for MRI, Lumirem® (ca. 40% cells labelled). Reasons for the low levels of labelling achieved in NSCs are not yet clear, however, a barrier to

particle uptake in NSCs could be their limited endocytotic activity. We recently showed using a high resolution membrane imaging technique (termed OTOTO-FESEM, described in **Section 2.4.4**) that cellular membrane activity can be correlated to MP uptake in cells of the CNS.[168] When the technique was used to visualise NSC membranes, these were found to be relatively quiescent, indicating low endocytotic activity. Low NSC membrane activity is most apparent when compared with microglia and astrocytes – two cell types with phagocytic and endocytotic functions in the CNS (**Figure 3.1**). Manipulating cells using magnets requires high intracellular iron content, in a large proportion of the transplant population. Therefore, it is critical to overcome low labelling of NSCs in order to achieve functional levels of intracellular MPs for therapeutic applications in MRI tracking or magnetic cell targeting.

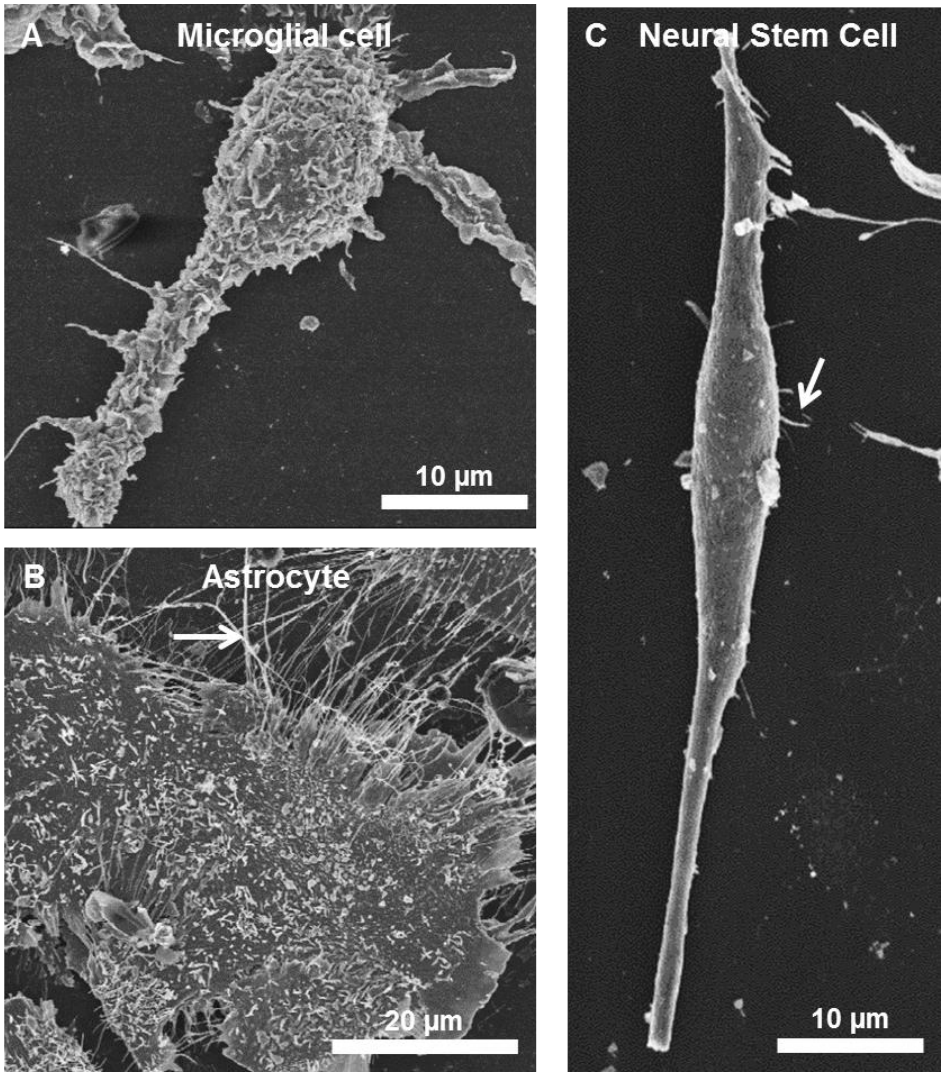

Figure 3.1. Comparison of relative membrane activity of neural cells. *Representative images of (A) a microglial cell (B) an astrocyte and (C) an NSC fixed by OTOTO and imaged using FESEM. Note that the membranes of the microglia and astrocyte cell seem more active displaying a greater extent of ruffling (especially apparent on the microglial cell) and cellular protrusions (arrows) than the NSC.*

In this context, several strategies have been used in an attempt to achieve highly loaded NSCs in order that they can be visualised by MRI; a technique widely studied for non-invasive tracking of

cells after transplantation. These include high iron concentrations in the media, long incubation times (>48 h), use of transfection agents and novel particle design (summarised in **Table 3.1**) which may all be disadvantageous in terms of a clinical labelling strategy. High iron concentrations could lead to cellular toxicity and also particle aggregation; undesirable from a clinical point of view as transplanting iron aggregates can lead to false identification of cell localisation. Long incubation times are inefficient for use in the clinic and increase chances of infection associated with longer culture periods. Transfection agents such as PLL and protamine sulphate are widely used in this field and can dramatically improve labelling, both percentage of labelled cells and extent of MP accumulation within labelled cells. For example, for a 48 h incubation period, proportions of NSCs labelled with Sinerem (clinical grade MP designed for lymph node imaging) increased from 50 to 100%, with large deposits of iron in each cell, when labelling was performed in the presence of PLL.[167] Although protamine sulphate is approved for clinical application, use of transfection agents to enhance MP uptake may not be a clinically viable strategy. A range of transfection agents have been shown to display dose dependent toxicity, including PLL, through mechanisms such as pore formation in the cellular membrane leading to an imbalance of the intracellular ionic environment.[165] Further, there is a risk of complexes precipitating when using MPs in conjunction with transfection agents. This can affect uptake dynamics or potentially lead to adverse immune reactions if the cells are to be transplanted.[169]

The capacity of a few novel particles to act as MRI contrast agents in NSCs has also been tested. A chitosan coated particle has been shown to provide *in vitro* contrast enhancement for MRI of labelled cells.[170] Chitosan is a natural cationic polymer capable of acting as a transfection agent and is therefore proposed to interact with the cell membrane to enhance particle uptake. In this study, chitosan coated MPs appeared to be more readily taken up than naked MPs and displayed large intracellular accumulations as judged by TEM. It was reported that no naked MPs were observed intracellularly resulting in greatly reduced MRI contrast enhancement compared to

chitosan coated MP labelled cells. However, some dissociation of chitosan from the MPs was observed which could lead to toxicity in a similar manner to other polycationic transfection agents i.e. pore formation in the cellular membrane and an intracellular ionic imbalance. Further, no information was provided on the extent of NSC labelling. Therefore, it is not clear whether the whole population of cells is labelled and ultimately trackable. Fluorescent silica MPs have also been synthesised and shown to internalise in NSCs.[171] These particles are designed to display high relaxivity values to increase the sensitivity of MP labelled cell tracking by MRI. In this study, NSCs were labelled with the silica MPs and injected intravenously into the tails of mice which had been experimentally treated to model stroke. NSCs were shown to localise to areas of ischemic brain by MRI which was confirmed with histological analysis. Although an interesting study, labelling was performed in the C17.2 NSC cell line (which may not be clinically relevant as explained in the General Introduction, **Section 1.13**) and no data was provided on the effect of labelling on differentiation of the stem cells; an important property given their potential to replace lost cell populations in lesion sites.

Cell type	Particle and labelling strategy	Proof of uptake	Labelling efficiencies	Functional readout?	Reference
Mouse NSCs	Feridex PLL	-	95%	*Ex vivo*, *In vivo* MRI	[66]
Human NSCs from Stem Cells Inc.	Feridex 24 h incubation + protamine sulphate	Prussian blue	98%	*In vivo* MRI	[172]
C17.2 NSC cell line	Feridex 24 h incubation	Prussian blue	85%	*In vivo* MRI	[96]
PC-12 cell line	Feridex complexed with viral vectors 6 h incubation	Prussian blue, MRI in vitro, AAS	Fe: 5.6 pg/cell	*In vitro* MRI though no values of relaxivity	[173]
Transduced cell lines to express transferrin receptor	MP conjugated to transferrin	Prussian blue, AAS	Fe: 0.25 pg/cell	In vitro MRI	[174]
Mouse NSCs	Endorem, Resovist and Sinerem 72 h incubation	Prussian blue	Endorem: 97% Resovist: 100% Sinerem: 15%	*In vitro* + *In vivo* MRI	[175]
Human NSC cell lines	Endorem 24 h incubation + PLL Sinerem 48 h incubation	Prussian blue	>80% ca. 70 and 50% for non-toxic doses of endorem and sinerem w/o TA	*In vivo MRI*	[167]
Rat NSCs	Feridex 48 h incubation	Prussian blue	100% Fe: 5.3 pg/cell	*In vivo MRI*	[176]
Rat NSCs not reported whether primary	Chitosan coated particle 2 h incubation	TEM, confocal	Not reported	NMR and MRI measurements on cells in gels	[170]
C17.2 NSC cell line	Silica MPs	Confocal, Prussian blue	Fe: 10 pg/cell	*In vivo* MRI	[171]
HB1.F3 human NSC cell line	Feridex 1 h incubation + PLL	Prussian blue	Fe: 260 pg/cell	*In vivo* magnetic targeting	[64]

Table 3.1. Labelling strategies and efficiencies achieved in NSCs. *AAS – atomic absorption spectroscopy; TA – transfection agent; NMR – nuclear magnetic resonance imaging.*

Novel particle engineering strategies are also being investigated to improve cell uptake. CPPs have been widely shown to be useful in increasing uptake of quantum dots, liposomes and nanoparticles.[177] CPPs are peptides which can cross cellular membranes and the most commonly used is the HIV-1 TAT peptide. One study has engineered MPs with TAT to improve gene delivery using MPs into the NT-2 human NSC cell line.[178] However, in this study the main target was U251 cells, an astrocytoma cell line, and no toxicity data was reported when delivering the MPs into NSCs. Although this may be a promising strategy, CPPs are associated with several concerns for potential therapeutic use. For example, it has been shown that gold nanoparticles modified with TAT can translocate into the nucleus,[179] especially undesirable for iron oxide based nanoparticles as free iron can cause oxidative damage to DNA.[166] In the same study, it was also observed that particles tended to be cleared from the cell over 24 h, possibly through exocytosis although this was not confirmed.[179] This last point results in the particles being ejected from the cells potentially before they have been useful for cell tracking or magnetic cell targeting. Currently, the use of CPPs to enhance uptake in neural cells is poorly researched both in terms of functional outcome and safety therefore their translation into the clinic is not expected to be imminent.

To avoid the use of transfection agents and modification of MPs, an alternative 'physical' particle delivery strategy could be to use magnetic fields to pull particles onto the surface of the cells. This strategy was explored in Chapter 2 and is widely used for magnetofection procedures (and most commonly for gene delivery grade particles but not MPs acting as labelling agents for MRI or magnetic targeting).[86] This approach utilises cells' natural endocytotic machinery[92] ensuring cells retain their membrane integrity (as opposed to transfection agent use) resulting in high safety. In addition, particle association with cells can be in the order of minutes and cells can be incubated with lower doses of particles whilst still achieving efficient labelling. Despite these advantages, detailed examination of this physical delivery strategy to enhance NSC labelling using functional MPs (e.g. capable of mediating magnetic cell targeting) has not been performed. It should be

noted that, although this strategy has proven efficacious in neural cells for transfection grade particles, these particles generally have a low iron content so are not suited for cell tracking through MRI or magnetic cell targeting. Further, the uptake of these particles in neural cells is predominately driven by the transfecting component; therefore, findings using these particles may not extrapolate to studies using particles proven efficacious for MRI or cell targeting (e.g. Feridex). In light of these observations, this chapter aims to investigate the use of magnetolabelling strategies (the application of static/oscillating magnetic fields during MP incubation) to overcome low intracellular particle accumulation in NSCs.

3.1.2 The need to investigate tailoring of MP magnetite content

In terms of a magnetolabelling approach, MP response to a magnetic field is proportional to its magnetic moment. Therefore, it may be predicted that a promising strategy to improve magnetolabelling efficiency would be to increase magnetite entrapment within MPs so that, in the presence of a magnetic field, MP sedimentation and subsequent cellular contact would be enhanced. Increasing particle magnetite content will also increase particle density which may have a further effect on the particles sedimentary properties additionally facilitating enhanced cellular uptake through increased contact. Application of magnetic fields and modulating magnetite content of MPs has shown benefits for labelling BAECs.[162] Here, three PLA-based particles of different iron content were added to the culture medium either in the absence or presence of a magnet beneath the culture plate for the duration of the labelling procedure (24 h). Greatest labelling efficiency (Fe: 26 pg/cell) was achieved using the highest magnetite content particle in conjunction with an applied magnetic field. Although interesting in terms of labelling endothelial cells, these cell types show relatively high levels of particle internalisation in the absence of uptake promoting strategies.[101] In addition, oscillating magnetic fields have been

shown to enhance uptake of transfection grade MPs in neural cells but were not studied here. Therefore, an additional goal of this chapter is to investigate how application of static and oscillating magnetic fields effects labelling of '*hard to transfect*' NSCs when using particles containing different magnetite contents.

3.1.3 Assessment of the translational potential of the developed protocols using *in vitro* models

The safety and utility of the developed protocols will also be tested by transplanting labelled NSCs into a slice model of SCI, to investigate cell survival and differentiation post-transplantation. Use of organotypic slices could reduce, refine and replace animal usage in accordance with the 3R's principle. As outlined in the General Introduction (**Section 1.14**) and Chapter 2 (**Section 2.1.3**) organotypic slice culture may be used for a rapid and cost effective assessment of transplantation into host tissue representative of *in vivo* environments. In Chapter 2 a slice model of the cerebellum was used as host tissue to test the transplantation of genetically engineered NSCs into a 'healthy' representation of CNS tissue (i.e. no injuries or disease states were induced in the model). The slice model of SCI, also developed in our laboratory, potentially has more clinical utility in representing a pathological condition for testing various nanotechnological interventions. To generate the model, spinal cords are dissected from mice, sliced longitudinally and these slices are cultured at an air-medium interface. A transecting lesion can then be introduced to mimic SCI. This model has been extensively characterised and shown to display signs of astrocyte scar formation, axonal regeneration and microglial infiltration into the lesion site; all characteristic features of *in vivo* SCI.[120] Therefore, the model provides a pathological system to test novel nanomaterials and cell transplantation but the utility of the model for investigating transplantation of labelled NSCs in the model has not been tested.

In addition to the slice model, an *in vitro* flow system will be used to examine whether magnetically labelled cells can be captured by magnetic force. In a similar manner to the *in vitro* slice model, this test could provide a rapid readout as to whether the developed protocols can sufficiently label cells for magnetic localisation strategies, reducing the reliance on animal models for these experiments. Use of these *in vitro* models may therefore provide two functional readouts important for assessing the ultimate translational potential of the developed protocols, namely, survival of the cells in host tissue mimicking injury pathology and capacity of the protocols to produce cells which can be trapped by magnetic force.

3.1.4 Chapter objectives

Given the lack of clinically applicable protocols for efficiently labelling NSCs, this chapter will explore whether modulation of the magnetite content of MPs in conjunction with application of magnetic fields can offer a safe, alternative strategy to enhance NSC labelling. This will be achieved using PLA-based particles, without a transfection component, whose magnetite content can be tuned to endow the particles with different magnetic properties. Importantly, this can be achieved without varying other key physicochemical properties of the particles including size and surface charge. This is critical for exclusively relating particle magnetite content to uptake as size and surface charge can both affect cellular internalisation. These particles have been kindly formulated by Dr Boris Polyak. For clarity and in order to be able to observe the differences between the particles, the formulation and characterisation (performed by Dr Boris Polyak and Dr Humphrey Yiu [Heriot Watt University, Edinburgh]) of these particles are outlined in the Methods and Results sections respectively. The specific objectives of this chapter are to:

(i) To investigate the effect of systematically modulating magnetite content on MP uptake in primary NSCs in the absence or presence of magnetic fields (static and oscillating).

(ii) To examine effects of the developed protocols on key regenerative features of the NSC population.

(iii) To investigate the utility of the slice model of SCI to assess survival and differentiation of labelled NSCs after transplantation.

(iv) To test the translational potential of the developed protocols by investigating magnetic cell targeting of labelled NSCs in an *in vitro flow* system.

3.2 Methods

All materials and methods are the same as for Chapter 2 including NSC derivation, media composition, fixation and immunostaining unless otherwise stated.

3.2.1 Reagents

Magnetic particles (BP): Poly(D,L-lactic acid) (PLA, average Mw: 75–120 kD), ferric chloride hexahydrate, ferrous chloride tetrahydrate, sodium hydroxide, oleic acid, and poly(vinyl alcohol) (PVA, 87-90% hydrolyzed, average Mw: 30-70 kD), were purchased from Sigma-Aldrich (St. Louis, MO, USA). PLA covalently labelled with BODIPY® 564/570 (Life Technologies™) was a generous gift of Dr. Robert Levy from the Children's Hospital of Philadelphia. All solvents were of HPLC grade and supplied by Fisher Scientific (Pittsburgh, PA, USA). Deionised water used in particle

synthesis procedures was obtained using a Milli-Q water purification system. Glass fiber 1.0 µm and 5.0 µm syringe driven filters were purchased from Millipore (Millipore, Bedford MA, USA).

Cell and slice culture: TrypLE was from Fisher. Amphotericin and DAPI were from Sigma.

3.2.2 Magnetic particle synthesis (BP)

To examine whether changing the physicochemical properties of magnetic particles affects their uptake by NSCs four particles were synthesised with different magnetite contents. A schematic of the synthesis is provided as **Figure 3.2**. A mass ratio of 1:3:7 of magnetite was used to prepare three MPs which resulted in a weight percent ratio of incorporated magnetite within their polymeric matrix of 1:3:5; originating the names for the MP formulations as MP-1X, MP-3X and MP-5X. A non-magnetic particle with no magnetite was also synthesised and termed Non-mag. Magnetite was prepared from ferric and ferrous chloride by alkaline precipitation (Massart method)[180] as previously described.[162,181] In brief, for MP-1X, 65 and 24 mg of ferric and ferrous chloride were dissolved in 9.04 mL of water and precipitated with 0.96 mL of 1N NaOH; for MP-3X, 195 and 72 mg of ferric and ferrous chloride were dissolved in 7.12 mL of water and precipitated with 2.88 mL of 1N NaOH; for MP-5X, 455 and 168 mg of ferric and ferrous chloride were dissolved in 3.28 mL of water and precipitated with 6.72 mL of 1N NaOH. After magnetic separation precipitated magnetite in each formulation was washed twice with degassed deionised water, re-suspended in 2 mL of ethanol and coated with 100 mg (for MP-1X), 150 mg (for MP-3X) or 200 mg (for MP-5X) oleic acid by heating under argon to 90°C for 10 min in a water bath. Phase-separation of excess oleic acid was achieved by drop-wise addition of 4 mL of water followed by two washes of the lipophilic magnetite with ethanol. The different amounts of lipophilic magnetite for the different formulations (28, 84 and 196 mg, based on the input of iron

salts) were dispersed in 6 mL of chloroform, forming stable magnetic fluids which were used for the rest of the particle formulations. PLA-based magnetite-loaded particles were prepared by the modified emulsification-solvent evaporation method as described elsewhere.[162,181] To formulate fluorescent PLA-based MPs, 180 mg of non-labelled PLA and 20 mg of fluorescently labelled BODIPY® (564/570) PLA were added to 6 mL of the appropriate magnetic fluid to form an organic phase. The organic phase was emulsified in 15 mL of pre-chilled 1.5% (w/v) PVA by sonication, and the organic solvents were removed by evaporation under reduced pressure at 30°C. The particles were passed through a 1.0 µm glass fibre before being lyophilised with 10% (w/v) trehalose as a cryoprotectant. Lyophilised MPs were kept at 4°C in 100 µL aliquots and re-suspended in deionised water before use.

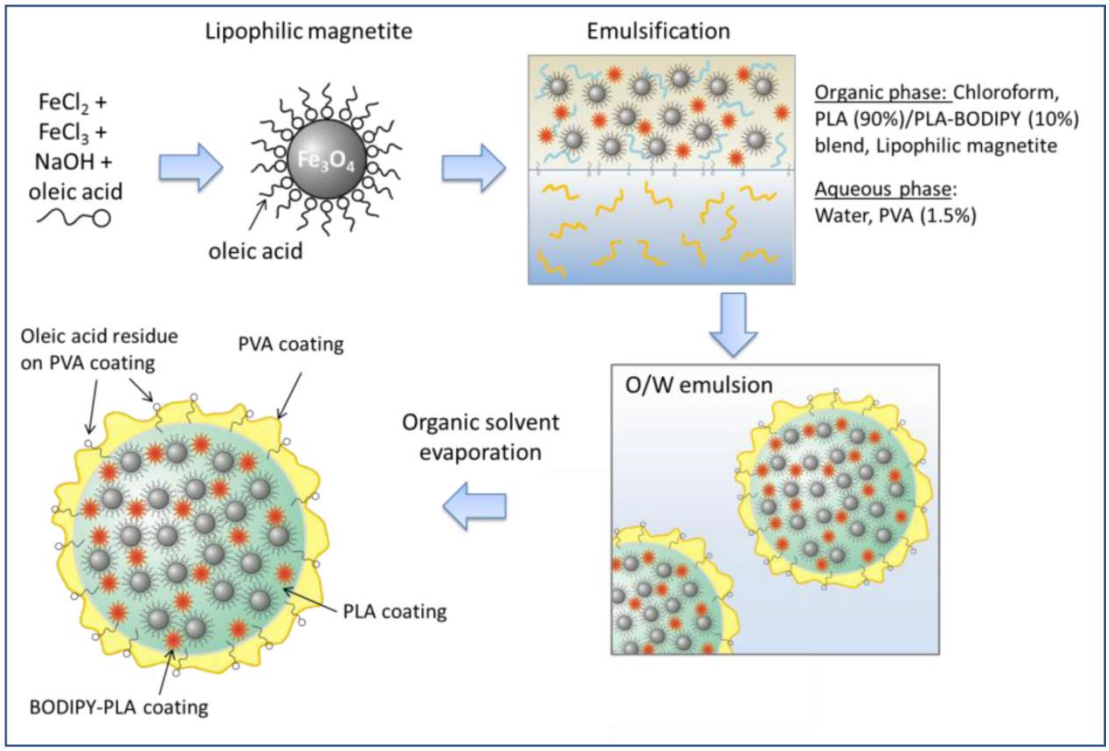

Figure 3.2. Schematic diagram for synthesis of PLA based MPs. *(BP + HY)*

3.2.3 MP characterisations (BP + HY)

Particle size and zeta-potential measurements were determined by DLS using a DelsaNano C particle size analyzer equipped with two laser diodes (658 nm, 30 mW, Beckman-Coulter, CA). The magnetic properties of MPs were obtained from the hysteresis curves of dry samples measured by an alternating gradient magnetometer (Princeton Instruments Corporation, Princeton, NJ, USA). The magnetite content of MPs was determined after MP degradation with 1N NaOH (90°C, 30 min), and dissolution of the iron precipitate in HCl, by spectroscopy (using Synergy 4TM multimode plate reader, BioTek Instruments, Inc. Winooski, VT, USA and UV compatible 96-well plates, BD Biosciences, Franklin Lakes, NJ, USA) and comparison to a standard curve.[162,181]

Fourier transform infrared (FTIR) spectroscopic analysis, to examine molecular composition of the particles, was carried out using a Perkin Elmer (Coventry, UK) Spectrum 100 spectrometer fitted with an attenuated total reflection sampling unit. For the sample measurement, 32 scans in the region from 650 to 4000 cm^{-1} were accumulated with a resolution of 4 cm^{-1}.

To examine the crystal structure of the particles, a Bruker D8 Advance diffractometer was used for powder XRD (x-ray diffraction) analysis on the particles with Cu Kα1 radiation (λ = 1.542 Å). The diffraction pattern was collected from 2θ = 5° to 80°, at a step size of 0.009° and a step time of 120 s.

CHN (carbon, hydrogen, nitrogen) elemental analysis was carried out using an Exeter CE-440 Elemental Analyser. The inorganic content of the particle samples was calculated based on the C% (with an accuracy of ± 0.2%) from the CHN analysis results.

3.2.4 Labelling NSC monolayers with MPs

In this chapter labelling of NSCs with the different particle formulations was assessed in monolayer cultures. As described in Chapter 2, this culture system has specific clinical advantages for transplantation but also for particle labelling (all cells are exposed to the particles and experience a uniform magnetic field application). NSCs were plated out at slightly lower concentrations than Chapter 2 (1.2×10^5 cells in 600 µL ML-M per well) as this achieved more spatial separation of cells adhered to the coverslip. This reduces cell clustering which can confound particle internalisation analysis. NSCs were plated in 24 well plates on coated glass (or aclar for TEM analysis) coverslips.

NSCs were cultured as monolayers for 24 h before changing to fresh ML-M with or without particles. To prepare particle suspensions, 100 µL lyophilised aliquots (containing the same number of particles for each particle type) were re-suspended in 100 µL water and added to ML-M to achieve the desired concentration. An optimal particle dose was established by incubating NSCs with increasing ratios of particle suspensions to ML-M (0.01, 0.1, 1, 2, 5 and 10 µL/mL) and observing cell adherence and morphology, to determine effect on cell health, and extent of uptake.

For subsequent experiments a concentration of 1 µL/mL was chosen (which correlated to approximately 13 µg/mL of dry weight for Non-mag particles, 15 µg/mL for MP-1X, 19 µg/mL for MP-3X and 26.5 µg/mL for MP-5X). Cells were incubated for 24 h under no-field or with exposure to static or oscillating (F = 4 Hz) magnetic fields for the first 30 min. Only one oscillating field of 4 Hz was chosen as it had been previously shown to be optimal for NSC transfection (Chapter 2, **Section 2.3.2**). Field application was also restricted to 30 min as significant particle aggregation on the surface of the cells was observed when incubating with the MP-5X formulation in combination with 24 h field application. After incubation, cells were washed 3-5 times with PBS to remove

particles not internalised. Cultures were then either: fixed for immunocytochemistry or TEM (**Section 3.2.8 and 3.2.9**), to assess particle uptake, numbers of nuclei and pyknotic nuclei per field and stem cell marker expression; dissociated for magnetic cell capture experiments (**Section 3.2.13**); or switched to differentiation medium and cultured for a further 7 days with media changes every 2-3 days, to assess NSC differentiation profiles post-labelling.

3.2.5 MTS assay

To investigate the effects of the labelling protocols on mitochondrial function, an MTS assay was performed. Here, NSCs were labelled as per the protocols described in **Section 3.2.4** in duplicate wells. After 24 h labelling, MTS reagent was added into the wells and incubated for 3 h. Blanks consisted of media containing the appropriate particles and controls were untreated cells. After 3 h incubation 200 µL aliquots from each well were added to a 96 well plate and the absorbance measured at 490 nm. Adjusted absorbance readings were calculated by averaging the results from the two duplicate wells and subtracting blank readings. These were then displayed as a percentage of the control readings.

3.2.6 Organotypic spinal cord slice derivation and culture

To generate organotypic SCI models to investigate labelled NSC transplantation, spinal cords from mice pups (post natal days 1–3) were dissected out into slicing medium and sliced longitudinally using a McIlwain tissue chopper (set to 350 µm). Slices were incubated on ice for 60 min before transfer to pre-cut Omnipore membranes sat on Millicell slice culture inserts. They were cultured in spinal cord slice culture medium (Chapter 2, **Table 2.4**) at 37^{o}C/5% CO_2 for a maximum of 14 days, with feeding every 2-3 days (80% medium change). To create a model of SCI, slices were

lesioned after 2-4 days in culture using a tool developed in the laboratory, constructed from two parallel scalpel blades, which allowed a section of tissue ca. 400 µm to be excised. Any remaining tissue in the lesion site was removed by careful aspiration which ensured complete transection between the two halves of the spinal cord allowing visualisation of regenerative events.

3.2.7 Labelled NSC transplantation into organotypic slice cultures of SCI

For transplantation of labelled NSCs into lesions of the organotypic SCI model, NSCs were labeled with DAPI at 20 µg/mL for 20 minutes and washed twice in PBS before 1.2 x10^4 NSCs were resuspended in 0.25 µL of ML-M. These were focally transplanted into lesion sites 24 h after lesioning. Slices were subsequently fixed 2 h, 48 h and 1 week post-transplantation.

3.2.8 Fixation

Cells and slices were fixed for immunocytochemistry as in Chapter 2 (**Section 2.2.14**). For examination of particle internalisation by TEM cells on aclar coverslips were fixed in 2.5% glutaraldehyde in SCB (0.1M sodium cacodylate buffer containing 2mM calcium chloride) for 2 h at RT. Glutaraldehyde fixed samples were washed three times in SCB before further processing.

3.2.9 TEM processing of NSCs

Glutaraldehyde fixed, NSC samples were post-fixed in 1% osmium tetroxide in SCB. Samples were washed three times in SCB then dehydrated through an ethanol series. Dehydrated samples were embedded in Spurr resin which was subsequently polymerized (60°C, 16 h). Samples were

sectioned perpendicular to the aclar sheet using a Reichert (Buffalo, NY, USA) Ultracut E microtome. As there was some difficulty in viewing sections which were mounted on grids due to bars obscuring the sample, formvar grids were utilised. These consist of a TEM grid with an empty middle section. Coating the grid with a thin layer of formvar (ca. 300 nm), which spans the middle section, allows sections to be mounted on an electron permeable membrane and for the whole section to be examined. Mounted sections were stained with 2% uranyl acetate in 70% ethanol (RT, 20 min) and 2% Reynolds lead citrate (RT, 5 min) before being examined.

3.2.10 Imaging

Fluorescence and light microscopy: Imaging was performed as in Chapter 2 (**Section 2.2.18**).

Z-stack microscopy: Z-stacks of NSCs labelled with PLA based MPs were obtained using a Nikon Eclipse 80i microscope fitted with a CA742-95 camera (Hamamatsu Photonics, Hamamatsu, Japan), with 1.0 µm incremental manual focus stepping. The resulting stacks were processed using Nikon NIS Elements (version 3.00).

TEM: Sections mounted on grids were examined using a JEOL (Tokyo, Japan) 100-CX transmission electron microscope operated at 100 kV. Images were captured using a SIS systems Megaview III digital camera (Olympus, Tokyo, Japan).

TEM of MP samples (BP) was performed by using JEM-1230 electron microscope (JEOL ltd, Japan) operated at 80kV. MP samples were diluted 1:10 with deionised water and deposited on carbon coated grids (Electron Microscopy Sciences, USA) with no use of contrast staining.

3.2.11 Assessment of PLA particle labelling efficiency

Particle internalization was quantified microscopically in fixed, nestin positive NSCs. Microscopic analysis of particle uptake was chosen as this permits analysis of particle internalisation and parameters of cell health to be conducted in parallel. In particular for particle uptake analysis, particle localisation within the cells can be discriminated from adherence to the cell membrane and the extent of particle uptake can also be assessed - important in primary NSCs which display heterogeneous particle uptake. Also, techniques such as flow cytometry do not allow evaluation of cellular morphology and therefore particle localisation within cells (e.g. peri-nuclear). Other techniques for assessing MP uptake into cells include colorimetric absorbance assays of lysed cells to measure 'intracellular' iron content, however, these values can be confounded by membrane bound MPs indicating that this may not be a robust measure for particle uptake in neural cells. Quadruple merged microscopic images (including phase images), taken at X400, were used to confirm whether particles were intracellular. Proportions of labelled cells and the extent of cellular labelling (unlabelled, low, medium or high labelling) were then determined from three fields with ca. 250 nuclei counted for each labelling condition. The extent of labelling was estimated by subjective assessment of the area occupied by particles within each cell: <10%, 10-50%, >50% of the average nuclear area being scored as 'low', 'medium' and 'high' labelling respectively, as previously described.[81,124] Iron quantification (related to the number of intracellular MPs) within cells was also determined spectrophotometrically after lysing cells with radioimmunoprecipitation assay buffer and dissolving the particles in 1N HCl (λ = 335 nm) which was performed by BP as described elsewhere.[162,181]

3.2.12 Examining the safety of labelling protocols

Using samples fixed at 24 h post-labelling, assessment was made of nuclei per field, pyknotic nuclei and the expression of NSC specific markers, nestin and SOX2 as in Chapter 2 (**Section 2.2.20 and 2.2.21**). Generation of daughter cells from labelled NSCs was assessed using samples fixed after 7 days differentiation (8 days post-labelling) by counting specific neural cell markers as in Chapter 2 (**Section 2.2.21**).

3.2.13 Assessment of magnetic localisation capability of MPs

To examine magnetic localisation of the labelled NSCs, cells were labelled for 48 h with application of the F = 4 Hz magnetic field for the first 30 min. Labelled cells were washed three times with PBS to remove free particles, then trypsinised (using TrypLE) and triturated to produce a single cell suspension. Cells were collected by centrifugation followed by two more washes with PBS before finally re-suspending in PBS at a concentration of 1 x 10^5 cells/mL. Labelled cells were subjected to a single pass through a 1.6 mm diameter tubular flow system (**Figure 3.3**). Preliminary experiments indicated that flow rates ≤1 mL/min resulted in high cell loss, presumably due to cellular adherence and aggregation within the flow system, whilst flow rates ≥4 mL/min resulted in minimal magnetic capture. Therefore, an optimal experimental flow rate of 2 mL/min was chosen with an approximate flow velocity of 1.7 cm/s broadly similar to blood flow rates in arterioles and venules.[182] To generate the magnetic field for cell capture, the tubing was placed on top of a magnetic plate (field strength: 316 ± 8 mT) and surrounded by two bar magnets (field strength: 410 ± 10 mT). Magnetic field strengths were measured by an F.W. Bell 5080 Gaussmeter (Pacific Scientific-OECO, Milwaukie, OR). Cell density was estimated before and after passage through the flow system using a haemocytometer and the percentage value for cell retention

within the system was calculated as (cell count after magnet application)/(cell count before magnet application) x 100.

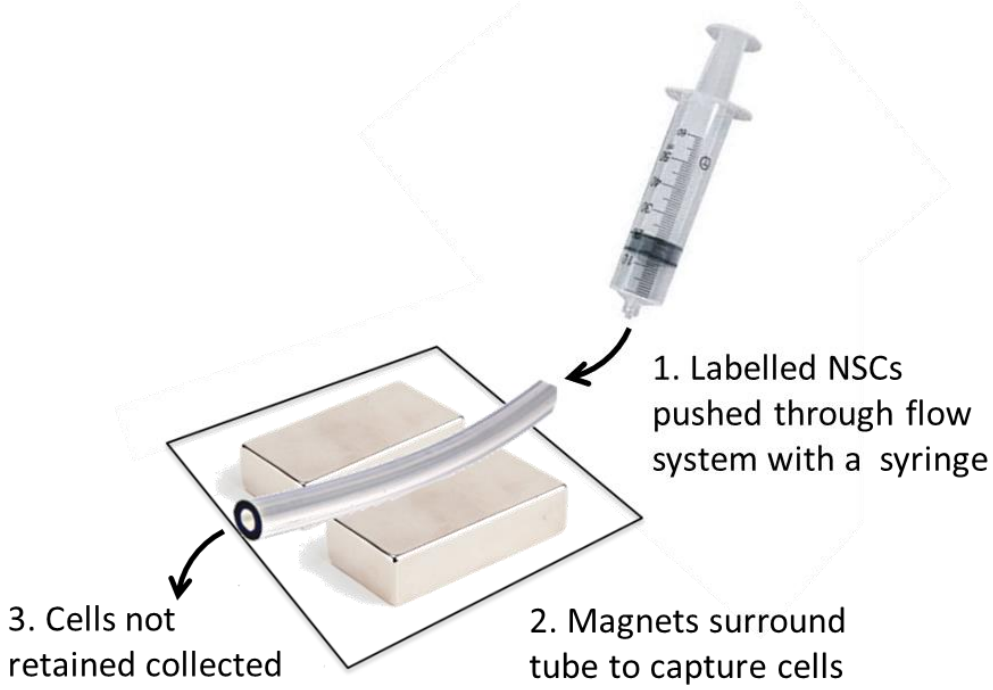

Figure 3.3. Schematic of the in vitro flow system used to assess the capability of magnetically capturing labelled NSCs.

3.2.14 Statistical analysis

Data was split into comparable groups (i.e. with only one variable change per group, for example: Non-mag, MP-1X, MP-3X and MP-5X uptake compared under the no-field condition only, represented a single dataset) for analysis by one-way ANOVA and Bonferroni's MCT using Prism software (version 4.03, Graphpad). Data are expressed as mean ± SEM with 'n' referring to the number of different cultures, each derived from a different mouse litter, except for the magnetic localisation experiments where 'n' refers to number of experiments. A two-way ANOVA was not performed in this chapter as comparisons were not made between groups of data sets.

Comparisons in this chapter are between field conditions for the same particle or between the different particles in each field.

3.3 Results

3.3.1 Culture purity

Monolayer NSC cultures were routinely produced displaying normal adherence, bipolar morphology and circular and intact DAPI nuclei staining as judged by light and fluorescence microscopy respectively. Cultures were also of high purity with 98.3 ± 0.7% (n = 5) and 96.4 ± 1.4% (n = 5) cells expressing nestin and SOX2 respectively.

3.3.2 Particle synthesis and characterisation (BP + HY)

Observation of the particles with TEM revealed they were of similar size with a spherical shape. However, each particle displayed a distinct pattern of magnetite distribution where packing density of magnetite appeared to increase from MP-1X to MP-5X (**Figure 3.4**).

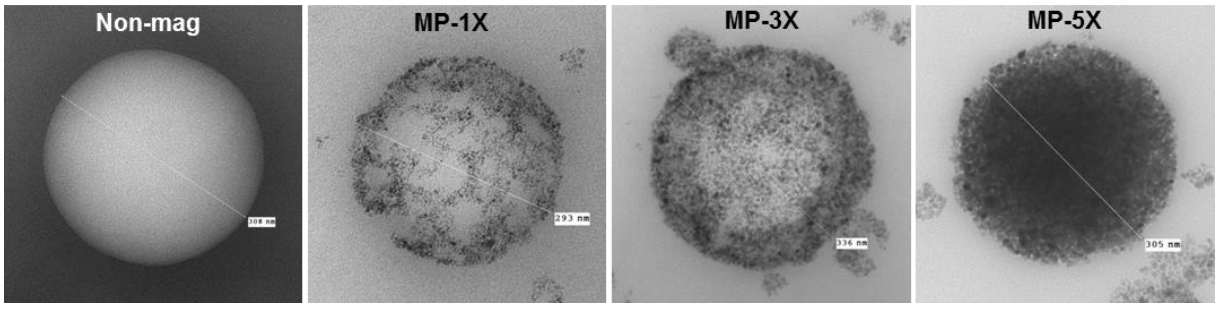

Figure 3.4. TEM analysis of MP formulations. *Images show particles were of a similar size and that iron appears to be more densely packed from MP-1X to MP-5X.*

The magnetic responsiveness of the particles matched this pattern of magnetite packing with no response shown from the Non-mag particles (as expected) and increasing response with increased magnetite content (**Figure 3.5A**). It is important to note here as well that the particles display superparamagnetic response curves with no significant hysteresis (**Figure 3.5A**). DLS confirmed particle size measurements from TEM (**Figure 3.5B** – values in **Table 3.2**) although the particle suspensions had a relatively high poly-dispersity index (0.15-0.23) indicating a heterogeneous size population. However, this was consistent among the formulations so was not a product of increased magnetite content. Zeta-potentials by DLS were all slightly negative with a small increase as magnetite content increased (**Table 3.2**). Size, zeta-potential and magnetisation data are summarised in **Table 3.2**.

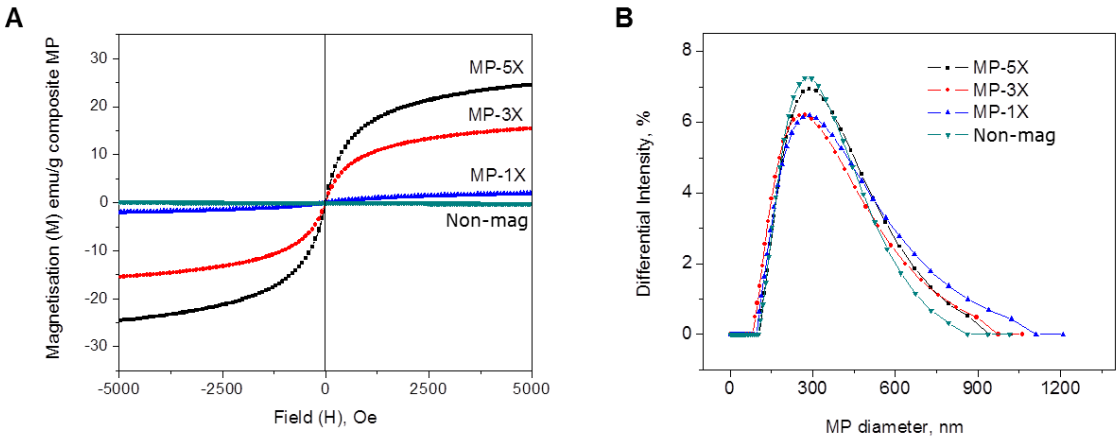

Figure 3.5. Magnetic responsiveness and size of the different particle formulations. *(A) Magnetisation curves of MP formulations measured by alternating gradient magnetometer. Note response increases with increasing magnetite content and curves are absent of hysteresis which is indicative of superparamagnetism. (B) Size distributions of the MP formulations by DLS indicating similar sizes.*

Formulation description	*Weight of formulation corresponding to magnetite (%)*	*MP average size (nm)*	*Poly-dispersity index*	*ζ-potential (mV)*	*Magnetization at 5 kOe (emu/g composite)*
MP-5X	35.4	278 ± 1.6	0.17	-14.4 ± 0.3	24.6 ± 1.2
MP-3X	19.2	254 ± 2.8	0.23	-11.5 ± 0.1	15.2 ± 1.0
MP-1X	6.7	262 ± 9.6	0.15	-9.5 ± 0.1	2.1 ± 0.1
Non-mag NP	-	267 ± 0.7	0.14	-9.0 ± 0.2	-

Table 3.2. Physicochemical properties of the formulated PLA- magnetite MPs.

Similar organic composition of the particles was confirmed using FTIR spectroscopy with expected peaks observed for PLA, oleic acid and PVA (**Figure 3.6A** - example peak identities are in the legend). XRD spectrum of all particles was dominated by PLA suggesting the magnetite is buried within a PLA matrix, however, XRD of the oleic acid coated iron oxide used to formulate the particles confirmed its magnetite nature (**Figure 3.6B**).

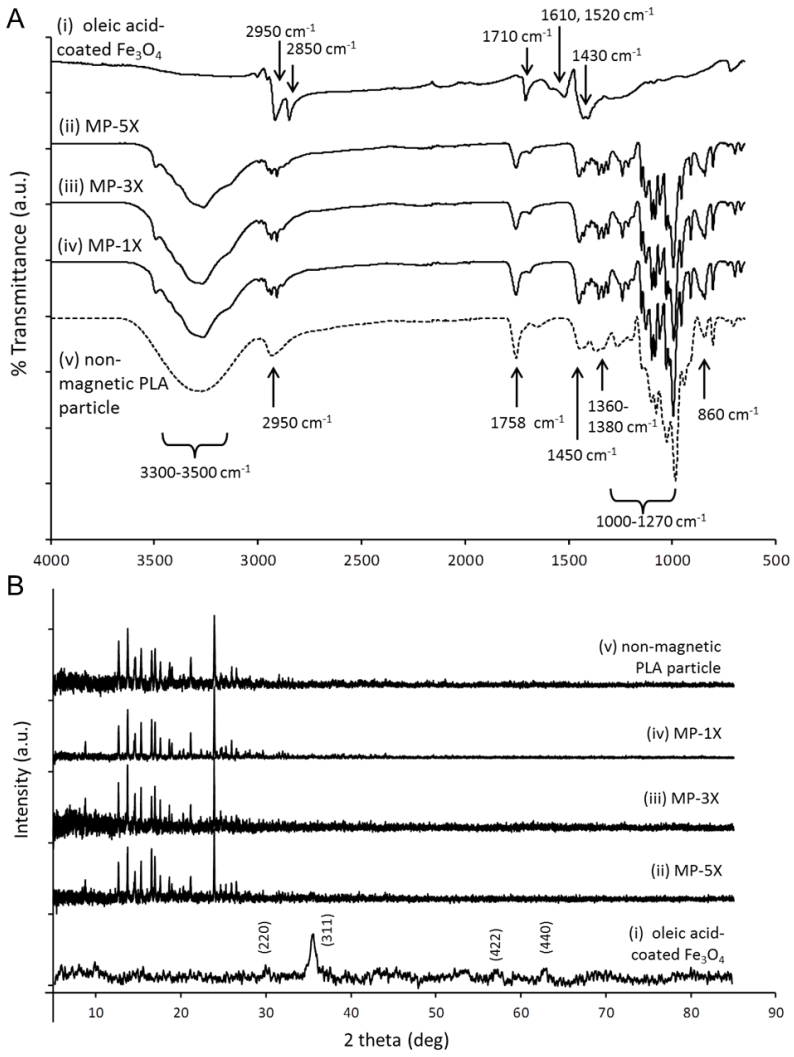

Figure 3.6. FTIR and XRD analysis of MP formulations. *(A) FTIR spectrum of the different MP formulations. Characteristic bands for oleic acids (CH stretching at 2950 and 2850 cm^{-1}, C=O stretching at 1710 cm^{-1} and CH_2 bending at 1430 cm^{-1}) were identified. The adsorption band at 1530 cm^{-1} is assigned as the COO stretching coordinated to iron atoms.*[183] *In all samples vibrational bands indicative of PLA were also observed (OH stretching at 3495 cm^{-1}, CH stretching at 2945 cm^{-1}, C=O stretching at 1758 cm^{-1}, CH_3 bending at 1450 cm^{-1}, CH_2 wagging at 1360-1380 cm^{-1} and C-O stretching at 1050-1270 cm^{-1}.*[184] *The broad peak at 3500 cm^{-1} is attributed to the OH stretching mode of PVA and moisture. (B) Powder XRD diffractions for the different MP formulations. The patterns in (i) are indicative of magnetite.*

3.3.3 Establishing optimal particle dose for labelling NSCs

Preliminary experiments indicated that MP-5X particles were taken up more readily than the other particle formulations. To achieve the experimental aim (investigating the modulation of magnetite content of particles independent of other factors such as surface chemistry or particle concentration) it is vital that the concentration of particles remains the same, therefore, as toxicity is related to levels of uptake, it was decided that an optimal concentration of MP-5X was established which would then be compared to equal amounts of the other particle formulations. For this, a series of MP-5X concentrations were tested from 0.01 µL/mL – 10 µL/mL. Particle uptake was found to be concentration dependant (**Figure 3.7**) with the highest levels of labelling achieved at 1 µL/mL. Concentrations of MP-5X tested above 1 µL/mL (2, 5 and 10 µL/mL) incurred substantial cell loss with the appearance of multiple rounded cells, indicative of cell death, which was attributed to excessive particle uptake by the NSCs. Given these findings it was decided that the concentration used for the rest of the experimental work would be 1 µL/mL.

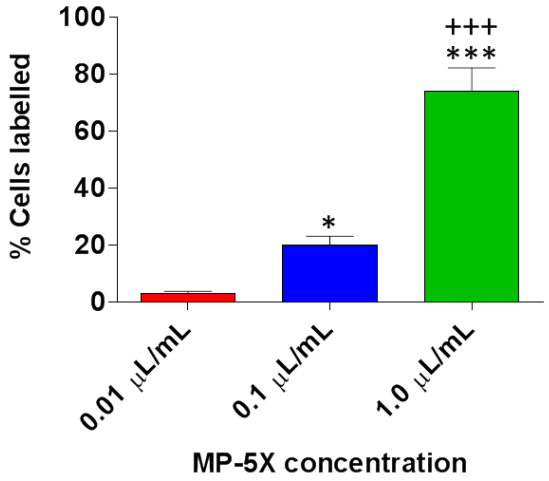

Figure 3.7. Optimising particle concentration for labelling NSCs. *(A) Bar chart depicting percentage of cells labelled when using different concentration of the MP-5X particle formulation. Statistical difference are *p<0.05 and ***p<0.001 vs 0.01 µL/mL; $^{+++}$p<0.001 vs 0.1 µL/mL one-way ANOVA with Bonferroni's MCT, n = 3).*

3.3.4 Confirmation of particle uptake in NSCs

After establishing a safe dose of particles it was assessed whether NSCs internalised the particles. Z-stack microscopy revealed both MP-1X and MP-5X particles accumulated within the cytoplasm, often localising in the peri-nuclear region, but rarely in the cellular processes (**Figure 3.8A**). TEM confirmed this pattern of internalisation although striking differences were seen between MP-5X and MP-1X particles (**Figure 3.8B**): MP-5X particles displayed a strongly electron dense ring-like structure and often appeared as clusters. This was in contrast to MP-1X which were always observed as single particles and had a similar ring-like structure but of apparently much less electron density. No particles were ever observed in the nucleus by z-stack microscopy or TEM and no particles were observed in control NSCs (not exposed to the particles).

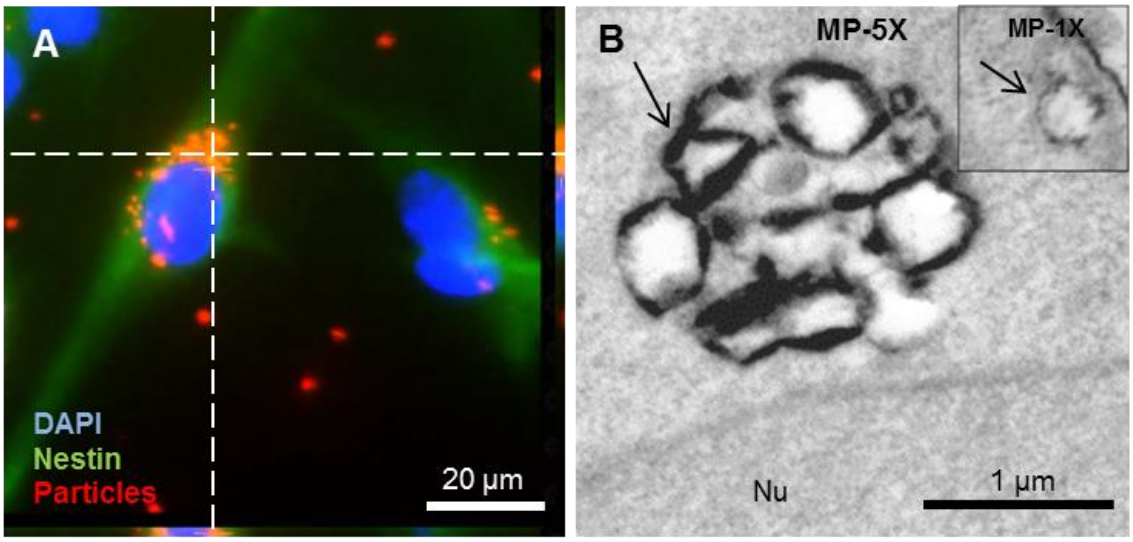

Figure 3.8. Confirmation of particle uptake in NSCs. *(A) Z-stack microscopy revealing clusters of peri-nuclear particles (MP-5X) which the z-stack indicates are in the same plane as the nucleus. (B) TEM section through a labelled cell shows a cluster of MP-5X particles, with a ring like structure of electron dense material, adjacent to the nucleus (Nu). The inset shows a MP-1X particle, always observed as single particles within the cytoplasm. Also, note the less electron dense ring-like structure corresponding to lower magnetite content than the MP-5X formulation.*

3.3.5 Effects of magnetite modulation and magnetic field application on MP uptake in cells

NSC labelling was observed in all conditions with intracellular patterns of labelling as described in **Section 3.3.4**. Basal levels of labelling were observed when using the Non-mag particles of approximately 35% with no effects on levels of labelling achieved when fields were applied. MP-1X labelling without field addition (39.6 ± 2.7%) was similar to that of the Non-mag particle labelling (**Figure 3.9A and 3.10**). However, field application systematically enhanced MP-1X labelling (**Figure 3.9A-B and 3.10**) from static field (53.4 ± 2.4%) to a maximum using the 4 Hz oscillating magnetic field (63.7 ± 3.5%). The percentage of labelled cells then increased with

increasing iron content (within each magnetic field condition) so that the following paradigm existed: MP-1X < MP-3X < MP-5X with optimal labelling achieved in this study using the MP-5X particles with the 4 Hz oscillating field (95.8 ± 1.0%, **Figure 3.9C and 3.10**). It should be noted that although there was a trend towards enhanced labelling when the oscillating field was applied for both MP-3X and MP-5X the increases were not statistically significant in terms of percentage of cells labelled.

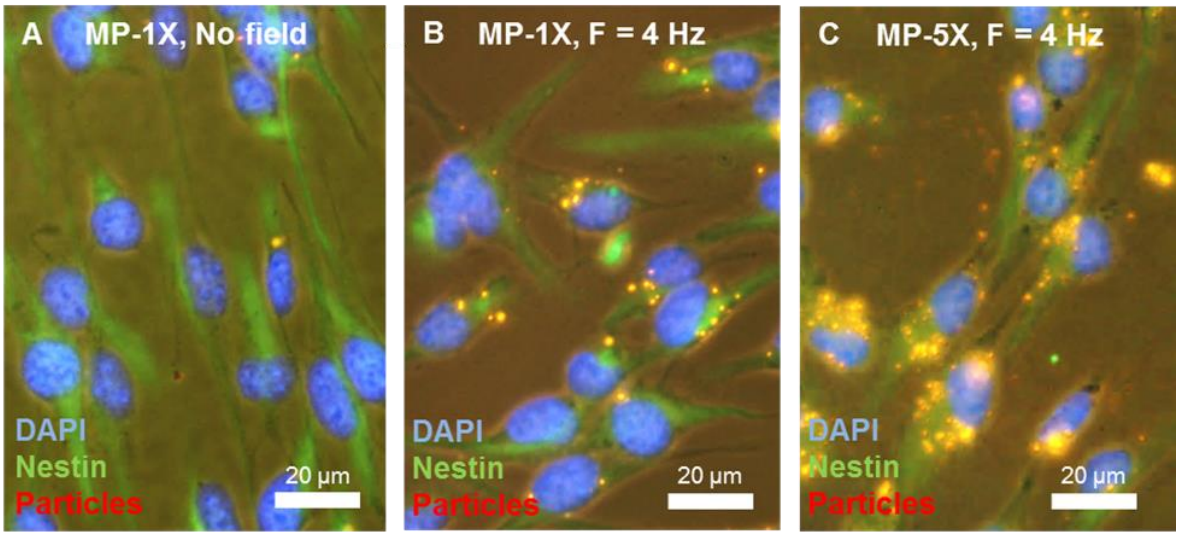

Figure 3.9. Differences in NSC labelling when using particles of different formulations under various magnetic field conditions. *NSCs labelled using MP-1X (A) without a field and (B) with application of an oscillating magnetic field (F = 4 Hz). (C) Optimal NSC labelling; achieved using MP-5X in conjunction with an oscillating magnetic field (F = 4 Hz). Numbers of NSCs labelled and the extent of particle uptake are quantified in Figures 3.10 and 3.11 respectively.*

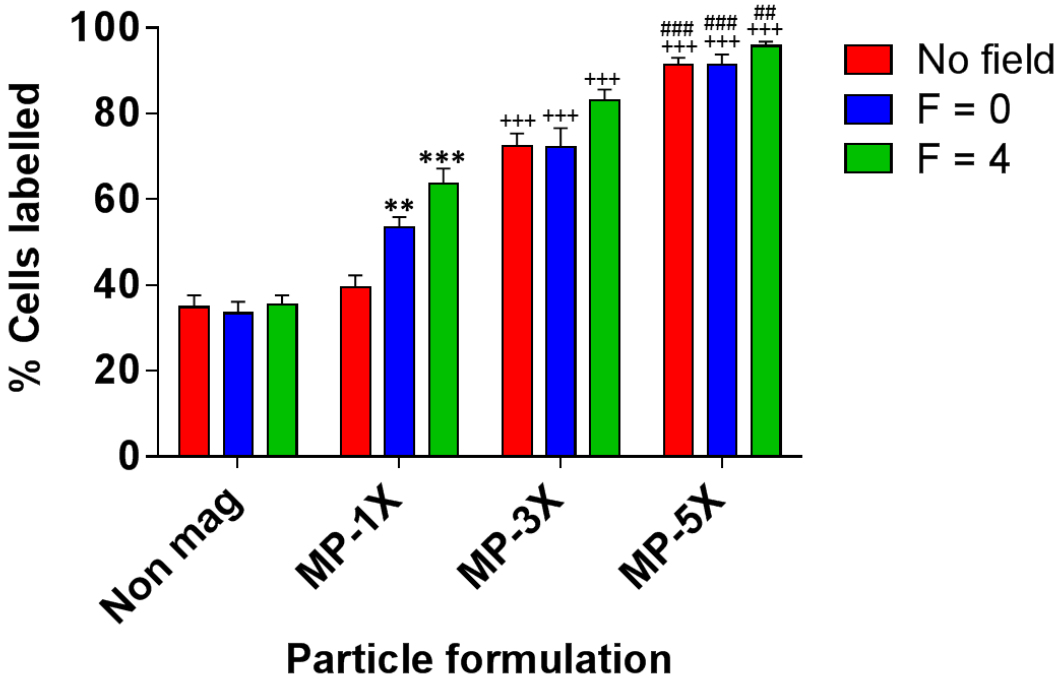

Figure 3.10. Quantification of NSC uptake of the different MPs. *Bar chart displaying percentage of NSCs labelled when using each particle formulation in conjunction with the indicated magnetic field. Statistical differences are: **p<0.01 and ***p<0.001 versus no-field condition labeling at the same particle iron concentration; $^{+++}$p<0.001 versus MP-1X labeling under the same field condition; $^{##}$p<0.01 and $^{###}$p<0.001 versus MP-3X labeling under the same field condition (one-way ANOVA with Bonferroni's MCT, n = 5).*

A semi-quantitative assessment was also made of the extent of uptake of each particle type which generally increased as particle magnetite content increased with more cells displaying 'medium' and 'high' levels of labelling when using MP-5X compared to MP-1X. Although there was a trend towards enhanced particle uptake when using applied magnetic fields, for a given particle formulation these were not statistically significant (**Figure 3.11**). At the optimal labelling condition the average iron content of NSCs was found to be 5.7 pg/cell as measured by spectrophotometry.

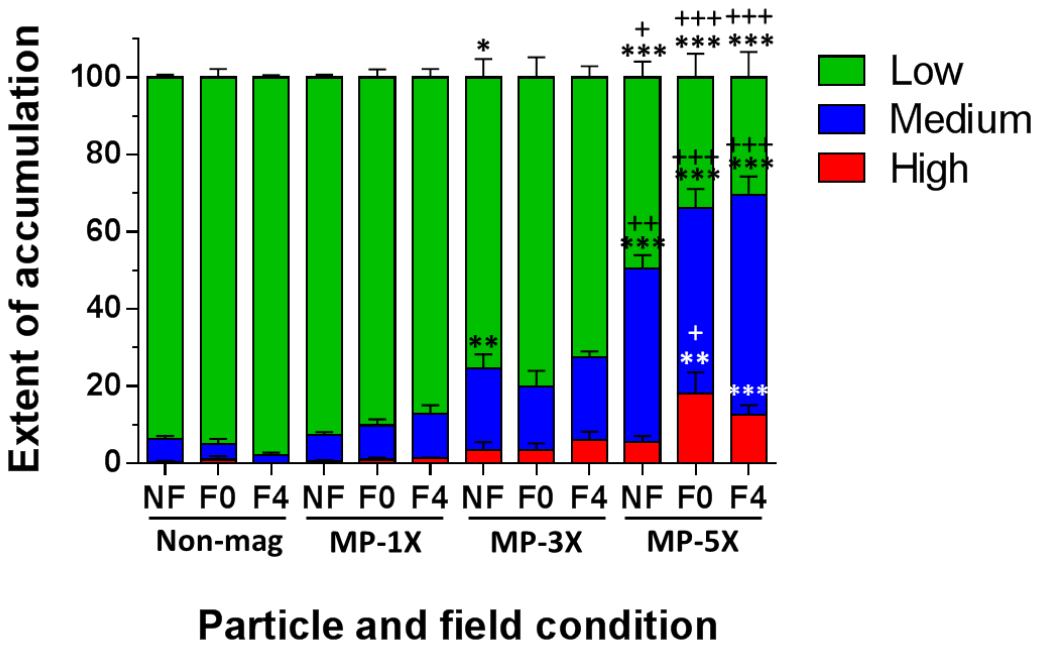

Figure 3.11. Semi-quantitative assessment of the extent of particle uptake. *Bar chart displaying the breakdown of labelled NSCs into cells displaying 'low', 'medium' and 'high' levels of labelling as judged by a semi-quantitative estimate of the area of internalised particles. Statistical differences were analysed between comparable low, medium and high groups and are: *p<0.05, **p<0.01 and ***p<0.001 versus MP-1X labeling under the same field condition; $^{+}$p<0.05, $^{++}$p<0.01 and $^{+++}$p<0.001 versus MP-3X labeling under the same field condition (one-way ANOVA with Bonferroni's MCT, n = 5).*

3.3.6 Labelling protocols do not affect cell health, proliferation or 'stemness' of NSCs

As described in Chapter 2 safety of novel nanotechnologies is essential and of paramount importance to their eventual adoption into clinical use. Therefore, a number of assessments of the safety of labelling NSCs with these novel particle formulations have been performed. Under phase microscopy, labelled cells were adhered to the substrate and displayed typical bipolar

morphology. Assessing the numbers of cells per field revealed no significant differences in the proliferation of the NSCs (**Figure 3.12A**). Cell viability, as judged by counting the percentage of abnormal (pyknotic) nuclei, was also low and similar across all conditions (**Figure 3.12B**). As a further measure of cell health a MTS assay was performed which showed there were no significant differences between the ability of cells from each condition to reduce the tetrazolium dye (**Table 3.3**). Taken with the microscopic analysis, which showed the cell numbers are equal between conditions, this result suggests that labelling did not affect cell metabolism.

Normal expression of NSC specific markers, nestin and SOX2, was maintained in cells that had taken up the particles under all conditions. The proportions of cells expressing the markers were also unaltered in all labelling conditions and similar to those in control cultures (**Figure 3.13A and B**).

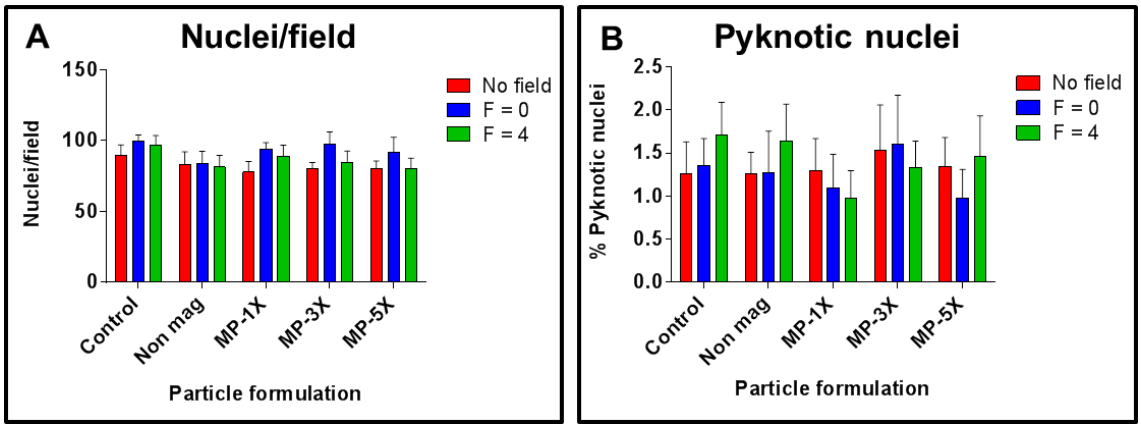

Figure 3.12. Effect of labelling on cell proliferation and viability. *Bar charts displaying quantification of (A) numbers of nuclei per field, a measure of the proliferative capacity of the cells, and (B) percentage of pyknotic nuclei, an indicator of cell death. Numbers are similar across all conditions suggesting the protocols are not having an effect on these measures of cell health.*

Field Condition	Particle Formulation				
	Non-mag	*MP-1X*	*MP-3X*	*MP-5X*	*Control*
No field	101.1 ± 10.8	97.3 ± 10.8	97.8 ± 10.5	97.8 ± 11.9	100.0 ± 9.3
Static field	100.8 ± 11.2	96.1 ± 13.1	92.4 ± 13.0	92.6 ± 12.9	
F=4Hz oscillating field	98.3 ± 10.9	92.5 ± 10.8	90.8 ± 11.4	93.8 ± 11.0	

Table 3.3. MTS assay absorbance readings from the different labelling conditions. *Absorbance readings are expressed as a percentage of the control. No significant differences were observed between the groups.*

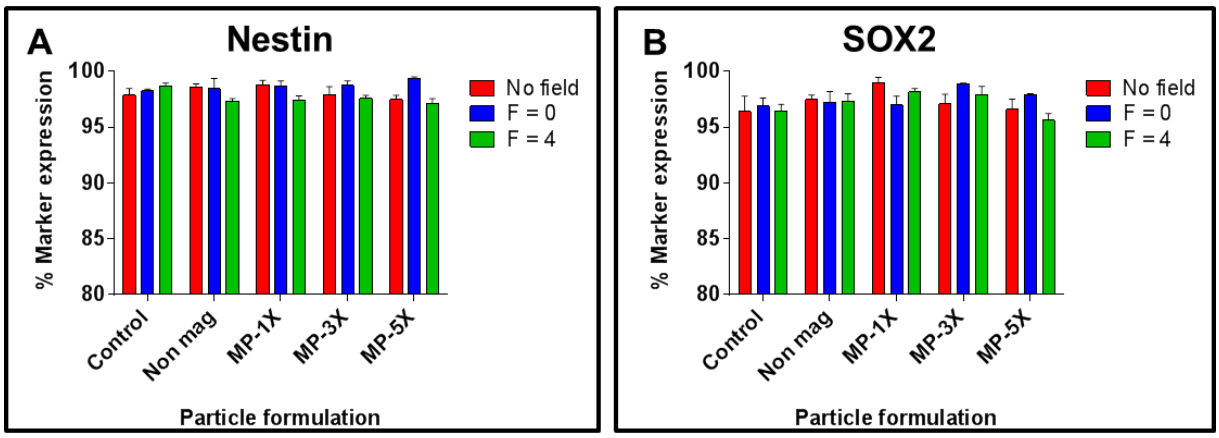

Figure 3.13. Labelling with the various particle formulations does not affect NSC marker expression. *Bar charts displaying the percentage of cells expressing the NSC specific markers (A) nestin and (B) SOX2 across all conditions.*

3.3.7 The developed protocols have no effect on the differentiation profile of NSCs

Part of the therapeutic potential of NSCs relies on their ability to generate their daughter cells for replacing cells that are lost or damaged in disease/injury. Therefore, an investigation of NSC progeny after labelling was performed. Daughter cells produced from labelled NSC populations had normal morphology and all cell types displayed some evidence of retaining the MPs (**Figure 3.14A-C**). This was most apparent in the astrocyte population where large particle accumulations were evident in a large majority of cells (**Figure 3.14A**). Neurons and oligodendrocytes were labelled to a lesser extent and often displayed small accumulations when intracellular MPs were observed (**Figure 3.14B and C**). Labelling NSCs under all conditions did not affect the proportions of cells that differentiate into astrocytes, neurons or oligodendrocytes (**Figure 3.14D-E**).

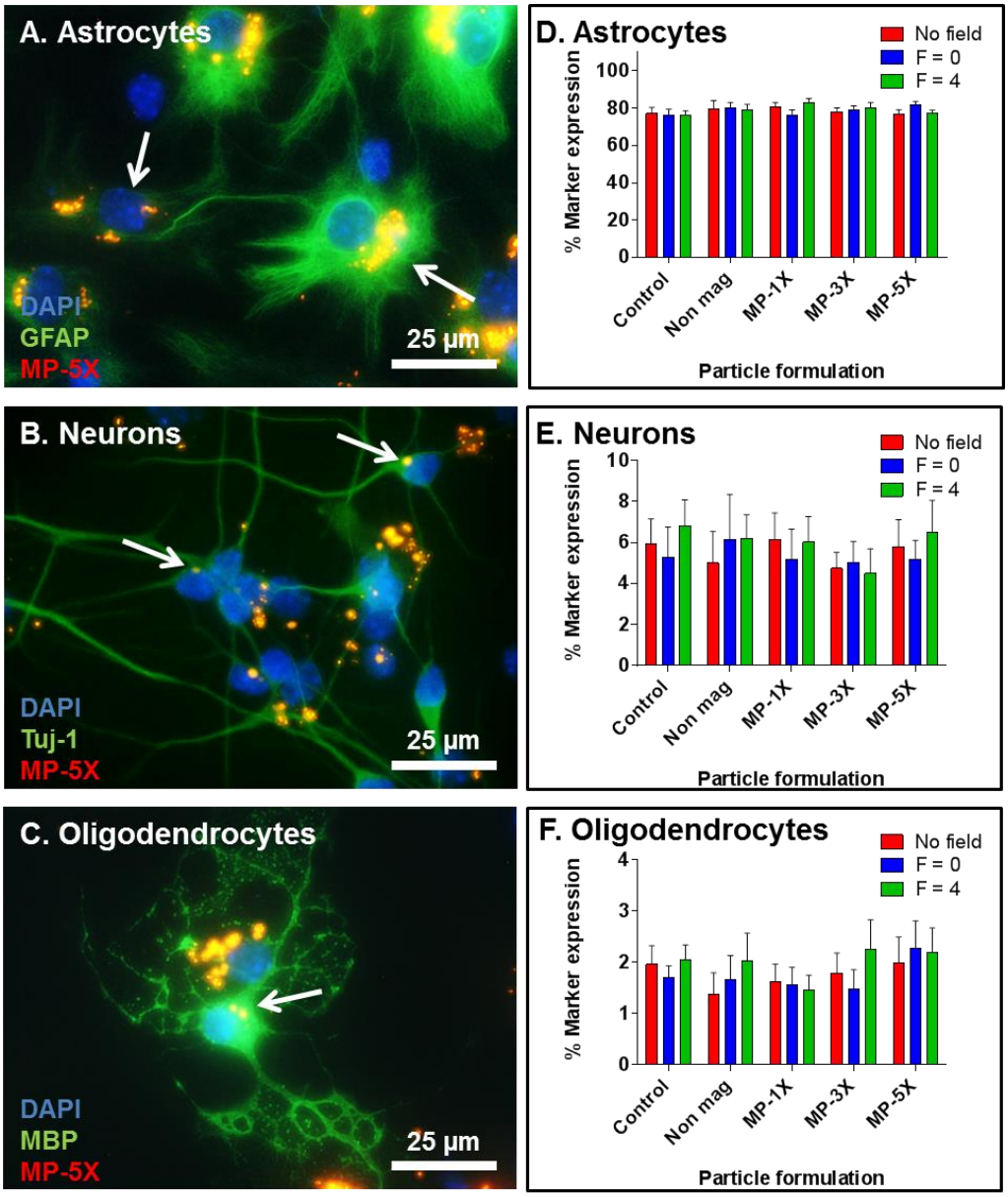

Figure 3.14. Post labelling differentiation of NSCs. *Representative images of the three major cell types generated from NSCs (A) astrocytes, (B) neurons and (C) oligodendrocytes. The images display examples of particle retention by the individual cell types indicated by the white arrows. Note that particle accumulations appear to be larger and more frequent in astrocytes (A) than in neurons (B) and oligodendrocytes (C). Bar charts displaying quantification of the proportions of (D) astrocytes, (E) neurons and (F) oligodendrocytes generated from NSCs from each condition between which there were no significant differences.*

3.3.8 NSCs could be trapped by magnetic force in an *in vitro* flow system

To test the functional utility of the formulated MPs, labelled NSCs were passed through an *in vitro* flow system and subjected to a magnetic field gradient designed to form a simulation of intravascular delivery and *in vivo* magnetic cellular capture. A basal level of retention was observed of 18.1 ± 4.9% of cells retained within the system when NSCs were labelled with the Non-mag particle. The percentage of cells trapped in the system increased along with increasing the magnetite content of the particles used to label the NSCs, up to a maximum of 66.7 ± 3.3% when labelling was performed with MP-5X (**Table 3.4**). Microscopic examination of the tubing after the magnetic localisation experiments revealed large aggregates of rounded bodies with the morphological appearance of trypsinised cells (see **Section 3.3.9** for an example of dissociated cells). These co-localised with particle fluorescence indicating the trapped labelled cells (**Figure 3.15**).

Particle formulation used to label NSCs	% Cell retention in flow system
Non mag	*18.1 ± 4.9*
MP-1X	*18.9 ± 9.0*
MP-3X	*40.1 ± 9.2*
MP-5X	*66.7 ± 3.3*** $^{++}$

Table 3.4. Magnetic localisation in an in vitro flow system. *Table shows percentage of cells retained after NSCs had been labelled with the indicated MP formulation and passed through an* in vitro *flow system which was exposed to a magnetic field gradient. Significant differences are: **p<0.01 vs Non-mag and $^{++}$p<0.01 vs MP-1X labelling (one-way ANOVA with Bonferroni's MCT, n = 3).*

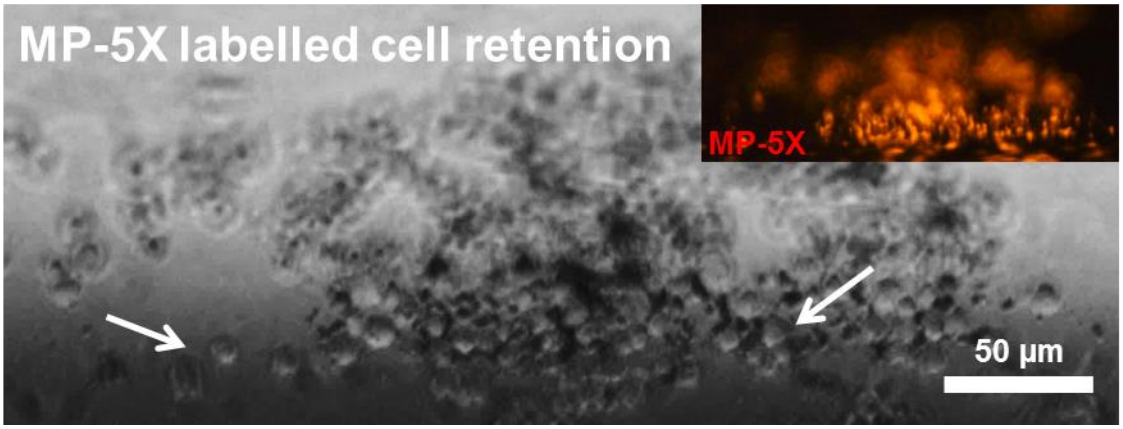

Figure 3.15. NSCs labelled with MP-5X could be magnetically localised in an in vitro flow system. *Representative image taken from the tubing next to the magnet after NSCs that had been labelled with MP-5X were passed through the flow system. Rounded cellular bodies can be seen indicative of trypsinised cells (white arrows). Inset shows the fluorescence counterpart indicating the cells that have accumulated are labelled with the fluorescent MP.*

3.3.9 Assessment of the transplantation of NSCs onto organotypic SCI slice models

To assess the utility of the organotypic slice cultures of SCI for investigation of protocol safety, NSCs labelled with MP-5X were transplanted into lesion sites. **Figure 3.16A** shows dissociated single NSCs, after trypsinisation, displaying retention of the MP label. Focal transplantation of labelled NSCs was achieved in the lesion of the slice (**Figure 3.16B**). 48 h post transplantation, cells co-labelled with DAPI (mostly absent within the slice body) and fluorescent particles were observed in areas of characteristic SCI pathology including axonal outgrowth (**Figure 3.16C**) and GFAP up-regulation (**Figure 3.16D**). One week post-transplantation, labelled cells appeared to be expressing the astrocytic marker GFAP (**Figure 3.16D, inset**) indicating NSC survival and differentiation in the slice. Labelled neurons were rarely observed and labelled oligodendrocytes

were never observed; similar to the pattern of labelling seen after differentiation on glass coverslips.

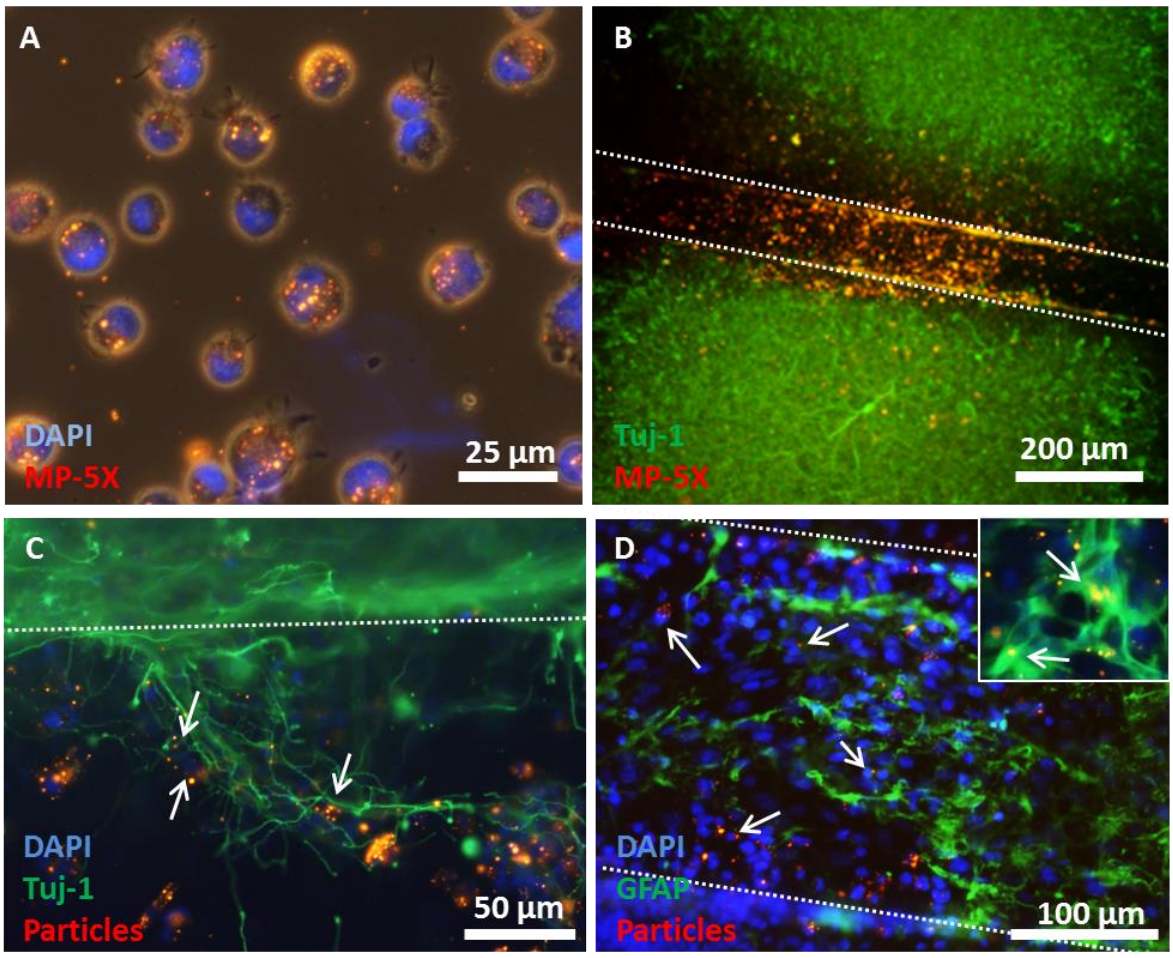

Figure 3.16. Labelled NSC transplantation into organotypic spinal cord slices. *(A) Representative image of dissociated NSCs retaining MP-5X after trypsinisation. The cells were also labelled with DAPI. (B) Focal transplantation of fluorescent MP labelled NSCs immediately after transplantation. Labelled NSCs (white arrows) were observed 48 h post-transplantation in areas of (C) axonal growth and (D) GFAP reactivity; hallmark features of SCI pathology. One week post-transplantation labelled cells were expressing the astrocytic marker GFAP (D - inset) indicating some NSCs had survived and differentiated into astrocytes within the lesion.*

3.3.10 MP-5X particles were retained in NSC daughter cells for up to three weeks

To examine the potential for long-term targeting strategies using these particles, MP-5X labelled NSCs were differentiated and cultured for three weeks. Cells still retained the particles up until this time-point (**Figure 3.17**) although the extent of labelling throughout the culture appeared to be less (estimated to be less than half the levels of labelling) than after one week in culture (**Figure 3.17 inset** and **Figure 3.11**) indicating some particle loss over the course of this experiment.

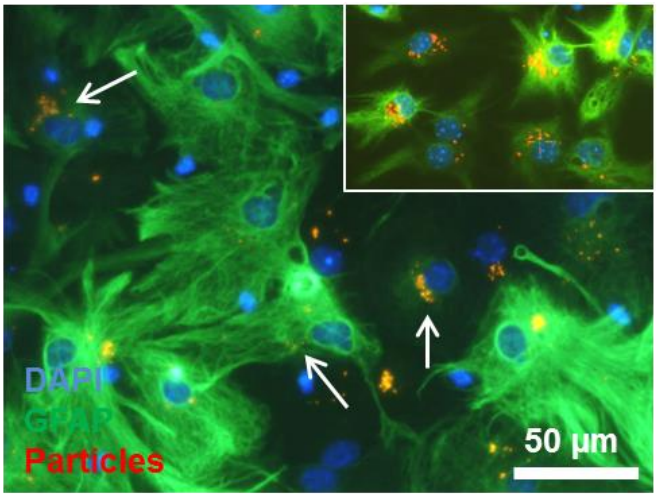

Figure 3.17. Daughter cells generated from labelled NSCs retain MPs for up to three weeks. *Representative image showing astrocytes generated from NSCs labelled with MP-5X still retain the label (white arrows) although the pattern of labelling is less extensive than in cultures differentiated for one week post labelling (**inset** and **Section 3.3.7**).*

3.4 Discussion

This is, as far as I am aware, the first study of systematically modulating particle magnetite content and assessing the impact on stem cell labelling alone and in conjunction with applied magnetic fields. It was found that, by simply increasing magnetite content of MPs, high labelling

can be safely achieved in a hard to label cell type without the use of chemical or biological strategies, which as discussed in the Introduction (**Section 3.1.1**) may not be suitable for clinical translation. As an alternative, the physical delivery strategy described in this chapter has considerable advantages for clinical use, including, a good safety profile and relatively simple and adoptable methodology. This has significant clinical implications for achieving high labelling efficiencies of novel designs of neuro-compatible MPs for a range of applications along with magnetic cell localisation. The protocols were also shown to impart functional benefit, at least in an *in vitro* flow system, where it was observed that MP labelled cells could be captured by magnetic force. Further, labelled cells survived and differentiated in a slice model of SCI. Taken together, these two findings demonstrate the potential clinical utility of using high magnetite content, PLA-based MPs as agents to facilitate magnetic NSC targeting to sites of injury and disease in the CNS.

3.4.1 Mechanisms of increased labelling utilising the described protocols

It is of interest that field application only significantly enhanced uptake of the MP-1X formulation, which has the lowest magnetite content, in a pattern reminiscent of that in MP mediated transfection of NSCs (Chapter 2); with the F = 4 Hz condition proving to be the most efficient in terms of percentage of cells labelled. It is well recognised that transfection grade particles have low iron content and good colloidal stability so they require a magnetic field to enhance their sedimentation on to the surface of the cells,[92] presumably a similar mechanism applies to the MP-1X formulation. The mechanism of oscillating magnetic field action in increasing cellular uptake is not yet known, however, was speculated to act through either increasing the dispersion of MPs in the media, therefore enhancing particle-cell contact, or stimulating the cellular membrane to promote endocytosis of the particles, or, be a combination of the two mechanisms. Whether, the

increase in MP-1X uptake after application of the oscillating fields follows the same mechanism as Neuromag (the particle used in Chapter 2) or whether there are even inter-particle differences in the interaction with magnetic fields cannot yet be elucidated. As in Chapter 2, it may be possible to study the mechanisms of action of the oscillating field by using the high resolution membrane imaging technique termed OTOTO-FESEM. To achieve this, FESESM could be used to visualise changes in the cellular membrane which may be indicative of increased endocytotic activity stimulated by application of magnetic fields.

In contrast to the MP-1X particle formulations, MP-3X and MP-5X showed no significant enhancement of the percentage of cells labelled or the extent of uptake of MPs after application of magnetic fields. However, the latter measure was conducted using a semi-quantitative analysis which may be limited in highlighting subtle differences in particle uptake between different field conditions. Our lab is currently investigating the use of confocal microscopy to measure the intracellular volume occupied by the particles as a more quantitative assessment of particle uptake. This approach may be used for future studies to examine the differences in uptake when using fluorescent particles. In this study, the fact that no differences were observed between field conditions may be explained in terms of the colloidal stability of the particles which, in sub-micron sized particles, depends on viscosity of the medium and particle density. It is likely that increasing particle iron content increases particle density sufficiently to facilitate sedimentation onto the surface of the cells and stimulate uptake mechanisms. Indeed, in recently published observations in our laboratory it was noted that when NSCs are incubated with MP-5X particles, membrane activity appeared to be up-regulated in comparison to labelling with the Non-mag particle formulations (paper attached as Appendix 3).[185] Specific membrane features that were enhanced are possibly related to particle uptake mechanisms and included membrane ruffling, filopodia (short 2-3 μm protrusions on the cell membrane), pits and nanopodia (cellular protrusions attached to the substrate). For the heavier particles this could mean that field application is

unnecessary to further enhance sedimentation and cell labelling (at least over 24 h) possibly demonstrating there is a '*magnetite limit*' where field application is no longer required to enhance labelling. However, it should be noted that there may be cell type differences in response to applying magnetic fields. For example, in the presence of a magnet, BAECs internalised ca. 90% of high iron content particles from the media in comparison to just 30% in the absence of a field (over a 24 h incubation period).[162] Although 24 h magnetic field application could represent an additional step to enhance particle labelling in NSCs, in this study particle aggregation of the MP-5X particles was noted over extended exposure to the magnet. As discussed in the Introduction (**Section 3.1.1**), particle aggregation can lead to non-internalised iron precipitates leading to false identification by MRI or adverse immune responses after transplantation. Therefore, this strategy may not be applicable in the context of translating this particle formulation into clinical use.

3.4.2 Clinical utility of the developed protocols for NSC transplantation therapy

Most studies to date involving the use of labelling NSCs with MPs have relied on the use of uptake enhancing strategies, including: lengthy incubation protocols; exposure to high particle concentrations; and transfection agents which as explained in the Introduction (**Section 3.1.1**) may not be clinically translatable. In addition, a large number of studies have reported their findings using NSC cell lines which may not represent particle uptake dynamics of primary NSCs (a more physiologically relevant cell population) and can display remarkable resistance to toxicity. The latter point means that safety data relating to developed protocols for cell tracking or magnetic cell localisation for labelled cell lines may not translate to primary NSCs. In this regard, the protocols developed here utilised primary NSCs, are rapid (24 h incubation) and can be performed in the absence of chemical or biological uptake enhancing strategies. High labelling

was reported (a maximum of ca. 96% cell labelled) with no obvious effects on key regenerative properties of the NSCs including proliferation, stem cell marker expression and differentiation. Further, labelled NSCs were captured in an *in vitro* flow system and survived and differentiated in a slice model of SCI demonstrating the potential for the protocols to be used for clinical magnetic cell targeting approaches. In combination with the technical simplicity of the protocols, translation of the approach into the clinic seems feasible.

In terms of clinical application, using the MP-5X particle in combination with a 4 Hz oscillating field resulted in the highest levels of labelling which corresponded to an average iron content per cell of 5.7 pg. Although this was proved here to be sufficient for cellular capture in an *in vitro* flow system, it is substantially lower than the levels of labelling (ca. 260 pg Fe/cell) achieved in NSCs magnetically localised in ischemic rat brains. It should be noted however that this latter study utilised an immortalised cell line combined with a transfection agent to enhance labelling.[64] Cell lines can display high uptake compared to primary cells. For example, PC-12 cells, often used as a neuronal cell line, displayed markedly greater labelling (ca. 77%) than primary neurons (ca. 13%) when comparing the same particle.[115] It remains to be determined if the extent of uptake achieved in this study will allow for magnetic targeting approaches *in vivo*. Of further clinical use, the average iron per cell reported in this study is comparable to the amounts reported from other studies which have tracked NSCs using MRI.[173,176] However, as iron content in cells is reduced over time due to proliferative dilution this amount may only be enough to track cells through one cell division; therefore intracellular iron may need to be increased. As this is the realistic maximum amount of iron that can be incorporated in the particle using this formulation method, particle design strategies to increase intracellular iron might involve utilising larger particles of the same formulation or utilising a different method of synthesis. For example, chemically binding PLA onto amine functionalised magnetite particles (prepared by silanisation) using EDC/NHS binding agents could reduce the amount of PLA which contributes to the final particle – increasing magnetite

content.[186] All novel particle designs would also have to be rigorously tested for safety and function.

Importantly for use in the clinic, all formulations tested were found to be safe with respect to key regenerative properties of the NSCs including cell proliferation, cell viability, stem cell marker expression, differentiation profiles and survival in an organotypic slice model. Indeed, it was desirable from the outset to formulate the particles with safe and potentially translatable components. In this regard, PLA is well known to be biocompatible and has been previously FDA approved for contact with biological fluids.[187,188] In addition, PLA is relatively stable, with extracellular degradation shown to last over weeks to months[189] and 15% degradation shown intracellularly over 3 days.[190] Confirming this, no evidence for particle degradation over a 24 h time period was observed in this study, as judged by TEM analyses. This could be a factor in the demonstrated safety of the particle, as our laboratory has previously shown that breakdown of MPs is a major correlate with toxicity,[124] possibly due to overwhelming the cell with intracellular iron. Therefore, particle stability is key for both retaining the MP for successful cellular imaging/targeting over the therapeutic time-course and for the safety profile. Magnetite based particles have been shown to be safe in animal studies[191,192] and some FDA approved magnetite particles are used as clinical grade contrast agents for MRI.[193] PVA and oleic acid used to stabilise the MPs are also considered safe, with PVA approved for embolization and neurological applications[194] and oleic acid rapidly absorbed and metabolic products utilised and excreted (according to www.fda.com). Therefore, in comparison to some novel particles that have been tested for labelling NSCs,[174,178] all the components of the particle are potentially safe highlighting the translational potential of the described protocols.

3.4.3 Particle formulation method could allow for modifications to enhance regenerative utility

Further advantages to regenerative neurology may be derived from the formulation method used to generate the particle in this study. Similar formulations to those presented here allow for biomolecule encapsulation within the polymer matrix – this can happen without modification of the biomolecule being necessary therefore avoiding altering the biological function of the drug – for release into target cells.[195] Further, degradation rates of the particles can be tuned by mixing PLA with a co-polymer poly(lactic-co-glycolic acid), PLGA, for slow release of incorporated drugs; this approach has been shown for release of the anti-proliferative drug, paclitaxel.[181] This could provide a novel approach for delivering drugs to the CNS, which is normally hampered by lack of drug penetration across the BBB. As discussed in the General Introduction (**Section 1.5**) combinatorial therapy is likely to be essential for promoting successful repair in the CNS and combining drug delivery with MP labelling of NSCs could be a promising strategy to achieve this.

3.4.4 *In vitro* tests could be suggestive of the *in vivo* potential of the labelling protocols

The translational potential of the developed labelling protocols was tested in two *in vitro* models. The first is a simple *in vitro* flow system. Here, MP labelled cells were effectively captured using magnetic force highlighting the functional capability of these particles to mediate magnetic cell localisation. The pattern of enhanced retention matched that of the particle labelling experiments, namely, MP-5X > MP-3X >MP-1X > Non-mag, suggesting this approach may provide reliable information on the ability to magnetically capture MP labelled cells. Improving the complexity of the flow system described in this chapter, for example, to provide continuous flow or performing the experiments with CSF, could allow a better representation of the *in vivo* response of MP labelled cells to magnetic localisation.

The second model involved transplantation of labelled NSCs onto organotypic slices mimicking SCI. In this study the slices demonstrated hallmark features of SCI pathology including axonal regeneration and evidence of astroglial scarring which is in agreement with the previous characterisation of these slices by our laboratory.[120] Post-transplantation, labelled NSCs predominately differentiated into astrocytes, a finding which has been shown for *in vivo* transplantation of NSCs into sites of SCI.[46] Crucially, for successful transplantation therapies, after one week, labelled cells were observed and predominately astrocytes. This suggests labelled NSCs can survive and differentiate in host tissue, indicating that the protocols developed for labelling NSCs are safe. Findings from the slice model could be important for future nanotechnology translational research as, compared with *in vivo* transplantation, the slice model described here offers several advantages, including: straightforward examination of cell fate and regenerative outcomes; technical simplicity; consistent generation of SCI lesions; and reduced animal suffering. In terms of clinical utility, the model mimics injured tissue and has previously been used to demonstrate the regenerative potential of using implantable nanofibres to promote axonal outgrowth from the lesion edges.[120] In combination with the data presented in this chapter, this suggests that the model could provide a platform to not only assess the survival and differentiation of transplanted labelled NSCs but also assess their functional capacity, for example, in terms of promoting axonal outgrowth. Indeed, slice models have previously shown utility for assessing magnetic stem cell targeting[80] and MRI capabilities[121] when utilising MP labelled NSCs.

Taking the findings from the two *in vitro* models, these results indicate that the protocols developed in this chapter could be useful for *in vivo* magnetic stem cell targeting applications, potentially for transplant into sites of SCI. For *in vivo* application, systemic delivery of cells reduces the risk of secondary damage; however, clearance of transplant cells by the macrophages in the lung, liver and kidney when delivered by this route is a well-known problem.[56] To counteract this,

labelled NSCs could be introduced in close proximity to sites of SCI (identified by MRI) via the spinal segmental arteries and external magnets used to hold and concentrate the transplanted cells in the desired location. This could potentially lead to greater beneficial effects compared to the transplantation of non-labelled cells. However, *in vivo* experiments would have to be conducted to assess the feasibility of this approach.

An important observation from both the transplantation experiments, and differentiation of the labelled NSCs on glass, is that astrocytes appear to dominate particle inheritance post-differentiation. This observation has significant implications for the manipulation of neurons and oligodendrocyte progeny of labelled NSCs after transplantation. This could be of importance in diseases such as Alzheimer's where the affected cell types are neurons, or multiple sclerosis whose main pathological feature is demyelination (secondary to oligodendrocyte loss). The reasons for this phenomenon are unclear. It could be that as the NSCs differentiate, cells destined to become neurons or oligodendrocytes eject the particle through exocytosis. Differentiating labelled NSCs whilst under time-lapse observation may be a strategy to confirm this. Daughter cell morphologies are straightforward to distinguish so cells that eject the particles could be identified. However, it will be of vital importance to overcome the labelling deficiency in neurons and oligodendrocytes for future clinical use of novel MPs. Although limited, some work has been performed on generating cell specific peptides for targeting cells of the CNS. One study has screened domains of GP1, a viral protein which semi-selectively infects glial cells of the CNS and identified a peptide they termed 'TD2.2'.[196] Fusion proteins were generated with EGFP attached to TD2.2 and applied to cultures of OPCs, astrocytes, NSCs and fibroblasts. Percentages of cells fluorescing in each culture; OPCs (41%), astrocytes (29%), NSCs (3%) and fibroblasts (3%), suggest some selectivity towards maturing and mature glial cells. It is especially interesting that OPCs were labelled to a much greater extent than NSCs potentially allowing a strategy to target this cell type in mixed co-cultures of cells, including differentiating NSCs.

3.4.5 Conclusions and future work

The data presented in this chapter demonstrate a rapid, safe and technically simple methodology to achieve efficient MP labelling in NSCs, a cell population of high clinical relevance. Further, the labelling procedures did not affect NSC differentiation and survival after transplantation into an organotypic model of SCI and resulted in labelled NSCs which were able to undergo magnetic capture, suggesting the developed protocols may be clinically translatable for neural cell therapies. The findings have relevance for the design of novel neurocompatible particles both for the functions outlined in this chapter and for multimodal functions such as gene delivery coupled with magnetic labelling. Delivering genetically engineered cell populations with the ability to magnetically guide them to sites of injury and visualise the transplant population could provide a step-change in the realisation of combinatorial therapies to promote repair in the CNS.

Future work will have to focus on increasing the iron content of cells which could be achieved by combining these protocols with other uptake enhancing strategies such as incorporation of CPPs into the particle design. Further, utilisation of the particles for delivery of drugs or genetic material could be an exciting avenue to pursue to explore the potential of these particles for delivering combinatorial therapies. In terms of the *in vitro* models of SCI and magnetic cell targeting, more physiologically relevant systems may be developed by combining magnetic cell targeting with the slice culture systems. Perfusion culture is well established and media could be pumped at physiologically relevant flow rates over the slice with magnets placed beneath the lesion sites. MP labelled cells could then be introduced and visualised by time-lapse microscopy to establish the number of MP labelled cells captured by the technique. This would have high

importance in terms of the 3R's principles of reducing animal usage as good experimental data could be obtained before ultimately progressing to animal studies.[b]

[b] Much of the data concerning labelling of NSCs with PLA based particles (Sections 3.3.2 – 3.3.8) has been published by Nanomedicine:NBM. The published paper is attached as Appendix 2 and has been licensed for use in this Thesis by Elsevier.

Chapter 4: Magnetofection of intraconstruct neural cells

4.1 Introduction

As described in the General Introduction (**Section 1.5**), transplantation of genetically modified NSCs can offer several benefits for repair in the CNS. However, it is hampered by poor functional integration of the transplant population. The main reason for this, also discussed in the General Introduction (**Section 1.6** – *barrier 4*), is the inability to control stem cell differentiation into the required functional cell types needed for repair following transplantation. Further, the majority of NSC transplant studies use cellular injection as a delivery method which has several disadvantages, such as cell death, poor cellular distribution throughout the lesion site, uncontrolled stem cell differentiation and a lack of 3-D reconstruction through the depth of the injury (**Section 1.6 –** *barrier 2*).

An exciting platform to address these multiple challenges could be to fuse cell transplantation with hydrogel technology, which has several clinical benefits for cell delivery (expanded in depth in the General Introduction, **Section 1.12**). For example, incorporating transplant cells within a polymer scaffold can promote cell survival and distribution throughout a 3-D matrix,[106–108,197] facilitating repair throughout the depth of a lesion site. In addition, hydrogel dimensions can be easily tuned to match those of the lesion. This is of particular importance in the CNS where lesion size can be quite varied. For example, in SCI, lesion size can affect one or more sections whose size can range from 6-13 mm in diameter with length of about 6 mm.[198] Therefore, it is essential that the implant can adopt a variety of shapes.

Further, hydrogel design strategies offer the potential to control stem cell differentiation and direct regeneration, to facilitate functional integration of the transplanted cells.[111,112,120,199] Combining scaffold materials into the hydrogel formulation can improve implant design by providing a guide for regenerating tissue and differentiating transplant populations. This strategy was demonstrated by Nomura *et al.* who seeded NSCs onto chitosan tubing for implantation into

sites of complete transecting SCI.[200] After transplantation, tissue bridges formed around the chitosan tubing within the lesion gap, containing a mixture of donor and host cells, with little evidence of repair in a no-channel group. NSCs displayed high survival and differentiated into astrocytes and oligodendrocytes within the lesion site. Although this study shows the potential of transplanting NSCs in combination with a scaffold capable of directing regeneration, no behavioural improvement was observed after transplantation suggesting further modifications are necessary to induce functional repair.

Similarly, most studies combining NSCs with hydrogels report enhanced survival of the cells post-transplantation, but not necessarily functional integration of the transplant population or behavioural improvements. For example, Bible *et al.* transplanted PLGA microparticles acting as a scaffold for the NSC cell line, MHP36, into ischemic areas within rat brains.[201] Cells survived implantation (although no quantification for extent of survival is shown) and differentiated into astrocytes and neurons showing the capacity for cell replacement. However, blood vessel penetration into the implant was not seen and no evidence was provided for axonal infiltration; two key regenerative targets for long term graft survival and functional integration respectively. Therefore it may be necessary to increase the complexity of the scaffold design to provide combinatorial modes of therapeutic intervention. One strategy to enhance the regenerative potential of NSC seeded scaffolds is to use genetically modified cells to release neurotrophic factors. As discussed in Chapter 2 (**Section 2.1**), genetically modifying NSCs can improve their ability to promote repair and this could represent the next steps in implant design for achieving combinatorial therapy. However, as far as I am aware, a thorough examination of the feasibility of combining genetically engineered NSCs with hydrogels has not yet been described in the literature.

4.1.1 Clinical considerations for combining genetically manipulated NSCs with hydrogels

In terms of associating genetically modified cells within an implantable matrix there are two main strategies: to engineer the cells prior to incorporation or perform '*intraconstruct genetic engineering'* at a desired time-point after the cells have been combined with the scaffolding. In this regard, engineering the population after incorporation into the hydrogel has several clinical advantages (summarised in **Figure 4.1**). These include: (1) No repeat culturing steps in cell plating, transfection and trypsinisation before incorporation into the matrix. This reduces risks of infection and cell loss associated with these procedures – important for safe and efficient production of therapeutic implants. (2) Rapid implantation after genetic manipulation. This is especially important in terms of non-viral plasmid delivery which results in transient expression of the desired protein; therefore, quicker implantation after manipulation allows for maximum therapeutic benefit derived from the expressed protein. (3) The ability to transplant mature populations of genetically modified cells. Differentiation of NSCs into their daughter cells may require several days, over which time there can be a dramatic reduction in expression of the therapeutic protein – leading to a loss of action after cell transplantation. Allowing the cells to mature on the scaffold before transfection offers a strategy to overcome this. This has implications for successful transplantation of mature oligodendrocytes or neurons which, due to fragile and more extensively branched processes, are more likely to die following either trypsinisation or transplant procedures.[202] Despite the clinical advantages of this approach, an intraconstruct engineering strategy for neural cells previously propagated within hydrogel materials has not yet been attempted.

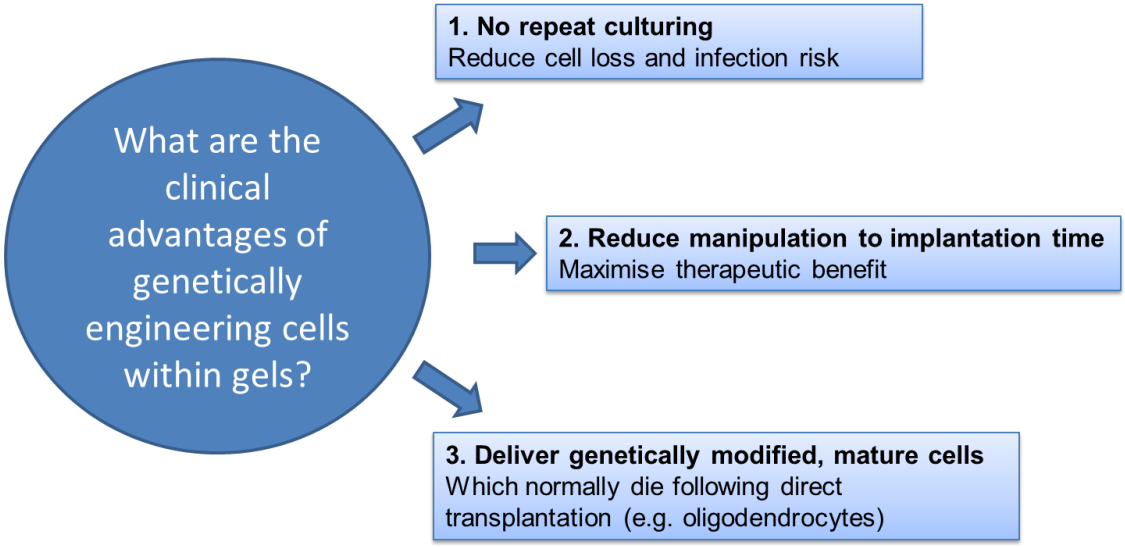

Figure 4.1. Schematic detailing the advantages of genetically engineering cells within scaffolds designed for implantation.

One interesting study has examined gene delivery to cells (in this case, the fibroblast cell line, NIH 3T3) previously propagated throughout 3-D collagen scaffolds.[203] In their initial experiments, they found that widely used non-viral transfection systems (based on lipoplexes and polymer particles) displayed negligible (<1%) transfection of cells within the 3-D scaffolds, representing a major barrier to this approach. However, based on these findings, the authors synthesised small MPs (ca. 45 nm in hydrodynamic diameter after complexing with DNA) which they predicted would be able to penetrate pores within the collagen. They subsequently applied their MP-DNA complexes to the 3-D cultures in the presence of a magnetic field to pull the complexes into the gel. Under optimal conditions (3 h magnetic field application) the authors reported transfection efficiency of 76%, assessed by flow cytometry. This strategy is particularly compelling for genetically engineering cells within hydrogels for clinical application, as the use of MPs for gene delivery offers several advantages to regenerative medicine including safety and non-invasive cell tracking through MRI (addressing *barriers 1 & 2* described in the General Introduction, **Section 1.6**). A

fusion of hydrogel technology, to improve cell survival and integration after transplantation, with MP mediated gene delivery could therefore simultaneously address multiple barriers to the translation of genetically engineered NSC transplantation therapy.

However, the results from this study cannot be extrapolated to NSCs due to cell intrinsic differences in the handling of MPs (described in the General Introduction, **Section 1.11**) and the potentially complex effects of MPs on NSCs. These include effects on NSC viability, proliferation, stemness and differentiation, which may all ultimately affect the clinical utility of novel genetic engineering procedures. In addition, an important step for the clinical application of magnetofection protocols could be the use of oscillating fields during transfection (demonstrated to improve MP mediated transfection efficiencies in Chapter 2) which have never been tested for hydrogel based magnetofection. Further, as the biology of cells cultured in hydrogels can be profoundly different compared to when they are grown on glass,[199,204] their interaction with MPs, and response to oscillating field magnetofection, cannot be extrapolated from previous magnetofection studies in NSCs grown on glass.

4.1.2 Objectives

Given the potential clinical benefits of fusing magnetofection technology with hydrogel culture of NSCs and the lack of studies of this nature in the literature, this chapter aims to examine the feasibility of such an approach. This will be initially achieved by culturing NSCs on top of pre-formed collagen hydrogels, a material currently used for several medical devices.[205] Culturing NSCs in this manner will be referred to as 2-D culture. Magnetofection procedures will then be tested for their efficiency to genetically manipulate the hydrogel cultured NSCs. The safety of developed protocols will also be investigated followed by a preliminary examination of the

efficiency of MP mediated gene delivery to NSCs cultured through the depth of collagen gels, which will be referred to as 3-D culture.

As this is the first time these protocols have been developed in the laboratory, techniques to observe the cell-hydrogel interaction also need to be developed. A high resolution imaging technique termed OTOTO-FESEM has been developed in this laboratory (described in Chapter 2, **Section 2.4.4**) which can allow detailed analysis of cellular membranes and polymeric materials. Using this technique it may be possible to examine features such as NSC invasion and association with the hydrogel and, in the case of magnetofection, particle-membrane interactions. Information such as this is important for assessing the biocompatibility of the hydrogel matrix and to potentially examine mechanisms of internalisation of MPs. Therefore, the specific objectives of this chapter are:

(i) To develop protocols to culture NSCs with collagen and develop microscopy techniques to examine their interaction with the collagen substrate.

(ii) To investigate the feasibility of genetically modifying intraconstruct NSCs (cultured in 2-D or 3-D) using magnetofection procedures.

(iii) To examine the safety of the magnetofection protocols and of culturing NSCs in collagen.

4.2 Materials and methods

All materials and methods are the same as for Chapter 2 including NSC derivation, media composition, fixation and immunostaining unless otherwise stated.

4.2.1 Reagents

Extra reagents not described in the previous chapters were collagen which was from Corning (Tewkesbury, MA, USA) and powdered Gibco MEMα which was purchased from Life Technologies. The latter was made into a 10X MEMα solution by dissolving 10.17 g MEMα and 2.2 g $NaHCO_3$ in 100 mL distilled water. The solution was pH adjusted to 7.4 and filter sterilised using a 0.2 µm filter. The other reagents used are as in previous chapters unless otherwise mentioned.

4.2.2 Collagen hydrogel formation

Collagen is stored in monomer form at 4°C dissolved in acetic acid. To form a gel, this solution has to be neutralised and warmed to at least room temperature. Under these conditions collagen polymerises and forms a hydrogel. In this chapter, collagen hydrogels were formulated for both 2-D and 3-D cell culture. For 2-D culture, hydrogels were pre-formed and NSCs seeded on to the top of the gel (**Figure 4.2A**). For 3-D culture, NSCs were incorporated into the collagen solution prior to setting (**Figure 4.2B**). In this manner NSCs could be captured in-between the collagen fibrils. For both culture systems, gels were set in 24 well plates on top of glass coverslips. This was found to be a useful insert to aid lifting the gel out of the well (especially important for the low density collagen gels, which could easily tear during manipulation). Using a needle point, the collagen gel could be separated from the walls of the well and then the point could also be used to lever the coverslip, and therefore the gel up for collection by curved tweezers.

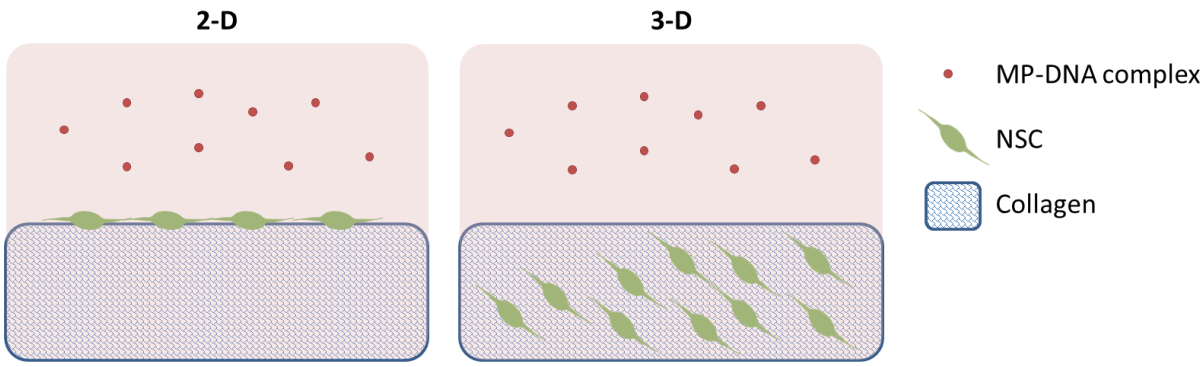

Figure 4.2. Schematic showing 2-D and 3-D culture of NSCs using collagen. *Schematics depicting NSCs grown on the top of a pre-set collagen gel, referred to as 2-D culture (A) and through the depth of the collagen gel, referred to as 3-D culture (B). For magnetofection, complexes (red circles) are added into the media above the gel.*

For gel formulation several reagents were combined including 10X MEMα (for biocompatibility), collagen (to form the gel), acetic acid (to adjust the concentration of the collagen) and NaOH (to neutralise the acetic acid). The formulae to calculate the required volumes of each reagent are given in **Table 4.1**. All reagents were kept on ice during the formulation procedures. For both 2-D and 3-D culture, collagen was dissolved in acetic acid to the required concentration before addition of 10X MEMα. This was then neutralised with NaOH and, for 2-D culture, 350 µL added immediately into each well of a 24 well plate before transfer to the incubator for 30 min (37°C) to set the gel. For 3-D culture, the neutralised solution was added to the cell suspension and thoroughly mixed before 250 µL added to wells of a 24 well plate and transferred to the incubator (30 min, 37°C). Following gelation, for 2-D culture 0.4 mLs of NSC suspension was added to each well; for 3-D culture 0.5 mLs of ML-M was added to each well.

Reagent (concentration)	*Formula to calculate required volume* **2-D**	**3-D**
10X MEMα	$V_M = V_F \times 0.1$	$V_M = V_F \times 0.1$
Collagen (C_S)	$V_C = (C_R \times V_F)/C_S$	$V_C = (C_R \times V_F)/C_S$
Cells (10 x 10^6 cells/mL)	N/A	$V_N = V_F \times 0.1$
Acetic acid (0.02M)	$V_A = V_F - V_C - V_M$	$V_A = V_F - V_C - V_M - V_N$
NaOH (1M)	$V_S = (V_A + V_C) \times 0.023$	$V_S = (V_A + V_C) \times 0.023$

Table 4.1. Formulae for deriving volumes of reagents to formulate collagen gels. *V_F – final volume; V_M – volume of MEMα; V_C – volume of collagen; V_N – volume of cell suspension; V_A – volume of acetic acid;* V_S = volume of NaOH; *C_R – required concentration of collagen; C_S – collagen stock concentration.*

4.2.3 2-D NSC culture on collagen hydrogels

In preliminary experiments, the optimal density of collagen was established for NSC culture. To investigate the effect of collagen density on NSC proliferation, stemness and differentiation, dissociated NSCs were seeded on to the top of pre-formed collagen gels of different density (0.6 – 3 mg/mL), in 24 well plates. NSCs were seeded at 3 x 10^4 cells/cm^2 in ML-M and either cultured for 3-5 days (until confluent) or changed to differentiation medium after 24 h and subsequently cultured for 7 days. Cells were then fixed in either 4% PFA (20 min, RT) for immunocytochemistry or 2% glutaraldehyde (2 h, RT) for FESEM.

For subsequent experiments investigating magnetofection of NSCs grown on the surface of pre-formed collagen gels, NSCs were cultured on 0.6 mg/mL density gels. Here, NSCs were allowed to attach to the collagen for 24 h before transfection was performed. This was carried out as a monolayer transfection as in Chapter 2 (**Section 2.2.7**) with application of the appropriate

magnetic field for 30 min at the start of transfection. In this instance controls involved just the application of DMEM:F12 to the wells. To assess the effect on the efficiency of magnetofection of leaving the complexes on for 48 h (i.e. a long particle incubation), transfection was performed using the same conditions without removal of complexes after 1 h. In all experiments, NSCs were fixed 48 h post-transfection to coincide with optimal GFP expression as previously reported.[30] Safety assessments were also performed at this time-point. For an assessment of the differentiation potential of magnetofected NSCs grown on collagen, ML-M was changed to differentiation medium 24 h post-transfection. GFP crystallisation was observed to occur over the course of the normal seven day differentiation protocol which confounded analysis of the numbers of GFP expressing cells and which cell types were expressing GFP. Therefore, cells were cultured for five days after the medium switch to try to reduce this problem (with feeding every 2-3 days) and then fixed (4% PFA, 20 min, RT).

4.2.4 3-D NSC culture in collagen hydrogels

Pilot experiments were also performed to assess whether magnetofection protocols could be utilised to transfect NSCs incorporated through the depth of the collagen matrix. The lowest density collagen, with the largest pore size, that could form a gel was found to be 0.3 mg/mL. As it has been reported that MP penetration into collagen matrices is dependent on particle size,[203] it was reasoned that using a low collagen density may allow for particle penetration through the pores of the gel and greater transfection compared to high density collagen. Indeed, in preliminary experiments when magnetofection was conducted on NSCs grown through 0.6 mg/mL density collagen gels, transfection efficiencies appeared to be markedly reduced compared to when NSCs were magnetofected after culture in 0.3 mg/mL gels. Therefore, gels of 0.3 mg/mL

collagen were subsequently used. The same transfection procedure was applied here as **Section 4.2.4** and complexes were left on for 48 h until fixation in 4% PFA (20 min, RT).

4.2.5 OTOTO processing of collagen gels for FESEM

Glutaraldehyde fixed samples were washed three times in SCB (defined in Chapter 3, **Section 3.2.8**) before post-fixation in a 1% osmium solution (RT, 1 h). Samples were then sequentially stained with the high affinity osmium binding agent thiocarbohydrazide (T) for 20 min then osmium (O) for 2 h (repeated twice) with six SCB washes between each step to obtain the OTOTO layering. Stained samples were dehydrated through a graded series of ethanols before critical point drying with liquid CO_2 as the transition fluid – CO_2 is used to replace the alcohol and is subsequently evaporated. Samples were then mounted on SEM stubs with application of silver paint around the coverslip edges to enhance conductivity.

4.2.6 Immunocytochemistry

Nestin and SOX2 staining was performed on PFA fixed samples and achieved as described previously (Chapter 2, **Section 2.2.17**). Modifications were made to the standard immunocytochemistry protocols described in this thesis for staining differentiated cells as, in early experiments, staining intensity was low and could not be distinguished from background staining. This was especially apparent when comparing fluorescent images to phase images (where cell morphologies can be distinguished) and an absence of staining for a particular cell type, e.g. neurons, was observed. Therefore, after fixation, samples were incubated in blocking solution for 1 h then primary antibody for 48 h before washing three times in PBS. Subsequently, samples were incubated in secondary antibody for 4 h and washed three times in PBS with an elongated

final washing step (at least 2 h) before mounting using Vectashield mounting medium with DAPI. The concentration of primary antibodies was also doubled so that concentrations used were GFAP (1:250), Tuj-1 (1:500) and MBP (1:100).

4.2.7 Imaging

Fluorescence and phase microscopy: Imaging and processing were performed as described in Chapter 2 (**Section 2.2.18**).

FESEM: Processed samples were examined using a Hitachi S4500 FESEM operated at 5kv accelerating voltage.

Confocal microscopy: Samples were examined using an Olympus FluoView FV1200. Images were captured and processed using FV10-ASW 4.1, Imaris 7.6.4 software.

4.2.8 Assessment of transfection efficiency

A microscopic method was chosen to analyse transfection efficiency of the NSCs grown on collagen. This allows for parallel assessments of transfection efficiency and cell health (including cell numbers, adherence and morphology) to be conducted. This is especially important in the context of examining the behaviour of transfected cells in a hydrogel environment (including integration and migration within the matrix) which could mimic a potential transplant scenario. However, NSCs propagated on collagen form spheres over time which prevents quantification of transfection efficiency, in terms of an absolute number of cells, as individual cells cannot be distinguished. Therefore, for a preliminary quantification of the efficiency of magnetofection protocols to transfect NSCs grown on collagen substrates, the proportions of transfected spheres

was assessed in three double merged images taken at X100 magnification. To further quantify the extent of transfection, numbers of GFP positive cells per field were counted and the proportions of transfected spheres which had two or more transfected cells within the sphere were also assessed using the same images. To quantify proportions of transfected astrocytes following magnetofection and differentiation on collagen, the same images used to assess neural marker expression were used to count the number of $GFAP^+$ cells, expressing GFP. This was expressed as a proportion of total $GFAP^+$ cells. This analysis was restricted to astrocytes as these cell types predominately retained expression of GFP after differentiation.

NSCs propagated and transfected in 3-D were examined by fluorescence and confocal microscopy. These images were used to estimate transfection efficiencies of the various magnetofection protocols when applied to 3-D cultures. An examination of NSC morphology and nestin expression was also performed. Quantification of the numbers of cells expressing GFP or positive for nestin was not possible in these studies due to the close proximity in 3-D of the cells. This confounded analysis meaning accurate numbers could not be generated.

4.2.9 Assessment of the safety of magnetofection of NSCs grown on collagen

Safety was assessed by examining the effect of magnetofection procedures on key regenerative properties of the NSCs. First, numbers of spheres per field were counted and sphere diameter was measured across three images taken at X100 magnification; two parameters which are representative of the proliferative capacity of NSCs. Stemness was assessed by evaluating NSC marker expression in triple merged images (DAPI, GFP and appropriate neural marker; either nestin or SOX2 for NSCs). Viability was investigated by performing LIVE/DEAD staining as described in Chapter 2 (**Section 2.2.12**) and images were taken at X200 magnification.

Differentiation of NSCs, under all conditions, was assessed by examining triple merged images (X400) of cells stained with the appropriate neural marker. Proportions of daughter cells generated were counted and an assessment made of the cell types expressing GFP in at least three images (>100 cells counted).

4.2.10 Statistical analysis

All comparable data was analysed using Prism software (version 6.03, Graphpad). Data are presented as mean ± SEM and statistical differences were measured by one-way ANOVA with Bonferroni's MCT. Repeat experiments ('n') are using cells derived from a different mouse litter.

4.3 Results

4.3.1 NSCs proliferate on collagen and display sphering behaviour which increases with collagen density

NSCs were successfully propagated on pre-formed collagen gels of varying density (0.6 – 3.0 mg/mL). Normal intact and circular nuclei were observed in the cells with the majority of cells positive for the NSC marker nestin, suggesting the cells are healthy and retain a stem cell phenotype (**Figure 4.3A-B**). Across all collagen densities, NSCs demonstrated a propensity to form spheres of aggregated cells, with this phenomenon most apparent when NSCs were cultured on the highest density collagen matrix, 3.0 mg/mL (**Figure 4.3B**). On lower density collagen more single cells were apparent and appeared to be spreading out from the neurosphere (**Figure 4.3A**). A high resolution imaging technique termed OTOTO was used to visualise NSCs grown on collagen and their interactions with the collagen substrate. Using this methodology, spheres of cells were

frequently observed (**Figure 4.3C**), confirming the finding from fluorescence microscopy that the NSCs tend to proliferate as spheres attached to the collagen. Dividing NSCs could also be observed suggesting the NSCs retain the ability to proliferate (**Figure 4.3D**). Further, bi-polar morphology of stem cells was apparent, with evidence of cellular protrusions extending into the fibre matrix of the collagen (**Figure 4.3D, inset**). Utilising this technique, membrane features can be observed, such as, filopodia (short 2-3 µm cellular projections), in high resolution (**Figure 4.3D**).

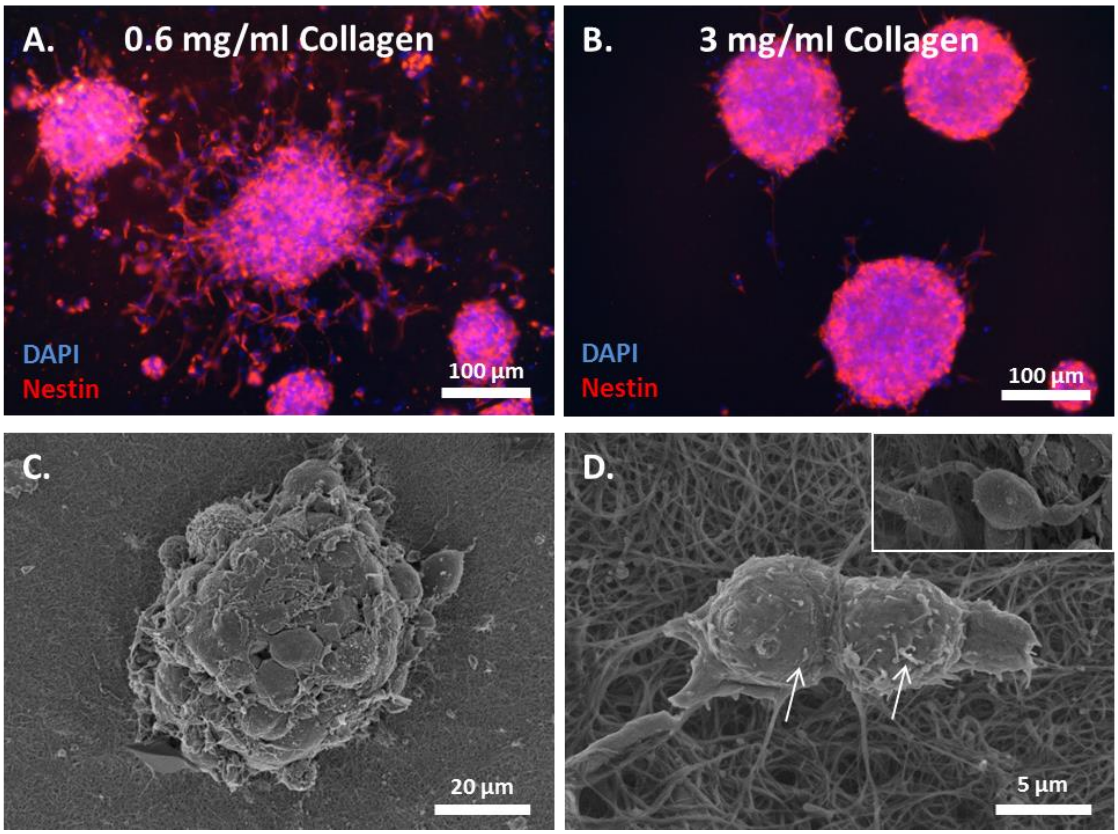

Figure 4.3. NSC propagation on collagen. *Representative fluorescent images of NSCs propagated for 4 days on (A) 0.6 mg/mL and (B) 3.0 mg/mL density collagen. Note that more cellular migration from the sphere seems to be apparent when NSCs are cultured on the lower density collagen. (C) FESEM image of NSCs after OTOTO processing forming a sphere on 0.6 mg/mL collagen. FESEM images of (D) dividing NSCs and (inset) a bipolar NSC following propagation on 0.6 mg/mL*

collagen and subsequent OTOTO processing. Arrows point to filopodia which can be observed on the membrane of the NSC.

4.3.2 NSCs differentiate on collagen into all the daughter cell types and can be visualised by fluorescence microscopy and FESEM

The developed staining protocols for fluorescence microscopy facilitated imaging of each of the daughter cell types generated from differentiated NSCs. Some problems in imaging arose from cells growing in different planes of focus, presumably due to undulation of the collagen and cells migrating through layers of the matrix (**Figure 4.4A-C**). Despite that, it was observed using fluorescence microscopy, that NSCs grown on collagen could be successfully differentiated into all the daughter cell types; astrocytes, neurons and oligodendrocytes (**Figure 4.4**). These appeared to be generated in similar proportions to those differentiated on glass (quantification performed in **Section 4.3.5**) with broadly similar and characteristic morphologies (**Figure 4.4** and see Chapter 2; Figure 2.11 and Chapter 3; Figure 3.14 for examples of differentiated cells cultured on a glass substrate). High magnification imaging using OTOTO-FESEM was also achievable after cells had been differentiated (**Figures 4.4D-F**) with some evidence of cell integration into the collagen matrix, especially evident in the case of a neuron that appears to be growing below the top layer of collagen (**Figure 4.4E**). Again, membrane features were straightforward to identify and a clear difference can be noted between the astrocytes, which appear to have an extensive covering of filopodia, and the neurons and oligodendrocytes which appear to be relatively quiescent (**Figure 4.4D-F**).

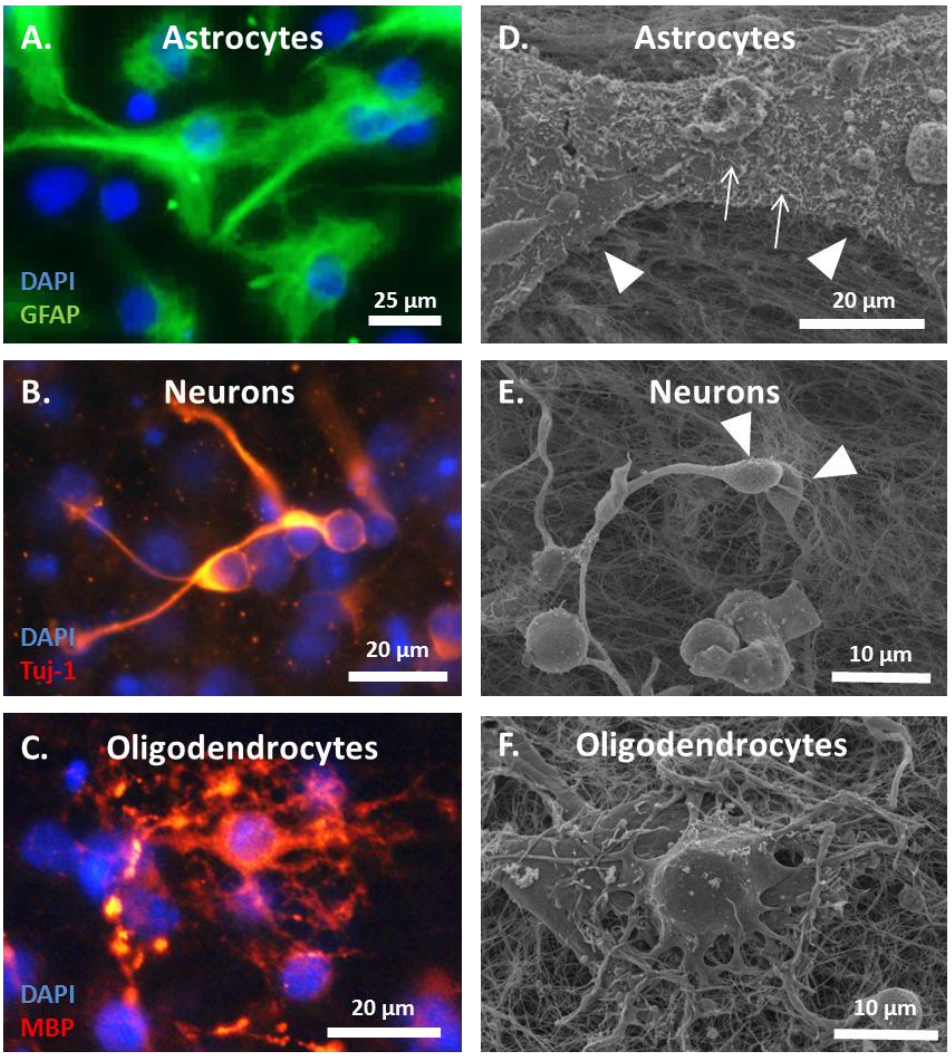

Figure 4.4. Differentiation of NSCs on collagen substrate. *Representative fluorescent images of (A) astrocytes, (B) neurons and (C) oligodendrocytes generated from NSCs propagated, and allowed to differentiate, on 0.6 mg/mL collagen. Daughter cells appear to have characteristic morphologies suggesting differentiation of NSCs on collagen is safe. Representative FESEM images following NSC differentiation on collagen and fixation using the OTOTO methodology of (D) astrocytes, (E) neurons and (F) oligodendrocytes. Arrow heads in (D) indicate two astrocytes in the image from a recent division and in (E) indicate neurons. Note membrane features such as filopodia can be readily identified (arrows in D) and cell protrusions appear to be growing underneath collagen fibrils (especially apparent in E).*

4.3.3 Magnetic field application can enhance MP mediated gene delivery to NSCs grown on collagen gels

To investigate the feasibility of MP mediated gene delivery to cells in collagen gels, NSCs were propagated on a collagen density of 0.6 mg/mL. At this stiffness it was observed that more single cells were present than on 3.0 mg/mL; possibly allowing MP access to a greater number of cells and therefore resulting in higher transfection efficiencies in a similar manner to monolayer vs neurosphere transfection, described in Chapter 2. After transfection, GFP expression was observed in nestin positive cells within spheres that had formed on the collagen and single cells separate from the spheres (**Figure 4.5**). Microscopic analysis of the NSCs revealed that a greater level of transfection was obtained after adding complexes in the presence of magnetic fields (**Figure 4.5**). Quantification of transfection efficiencies revealed that application of a static and an oscillating magnetic field significantly enhanced the number of transfected spheres compared to no-field transfection (**Figure 4.6A**). Application of an oscillating field also significantly enhanced the number GFP expressing cells per field compared to no-field, whereas no significant effect was observed with static field application compared to no-field (**Figure 4.6B**). A tendency towards increased proportions of spheres displaying two or more transfected cells was noted when using the oscillating field in comparison to no-field and static field conditions (**Figure 4.6C**).

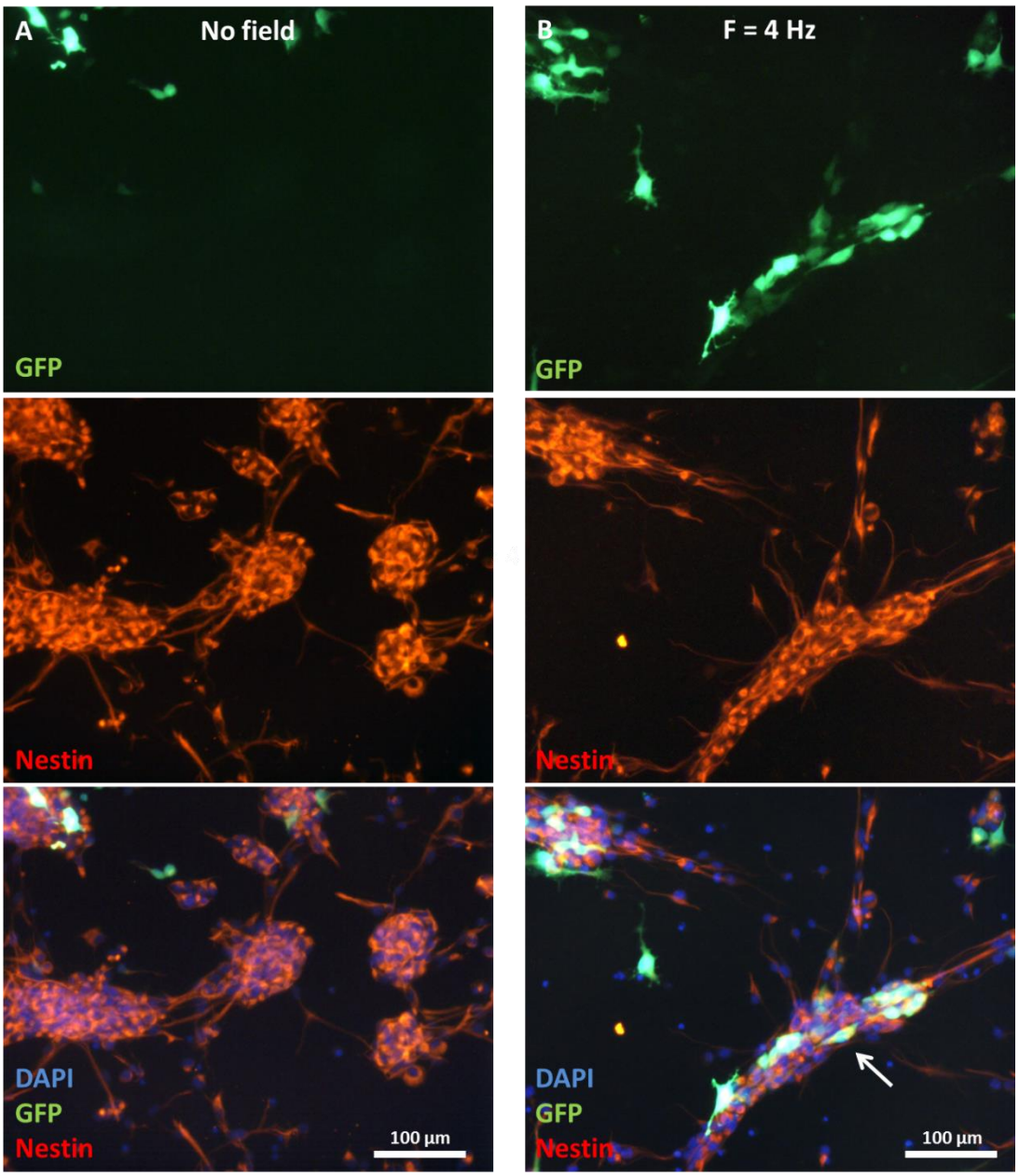

Figure 4.5. Field application enhances MP mediated gene delivery in NSCs grown on collagen gels. *Representative images of NSCs grown on 0.6 mg/mL collagen and transfected under (A) no field or (B) F = 4 Hz oscillating magnetic field. White arrow indicates GFP expressing cell co-expressing nestin. Note that more cells appear to be expressing GFP in the F = 4 Hz condition than in the no field condition which has been quantified in* ***Figure 4.6****.*

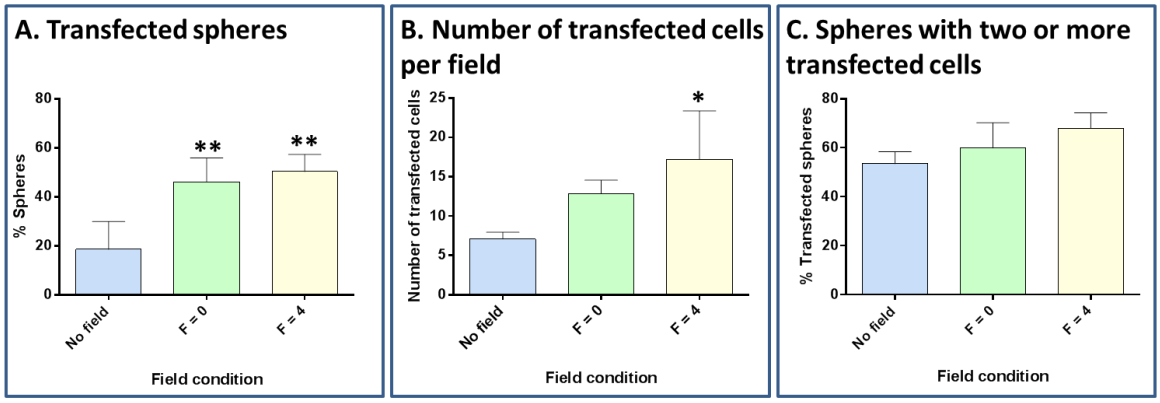

Figure 4.6. Quantification of transfection efficiency of magnetofection in NSCs propagated on collagen. *Bar charts depicting (A) proportions of transfected spheres (B) number of transfected cells per field (C) proportions of transfected spheres which contain two or more transfected cells across the different transfection conditions. Significant differences are **p<0.01 and *p<0.05 vs no-field (one-way ANOVA and Bonferroni's MCT, n = 4).*

4.3.4 The developed protocols have no effect on NSC proliferation, stemness and viability

Following magnetofection of NSCs grown on collagen, healthy spheres containing phase bright cells were observed in all conditions, including controls where no MPs were added. Quantification of spheres revealed no differences in sphere number or size across all conditions (**Figure 4.7A-B**). **Figure 4.7C** shows recently divided NSCs, both positive for nestin, indicating magnetofection does not affect cell division events. Further, all spheres observed microscopically were nestin or SOX2 positive and all transfected cells were also nestin or SOX2 positive (**Figure 4.7C-D**), demonstrating magnetofection protocols have no effect on stem cell marker expression. As a further assessment of the safety of magnetofection a LIVE/DEAD assay was performed. High NSC viability was observed after oscillating field magnetofection (estimated to be above 90%) which was similar to control cells where no particles were added (**Figure 4.8**). Dead cells were observed in the spheres

although the majority of dead cells appeared as single cells, outside of spheres. The high viability across all conditions observed here also suggests that culturing NSCs on collagen is safe.

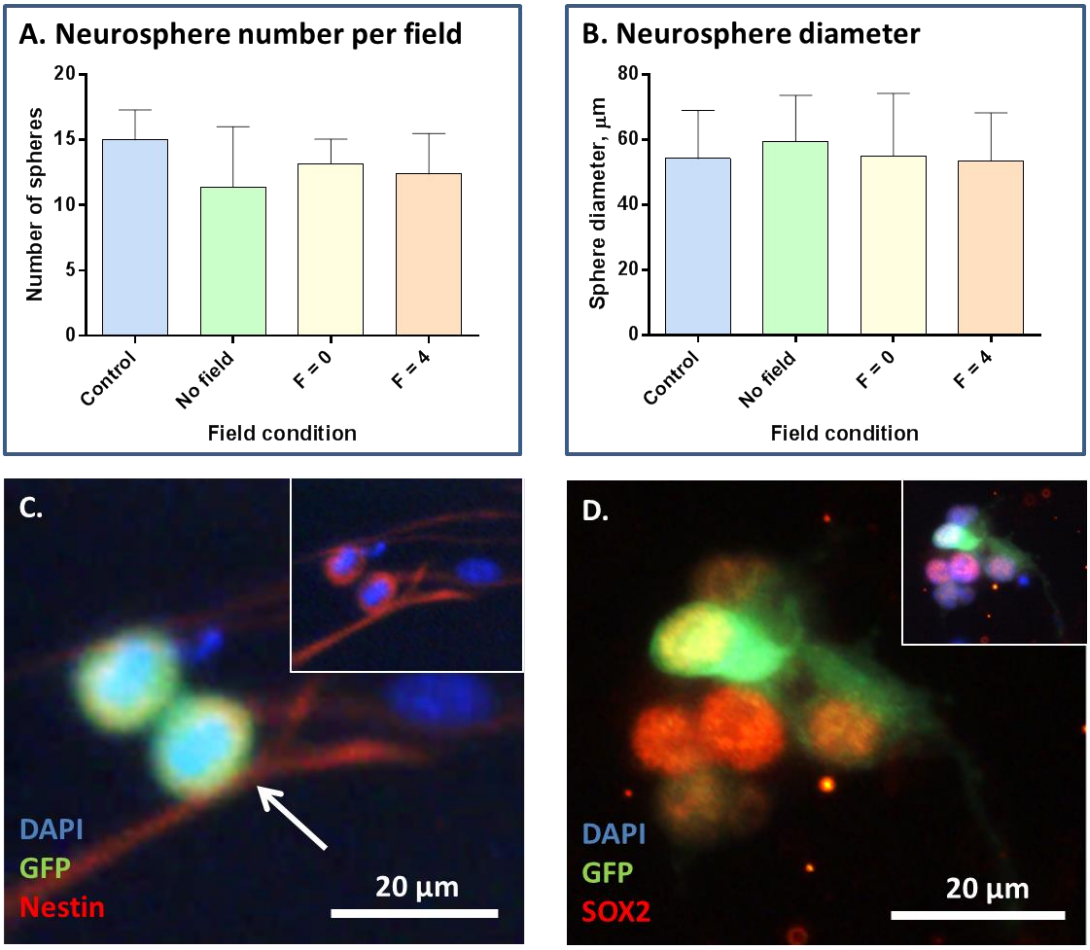

Figure 4.7. Safety assessments of the magnetofection procedures. *Bar charts depicting (A) numbers of neurospheres per field and (B) sphere diameter after transfection of NSCs on collagen across all conditions. (C) Cellular division of transfected NSCs on collagen (F = 4 Hz) producing two nestin positive cells which are both expressing GFP, indicated by white arrow. (C – inset) Double merged image showing same area as (C). (D) Representative image of a SOX2 positive sphere after transfection under the 4 Hz oscillating field condition with GFP expressing cells that are also positive for SOX2. (D – inset) Triple merged image of same area as (D) with the addition of DAPI staining to show the nuclei.*

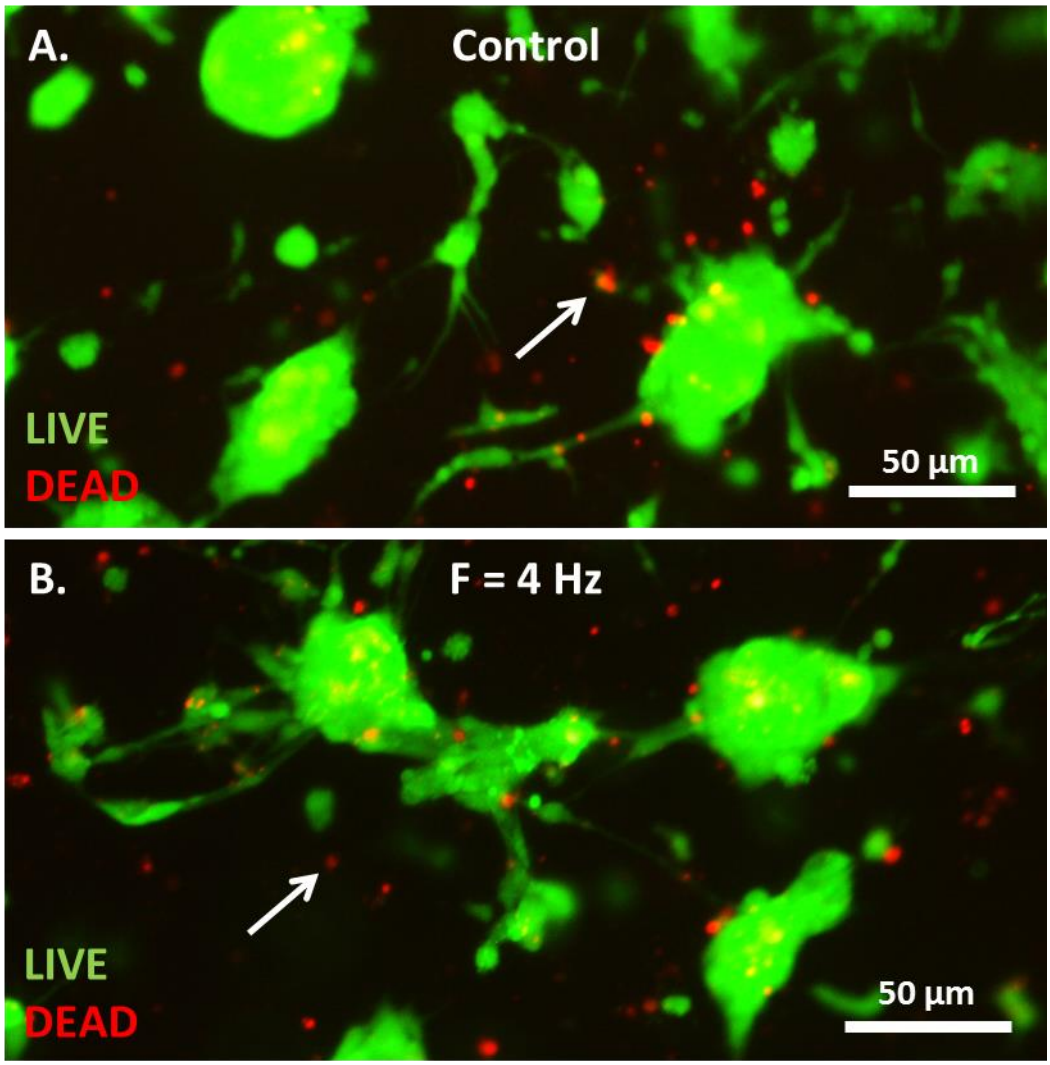

Figure 4.8. LIVE/DEAD assay of transfected cells on collagen. *LIVE/DEAD staining of NSCs grown on collagen either (A) under control conditions or (B) transfected under the 4 Hz oscillating field. Live cells appear green and dead cells appear red. Note the majority of dead cells appear to be single cells outside of spheres shown by the white arrows. Similar proportions of LIVE and DEAD cells appear to be present in each condition. However, quantification was not performed in this experiment as single cells could not be distinguished.*

4.3.5 Magnetofected NSCs differentiated normally on collagen

The ability of NSCs to generate their daughter cells on collagen was not affected by magnetofection protocols, with astrocytes, neurons and oligodendrocytes all produced (**Figure 4.9A-C**). Daughter cells were also produced in similar proportions across all conditions indicating magnetofection has no effect on the differentiation profile of NSCs (**Figure 4.9D-F**). It should be noted that daughter cells are generated in similar proportions to those observed on glass in the previous chapters (Chapter 2, **Section 2.3.6** and Chapter 3, **Section 3.3.7**). The majority of transfected cells were astrocytes with small numbers (< 3%) of transfected neurons observed. The proportions of GFP expressing astrocytes (no-field – 3.5 ± 1.6%; static field – 5.7 ± 2.1%; F = 4 Hz – 9.1 ± 1.5%) followed a similar pattern to the numbers of transfected cells counted per field in NSCs, although no significant differences were found.

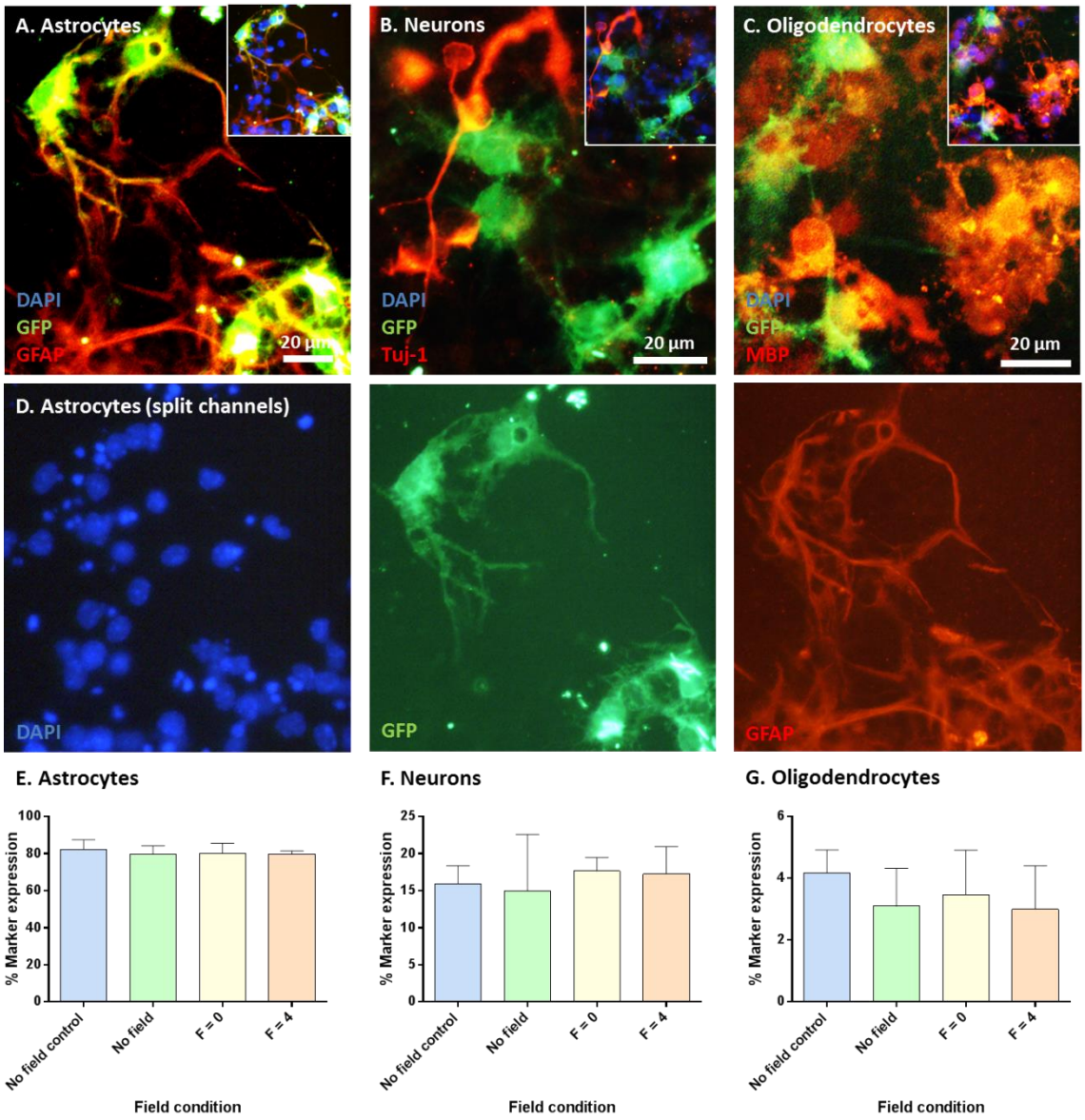

Figure 4.9. Differentiation of magnetofected NSCs on collagen. *Representative fluorescent images of (A) astrocytes, (B) neurons and (C) oligodendrocytes generated from NSCs transfected under the F = 4 Hz condition and allowed to differentiate on collagen. (D) Separate channels for each fluorophore from (A). The majority of transfected daughter cells were astrocytes and the overlap of GFP expression with GFAP staining can be observed in (A and D). GFP expressing cells with the morphological appearance of astrocytes can also be observed next to cells staining positive for (B) Tuj-1 and (C) MBP. Bar charts displaying quantification of the proportions of (D) astrocytes, (E) neurons and (F) oligodendrocytes generated under all tested conditions.*

Proportions of daughter cells generated appear to be similar across all conditions suggesting that the protocols are not having an effect on the differentiation profile of NSCs.

4.3.6 Field application has no effect with longer particle incubations

When complexes were incubated with the constructs for 48 h before terminating the experiment, proportions of transfected spheres were approximately 56% regardless of field condition (**Figure 4.10A**). This is slightly higher than the optimal condition from the 1 h incubation experiments (ca. 50% at F = 4 Hz). An increase was noted in numbers of GFP expressing cells per field when incubating the complexes for 48 h (ca. 26 per field; all groups) as compared to 1 h (17.2 ± 3.6 per field; F = 4 Hz); however, this had no effect on the proportions of spheres with two or more transfected cells which were similar across all conditions and matched that achieved in the F = 4 Hz group (ca. 67%) from the 1 h incubation experiments (**Table 4.2**). Preliminary safety assays indicated that incubating the complexes for 48 h had no effect on sphere number (**Figure 4.10B**) and size (**Figure 4.10C**) suggesting there is no significant effect on proliferation of NSCs, although a thorough safety assessment will have to be performed to confirm the safety of these procedures.

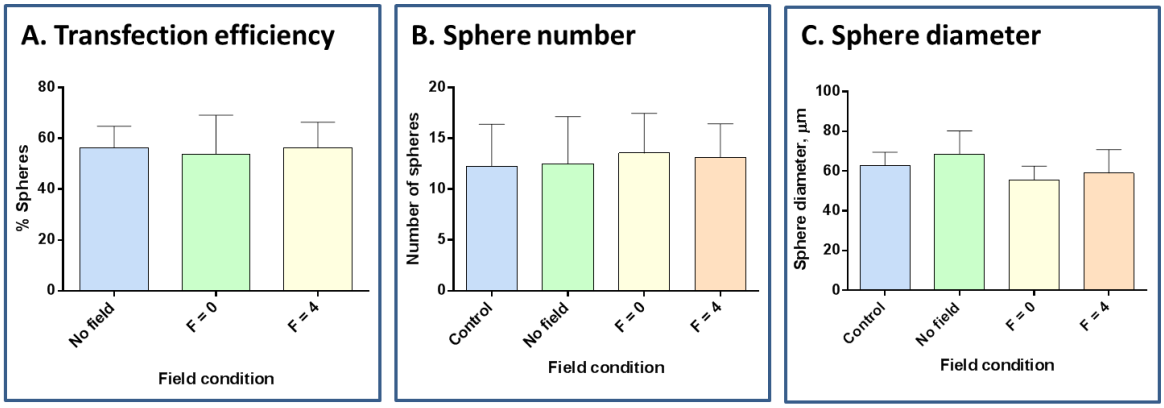

Figure 4.10. The effect on transfection efficiency after incubating the complexes for 48 h. *Bar charts displaying (A) proportions of transfected spheres grown on collagen after incubating complexes for 48 h under different field conditions, (B) sphere number per field 48 h post-transfection across all conditions and (C) sphere diameter 48 h post-transfection across all conditions.*

	Transfection condition			
	48 h incubation			**1 h incubation**
	No field	*F = 0 Hz*	*F = 4 Hz*	*F = 4 Hz*
Number of GFP$^+$ cells per field	25.1 ± 4.9	24.4 ± 3.5	29.9 ± 9.1	17.2 ± 3.6
Proportions of spheres displaying two or more transfected cells, %	66.8 ± 7.0	61.8 ±10.0	68.9 ± 8.1	67.9 ± 3.2

Table 4.2. Quantification of magnetofection efficiency in NSCs grown on collagen and transfected under different conditions.

4.3.7 Oscillating fields enhance transfection efficiency in NSCs incorporated in 3-D collagen constructs

In pilot experiments, NSCs were also successfully propagated in 3-D by incorporation into collagen gels before polymerisation. Nestin positive cells, with some displaying characteristic bipolar morphologies, could be seen throughout the gel (**Figure 4.11** and **Video 4.1**). Following

transfection, GFP expressing cells were also within the collagen matrix, and appeared throughout the gel, although were mainly found near the surface of the gel (**Figure 4.11**). Field application (F = 4 Hz) appeared to markedly enhance transfection levels as greater numbers of GFP expressing cells could be seen per unit area (**Figure 4.12**). However, transfection efficiency was low after oscillating field magnetofection with ca. 2-3% of cells expressing GFP from the total population.

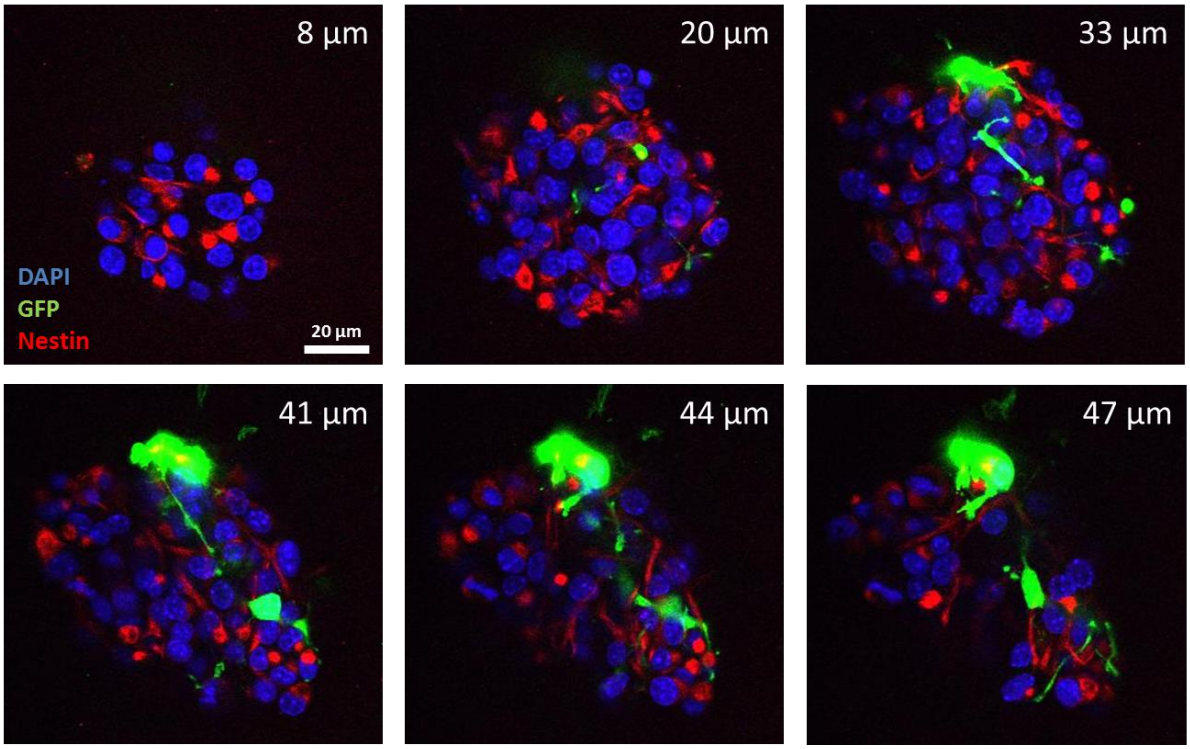

Figure 4.11. Confocal imaging of NSCs magnetofected after incorporation into a collagen scaffold. *Selected slices from confocal z-stack analysis at various heights through the gel with measurements taken from the base of the sphere. Scale is the same for each image. Corresponding z-stack movie is attached on CD as 'Z-stack of transfected sphere'.*

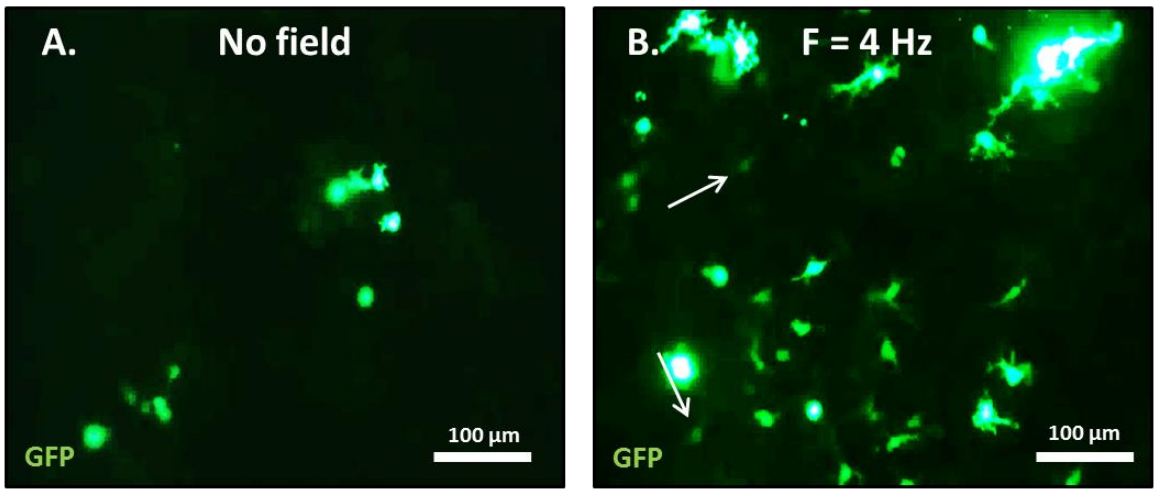

Figure 4.12. Magnetofection of NSCs incorporated into a collagen scaffold. *Representative fluorescent images of NSCs grown in 3-D transfected with MPs under (A) no-field or (B) a 4 Hz oscillating field. White arrows in (B) point to faint, GFP positive cells that are also out of focus suggesting transfection is occurring at different depths within the gel.*

4.4 Discussion

As far as I am aware, this is the first time that primary NSCs cultured within a potentially implantable hydrogel matrix have been genetically engineered *in situ*. Further, gene delivery was achieved using MPs and could be significantly enhanced by application of magnetic fields. Utilising the MP platform for this purpose could also provide a strategy to enable non-invasive graft monitoring after transplantation to examine cell localisation, survival and integration. Given the clinical advantages of hydrogel application (in improving transplant survival and integration), the data presented in this chapter could have particular impact for regenerative neurology in the development of protocols to produce complex implants capable of achieving multiple therapeutic goals. The clinical utility of this approach is also demonstrated with the lack of an effect on NSC

viability, stemness, division or differentiation – key regenerative properties of the transplant population.

4.4.1 Clinical utility of the developed protocols

In terms of utilising hydrogel technology for CNS therapy, gels can be pre-formed prior to transplantation or injected and allowed to set *in situ*. The advantages of an injectable hydrogel include minimally invasive application and the ability to fill a variety of lesion shapes and sizes – often present in the CNS after disease or injury. Transplantable hydrogels on the other hand can be several orders of magnitude more complex with incorporation of multiple cell types arranged in specific 3-D architectures to better mimic the surrounding tissue and promote functional repair. Further, a defined structural implant can be produced to facilitate directed tissue regeneration by spatially controlling guidance cues within the matrix. This is especially important for the guidance of axonal growth as stiffer substrates can be incorporated which are required by the axonal growth cone to 'pull' on.[106] Features such as this are difficult to achieve in injectable systems.

In the study presented here, NSCs were successfully cultured on pre-formed collagen hydrogels with dividing NSCs observed by FESEM and differentiation into their daughter cells (astrocytes, neurons and oligodendrocytes). In addition, NSCs were successfully cultured by encapsulation into a collagen scaffold with numerous bipolar, nestin positive cells (indicative of normal NSC morphology) observed by confocal microscopy, suggesting culture of NSCs with collagen is safe. Although collagen is rarely found in the CNS, it has been used for many neural applications, including implantation with NSCs into sites of injury and disease.[106] It has several advantages for regeneration in the CNS including the ability to reduce glial scarring, possibly by providing a scaffold for astrocytes to migrate into, and facilitating axonal growth and blood vessel infiltration

through the matrix.[105] Further, collagen hydrogels have been shown to closely match the stiffness of neural tissue which is thought to be important for implant acceptance. For the collagen density used in this study, the stiffness has been reported to be about 1 kPa[206] which is in the range of reported brain tissue stiffness (ca. 0.5 – 3 kPa).[207,208] In terms of cell transplantation, it has been shown that when cells are mixed with collagen scaffolding prior to implantation, histological and functional readouts can be improved compared to transplanting cells alone. This has not been explicitly proven for NSC transplantation with collagen; however, Lu *et al.* transplanted MSCs with or without collagen into areas of traumatic brain injury in rats.[209] The authors found that lesion volume was reduced (16 vs 11% of original lesion volume) and numbers of MSCs (ca. 14 vs 4 per mm^2) was increased in the collagen-cell group compared to cells alone. These differences also correlated to improved behavioural outcomes in the collagen-cell group compared to cells alone when tested using a modified neurological severity score, indicating the clinical benefits of using collagen scaffolds.

In this study, NSCs cultured on the collagen appeared to form spheres after two or more days in culture. In terms of transplantation, spheres are thought to be more protective of NSCs.[129] Combining the protective nature of sphere transplantation with cellular support from the collagen hydrogel could be a beneficial strategy to improve cell survival after transplantation – a key barrier to translation of NSC transplantation highlighted in the General Introduction (**Section 1.6**). Data from the literature and this chapter suggest that collagen may be used as a CNS compatible hydrogel for implantation of an NSC-collagen scaffold. Therefore, collagen seems a reasonable material to associate with NSCs to investigate intraconstruct genetic engineering.

The data presented in this chapter indicate that magnetofection can be used to genetically engineer NSCs cultured using clinically translatable hydrogel matrices. Previous reports have genetically engineered NSCs cultured with Matrigel™ and an Atelocollagen scaffold;[123] however,

Matrigel™ is currently not clinically translatable due to xenogenic components. Lack of flexibility and poor matching of CNS tissue stiffness associated with the Atelocollagen scaffold may also prevent application in the CNS. In addition, in this particular study, no information was provided on NSC invasion into the substrate (whether the cultures were dispersed throughout the matrix), transfection efficiency or safety of the procedures limiting the clinical relevance of this study. Further, this study involved combining the transfection complexes with the scaffold material before seeding the NSCs. In terms of clinical application, the protocols described in this chapter are suited to transfecting cells which have been previously cultured on the scaffold. This has particular relevance when cells are desired to adopt a specific 3-D architecture to enable their regenerative function (e.g. formation of neurospheres for cell protection post-transplantation). Applying the transfection complexes shortly before implantation, in a manner similar to that described in this chapter, can therefore maximise the time-course of therapeutic protein delivery.

Further clinical advantages of the methodologies described in this chapter derive from the use of MPs to deliver genetic material. Clinical advantages of MP mediated gene delivery compared to viral transduction and other non-viral manipulation techniques have already been discussed in depth (multiple sections in the General Introduction and Chapter 2). However, a few key features are highlighted in the following section. Importantly, the protocols were shown to be safe and transfection could be achieved after a relatively rapid incubation time (1 h with application of magnetic fields). The procedures are also straightforward, allowing operation by non-skilled personnel, of importance to wide-spread clinical adoption. An additional point to note here is that it may be necessary for transfection complexes to be 'driven' into the hydrogel; especially for cells cultured throughout the matrix. Confirming this, Zhang *et al.* observed negligible transfection efficiencies in NIH 3T3 cells cultured within collagen hydrogels when using non-viral transfection techniques such as lipofection which rely on diffusion to contact cells.[203] Therefore, magnetofection protocols may be vital for genetic manipulation of cells within hydrogel matrices.

The preliminary data presented in this chapter, regarding magnetofection of NSCs cultured in 3-D collagen matrices, suggest this may be the case with a dramatic increase in GFP expressing cells when utilising magnetic fields compared to no-field transfection.

For cells cultured on top of the hydrogel matrix, application of magnetic fields increased transfection efficiencies although no difference was observed between static or oscillating fields. Application of the static component of the magnet field is likely to increase transfection efficiencies through a similar mechanism to that described previously, namely, drawing the particles onto the cell surface and increasing cell-particle contact.[92] The reason for the absence of an effect when using the oscillating field is not currently known. However, a recent study suggested that the cell substrate might affect the efficiency of oscillating magnetic fields to transfect cells using MPs.[210] Here, cardiomyocytes were plated on collagen coated or uncoated surfaces which the authors referred to as adherent or semi-adherent cell states respectively. After oscillating field magnetofection, adherent cells displayed higher transfection than semi-adherent cells suggesting a possible change in membrane responsiveness to an oscillating field. If the oscillating field acts through a mechanical stimulation of the membrane and cellular machinery to increase transfection, these processes might not be as effective in less 'tense' cells. Culturing NSCs on substrates of different stiffness does alter the elastic moduli of the cells – on softer gels, cells have lower elastic moduli[199] – therefore the membrane may be less easy to deform to ultimately stimulate a response. Assessing membrane activity may be a strategy to observe whether this is the case. The fact that OTOTO-FESEM protocols can facilitate detailed examination of cellular membranes and interactions with the collagen substrate may mean this technique can provide a reasonable methodology to achieve this.

However, an increasing trend was observed from static to oscillating field magnetofection for number of GFP positive cells per field and number of spheres displaying two or more transfected

cells, suggesting there may be a limitation to the methods of analysis. Further, following 48 h incubation of complexes greater numbers of transfected cells per field were observed than the F = 4 Hz condition from the 1 h incubation group. However, this did not correlate with an increase in the percentage of spheres that were transfected. Enzymatically dissociating the construct and counting individual cells could be one future strategy to examine whether oscillating fields transfect more cells than static fields.

Although a direct comparison cannot be made, MP mediated transfection efficiency appeared to be less in NSCs cultured on hydrogels than that achieved in NSCs cultured on glass. This is especially true in the case of magnetofection in NSCs cultured throughout the collagen hydrogel where transfection efficiencies were estimated to be between 2 and 3%. It is likely therefore that transfection will need to be improved for both scenarios in order to be clinically useful. A number of different strategies could be employed in order to potentially achieve this. The previous study by Zhang *et al.* used small nanoparticles to achieve transfection (ca. 45 nm in hydrodynamic diameter) of cells cultured in 3-D collagen gels.[203] In their preliminary experiments, the authors also tested a commercial MP, PolyMag, which has a larger hydrodynamic diameter of ca. 250 nm and found this achieved less than 5% transfection efficiency. Although the chemistries of these two particles are different, which can significantly affect cellular uptake mechanisms, reducing particle size could be a reasonable strategy to increase gel penetration of the particles and subsequent transfection. Another more complex technique to improving particle uptake in cells within collagen gels could be to complex particles to CPPs, demonstrated by Child *et al*.[211] Here, MPs were complexed to the CPP, penetratin, and applied to a fibroblast cell line cultured throughout a collagen gel. With application of a magnetic field, only penetratin coated particles (and not "plain" particles) were observed to be taken up by cells at 500 µm depth within the gel. In this study no quantification was performed of cellular uptake in the whole cell population, but attaching CPPs to particles has been shown to enhance particle uptake previously,[177,178]

suggesting this is a promising strategy for enhancing particle uptake in cells cultured within a 3-D scaffold. Multifection, as described in Chapter 2 (**Section 2.4.1**), or longer field application could be used although would increase procedure time which may be disadvantageous from a clinical perspective if transfection needs to be performed immediately prior to implantation.

In areas with fewer resources this might not be possible as access to magnetic equipment may be limited, requiring alternative strategies to enhance transfection. In this respect, it is of interest that incubation of constructs with complexes for 48 h resulted in high transfection (56% of neurospheres) without the need for magnetic field application. This is in agreement with a similar result obtained by Child *et al.* with their plain MPs (counterparts to the penetratin particles described above).[211] Here, an 18 h incubation period resulted in improved particle association with the gel compared to 1 h incubation. However, although magnetic field application improved uptake over 1 h no effect was observed over the 18 h incubation period. As cells are at various heights in the medium, due to culture with collagen, the complexes may be able to sediment over a shorter period of time and contact more cells than when the cells are cultured in monolayer format. In this manner, magnetic field application is not required to enhance the sedimentation of the complexes to achieve optimal transfection. Lengthening incubation periods could therefore provide a simple means to enhance the intraconstruct engineering of neural cells by MPs, facilitating wide-spread use.

Different materials may ultimately be used in clinical application. The procedures described are straightforward; however, it is difficult to predict how they would translate across various materials as there are numerous discrepancies in the literature reporting different responses of NSCs to a range of materials. It is likely that varying the chemical and physical properties of the hydrogel matrix will affect NSC biology and subsequent interactions with MPs, therefore results from this study may not extrapolate to other biomaterials. In addition, changes in porosity of the

hydrogel will likely effect particle penetration into the gel. Demonstrating this principle, in preliminary studies investigating transfection of NSCs propagated in higher density collagen than reported in this chapter, I found transfection levels to dramatically drop-off. This could possibly be a result of reduced pore size and leading to poor particle penetration. A detailed assessment still needs to be performed to assess the extent of particle penetration into gels and to develop techniques to improve this.

A final point to note is that after differentiation of the collagen associated magnetofected NSCs, a multicellular construct containing genetically modified cells is obtained. As far as I am aware this is the first time that multiple, genetically engineered, neural cell types have been cultured in a single hydrogel system. The data provides promise for producing complex, multicellular implants using neurocompatible protocols – as both collagen and magnetofection have been shown to be safe for use with neural cells. This has implications for implantation of mature cells not usually amenable to transplantation, such as neurons or oligodendrocytes. Of particular interest could be promoting repair in accessible sites such as in SCI where implanted neurons can aid in reconnecting lost electrical circuitry, therapeutic biomolecules can promote axonal growth and oligodendrocytes can provide protection for the regenerating axons.

4.4.2 Conclusions and future work

The data presented in this chapter show that it is feasible to safely genetically engineer intraconstruct NSCs cultured with collagen, important due to the combined advantages of hydrogel and MP technology for NSC transplantation. For this preliminary study, relatively simple technologies have been used – the collagen gel was unmodified and Neuromag is primarily designed for gene delivery. However, the findings prove that intraconstruct cell engineering is

possible and could be useful with further improvements in transfection efficiency and sophisticated hydrogel design.

For example, hydrogels not only provide support for the transplant population but can be further functionalised to influence the transplanted cells and the host tissue. Incorporating growth factors into their formulation can improve NSC survival and differentiation into required cell types. Controlled differentiation of NSCs into neurons was observed after transplantation with a GDNF functionalised poly-caprolactone scaffold. In this scenario, neurite extension into the scaffold was also increased compared to an unfunctionalised scaffold.[212] Promotion of oligodendrogenesis from NSCs transplanted with a hyaluronan/methyl cellulose hydrogel has also been performed by immobilising PDGF-α onto the scaffold. Upon transplantation of the cell-polymer matrix, sparing of perilesional host oligodendrocytes and neurons was also observed with a reduction in injury site cavitation when compared to transplantation of NSCs alone.[213] These two studies suggest that NSC differentiation can be controlled by hydrogel formulation, facilitating repair for different injury paradigms. Coupled with genetic manipulation of the cells to also secrete disease specific therapeutic biomolecules this approach is attractive for providing advanced repair in the CNS.

In terms of the particles used, more clinically relevant particles could also be studied. Particles with higher iron content and different chemistries may be more amenable to hydrogel penetration and cellular uptake. Technologies such as plasmid mini-circles could also aid in reducing complex size. Here, non-essential DNA, such as bacterial promoters and antibiotic resistance genes are removed resulting in much smaller plasmids.[214] Therefore, combining small MPs with small plasmids might improve complex penetrance. These strategies could improve transfection levels overall but also provide a system for monitoring the graft post-implantation through MRI detection of MPs. It would be interesting to investigate this potential in future

studies. However, this preliminary study provides a platform from which sophisticated implantable hydrogels may be developed.

Chapter 5: Final conclusions and future directions

5.1 Summary of key thesis findings

Chapter 2. Safe and efficient gene delivery to NSCs grown as monolayers and neurospheres using magnetofection protocols

Oscillating magnetic fields were found to produce optimal MP transfection efficiency in NSCs cultured as neurospheres and monolayers. Monolayers displayed higher transfection efficiency than neurospheres (ca. 33 vs 10%) with a frequency of 4 Hz proving optimal, for both culture systems, in these studies. Standard safety assessments (of cell viability, proliferation, stemness and differentiation) proved that oscillating magnetofection protocols were non-toxic in both culture systems. GFP expressing daughter cells generated from transfected NSCs were mostly astrocytes with very few transfected neurons detected (<1% in daughter cells generated from monolayer NSCs) and no transfected oligodendrocytes observed. A preliminary proteomics analysis of monolayers showed proteins expressed and their levels of expression in magnetofected NSCs could be interrogated. GFP was positively identified within magnetofected samples suggesting the ability to perform analysis of safety and transfection success using one-step protocols. Further safety was demonstrated in monolayers by survival and differentiation of magnetofected NSCs after transplantation into cerebellum slice cultures. This test also shows the potential of using slice cultures as low cost and high throughput means of testing novel nanomaterial technologies designed to enhance NSC transplantation therapy.

Chapter 3: Developing high iron content particles for the efficient labelling of NSC transplant populations

In terms of NSC labelling with MPs, increases in iron content of non-functionalised PLA based MPs were found to lead to increases in NSC labelling. Using the lowest iron content particles field

application enhanced labelling in a pattern similar to that achieved with the Neuromag transfection grade particles (which also have low iron content). However, a high iron content particle was found to efficiently label NSCs (ca. 93% labelling) without need for magnetic field application. All labelling procedures were shown to be safe in terms of cell viability, proliferation, stemness and differentiation. Post-differentiation, astrocytes often displayed large accumulations of particles compared to single particles observed in neurons and oligodendrocytes – a similar finding to MP transfected NSCs where most daughter cell expressing GFP were astrocytes. MP labelled NSCs could be trapped in an *in vitro* flow system by application of a magnetic field. The efficiency of cell retention achieved after magnetic trapping of NSCs labelled with the different particle formulations was: Non-mag < MP-1X < MP-3X < MP-5X – reminiscent of the pattern of labelling of the NSCs with the different particle formulations. MP labelled NSCs survived after transplantation into slice models of SCI and appeared to retain the magnetic label. Labelled NSCs also differentiated, mostly into astrocytes consistent with NSC differentiation *in vivo*. In addition, the SCI slice model displayed characteristic hallmarks of SCI pathology including axonal regeneration and reactive astrocytosis. Along with the data collected using the cerebellum slices, the data utilising the SCI slice model suggest that these systems may be used to test nanotechnology as a means of improving NSC transplantation. The added benefit of the SCI slice model is that it mimics an injury site so potentially has more clinical relevance.

Chapter 4: Magnetofection of intraconstruct neural cells

NSCs were also successfully propagated and differentiated using collagen hydrogels as a substrate. Both fluorescence microscopy and FESEM could be used to visualise the NSCs and their daughter cells. The feasibility of magnetofection was demonstrated in NSCs cultured using collagen with transfection efficiency enhanced by application of magnetic fields, although no

additional benefit was seen by applying an oscillating field compared to a static field during transfection. Protocols developed here were also shown to be safe in terms of cell viability, proliferation, stemness and differentiation. Daughter cells generated from transfected NSCs grown on collagen and subsequently differentiated continued to express GFP, with the majority of transfected cells appearing to be astrocytes. Therefore, a multicellular collagen hydrogel was created also containing genetically engineered cells. A pilot study also demonstrated that MP mediated transfection of NSCs cultured throughout the collagen hydrogel was feasible and that application of an oscillating field appeared to show the highest transfection efficiency. Using confocal microscopy, GFP expressing nestin positive cells could be observed throughout the hydrogel indicating the safety of the developed protocols i.e. neither culture throughout collagen nor MP mediated transfection appeared to alter NSC specific marker nestin expression.

5.2 Implications of findings and future research directions

Taken together, the data in this thesis suggests that magnetofection may be used as a clinical grade transfection protocol for neural transplant populations. In order to apply this strategy in the CNS, introducing multiple therapeutic genes would be desirable to achieve several repair goals simultaneously. Single gene delivery has been demonstrated in this thesis; however, dual delivery (separate plasmids encoding GFP and RFP) has been demonstrated to OPCs[143] and to NSCs in our laboratory (paper in preparation). Therefore, enhancing the complexity of therapeutic gene delivery seems feasible. A further step in this regard could be to introduce temporal control over therapeutic genes after delivery. This would be especially important in neural repair where controlled biomolecule release could allow targeted regenerative events to occur sequentially, for example, break down of the glial scar followed by promotion of axonal outgrowth. To achieve this, plasmids could be engineered with inducible systems such as the tetracycline-on system.

Using this system, expression of GDNF from transduced MSCs has been shown to remain 'off' until activated by doxycycline,[215] a drug which has the potential to be used *in vivo*.[216]

Some genetic diseases highlighted in this thesis would also benefit from sustained gene expression to correct defective phenotypes resulting from misexpression of the target gene. Although plasmid delivery generally results in transient gene expression, there are multiple strategies for increasing the duration of expression.[217] One particular strategy is to utilise the sleeping beauty transposon system which is capable of transferring the desired gene from the plasmid into a targeted site within the genome.[218] This can enable sustained expression and, concomitantly, reduce risks associated with insertional mutagenesis. In this manner, a technique combining the sleeping beauty transposon system and electroporation to stably introduce a gene encoding a CD19 antigen (which recognises a specific leukaemia cell lineage), into T-cells before transplantation, has been approved for clinical trials (identifier: NCT00968760).[219] Therefore, this could represent an area of investigation in order to safely achieve long term gene expression in NSCs following magnetofection.

Further to gene delivery, data in this thesis also suggest that high iron content PLA based MPs could be used as neurocompatible particles for magnetic stem cell targeting. Along with data from other studies, demonstrating the capability of MPs to label transplant cells for tracking via MRI,[67,70] these findings indicate that novel multifunctional MPs could be used as a tool to achieve multiple biomedical outcomes. This will require testing of a range of particle formulations (which can differ in size, shape and surface chemistries) for transfection efficiency, NSC targeting capability and MRI contrast enhancement alongside toxicity analyses. With the wealth of materials available, assessing numerous particles for their translational potential will require detailed and high throughput tests. Developing the functional and safety assays and *in vitro* slice

models described in this chapter could provide methodologies to achieve this; without resorting to animal testing.

A major step in enhancing the high throughput capability of the *in vitro* tests is to adapt the protocols to automation. Automation of cell culture and online monitoring can already be achieved.[132,133,220] For measurement of fluorescent endpoints (which can provide information on viability, proliferation, stem cell marker expression, differentiation and transfection efficiency if using a reporter gene) automated cell culture could be coupled with high content imaging – a technique which is emerging as a popular tool for drug discovery.[221] Here, characteristics such as fluorescence intensity (for assessments of transfection efficiency or LIVE/DEAD staining) and shape (for assessments of fragmented nuclei and cellular morphology) can be interrogated by computerised imaging software to generate data on cell behaviour after treatment with various nanoparticle formulations. Using these protocols large numbers of wells can be treated, and endpoints measured, to provide powerful statistical analysis of differences between the particles in each category (in cell behaviour and transfection readouts). Currently, this is mostly achieved using cell lines with easily definable endpoints, such as, nuclear fragmentation as an indicator of cellular toxicity. Adapting these protocols for primary neural cells and more complex readouts (such as differentiation analysis) could create rapid tests for assessing the usefulness of nanotechnologies in regenerative neurology.

In addition to fluorescent readouts, automation of a molecular analysis performed using mass spectrometry (as described in Chapter 2) also seems feasible. Additional steps to cell culture and particle addition would include trypsinisation, cell lysis, protein extraction and separation which could all be optimised for online performance. Mass spectrometry is a fully automated procedure which outputs peptide fragmentation patterns to an external computer. With parallel research identifying important biomarkers for safety and transfection outcomes, these patterns could be

matched by the computer to a database containing these biomarkers, therefore providing a rapid non-biased analysis of transfection and safety of the tested nanoparticles.

Automating and monitoring slice culture may prove more challenging as moving slices requires delicate handling and the fact they are cultured on membranes restricts real time imaging. One possibility for their future application in nanomaterial testing, is that the culturing and manipulation of slices will be done manually and only promising nanotechnologies, identified in previous rounds of testing, assessed. However, after fixation, slices could be transferred to vessels where staining and subsequent imaging could be automated. Smart, high content imaging software could then be used to gather data on safety and functional readouts of fluorescence images, such as, fragmented nuclei or axonal outgrowth. If a list of simple and powerful outputs can be generated this will greatly expand the utility of slice culture as a strategy to assess advances in nanotechnology for neurological repair, especially in comparison to animal models.

Further development of the *in vitro* tests described in this thesis should focus on enhancing their predictive utility to accurately represent cellular and host tissue responses to nanomaterials; which could be achieved by utilising human cells and tissue. Human NSCs have been propagated as monolayers[128] and neurospheres[126] so would be amenable to the manipulations and standard safety and functional (assessing transfection efficiency) assays described in this chapter. However, oscillating field magnetofection protocols have never been tested in primary human neural cells. Therefore, it is not known whether there will be a difference in human cellular responses to MPs deployed with these oscillating fields compared to the mouse cells used in this study, representing a significant knowledge gap for the translation of this technology. In addition to testing the developed protocols on human cells, in order to achieve clinically relevant safety and functionality information, novel nanotechnologies may be tested on slices derived from human tissue. Such slice models would have to be developed in collaboration with hospital departments

but could provide valuable information on human tissue responses to nanomaterials – before their use in humans and with better predictive quality than that achieved using *in vivo* animal models. With detailed research into how molecular responses to nanomaterial manipulation and subsequent behaviours in tissue slices represent *in vivo* responses, sophisticated models such as this could lead to successful and safe clinical trials, reducing associated cost and risk.

In terms of utilising hydrogels as cell delivery systems, enhancing the complexity of the hydrogel system was discussed in detail in Chapter 4 (**Section 4.4.1**). Testing of various materials is vital as different materials can have distinct advantages for neuroregeneration. For example, self-assembling peptides have only recently been described for neurological applications. These materials offer a greater control over hydrogel stiffness than natural materials such as collagen, important to be able to accurately match the implant to the destination tissue stiffness. In addition, tight control over hydrogel stiffness may also impart some control over encapsulated NSC differentiation crucial for functional integration of transplanted cells. As cellular responses can vary when cultured on substrates which only have small changes in mechanical properties (tens of Pascals)[105] materials such as self-assembling peptides will be crucial in determining, with high precision, the optimal hydrogel stiffness for implantation area and desired transplant cell phenotypes.

Using MPs can enhance the regenerative potential of the cells embedded in hydrogels as discussed in Chapter 4. Further investigations into how particles interact with cells within the matrix could be useful to inform future particle design in order to enhance particle uptake. The FESEM-OTOTO technique could be used as a high-resolution imaging modality to probe particle cell interaction. Using this technique, iron oxide particles can be examined using energy dispersive microanalysis, to detect their associated iron, and membrane features involved in particle uptake such as filopodia and membrane ruffles can also be identified in parallel. [185] Data generated from

such studies could highlight differences in particle handling by the cell membrane in response to different particle formulations. Time-lapse microscopy may also be a valuable tool in this regard to assess the kinetics of particle uptake, important for developing optimal labelling protocols, and their subsequent cellular handling. The latter point is especially of relevance to the long term retention of MPs which impacts on the ability to track labelled cells by MRI.

Finally, the protocols described in this chapter appear to have clinical potential given the safety of the nanomaterials tested. Several MP formulations have been previously approved for clinical use by the FDA for MRI,[76] and also as iron supplements for anaemia,[222] and MRI facilities are widely available. Genetically engineered cells have also been approved for clinical trials within the CNS,[223] with non-viral delivery regarded as safer than viral manipulation of transplant populations. Implantation of hydrogels is still rare in the CNS; however, several polymer formulations have been used for other clinical applications, such as in cartilage and intervertebral disc repair,[103] and given their extensive advantages to cell transplantation therapy, it is likely that efforts will be focussed on translation into CNS applications. Therefore, the findings in this thesis represent important steps in developing translatable protocols for genetic manipulation, efficient cell delivery and potentially non-invasive tracking and functional integration of NSCs after transplantation. It is hoped that, with further improvements to particle uptake and hydrogel design (for which strategies have been outlined in the various chapters), these protocols could facilitate development of the next generation of therapies in regenerative neurology by combining nanotechnology with cell transplantation.

Appendix 1. Nanomedicine:NBM publication.

"*Magnetic nanoparticle mediated transfection of neural stem cell suspension cultures is enhanced by applied oscillating magnetic fields*".

Adams, CF. Pickard, MR. Divya, DM. Nanomedicine:NBM, 2013

This publication contains data found in Chapter 2 which has been licensed for use in this Thesis by Elsevier.

BASIC SCIENCE

Nanomedicine: Nanotechnology, Biology, and Medicine
9 (2013) 737–741

nanomedicine
Nanotechnology, Biology, and Medicine

Short Communication

Magnetic nanoparticle mediated transfection of neural stem cell suspension cultures is enhanced by applied oscillating magnetic fields

Chris F. Adams, MSc, Mark R. Pickard, PhD, Divya M. Chari, DPhil*

Cellular and Neural Engineering Group, Institute for Science and Technology in Medicine, Keele University, Keele, Staffordshire, United Kingdom

Received 5 March 2013; accepted 31 May 2013

Abstract

Safe genetic modification of neural stem cell (NSC) transplant populations is a key goal for regenerative neurology. We describe a technically simple and safe method to increase transfection in NSCs propagated in the neurosphere (suspension culture) model, using magnetic nanoparticles deployed with applied oscillating magnetic fields ('magnetofection technology'). We show that transfection efficiency was enhanced over two-fold by oscillating magnetic fields (frequency = 4 Hz). The protocols had no effect on cell viability, cell number, stem cell marker expression and differentiation profiles of 'magnetofected' cultures, highlighting the safety of the technique. As far as we are aware, this is the first successful application of magnetofection technology to suspension cultures of neural cells. The procedures described offer a means to augment the therapeutic potential of NSCs propagated as neurospheres – a culture model of high clinical translational relevance – by safe genetic manipulation, with further potential for incorporation into 'magneto-multifection' (repeat transfection) protocols.

From the Clinical Editor: This team of investigators describe a simple and safe method to increase transfection in neural stem cells using magnetic nanoparticles deployed with oscillating magnetic fields, demonstrating a greater than two-fold transfection efficiency increase by applying low frequency magnetic oscillation.

Key words: Neural stem cell; Neurosphere; Magnetic nanoparticle; Transfection; Nonviral

The central nervous system (CNS, i.e. brain and spinal cord) displays limited regeneration post-injury, generally leading to poor clinical prognoses. Current treatments can prevent further degeneration, but successful repair and return of functionality are key goals for regenerative neurology. Transplantation of repair mediating cell populations is a promising strategy to enhance repair (via replacement of damaged cells or protective bystander effects e.g. releasing therapeutic biomolecules).[1] Neural stem cells (NSCs), including genetically engineered populations, are a key transplant population in this regard given their high integrative capacity and differentiation into the three major cell populations of the CNS (neurons, astrocytes and oligodendrocytes).[2] Several studies using NSCs have progressed to the stage of clinical trials,[1] highlighting their major translational potential for regenerative medicine.

In this clinical context, transplantation of NSCs grown as 'neurospheres' (a suspension culture model used globally to propagate NSCs, including those of human origin) rather than dissociated cells offers several key advantages. Firstly, high NSC survival has been observed following transplantation of neurospheres in various models of CNS pathologies, including spinal cord injury,[3] possibly due to the maintenance of cell-cell contacts and associated pro-survival cell signalling.[4] Secondly, neurosphere cultures yield high cell numbers within a relatively small surface area, facilitating the provision of large cell numbers for transplantation (e.g. 8–12 foetuses are required per patient for grafting in Parkinson's disease[5]), which is currently a major barrier to clinical translation.

Abbreviations: CNS, central nervous system; DAPI, 4′,6-diamidino-2-phenylindole; EGF, epidermal growth factor; FGF-2, basic fibroblast growth factor; GFAP, glial fibrillary acidic protein; GFP, green fluorescent protein; MBP, myelin basic protein; MNP, magnetic nanoparticle; NSC, neural stem cell; OPC, oligodendrocyte precursor cell; SEM, standard error of the mean; Tuj-1, neuron-specific class III beta-tubulin.

This work was funded by grants from the British Biotechnology and Biological Sciences Research Council (BBSRC) and the Engineering and Physical Sciences Research Council (EPSRC) via the Doctoral Training Centre in Regenerative Medicine.

*Corresponding author: Cellular and Neural Engineering Group, Institute for Science and Technology in Medicine, Keele University, Keele, Staffordshire ST5 5BG, United Kingdom.

E-mail address: d.chari@keele.ac.uk (D.M. Chari).

1549-9634/$ – see front matter © 2013 Elsevier Inc. All rights reserved.
http://dx.doi.org/10.1016/j.nano.2013.05.014

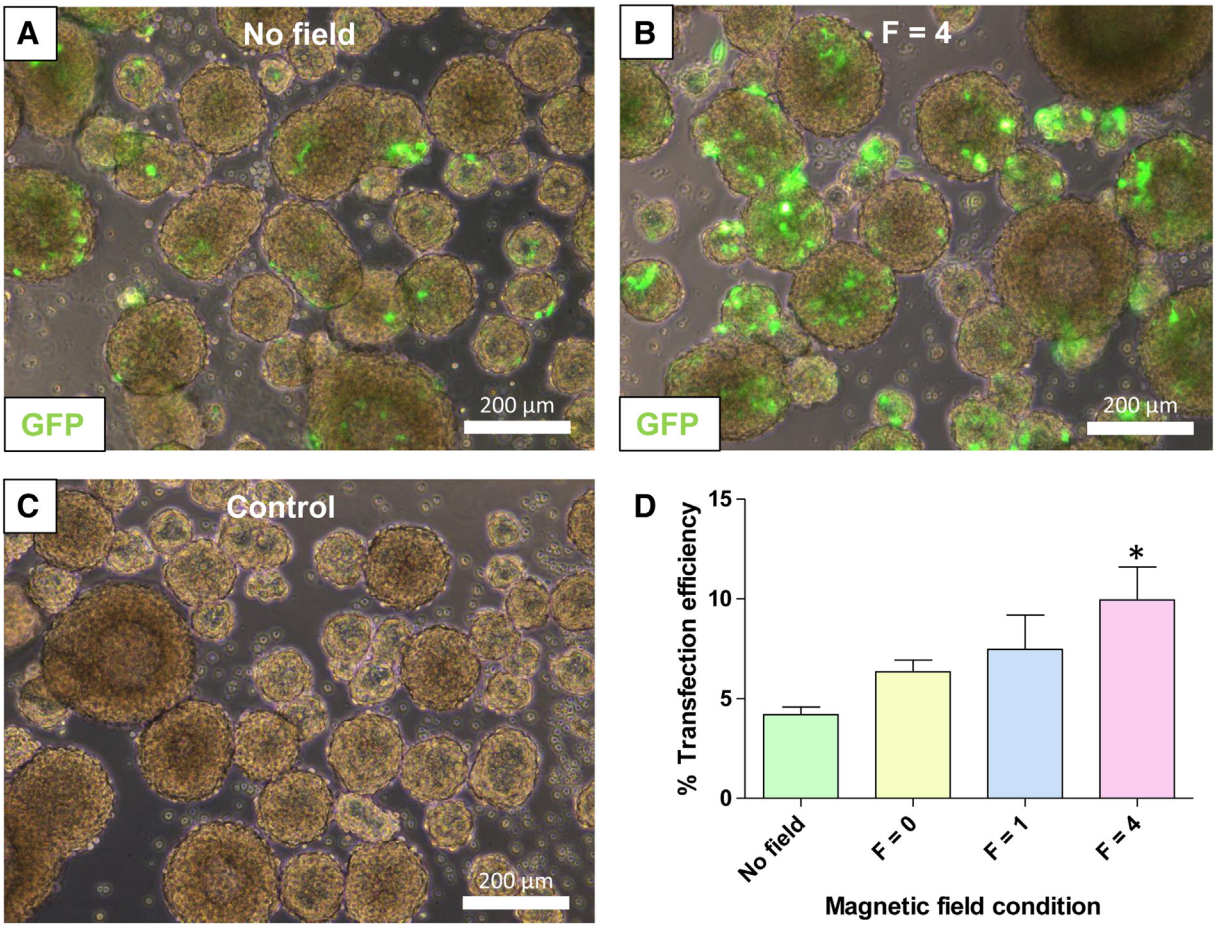

Figure 1. Effects of Magnetic Fields on Neurosphere Transfection. Double merged images of neurospheres 48 hours after MNP mediated transfection performed using **(A)** no field **(B)** a 4 Hz oscillating magnetic field compared with **(C)** neurospheres treated with plasmid alone, in the no field condition. **(D)** Bar chart displaying mean transfection efficiencies under all conditions, $*P < 0.05$ versus no field, n = 6 cultures (one way ANOVA and Bonferroni's MCT).

Currently, genetic engineering of NSCs (to augment their therapeutic potential) overwhelmingly relies on viral methods that are associated with numerous disadvantages including safety risks and costly scale-up production procedures.[6] In this context, magnetic nanoparticles (MNPs) offer significant advantages as nonviral gene delivery agents, with transfection significantly enhanced using 'magnetofection' methods (application of static/oscillating magnetic fields to assist MNP mediated biomolecule delivery).[7] We recently demonstrated that neurospheres can be successfully transfected using MNPs, although application of a static magnetic field had no effect on transfection levels.[8] However, we recently proved that application of *oscillating* magnetic fields, generated by high gradient NdFeB magnets, dramatically enhance transfection in monolayer (2D) cultures of major neural transplant populations such as oligodendrocyte precursor cells (OPCs).[9]

To date, the effects of oscillating magnetic fields have not been tested in the context of neurosphere transfection and indeed, as far as we are aware, in any suspension culture system. Given the translational advantages of the neurosphere culture system, the goals of this study were to determine the effects of oscillating magnetic fields on MNP mediated transfection, and to evaluate the safety of the procedures used.

Methods

Expanded methods are in Supplementary Information. Briefly, mouse subventricular zone-derived NSCs were maintained as neurospheres.[8] For magnetofection experiments, at 24 hours after passage, transfection with pmaxGFP:MNP complexes (or pmaxGFP only for controls) was performed previously[8] under four magnetic field conditions: no field, static field and oscillating fields (1 and 4 Hz).

All quantitative analyses have been performed using a combination of phase and fluorescence microscopy observations, to allow for readouts of transfection efficiency as well as morphological assessments (for procedural safety) to be carried out in parallel. At 48 hours post-transfection (time point which coincides with peak green fluorescent protein [GFP] expression, as previously reported[8]), neurospheres were dissociated for determination of transfection efficiency (% GFP expressing cells), total cell number and cell viability (by trypan blue exclusion). Cells were then replated as monolayers in appropriate media for quantitation of pyknotic nuclei (nuclear shrinkage or chromatin fragmentation indicative of cell death) and determination of NSC phenotype and differentiation potential. Immunocytochemistry was performed

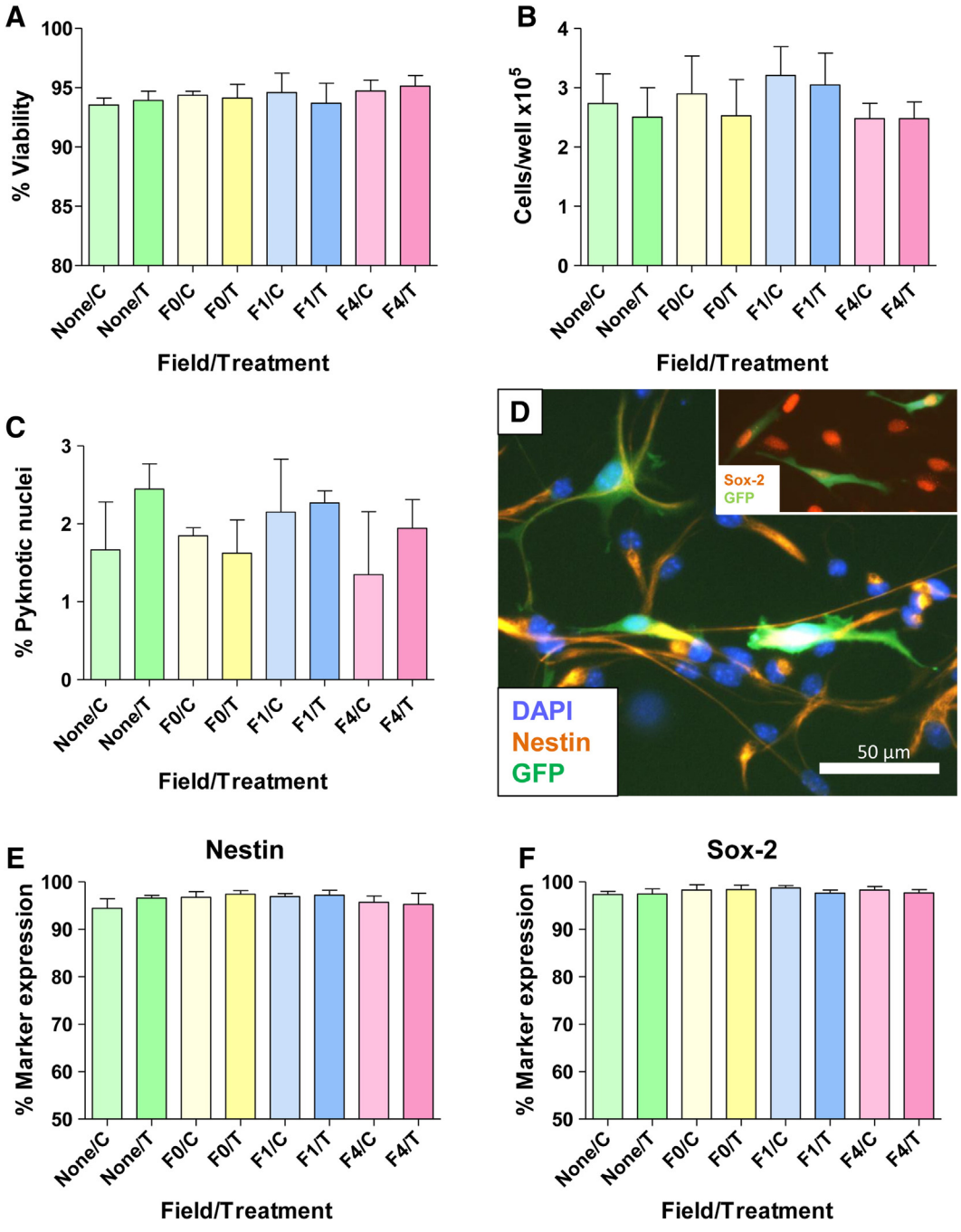

Figure 2. Viability and 'stemness' of transfected NSCs. Bar charts displaying **(A)** mean cell viabilities of NSCs, n = 5, **(B)** mean cell number per well, n = 5 and **(C)** percentage pyknotic nuclei, n = 3, across all conditions. Merged images of magnetofected (F = 4 Hz), GFP^+ NSCs, staining for NSC markers nestin **(D)** and Sox-2 (inset). Bar charts displaying percentage of nestin **(E)** and Sox-2 **(F)** positive cells, n = 4 cultures. None: no field, F(N): frequency of oscillation, C: control, T: transfected.

to detect NSC specific markers nestin and Sox-2 (quantified at 72 hours post-transfection), and for glial fibrillary acidic protein (GFAP – astrocytes), neuron specific class III beta-tubulin (Tuj-1 – neurons) and myelin basic protein (MBP – oligodendrocytes) for differentiation profile analysis (quantified at 9 days post transfection).

All data were analysed by one-way ANOVA and Bonferroni's multiple comparison test (MCT) using Graphpad Prism software (version 4.03). Data are expressed as mean ± SEM.

Results

Effects of magnetic fields on neurosphere transfection

Under all experimental conditions, neurospheres appeared intact and of similar size, with GFP expressing cells present throughout transfected spheres (Figure 1, *A–C*). At 48 hours, basal transfection (no field) was found in 4.2 ± 0.4% of cells. Application of all fields showed a tendency to increase

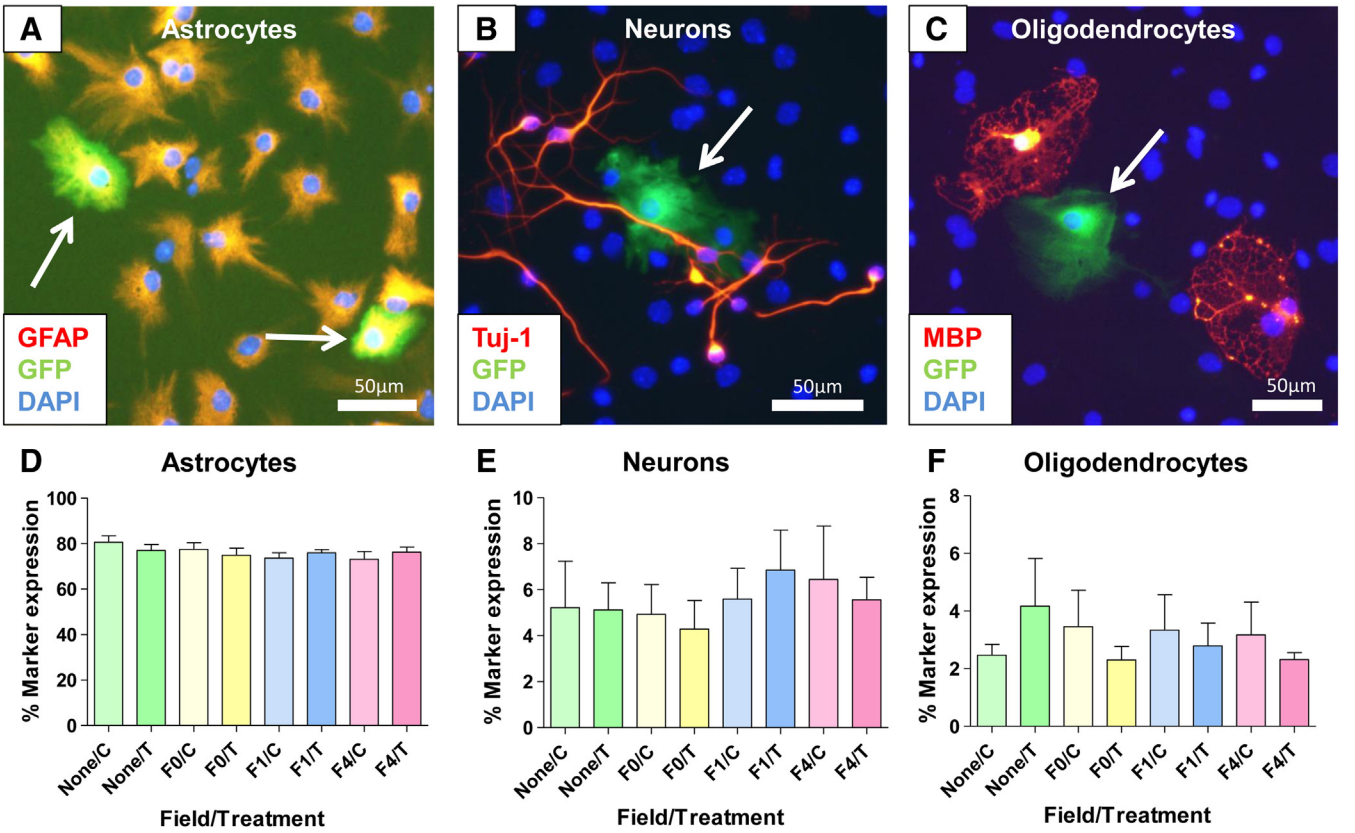

Figure 3. Differentiation profiles of transfected NSCs. Triple merged images of magnetofected (F = 4 Hz) NSCs post-differentiation showing cells positive for GFAP **(A)** Tuj-1 **(B)** and MBP **(C)**. GFP expressing $GFAP^+$ cells are seen in (A, arrows) and GFP^+ cells with the morphological appearance of astrocytes in (B and C, arrows). **(D-F)** Bar charts showing proportions of GFAP, Tuj-1 and MBP positive cells, n = 4 cultures. None: no field, F(N): frequency of oscillation, C: control, T: transfected.

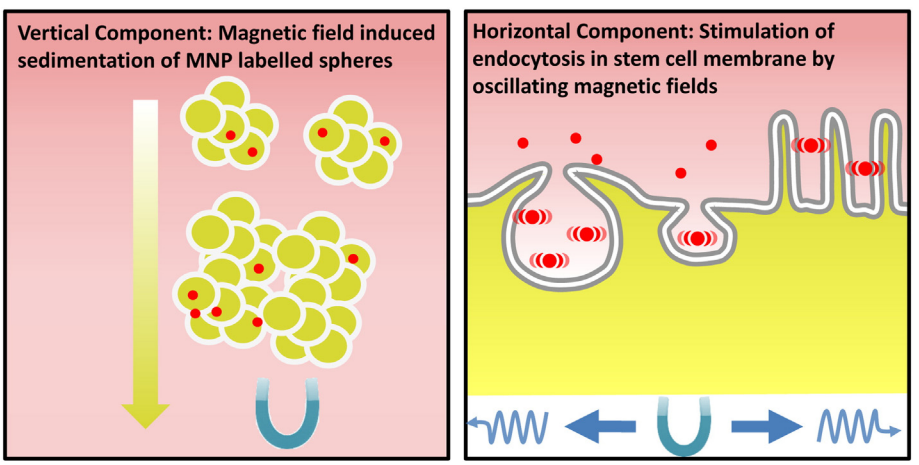

Figure 4. Proposed mechanism of transfection of neurospheres. Schematic diagram illustrating a hypothetical model to explain the mechanism of oscillating field enhancement of transfection in neurospheres.

transfection levels; the increase was maximal and statistically significant for the 4 Hz condition [approximately two-fold increase (9.9 ± 1.7%)] (Figure 1, *A*, *B* & *D*). Monitoring of spheres at 12 hour time points post-transfection revealed a similar pattern in GFP expression (F = 4 Hz > no field and F = 0 Hz) to that seen at 48 hours. Transfected cells were not observed under any condition in the plasmid only, control cultures.

Viability, 'stemness' and differentiation profiles of transfected NSCs

NSC viability, cell number and percentage of pyknotic nuclei were similar across all conditions (Figure 2, *A*, *B* & *C*). Further, co-localisation of NSC markers and GFP was observed (Figure 2, *D*) and the protocols had no effect on the expression of nestin and Sox-2

(Figure 2, *E* & *F*). The differentiated progeny of transfected NSCs were exclusively astrocytes (Figure 3, *A–C*); transfected neurons/oligodendrocytes were never observed in these experiments. NSC differentiation profiles were also unaffected post transfection - similar proportions of astrocytes, neurons and oligodendrocytes were generated under all conditions (Figure 3, *D–F*).

Discussion

We report here a simple method to enhance MNP mediated gene transfer in a widely used NSC culture model. Technical ease, accompanied by high safety, as evidenced by negligible effects on 'stemness' and differentiation profiles, highlight the clinical potential of this technique. We previously showed that 'multifection' (repeat transfection) can safely enhance MNP based gene transfer in neurospheres.[8] Future work will focus on repeat transfection in conjunction with oscillating magnetic fields, and we predict that the safety of the protocols reported here will easily extrapolate to such a 'magneto-multifection' approach to further augment transfection levels. With further development, combined neurosphere culture and magnetofection could also be amenable to automation - essential for reproducible and scalable production of genetically engineered cell transplant populations,[10] including human NSCs for clinical use.

The underlying mechanism for enhanced transfection by oscillating magnetic fields in neurospheres in the current experiments is unclear. It is well established that static magnetic fields assist transfection by increasing particle-cell contact, and that MNP uptake occurs via various forms of cellular endocytosis.[7] Further, magnetofected NSCs (in monolayer cultures) which have been exposed to high frequency (4 Hz) fields reveal a greater degree of membrane ruffling compared with untreated cultures (our unpublished observations), suggesting endocytotic stimulation. Taking these observations together, we propose a model to explain our findings wherein sedimentation of MNP labelled spheres (through the vertical component of the magnetic field) would increase particle-cell contact, the first barrier to transfection when using MNPs.[7] Subsequent stimulation of NSC membrane endocytotic activity (by the horizontal magnetic field component) may provide a reasonable explanation for the observed oscillation dependent increase in transfection (Figure 4).

In conclusion, we believe this study highlights the efficacy of the MNP vector platform for technically simple gene transfer to neurospheres for translational applications in transplantation neurobiology.

Appendix A. Supplementary data

Supplementary data to this article can be found online at http://dx.doi.org/10.1016/j.nano.2013.05.014.

References

1. Trounson A, Thakar RG, Lomax G, Gibbons D. Clinical trials for stem cell therapies. *BMC Med* 2011;**9**:52.
2. Pluchino S, Quattrini A, Brambilla E, Gritti A, Salani G, Dina G, et al. Injection of adult neurospheres induces recovery in a chronic model of multiple sclerosis. *Nature* 2003;**422**:688-94.
3. Akesson E, Piao JH, Samuelsson EB, Holmberg L, Kjaeldgaard A, Falci S, et al. Long-term culture and neuronal survival after intraspinal transplantation of human spinal cord-derived neurospheres. *Physiol Behav* 2007;**92**:60-6.
4. Campos LS. Neurospheres: insights into neural stem cell biology. *J Neurosci Res* 2004;**78**:761-9.
5. Ali F, Stott SR, Barker RA. Stem cells and the treatment of Parkinson's disease. Exp Neurol Published Online First: 6 January 2013.
6. Rogers ML, Rush RA. Non-viral gene therapy for neurological diseases, with an emphasis on targeted gene delivery. *J Control Release* 2012;**157**:183-9.
7. Plank C, Zelphati O, Mykhaylyk O. Magnetically enhanced nucleic acid delivery. Ten years of magnetofection-progress and prospects. *Adv Drug Deliv Rev* 2011;**63**:14-5.
8. Pickard MR, Barraud P, Chari DM. The transfection of multipotent neural precursor/stem cell transplant populations with magnetic nanoparticles. *Biomaterials* 2011;**32**:2274-84.
9. Jenkins SI, Pickard MR, Granger N, Chari D. Magnetic nanoparticle-mediated gene transfer to oligodendrocyte precursor cell transplant populations is enhanced by magnetofection strategies. *ACS Nano* 2011;**5**:6527-38.
10. Thomas RJ, Hope AD, Hourd P, Baradez M, Miljan EA, Sinden JD, et al. Automated, serum-free production of CTX0E03: a therapeutic clinical grade human neural stem cell line. *Biotechnol Lett* 2009;**31**:1167-72.

Appendix 2. Nanomedicine publication II.

"*Increasing magnetite contents of polymeric magnetic particles dramatically improves labeling of neural stem cell transplant populations*".

Adams, CF. Rai, A. Sneddon, G. Yiu, HHP. Polyak, B. Chari, DM. Nanomedicine:NBM, 2015

This publication contains data from Chapter 3 which has been licensed for use in this Thesis by Elsevier.

BASIC SCIENCE

Nanomedicine: Nanotechnology, Biology, and Medicine
11 (2015) 19–29

nanomedicine
Nanotechnology, Biology, and Medicine

Original Article

nanomedjournal.com

Increasing magnetite contents of polymeric magnetic particles dramatically improves labeling of neural stem cell transplant populations

Christopher F. Adams, MSc[a], Ahmad Rai, MD[b], Gregor Sneddon, MChem[d], Humphrey H.P. Yiu, PhD[d], Boris Polyak, PhD[b,c,*], Divya M. Chari, DPhil[a,**]

[a]*Cellular and Neural Engineering Group, Institute for Science and Technology in Medicine, Keele University, Keele, Staffordshire, United Kingdom*
[b]*Department of Surgery, Drexel University College of Medicine, Philadelphia, PA, USA*
[c]*Department of Pharmacology and Physiology, Drexel University College of Medicine, Philadelphia, PA, USA*
[d]*Department of Chemical Engineering, School of Engineering and Physical Sciences, Heriot-Watt University, Edinburgh, United Kingdom*

Received 21 March 2014; accepted 10 July 2014

Abstract

Safe and efficient delivery of therapeutic cells to sites of injury/disease in the central nervous system is a key goal for the translation of clinical cell transplantation therapies. Recently, '*magnetic cell localization strategies*' have emerged as a promising and safe approach for targeted delivery of magnetic particle (MP) labeled stem cells to pathology sites. For neuroregenerative applications, this approach is limited by the lack of available neurocompatible MPs, and low cell labeling achieved in neural stem/precursor populations. We demonstrate that high magnetite content, self-sedimenting polymeric MPs [unfunctionalized poly(lactic acid) coated, without a transfecting component] achieve efficient labeling (≥90%) of primary neural stem cells (NSCs)—a '*hard-to-label*' transplant population of major clinical relevance. Our protocols showed high safety with respect to key stem cell regenerative parameters. Critically, labeled cells were effectively localized in an *in vitro* flow system by magnetic force highlighting the translational potential of the methods used.

From the Clinical Editor: Utilizing self-sedimenting polymeric magnetic particles, the authors demonstrate an efficient method for magnetically labeling primary neural stem cells for magnetic localization in the central nervous system.

Key words: Polymeric magnetic particles; Neural stem cells; Labeling; Transplant cells; Magnetic cell targeting

Advances in stem cell technology have had a major impact in the field of regenerative neurology. Several transplant cell populations show improved neurological outcomes in pre-clinical models of injury and disease, including spinal cord injury (SCI), stroke, Parkinson's disease, Huntington's disease and birth defects.[1] A major obstacle in the translation of cell transplantation is the safe and efficient delivery of cells to sites of disease/injury. The two main methods for cell delivery (systemic and direct local injection) have associated problems in this regard. Injecting cells systemically can lead to their eventual clearance in the spleen, liver or lung resulting in low cell accumulation at the desired site.[2,3] Multiple direct injections can result in secondary pathology due to blood brain barrier damage, bleeding or embolization.[4] To overcome these issues, several reports have shown that transplant cells labeled with magnetic particles (MPs) can be efficiently "trapped" at foci of injury by application of a magnetic field gradient, as part of so called '*magnetic cell localization*' strategies.[5–9] Application of fields

This work is supported by a research grant from the Biotechnology and Biological Sciences Research Council, UK (DMC), the Engineering and Physical Sciences Research Council funded Doctoral Training Centre in Regenerative Medicine (CFA) and by the USA Award Number 5R01HL107771 from the National Heart, Lung and Blood Institute (BP). The content is solely the responsibility of the authors and does not necessarily represent the official views of the National Heart, Lung and Blood Institute or the National Institutes of Health.

This work has been presented as a poster at the Cell Tracking Symposium, Liverpool University, July 2013, Doctoral Training Centre in Regenerative Medicine's Joint Conference, Sheffield University, July 2013 and the FIRM symposium, Girona, September 2013.

*Correspondence to: B. Polyak, Department of Surgery and Department of Pharmacology and Physiology, Drexel University College of Medicine, Philadelphia, USA.

**Correspondence to: D. Chari, Cellular and Neural Engineering Group, Institute for Science and Technology in Medicine, Keele University, Keele, Staffordshire, United Kingdom.

E-mail addresses: bpolyak@drexelmed.edu (B. Polyak), d.chari@keele.ac.uk (D.M. Chari).

http://dx.doi.org/10.1016/j.nano.2014.07.001
1549-9634/

over sites of pathology can trap systemically injected cells as they pass through the vasculature.[6,8] This would offer considerable benefits if used in conjunction with the 'homing' capability of some stem cell types to sites of injury (after intravenous administration).[10] Field application has also been suggested to localize cells near injury sites after intrathecal injection[7] and can thereby remove the need for multiple injections over time. Enhanced cell accumulation using this method has been shown in the heart,[9] on the surface of intraarterial steel stents[8] and also for some neurological applications.[5–7]

Despite being a promising method to safely enhance cell accumulation at injury sites, a major limiting factor for neurological applications is the relatively low MP labeling efficiency achieved in stem cell transplant populations; few neurocompatible particles have been developed for neurological use. Diverse chemical/biological strategies have been adopted to promote intracellular MP accumulation. These include chemical transfection coating agents (such as chitosan or polylysine)[6,11,12] or cell uptake enhancing molecules (such as the RGD/TAT peptides).[13] While effective from a research perspective, such strategies are not optimal in the clinical context as the related methods can be time consuming, involve significant technical challenges in generating nanoparticle constructs, and are limited by non-specificity of cellular targets. Moreover, these can be associated with cellular toxicity[14,15] and the effects of targeting molecules on neural cell physiology are poorly understood.

As an alternative *physical* delivery approach, MPs have been deployed with external magnetic fields to enhance cellular uptake.[16,17] From a translational perspective, these magnetic assistive methods rely on intrinsic endocytotic uptake mechanisms of cells and have high associated safety.[16] As magnetic force is proportional to the particle magnetic moment, magnetite entrapment within MPs is a major parameter that can influence cell–particle interactions and cellular uptake. Despite this, the relationship between magnetite concentration, applied magnetic fields and cellular labeling in '*hard-to-label*' stem cell transplant populations has never been investigated. It should be noted that studies investigating the relationship between magnetic force and cell loading in neural cells, using applied magnetic fields, have primarily used transfection (gene delivery) grade MP reagents, many of which have low iron content, and where particle uptake is strongly influenced by properties specific to the transfecting component.[18] As such, these cannot provide insights into the relationship between MP magnetite content and '*magnetolabeling*' of stem cells.

To address these issues, the goal of this study is to investigate the effects of systematically modulating MP magnetite concentration on labeling of multipotent, primary neural stem cell (NSC) transplant populations, in conjunction with applied magnetic fields (static and oscillating). The translational potential of the labeling methods has been evaluated by assessing the magnetic cell localization potential of the labeled NSCs in a flow system, using applied magnetic force. NSCs were selected as the target stem cell population given their high clinical relevance for the repair of neurological injury and their capacity to migrate towards sites of pathology, a phenomenon termed '*pathotropism*'. Available MP labeling studies indicate that NSCs have intrinsically low MP labeling efficiencies in the absence of delivery enhancing strategies,[19–21] making these an ideal test population for the current study.

Methods

Magnetic particle formulation and characterization

Fluorescent poly(lactic acid) (PLA) coated non-magnetic (termed Non-mag) and MP samples with varied magnetite content (MP-1X, MP-3X and MP-5X, indicating their relative magnetite content) were prepared using published methods.[17,22] Expanded methods including reagent information/particle formulation are in Supplementary Information. Particles were fully characterized using dynamic light scattering (DLS), transmission electron microscopy (TEM), magnetometry, zeta potential measurement, Fourier-transform infrared (FTIR) spectroscopy, elemental analysis, and powder x-ray diffraction (XRD). Full experimental details are also in the Supplementary Information. Figure 1 illustrates a schematic procedure for preparing the PLA MPs.

Preparation of NSC cultures and MP labeling procedures

NSCs derived from the subventricular zone of CD1 mouse pups (postnatal days 1-3)[23] were maintained as neurospheres in complete medium (defined in Supplementary Information). Neurospheres (passages 1-3) were dissociated to a single cell suspension and maintained as monolayers by plating 1.2×10^5 cells in 600 μL of monolayer medium (defined in Supplementary Information) onto glass coverslips (or aclar for TEM) coated with poly-ornithine and laminin in 24 well plates. Cells were allowed to adhere for 24 hours before changing to fresh monolayer medium with or without particles.

To prepare particle suspensions, lyophilized aliquots (containing the same number of particles for each particle type) were re-suspended in water and added to monolayer medium so that final suspensions contained a 1:1000 ratio of particle solution to medium (approximately 15 μg/mL of dry weight for MP-1X, 19 μg/mL for MP-3X and 26.5 μg/mL for MP-5X). Cells were incubated for 24 hours under no field, static (oscillation frequency: $F = 0$ Hz, 200 μm amplitude) or oscillating ($F = 4$ Hz, 200 μm amplitude) magnetic fields for the first 30 minutes. Field application was restricted to 30 minutes as heating effects were observed in pilot experiments using oscillating fields for longer time periods, and static fields applied for 24 hours resulted in significant particle aggregation. After incubation, cells were washed 3-5 times with phosphate buffered saline (PBS) to remove particles not internalized. Cells were fixed using 4% paraformaldehyde (15 minutes, room temperature) for immunocytochemistry or 2.5% glutaraldehyde for TEM analysis or switched to differentiation medium (complete medium minus growth factors, supplemented with 1% FCS). Cells in differentiation medium were cultured for a further 7 days with medium changes every 2-3 days. TEM samples were processed as previously described.[24]

Assessment of proliferation, stemness and differentiation of labeled NSCs

To assess safety of the procedures, cells fixed at 24 hours post particle addition were stained for the NSC specific markers

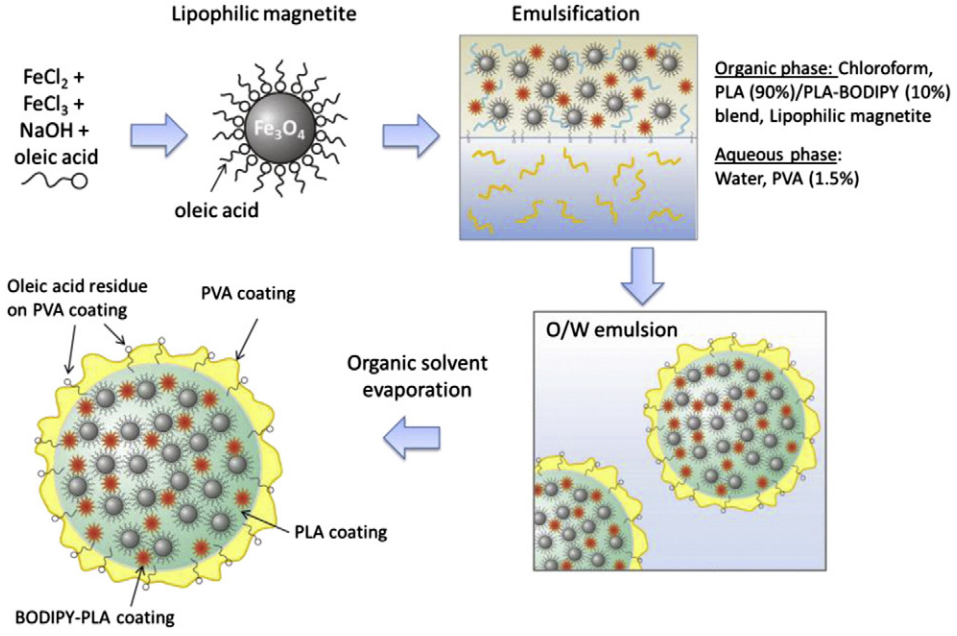

Figure 1. Schematic illustration for the step-wise synthesis of the PLA-coated MPs.

nestin (NSC-specific cytoskeletal protein) and Sox-2 (a transcription factor). Double merged fluorescence images using specific markers and DAPI (nuclear marker) were used to count the proportions of cells expressing each marker under different conditions. Counts from control cultures were used to estimate culture purity. To further examine safety of the procedures, the images were also used to estimate numbers of nuclei per field and percentage of pyknotic nuclei (an indicator of cell death evidenced by nuclear shrinkage, fragmentation or DNA condensation). Three fields were assessed, with at least 100 nuclei assessed for each condition. These methods of safety analysis allow for qualitative microscopic evaluation of cell health (through observations of cell morphology), and quantitative measurements to be performed on the same sample. As an additional measure of toxicity, an MTS (mitochondrial toxicity) assay was performed according to the manufacturer's instructions (Supplementary Information).

To assess the proportions of each daughter cell type generated from labeled NSCs, differentiated cells were fixed at 1 week following 24 hours of labeling of parent NSCs (therefore 8 days post-labeling) and cells expressing neural cell markers GFAP (astrocytes), Tuj-1 (neurons) or MBP (oligodendrocytes) were counted (100-200 nuclei per condition) using a minimum of three double merged fluorescent images.

Assessment of particle uptake in NSCs

Particle internalization was quantified microscopically in nestin (NSC specific, cytoskeletal protein) positive NSCs. We previously validated the microscopic method of analysis used here for assessing particle uptake in a range of neural cells.[24,25] This approach was chosen as simultaneous assessment of particle uptake and features of cell health, such as adherence and morphology, can be conducted. Particle localization within the cells can be discriminated from adherence to the cell membrane and the extent of particle uptake can also be assessed—particularly important in primary NSCs which display heterogeneous particle uptake. Measurements of '*intracellular*' iron content (using colorimetric absorbance assays of lysed cells) in neural cells can include substantial proportions of extracellular (membrane-bound) iron oxide particles, suggesting that this method alone cannot be used as a robust indicator of labeling.[26] Quadruple merged microscopic images (including phase images) were assessed in order to confirm whether particles were intracellular. Three fields totaling *ca*. 250 nuclei were counted for each labeling condition. Proportions of labeled cells were determined and cells scored for extent of labeling (unlabeled, low, medium or high labeling). The extent of labeling was determined by subjective assessment of the area within each cell occupied by particles: $<10\%$, 10-50%, $>50\%$ of the average nuclear area being scored as 'low', 'medium' and 'high' labeling respectively, as previously described.[24,25] In addition to the microscopic analysis, MP quantification within cells was determined spectrophotometrically after lysing cells with radioimmunoprecipitation assay buffer and dissolving the particles in 1 N HCl (λ = 335 nm) as described elsewhere.[17,22]

Assessment of magnetic localization capability of MPs

To examine magnetic localization of the labeled NSCs, cells were labeled for 48 hours with application of the $F = 4$ Hz magnetic field for the first 30 minutes. Labeled cells were washed three times with PBS to remove free particles, then trypsinized (using TrypLE) and cells triturated. Cells were collected by centrifugation followed by two more washes with PBS before finally re-suspending in PBS at a concentration of 10^5 cells/mL. Labeled cells were subjected to a single pass through a 1.6 mm diameter tubular flow system. Preliminary experiments indicated

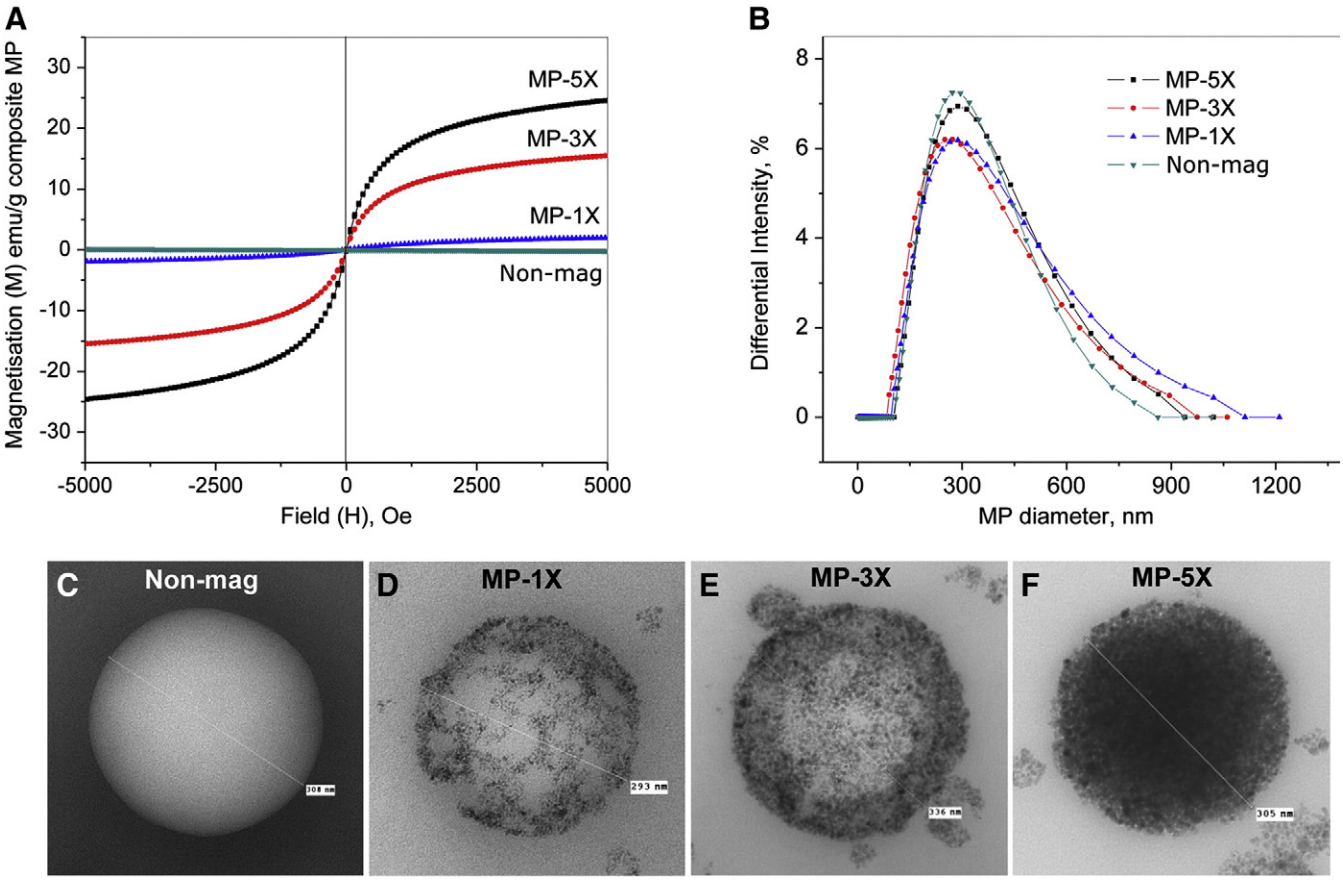

Figure 2. Size and magnetization of MP formulations. **(A)** Magnetization curves of MP formulations. All MP formulations have negligible remnant magnetization, an indicative of superparamagnetism **(B)** Particle size distribution by DLS. Transmission electron micrographs of **(C)** Non-mag, **(D)** MP-1X, **(E)** MP-3X and **(F)** MP-5X particle formulations.

that flow rates ≤ 1 mL/minute resulted in high cell loss, presumably due to cellular adherence and aggregation within the flow system, whilst flow rates ≥ 4 mL/minute resulted in minimal magnetic capture. Therefore, an optimal experimental flow rate of 2 mL/minute was chosen with an approximate flow velocity of 1.7 cm/second broadly similar to blood flow rates in arterioles and venules.[27] To generate the magnetic field for cell capture, the tubing was placed on top of a magnetic plate (field strength: 316 ± 8 mT) and surrounded by two bar magnets (field strength: 410 ± 10 mT). Magnetic field strengths were measured by an F.W. Bell 5080 Gaussmeter (Pacific Scientific-OECO, Milwaukie, OR). Cell density was estimated before and after passage through the flow system using a hemocytometer and the percentage value for cell retention within the system was calculated as $\frac{\text{cell count after magnet application}}{\text{cell count before magnet application}} \times 100$.

Statistical analysis

Data were split into comparable groups (i.e. with only one variable change per group, for example: Non-mag, MP-1X, MP-3X and MP-5X uptake compared under the no field condition only, represented a single dataset) for analysis by one-way ANOVA and Bonferroni's multiple comparison test (MCT) using GraphPad 4 software (version 4.03). Data are expressed as mean ± SEM with '*n*' referring to the number of different cultures, each derived from a different mouse litter, except for the magnetic localization experiments where '*n*' refers to number of experiments.

Results

Particle formulation and characterization

We formulated MPs of distinct magnetite content with the nomenclature Non-mag, MP-1X, MP-3X and MP-5X, to provide MPs with a range of magnetic responses—the nomenclature is based on the weight percent ratios of incorporated magnetite within the polymer matrix (given in Supplementary Table 1). The MPs exhibited dose-dependent superparamagnetic behavior showing no significant hysteresis (Figure 2, *A*). The average normalized values of MP magnetizations calculated at 5.0 kOe (saturation magnetization) were found to be 2.1, 15.3 and 24.6 [emu/g composite] for MP-1X, MP-3X and MP-5X respectively. The average MP hydrodynamic diameters ranged from 262 to 278 nm for different magnetite concentrations (by DLS) with a relatively high polydispersity index (PDI) of 0.15-0.23 (Supplementary Table 1). In particle size distribution analysis, the PDI is a measure of the width of the particle size distribution being calculated as the square of the standard deviation divided by mean nanoparticle

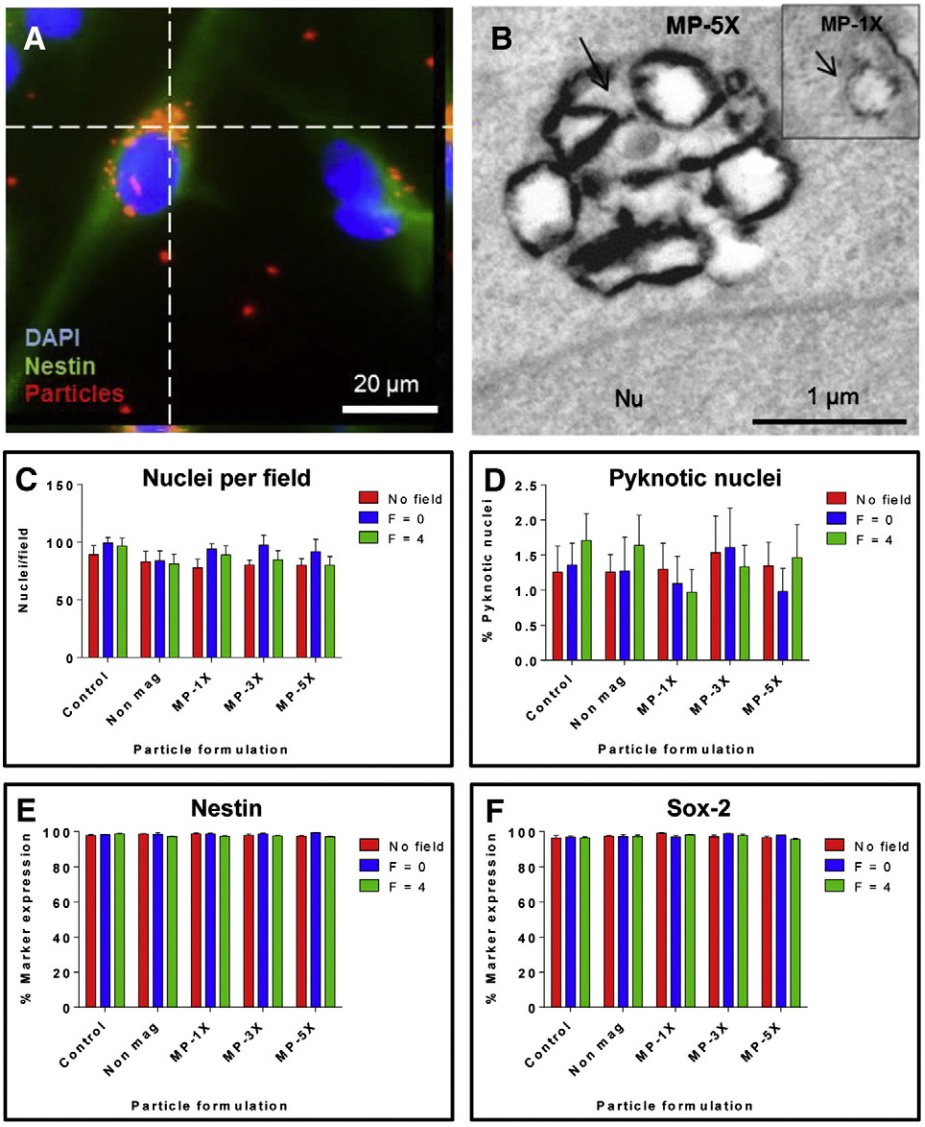

Figure 3. Particle uptake confirmation and toxicity in NSCs. **(A)** Representative triple merged z-stack image of NSCs labeled with MP-5X showing internalized particle accumulation around the nucleus **(B)** TEM micrograph of internalized MP-5X particles with comparative image of internalized MP-1X (inset) both indicated by black arrows. Bar charts displaying quantification of **(C)** nuclei per field, representing cell proliferation, **(D)** pyknotic nuclei, indicative of cell death, and percentage of cells expressing the NSC specific markers **(E)** nestin and **(F)** Sox-2. No significant toxicity or differences in NSC marker expression were found in any of the labeling conditions, $n = 4$.

diameter. Indices less than 0.1 typically describe the system as "*monodisperse*". The PDIs of 0.15-0.23 show that our particles are "*polydisperse*", but overlapping MP size distribution curves indicate that the MP size distribution and PDI are independent of magnetite concentration in MPs and are predetermined by the MP formulation method *per se*. MP sizes obtained by TEM were in agreement with DLS data (Figure 2, *B-F*) and magnetite crystal density in these images was consistent with the extent of magnetite loading (Figure 2, *C-F*). Zeta potential, a measure of surface charge, can influence particle stability, interactions with cell membranes, cellular uptake and intracellular trafficking.[28–31] Zeta potentials of the studied formulations were slightly negative (−9.46 to −14.4 mV) and systematically increased from MP-1X to MP-5X (Supplementary Table 1). Usually PLA has uncapped end carboxyl groups that result in a relatively high (above −30 mV) negative surface charge of particles dispersed in a neutral buffer.[32] However, when PLA particles are formulated with poly(vinyl alcohol) (PVA) as an emulsifier, the zeta potential becomes less negative (−6 to −10 mV at pH7)[33] because the PVA coating shields the charged surface groups of PLA. The slight systematic elevation in zeta potential for higher magnetite loads could be attributed to increase in free oleic acid molecules engrafted between PVA chains at the MP surface as previously proposed.[34] However, the stabilization of MPs in the present study was mainly due to steric hindrances between PVA chains on the surface of neighboring MPs rather than by charge due to low values of zeta potential of our MPs.[32,33] The nearly identical MP size for all three magnetite concentrations, and proportionally increased magnetic

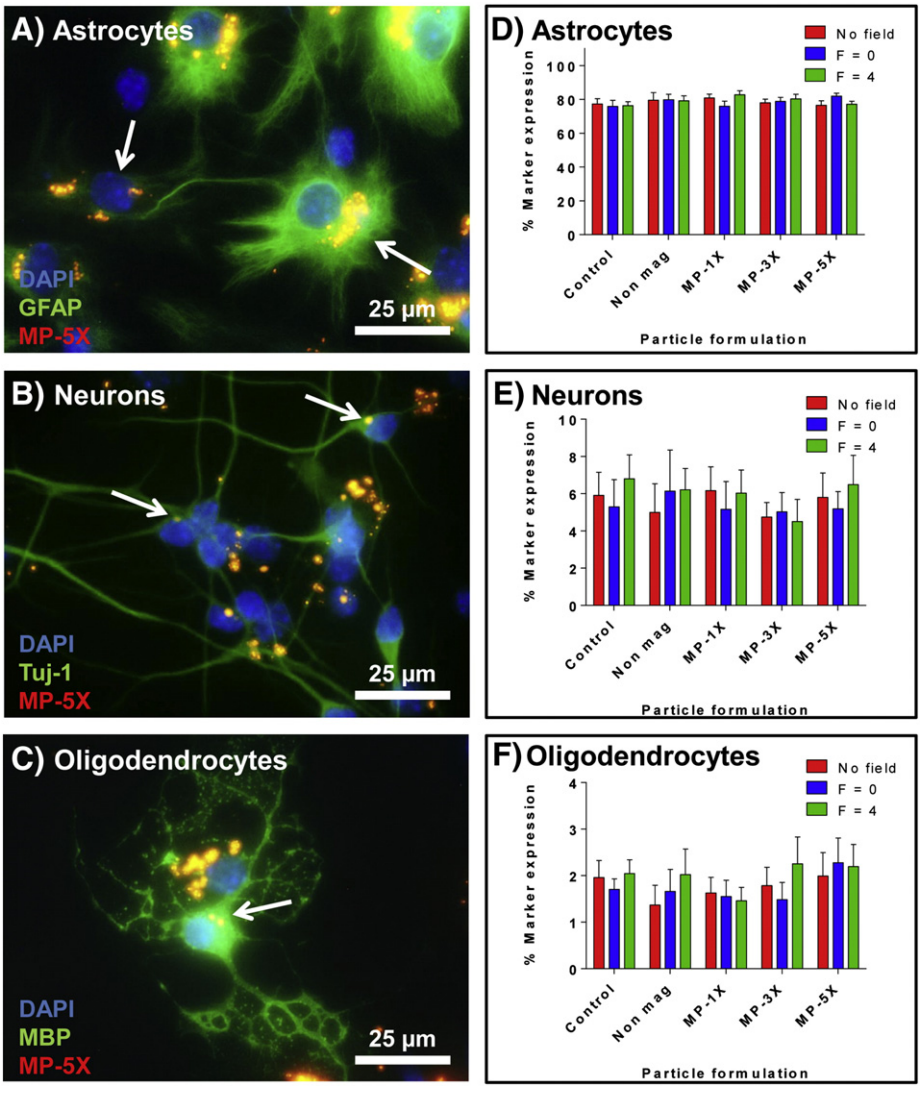

Figure 4. Assessment of the differentiation potential of NSCs after labeling with the different particle formulations. Representative triple merged z-stack images of **(A)** GFAP positive astrocytes **(B)** Tuj-1 positive neurons and **(C)** MBP positive oligodendrocytes generated from NSCs labeled with the MP-5X formulations under the $F = 4$ Hz magnetic field. White arrows point to labeled cells. Note large accumulations of particles within astrocytic progeny compared with relatively small accumulations in neurons and oligodendrocytes. Bar charts displaying quantification of the proportions of **(D)** astrocytes **(E)** neurons and **(F)** oligodendrocytes generated from cells labeled with the different particle formulations and under various field conditions. No significant differences in expression of the neural markers were found in any of the labeling conditions, $n = 3$.

responsiveness for particles of higher magnetite loadings, suggests that the differences in magnetic responsiveness are due to different magnetite content within the polymeric core, which is supported by our TEM data (Figure 2, *C-F*).

Results from FTIR spectroscopy indicated that the particles were similar in organic composition with expected peaks observed for PLA, oleic acid and PVA (Supplementary Figure 1, *A*). Full peak assignment can be found in the Supplementary Information. XRD patterns of the samples were dominated by the PLA coating regardless of MP content, suggesting that the magnetite core particles are buried under a layer of PLA. Nonetheless, the XRD pattern for the oleic acid-coated magnetite particles (Supplementary Figure 1, *B*.i) confirmed the magnetite nature of the core.

Characterization of primary stem cell cultures used for MP labeling

Monolayer cultures routinely established for these experiments were of high purity with 98.3 ± 0.7% ($n = 5$) and 96.4 ± 1.4% ($n = 5$) cells expressing nestin and Sox-2 respectively. NSCs displayed typical bipolar morphology and normal, rounded nuclei as judged by phase contrast microscopy and DAPI staining.

Confirmation of MP uptake and safety analyses

Z-stack fluorescence microscopy (to rule out cell surface particle adherence) showed that NSCs labeled with MPs displayed cytoplasmic and perinuclear particle accumulations (Figure 3, *A*); TEM analysis further confirmed this pattern of internalization

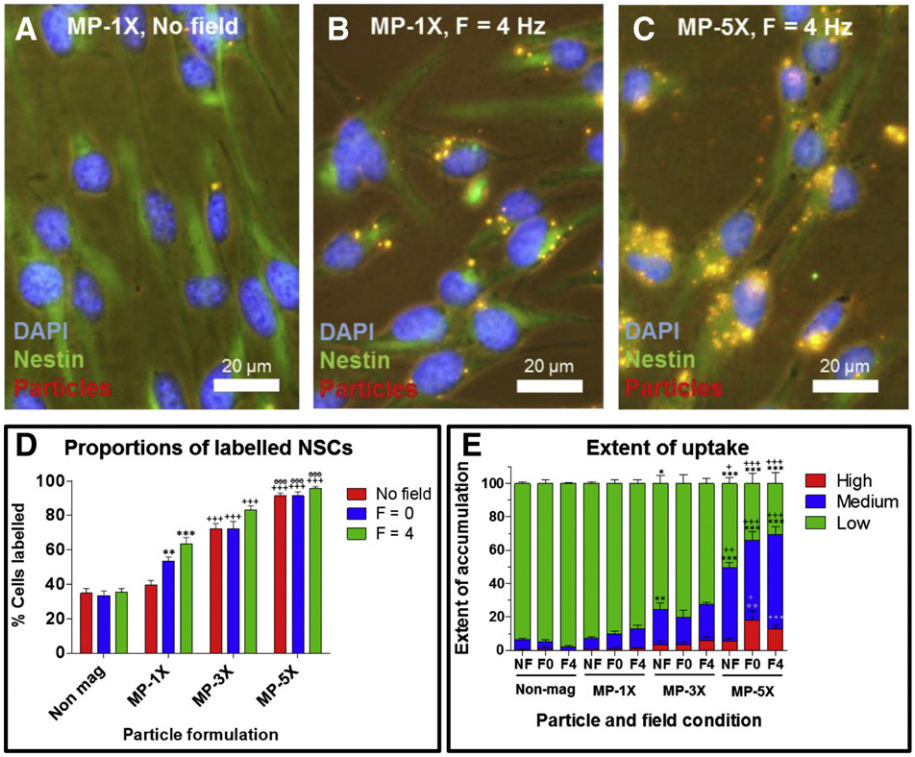

Figure 5. Assessment of test particle formulation uptake in NSCs under different magnetic fields. Representative triple merged images of NSCs labeled with MP-1X under **(A)** no field and **(B)** $F = 4$ Hz magnetic fields and **(C)** MP-5X under $F = 4$ Hz magnetic field. **(D)** Bar chart displaying quantification of percentage of NSCs labeled with the various particle formulations under different magnetic fields. Statistical differences are: $^{*}P < 0.05$ and $^{***}P < 0.001$ versus no field condition at the same particle iron concentration; $^{+++}P < 0.001$ versus MP-1X under the same field condition; $^{□□}P < 0.01$ and $^{□□□}P < 0.001$ versus MP-3X under the same field condition. **(E)** Bar chart displaying semi-quantitative analysis of extent of particle uptake using the various particle formulations under the different magnetic field conditions. Comparable low, medium and high groups were analyzed for statistical differences and are: $^{*}P < 0.05$, $^{**}P < 0.01$ and $^{***}P < 0.001$ versus MP-1X under the same field condition; $^{+}P < 0.05$, $^{++}P < 0.01$ and $^{+++}P < 0.001$ versus MP-3X under the same field condition (one way ANOVA with Bonferroni's MCT, $n = 5$).

(Figure 3, *B*). MP-5X strikingly demonstrated electron dense rings (Figure 3, *B*), reflecting their high magnetite content, and were usually found in clusters. A similar, although correspondingly less dense, ring like structure was seen for internalized MP-1X, which were usually observed as single particles within the cells (Figure 3, *B*, inset). Particles displayed similar magnetite content to that seen in the whole particle TEM images (Figure 2, *C-F*), however, sectioning through the particle results in the ring like structures of electron dense material observed here. No intra-nuclear particles were observed, under any conditions.

Post labeling, several parameters were investigated to examine if the labeling protocols had any associated toxicity. NSC counts were found to be similar across all conditions, with cells retaining their bipolar morphology and substrate adherence. Counts of nuclei/field (an estimation of NSC proliferative capacity), counts of pyknotic nuclei (indicative of cell death), and estimates of cell viability using the MTS assay were also similar across all conditions (Figure 3, *C* and *D* and Supplementary Table 2 respectively). Further, no significant differences were observed in the proportions of cells expressing NSC-specific markers nestin and Sox-2 (Figure 3, *E* and *F*).

All three major cell types of the central nervous system (CNS) could be generated from labeled NSCs with similar proportions generated across all conditions (Figure 4, *A-F*), suggesting that our protocols did not adversely affect the differentiation capabilities of labeled NSCs. Particles were found to be '*inherited*' primarily into astrocytes, with smaller accumulations noted in neuronal and oligodendrocyte progeny of the labeled NSCs.

Effects of magnetite modulation and applied magnetic fields on MP uptake in NSCs

Labeled cells under all conditions displayed internalized particles throughout the cell body but rarely in the processes (Figure 5, *A-C*). For non-magnetic particles, basal levels of labeling (under the no field condition) were approximately 35%, with low levels of particle accumulation (Figure 5, *D*); as expected, no labeling enhancement was induced by applied fields. The proportions of cells labeled with MP-1X, was systematically improved from basal levels (39.6 ± 2.7%, Figure 5, *A* and *D*) upon application of both static (53.4 ± 2.4%) and oscillating (63.7 ± 3.5%, Figure 5, *B* and *D*) magnetic fields. For all field conditions, the percentage of cells labeled was greater when using MP-3X and MP-5X, compared with MP-1X, with the highest proportions of cells being labeled when using MP-5X, up to a maximum of 95.8 ± 1.0% when using the oscillating magnetic

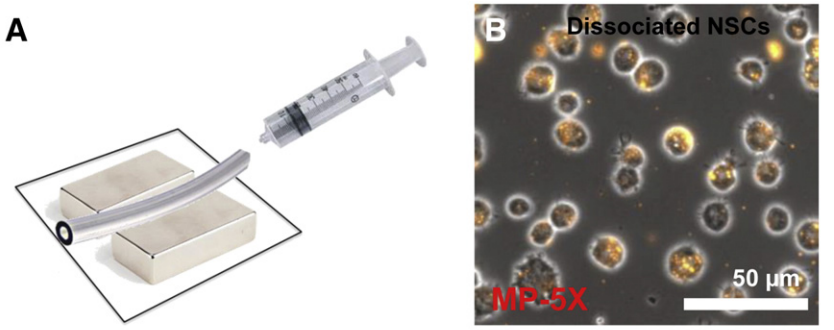

C

Particle formulation used to label NSCs	% Cell retention in flow system
Non mag	*18.1 ± 4.9*
MP-1X	*18.9 ± 9.0*
MP-3X	*40.1 ± 9.2*
MP-5X	*66.7 ± 3.3*

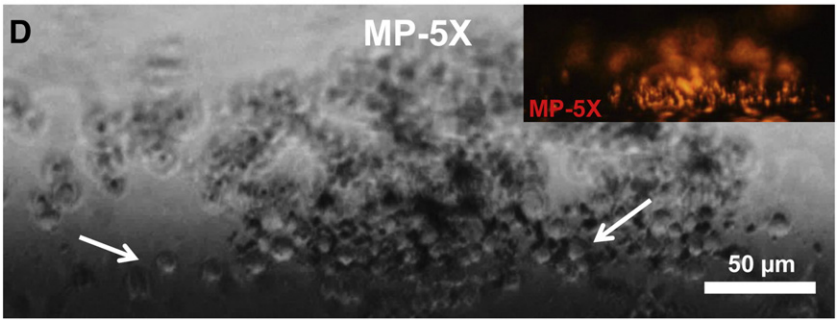

Figure 6. Assessment of magnetic localization capability of the different particle formulations on NSCs within a flow system. **(A)** Schematic diagram of the flow system consisting of tubing placed on a magnetic plate surrounded by two bar magnets all of which provide magnetic field gradients for cell capture. **(B)** MP-5X labeled NSCs after trypsinization showing typical rounded morphologies and particle accumulations. **(C)** Table depicting the percentage of NSC retention after labeling with the different particle formulations and passage through an *in vitro* flow system in the presence of magnetic fields. **(D)** Representative counterpart phase and fluorescent (inset) images depicting aggregation of MP-5X labeled NSCs in the flow system at the site of magnet application. White arrows in this image indicate rounded cells.

field (Figure 5, *D*). Under these optimal labeling conditions (MP-5X, $F = 4$ Hz oscillating magnetic field) approximately 5.7 pg Fe/cell was measured using spectrophotometry.

In marked contrast to MP-1X, field application had no significant effect on the proportions of cells labeled with either MP-3X or MP-5X, although oscillating fields did show some tendency to increase labeling. In parallel with increased proportions of labeled cells, higher magnetite concentration also led to larger particle accumulations within cells, with a progressive shift towards a greater proportion of cells displaying 'high' and 'medium' levels of labeling compared with lower magnetite content particles (Figure 5, *E*). Although the rate of MP-5X sedimentation was found to be 200 times greater upon application of a magnetic field (data not shown), it should be noted here that for a given particle formulation, the percentage of labeled cells was independent of the applied field (Figure 5, *E*).

Assessment of NSC localization capability of MPs in an in vitro flow system

The ability of MPs to localize labeled NSCs was assessed in a flow system with applied magnetic fields/gradients, as shown (Figure 6, *A*). After trypsinization and dissociation, a single cell suspension was obtained with clear intracellular accumulations visible within cells (Figure 6, *B*). Some cell attrition was seen in all conditions after passage through the flow system, with a basal cell retention by the system of 18.1 ± 4.9% when using NSCs labeled with non-magnetic particles (Figure 6, *C*). A similar retention level was seen in NSC retention for cells labeled with MP-1X (the particle formulation with the lowest magnetite content), however, cell retention increased as cells were labeled with particles of increasing magnetite content to a maximum of 66.7 ± 3.3% when using the MP-5X particles (3.7-fold greater

than basal levels of cellular retention). Microscopic examination of the flow tube in the area of magnet application revealed striking cell localization using cells labeled with MP-5X (Figure 6, *D*).

Discussion

This study demonstrates for the first time that increased MP magnetite content can safely and systematically improve labeling of clinically important but hard-to-transfect NSCs (in the absence of any cellular delivery enhancing strategies) using technically simple, inexpensive and one-step protocols. The potential translational utility of the particles has been proven for magnetic localization of labeled NSCs using a simple *in vitro* system. Further research will be required to confirm that our findings can be extrapolated to neurological lesions using live animal models of neurological injury and disease and various routes of cell administration, in conjunction with magnetic field application. The enhancement of cell labeling with particles of increasing magnetite content was reflected in the improved efficacy of magnetic cell capture, likely due to greater magnetic forces acting upon cells with higher magnetite content.

The pattern of increase in cell labeling using MP-1X with applied fields is similar to that observed when using commercial transfection grade MPs for gene delivery applications.[35,36] It is of note that such commercial magnetofection-compatible particles typically tend to have a good colloidal stability and therefore low sedimentary properties of the particles, necessitating application of magnetic fields to promote particle–cell contact.[37] In this context, gravitational sedimentation of sub-micron sized particles depends on several factors including particle diameter/density and fluid viscosity/density.[38] With other parameters being constant, the gravitational sedimentary forces due to the increased particle density (as a result of higher magnetite content) are likely sufficient to induce particle sedimentation, cellular contact and hence increased uptake by NSCs to achieve efficient cell labeling. Therefore, our results suggest a MP '*magnetite limit*', beyond which magnetic field application strategies *do not* offer a significant benefit for cell loading, at least in the case of NSCs. However, it should be noted that intercellular differences appear to exist; indeed in cells such as bovine aortic endothelial cells, MP loading can be dramatically improved using magnetic fields in conjunction with high magnetite particles.[17]

Using our experimental flow system, efficient magnetic targeting of NSCs was achieved after one pass through the magnetic system. Intraarterial and intravenous deliveries have both been utilized for clinical cell delivery to the CNS.[1,39] However, a well-recognized problem with intravascularly delivered cells is subsequent clearance by the tissue macrophage system.[2,3] In terms of an effective clinical delivery strategy, cells injected close to the injury site (by delivery via local blood vessels supplying the area of injury) could be trapped by magnetic field application thereby providing a means to limit this problem. For example, labeled NSCs could be introduced near known anatomical sites of pathology (determined by MRI) via the spinal segmental arteries (accessed through the aorta by catheterization of the femoral artery under fluoroscopic guidance). These could subsequently be localized to areas of pathology via external magnets applied over sites of SCI, potentially leading to greater beneficial effect when compared with non-targeted NSCs. Systemic delivery reduces the risk of secondary damage from local invasive surgical procedures. Further, smaller numbers of cells can be administered due to a higher percentage of cell integration at the desired sites, while reducing off-target effects such as non-targeted integration, as well as costs associated with cell production.

The test particles used were formulated with biocompatible and biodegradable components, which have the potential for clinical application. PLA, comprising the core, is a well-known non-toxic bio-absorbable polymer, approved by the US Food and Drug Administration (FDA) in the early 1970s for direct contact with biological fluids.[40,41] Slow PLA degradation has been reported both extracellularly (weeks to months)[42] and intracellularly (15% degradation over 3 days)[43] and our TEM data also suggest minimal particle degradation and iron leaching in NSCs over 24 hours. This indicates that the degradation time-frame of PLA, could be sufficient to enable stem cell targeting of therapeutic cells laden with intact or minimally degraded particles over the experimental or therapeutic time course. PVA, a MP surface stabilizer is also approved by the US FDA for general and neurological embolization use.[44] Oleic acid used to stabilize magnetite nanoparticles is considered as a safe material; it is rapidly absorbed after oral administration, metabolized, and the metabolic products are utilized and excreted (www.fda.gov). Magnetite nanoparticles have been shown to be safe in animal studies[45,46] and approved by the US FDA for use in humans as an MRI contrast agent.[47]

In addition, the process used here to formulate the polymeric magnetite-loaded particles could offer further advantages for regenerative applications. First, the polymer matrix of such particles can be impregnated with additional bioactive molecules that can be released intracellularly to influence biological processes[48]—these can be incorporated within the polymeric matrix without chemical reactions, an important factor for preserving bioactivity. Additionally, blending the polymeric matrix with a fluorescently labeled polymer (such as BODIPY® 564/570 used in this study) produces fluorescent MPs that offer potential for multimodal tracking by fluorescence microscopy and MRI. Indeed, the cellular iron loading under optimal labeling conditions of 5.7 pg Fe/cell is in line with other reported values in NSCs and can facilitate cell tracking by MRI.[21,49] Second, controlled release of bioactive molecules as well as particle degradation characteristics can be readily modulated by the choice of matrix constituents.[50] For example, we previously showed that magnetic polymeric particles prepared with poly(lactic-co-glycolic acid) at various copolymer ratios enabled tuning of particle degradation rates, thereby modulating the release profiles of the incorporated anti-proliferative drug paclitaxel.[22] Finally, these polymeric particles can be further surface functionalized (to bear charge or specific biological ligands) to enable binding of nucleic acids for gene transfer in potential multimodal applications, highlighting their versatility.[34]

Under all test conditions, the high viability we observed in NSCs post-labeling is likely due to the labeling method exploiting natural cellular internalization mechanisms, combined with the slow degradation profile of the PLA matrices of the

particles. Previous ultrastructural studies from our laboratory indicate that rapid particle degradation and extensive iron leaching within neural cells are the major pathological correlates of MP-induced cellular toxicity,[24] highlighting the translational benefits of the biocompatible coatings used here. Additionally, the labeling protocols had no effect on the differentiation of NSCs into their daughter phenotypes, vital for successful cell replacement after transplantation, further highlighting their translational utility for clinical applications.

Appendix A. Supplementary data

Supplementary data to this article can be found online at http://dx.doi.org/10.1016/j.nano.2014.07.001.

References

1. Aboody K, Capela A, Niazi N, Stern JH, Temple S. Translating stem cell studies to the clinic for CNS repair: current state of the art and the need for a Rosetta stone. *Neuron* 2011;**70**:597-613.
2. Hauger O, Frost EE, van Heeswijk R, Deminière C, Xue R, Delmas Y, et al. MR evaluation of the glomerular homing of magnetically labeled mesenchymal stem cells in a rat model of nephropathy. *Radiology* 2006;**238**:200-10.
3. Kraitchman DL, Tatsumi M, Gilson WD, Ishimori T, Kedziorek D, Walczak P, et al. Dynamic imaging of allogeneic mesenchymal stem cells trafficking to myocardial infarction. *Circulation* 2005;**112**:1451-61.
4. Li L, Jiang Q, Ding G, Zhang L, Zhang ZG, Li Q, et al. Effects of administration route on migration and distribution of neural progenitor cells transplanted into rats with focal cerebral ischemia, an MRI study. *J Cereb Blood Flow Metab* 2010;**30**:653-62.
5. Carenza E, Barceló V, Morancho A, Levander L, Boada C, Laromaine A, et al. In vitro angiogenic performance and in vivo brain targeting of magnetized endothelial progenitor cells for neurorepair therapies. *Nanomedicine* 2014;**10**:225-34.
6. Song M, Kim Y-J, Kim Y, Roh J, Kim SU, Yoon B-W. Using a neodymium magnet to target delivery of ferumoxide-labeled human neural stem cells in a rat model of focal cerebral ischemia. *Hum Gene Ther* 2010;**21**:603-10.
7. Vaněček V, Zablotskii V, Forostyak S, Růřička J, Herynek V, Babič M, et al. Highly efficient magnetic targeting of mesenchymal stem cells in spinal cord injury. *Int J Nanomedicine* 2012;**7**:3719-30.
8. Polyak B, Fishbein I, Chorny M, Alferiev I, Williams D, Yellen B, et al. High field gradient targeting of magnetic nanoparticle-loaded endothelial cells to the surfaces of steel stents. *Proc Natl Acad Sci U S A* 2008;**105**:698-703.
9. Cheng K, Li T, Malliaras K. Magnetic targeting enhances engraftment and functional benefit of iron-labeled cardiosphere-derived cells in myocardial infarction. *Circulation* 2010;**106**:1570-81.
10. Pluchino S, Quattrini A, Brambilla E, Gritti A, Salani G, Dina G, et al. Injection of adult neurospheres induces recovery in a chronic model of multiple sclerosis. *Nature* 2003;**422**:688-94.
11. Cohen ME, Muja N, Fainstein N, Bulte JWM, Ben-Hur T. Conserved fate and function of ferumoxides-labeled neural precursor cells in vitro and in vivo. *J Neurosci Res* 2010;**88**:936-44.
12. Bakhru SH, Altiok E, Highley C, Delubac D, Suhan J, Hitchens TK, et al. Enhanced cellular uptake and long-term retention of chitosan-modified iron-oxide nanoparticles for MRI-based cell tracking. *Int J Nanomedicine* 2012;**7**:4613-23.
13. Delehanty JB, Boeneman K, Bradburne CE, Robertson K, Bongard JE, Medintz IL. Peptides for specific intracellular delivery and targeting of nanoparticles: implications for developing nanoparticle-mediated drug delivery. *Ther Deliv* 2010;**1**:411-33.
14. Arbab AS, Yocum GT, Wilson LB, Parwana A, Jordan EK, Kalish H, et al. Comparison of transfection agents in forming complexes with ferumoxides, cell labeling efficiency, and cellular viability. *Mol Imaging* 2004;**3**:24-32.
15. Lee SH, Castagner B, Leroux J-C. Is there a future for cell-penetrating peptides in oligonucleotide delivery? *Eur J Pharm Biopharm* 2013;**85**:5-11.
16. Plank C, Zelphati O, Mykhaylyk O. Magnetically enhanced nucleic acid delivery. *Adv Drug Deliv Rev* 2011;**63**:1300-31.
17. MacDonald C, Barbee K, Polyak B. Force dependent internalization of magnetic nanoparticles results in highly loaded endothelial cells for use as potential therapy delivery vectors. *Pharm Res* 2012;**29**:1270-81.
18. Soenen SJ, De Smedt SC, Braeckmans K. Limitations and caveats of magnetic cell labeling using transfection agent complexed iron oxide nanoparticles. *Contrast Media Mol Imaging* 2012;**7**:140-52.
19. Politi LS, Bacigaluppi M, Brambilla E, Cadioli M, Falini A, Comi G, et al. Magnetic-resonance-based tracking and quantification of intravenously injected neural stem cell accumulation in the brains of mice with experimental multiple sclerosis. *Stem Cells* 2007;**25**:2583-92.
20. Neri M, Maderna C, Cavazzin C, Deidda-Vigoriti V, Politi LS, Scotti G, et al. Efficient in vitro labeling of human neural precursor cells with superparamagnetic iron oxide particles: relevance for in vivo cell tracking. *Stem Cells* 2008;**26**:505-16.
21. Chen C-CV, Ku M-C, DMJ, Lai J-S, Hueng D-Y, Chang C. Simple SPION incubation as an efficient intracellular labeling method for tracking neural progenitor cells using MRI. *PLoS One* 2013;**8**:e56125.
22. Johnson B, Toland B, Chokshi R, Mochalin V, Koutzaki S, Polyak B. Magnetically responsive paclitaxel-loaded biodegradable nanoparticles for treatment of vascular disease: preparation, characterization and in vitro evaluation of anti-proliferative potential. *Curr Drug Deliv* 2010;**7**:263-73.
23. Pickard MR, Barraud P, Chari DM. The transfection of multipotent neural precursor/stem cell transplant populations with magnetic nanoparticles. *Biomaterials* 2011;**32**:2274-84.
24. Jenkins S, Pickard M, Furness D, Yiu H, Chari D. Differences in magnetic particle uptake by CNS neuroglial subclasses: implications for neural tissue engineering. *Nanomedicine (Lond)* 2013;**8**:951-68.
25. Pickard M, Jenkins S, Koller C, Furness D, Chari D. Magnetic nanoparticle labeling of astrocytes derived for neural transplantation. *Tissue Eng Part C Methods* 2010;**17**:89-99.
26. Luther EM, Petters C, Bulcke F, Kaltz A, Thiel K, Bickmeyer U, et al. Endocytotic uptake of iron oxide nanoparticles by cultured brain microglial cells. *Acta Biomater* 2013;**9**:8454-65.
27. Marieb EN. The cardiovascular system: blood vessels. In: Murray MA, editor. *Hum Anat Physiol Int Ed*San Francisco: Pearson Education; 2004. p. 721-39.
28. Albanese A, Tang PS, Chan WCW. The effect of nanoparticle size, shape, and surface chemistry on biological systems. *Ann Rev Biomed Eng* 2012;**14**:1-16.
29. Fröhlich E. The role of surface charge in cellular uptake and cytotoxicity of medical nanoparticles. *Int J Nanomedicine* 2012;**7**:5577-91.
30. Labille J, Brant J. Stability of nanoparticles in water. *Nanomedicine (Lond)* 2010;**5**:985-98.
31. Zhao F, Zhao Y, Liu Y, Chang X, Chen C, Zhao Y. Cellular uptake, intracellular trafficking, and cytotoxicity of nanomaterials. *Small* 2011;**7**:1322-37.
32. Gref R, Miralles G, Dellacherie É. Polyoxyethylene-coated nanospheres: effect of coating on zeta potential and phagocytosis. *Polym Int* 1999;**48**:251-6.
33. Sahoo SK, Panyam J, Prabha S, Labhasetwar V. Residual polyvinyl alcohol associated with poly (D, L-lactide-co-glycolide) nanoparticles affects their physical properties and cellular uptake. *J Control Release* 2002;**82**:105-14.
34. Chorny M, Polyak B, Alferiev IS, Walsh K, Friedman G, Levy RJ. Magnetically driven plasmid DNA delivery with biodegradable polymeric nanoparticles. *FASEB J* 2007;**21**:2510-9.
35. Jenkins SI, Pickard MR, Granger N, Chari DM. Magnetic nanoparticle-mediated gene transfer to oligodendrocyte precursor cell transplant

populations is enhanced by magnetofection strategies. *ACS Nano* 2011;**5**:6527-38.
36. Pickard M, Chari D. Enhancement of magnetic nanoparticle-mediated gene transfer to astrocytes by "magnetofection": effects of static and oscillating fields. *Nanomedicine (Lond)* 2010;**5**:217-32.
37. Arsianti M, Lim M, Marquis CP, Amal R. Assembly of polyethylenimine-based magnetic iron oxide vectors: insights into gene delivery. *Langmuir* 2010;**26**:7314-26.
38. Ganguly S, Chakraborty S. Sedimentation of nanoparticles in nanoscale colloidal suspensions. *Phys Lett A* 2011;**375**:2394-9.
39. Sahni V, Kessler JA. Stem cell therapies for spinal cord injury. *Nat Rev Neurol* 2010;**6**:363-72.
40. Gupta B, Revagade N, Hilborn J. Poly(lactic acid) fiber: an overview. *Prog Polym Sci* 2007;**32**:455-82.
41. Lin Xiao M, Wang B, Yang G, Gauthier M. Poly(lactic acid)-based biomaterials: synthesis, modification and applications. In: Ghista D, editor. *Biomed Sci Eng Technol InTech*; 2012. p. 247-82.
42. Grayson ACR, Voskerician G, Lynn A, Anderson JM, Cima MJ, Langer R. Differential degradation rates in vivo and in vitro of biocompatible poly(lactic acid) and poly(glycolic acid) homo- and co-polymers for a polymeric drug-delivery microchip. *J Biomater Sci Polym Ed* 2004;**15**:1281-304.
43. Tengood JE, Alferiev IS, Zhang K, Fishbein I, Levy RJ, Chorny M. Real-time analysis of composite magnetic nanoparticle disassembly in vascular cells and biomimetic media. *Proc Natl Acad Sci U S A* 2014; **111**:4245-50.
44. Worthington-Kirsch RL, Siskin GP, Hegener P, Chesnick R. Comparison of the efficacy of the embolic agents acrylamido polyvinyl alcohol microspheres and tris-acryl gelatin microspheres for uterine artery embolization for leiomyomas: a prospective randomized controlled trial. *Cardiovasc Interv Radiol* 2011;**34**:493-501.
45. Jain TK, Reddy MK, Morales MA, Leslie-Pelecky DL, Labhasetwar V. Biodistribution, clearance, and biocompatibility of iron oxide magnetic nanoparticles in rats. *Mol Pharm* 2008;**5**:316-27.
46. Weissleder R, Stark DD, Engelstad BL, Bacon BR, Compton CC, White DL, et al. Superparamagnetic iron oxide: pharmacokinetics and toxicity. *AJR Am J Roentgenol* 1989;**152**:167-73.
47. Tartaj P. Nanomagnets for biomedical applications. In: Hari Singh N, editor. *Encycl Nanosci Nanotechnol*, vol. 6. American Scientific Publishers; 2003. p. 823.
48. Santos T, Ferreira R, Maia J, Agasse F, Xapelli S, Cortes L, et al. Polymeric nanoparticles to control the differentiation of neural stem cells in the subventricular zone of the brain. *ACS Nano* 2012;**6**: 10463-74.
49. Miyoshi S, Flexman JA, Cross DJ, Maravilla KR, Kim Y, Anzai Y, et al. Transfection of neuroprogenitor cells with iron nanoparticles for magnetic resonance imaging tracking: cell viability, differentiation, and intracellular localization. *Mol Imaging Biol* 2005;**7**:286-95.
50. Shive M, Anderson J. Biodegradation and biocompatibility of PLA and PLGA microspheres. *Adv Drug Deliv Rev* 1997;**28**:5-24.

Appendix 3. Particle and Particle Systems Characterization publication.

"*Early membrane responses to magnetic particles are predictors of particle uptake in neural stem cells*"

Fernandes, A. Adams, CF. Jenkins, SI. Furness, DN. Chari, DM. Particle and Particle Systems Characterization, 2015.

This article is referred to in Chapter 3 and describes the OTOTO-FESEM technique. The full article has been reproduced here with permission from John Wiley and Sons.

Particle & Particle Systems Characterization
www.particle-journal.com

Early Membrane Responses to Magnetic Particles are Predictors of Particle Uptake in Neural Stem Cells

*Alinda R. Fernandes, Christopher F. Adams, David N. Furness, and Divya M. Chari**

Magnetic particles (MPs) offer several advantages for neural cell therapy, but limited particle uptake by neural cells is a barrier to translation. It is recently proved that tailoring particle physicochemical properties (by enhancing their iron content) dramatically improves uptake in neural stem cells (NSCs)—a major transplant population. High-throughput screening of particles with varying physicochemical properties can therefore aid in identifying particles with optimal uptake features, but research is hampered by the lack of simple methodologies for studying neural cell membrane responses to nanoparticle platforms. A high-resolution–high throughput method has been used to study early membrane responses of primary rodent NSCs to particles of variant magnetite loading, to attempt to correlate these responses with known particle internalization profiles. Membrane imaging is enhanced through sequential staining with osmium (O) and thiocarbohydrazide (T), a method termed OTOTO, combined with field-emission scanning electron microscopy (FESEM). A five-point classification system was used to systematically evaluate early MP-induced membrane responses to particles possessing distinct physicochemical properties. Significantly different profiles of membrane activation were noted that correlate with particle uptake profiles. It is suggested that our method can serve as a valuable predictor of particle internalization in neural cells for diverse particle platforms.

1. Introduction

Magnetic particles (MPs) are versatile tools for diverse applications in neuro-nanotechnology. A major emergent application area is in neural cell therapies where MPs can mediate transplant cell imaging in vivo,[1,2] magnetic cell targeting to foci of pathology[3] and can also function as vectors for genetic engineering of neural cell populations.[4–6] For such applications, the limited uptake of MPs by neural transplant cells has widely been considered a significant barrier to translation, necessitating the use of chemical transfection agents or targeting peptides to enhance uptake—approaches that may be toxic and alter cellular physiology.[7,8] By contrast, we recently proved that simple tailoring of particle properties by enhancement of the iron content of polymeric MPs can lead to efficient and safe labeling of an important "hard to label" transplant population—neural stem cells (NSCs) (see Figure S1, Supporting Information). In this study, non-magnetite particles (termed non-Mag) showed labeling efficiencies of ca. 35% but on application of particles with enhanced magnetite loading (termed 5× particles), cell-labeling efficiency dramatically improved to ca. 96%. 5× particle-labeled NSCs were shown to be amenable to magnetic cell localization strategies in a flow system, highlighting the translational benefits of such labeling approaches.[9] NSCs offer key benefits post-transplantation in several neural pathologies such as spinal cord injury[10] and Parkinson's models,[11] with clinical trials being commenced in some centers.[12] Therefore, our findings suggest that investigations into the influence of chemical and physical modifications of particle properties on cellular uptake can be of significant value in informing the development of tailored, neurocompatible platforms for neural cell therapies. In this context, the neural cell plasma membrane is a critical mediator of particle uptake, both in sensing extracellular particles and through a range of uptake events such as endocytosis and micropinocytosis.[13] As such, it can be predicted that early changes/activation profiles in the cellular membrane following interaction with nanoparticles will be informative predictors of subsequent particle uptake.

Despite this, our understanding of the relationship between the physicochemical properties of particles and their influence on neural cell uptake is very limited. An important point to note is that research in this area is significantly hampered by the lack of high throughput and simple methods for studying neural cell responses to nanoparticle platforms. Current methods are heavily reliant on conventional fluorescence and confocal microscopy, permitting examination of large cell numbers but at low resolution, meaning membrane events cannot be reliably studied. Emergent methodologies involving the study of model biological membranes using atomic force microscopy (AFM), optical tweezers, and electrophysiological measurements are useful to some extent, though direct unequivocal visualization of particle–membrane binding is challenging due to the intrinsically low resolution of these methods and subjective data interpretation.[14] Transmission electron microscopy (TEM; conventional or cryo-TEM) is a commonly

Dr. A. R. Fernandes, C. F. Adams, Prof. D. N. Furness, Prof. D. M. Chari
Cellular and Neural Engineering Group
Institute for Science and Technology in Medicine
Keele University
Newcastle Under Lyme
Staffordshire, ST5 5BG, UK
E-mail: d.chari@keele.ac.uk

DOI: 10.1002/ppsc.201400231

used high-resolution approach for ultrastructural analyses of membrane features. Although this is an excellent approach for detailed membrane analyses, the method is associated with high technical complexity, lengthy protocols, laborious quantification procedures and is typically very low throughput. Given the drawbacks of current methods, there is a substantial need for a simple, cost effective, and rapid experimental/analytical approach to study membrane responses to nanoparticles for neuro-nanotechnology research.

Scanning electron microscopy (SEM), specifically field-emission (FESEM) could offer a realistic solution to the above challenges. The resolution of FESEM can be enhanced by sequential-repeat staining of cells using osmium (O) and a high-affinity osmium binding agent, thiocarbohydrazide (T) (a method known as OTOTO)[15] enabling reliable analysis of ultrastructural membrane features at the nanoscale level. We recently proved that this high throughput, high-resolution method can be used to reliably examine detailed intercellular membrane differences between the major classes of brain cells (derived from NSCs), on stimulation with transfection-grade MPs.[16] However, it has never been established if this simple approach can be employed to identify distinctive membrane responses to MPs possessing differing physiochemical properties, in order to correlate particle properties with known cellular uptake profiles. The goal of this study therefore was to use the OTOTO–FESEM approach to examine early membrane responses of primary rodent NSCs to MPs of varied iron content, (specifically the non-Mag and 5× particles used in conjunction with a 4 Hz oscillating magnetic field, conditions that resulted in the highest uptake levels of these particles, as previously reported).[9] We reasoned that employing particles with distinct physical properties, that in turn show dramatically different uptake levels in NSCs, would enable a robust dissection of differences in the induced membrane responses of the stem cells. We describe a five-point classification system of membrane features (corroborated by TEM analysis), allowing for systematic quantification of cell-surface activity in response to MP stimulation.

2. Results and Discussion

2.1. Identification of MPs on Stem Cell Membrane Surfaces

Both particles used here have been fully characterized previously using powder X-ray diffraction (XRD), dynamic light scattering (DLS), TEM of both naked and intracellular particles in NSCs, SQUID magnetometry, Fourier-transform infrared (FTIR) spectroscopy, and elemental analysis.[9] FESEM images of magnetite-loaded particles (**Figure 1**A) and non-magnetite particles (inset) show similar diameters. Fluorescence microscopy revealed "chains" of particles associated with the surface

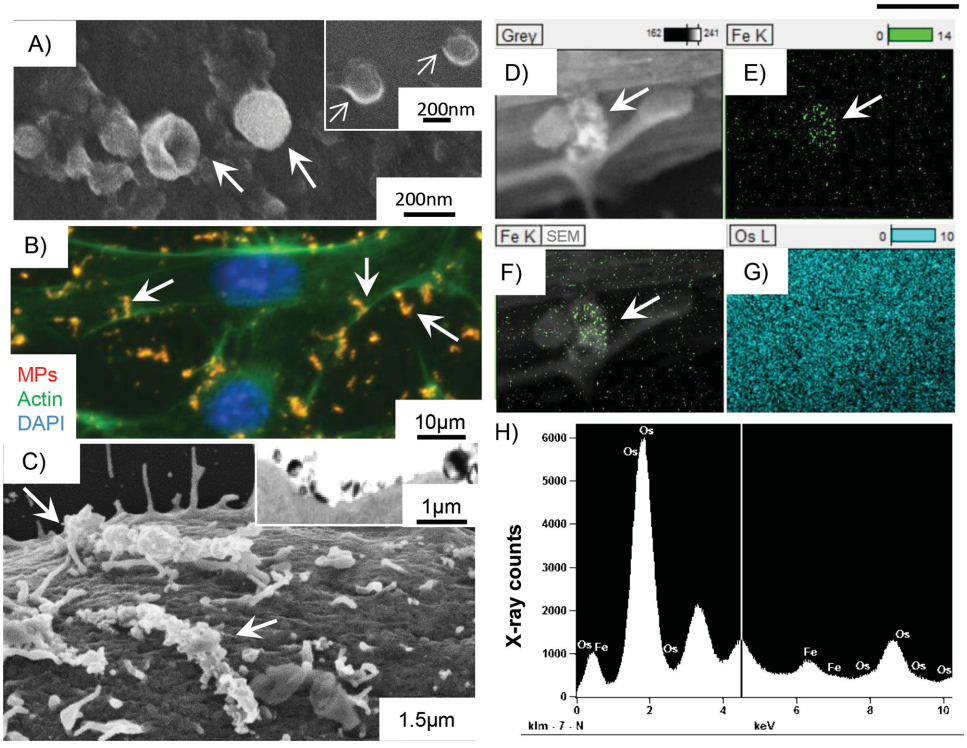

Figure 1. Particle identification using FESEM and EDX. A) FESEM image of magnetite-loaded particles (white arrows) and non-magnetite-loaded particles (inset) showing similar particle diameters. B) Magnetite-loaded particles appear as cell surface chain-like aggregates in the fluorescence image (white arrows), confirmed by FESEM (C, white arrows) and TEM (C, inset). D–F) EDX analysis showing iron signal from particles on the NSC membrane surface; D) FESEM–particle cluster indicated by arrow; E) iron EDX analysis; and F) merged image. G) Osmium detected by EDX over the entire cell surface. H) Spectral mapping of magnetite-loaded particle location showing a distinct iron peak (6.4 keV), which was absent in non-magnetite particle spectra.

of phalloidin-labeled NSCs (Figure 1B). This finding was corroborated by OTOTO–FESEM (Figure 1C) and TEM (inset). The lengths of these particle chains were observed to be similar in the FESEM and fluorescence images (3–4 μm). Elemental mapping using energy-dispersive X-ray microanalysis (EDX) showed a discrete iron signal corresponding to surface-associated particle chains (Figure 1D–F), distinct from the widely distributed osmium signal (Figure 1G), which is present due to the OTOTO processing. Spectral analysis of particles confirmed the presence of iron with a peak at 6.4 keV (Figure 1H) that was absent in cells treated with non-magnetite particles (data not shown). In contrast to magnetite- loaded particles, it proved difficult to reliably generate equivalent images for non-magnetite particles, as we were unable to use X-ray microanalysis to robustly identify these particles on the cell surface.

Therefore, identification and direct observation of metallic MP interactions with the NSC surface were feasible using OTOTO–FESEM and paralleled observations using standard fluorescence microscopy. Combined use of our method with EDX suggests that the approach can be exploited in the future to study particle–membrane interactions for particles with a range of metal cores, without resorting to technically challenging sectioning procedures, as with TEM. A further significant advantage of OTOTO processing for analysis of synthetic particles, including nanoparticles, is that the need for a gold coating of the sample (after critical point drying) is avoided. Gold coating can potentially obscure small diameter nanoparticles, and is not compatible with backscatter electron detection, which can be used to detect metal-containing particles, for example, iron oxide particles.[16]

2.2. OTOTO–FESEM Allows for Examination of Parameters of Cell Safety and Overall Cell Membrane Activity

Cells in our samples appeared to be of high viability in both particle stimulated (magnetite-loaded and non-magnetite particles) and unstimulated cultures (no particles), as judged by normal membrane integrity and cellular adherence, and the characteristic bipolar morphology of NSCs (**Figure 2**A). Further, mitotic NSCs were frequently observed (Figure 2A, inset). This is in line with our previous observations where the polymeric particles used showed little evidence of toxicity based on normal adherence, absence of cellular detachment/rounding, normal morphology, and observation of dividing stem cells (a key property underpinning their regenerative potential). Therefore, the OTOTO method allows for a high throughput and detailed analysis of cellular safety profiles, which parallel observations from standard and widely used fluorescence microscopy methods.

Clear differences in membrane features were apparent between unstimulated and MP-stimulated cultures with greater overall cellular membrane activity obvious after MP stimulation (Figure 2B,C). Consistent with these observations, dextran uptake (indicative of macropinocytotic activity) was increased in MP-stimulated NSCs (Figure 2D) compared to unstimulated control cultures (inset); non-magnetite particle-treated cultures demonstrated similar results to unstimulated cultures (data not shown).

The OTOTO methodology allowed for high-resolution analysis of several cells per sample. Sample processing using the method was technically simple and rapid (one day), with the ability to simultaneously process large sample numbers for imaging and analysis. Ultrastructural analyses such as TEM enable direct observation of particle uptake processes, and identification of specific endocytotic events by visualization of endocytotic structures and vesicle formation. However, this is a time- and labor-intensive process,[18] and few uptake events may be observed in an individual sample, consisting as it does of an ultrathin section (typically 30–100 nm, rarely exceeding 150 nm, as electrons less readily pass through biological material of this thickness).[17] Additionally, artifacts may be introduced into TEM samples due to damage during the sectioning process, which can be a particular problem for the study of cellular interactions with synthetic materials, as the interface between "soft" biological material and "hard" synthetic particles can be altered.[19]

OTOTO preparation also allowed for a greater proportion of each cell's membrane to be studied compared with TEM samples. Following OTOTO, an entire coverslip could be placed into the scanning electron microscope, allowing therefore for an entire culture (and treatment condition) to be analyzed. By comparison, for TEM samples, the resin within which cells are embedded typically needed to be broken into smaller pieces to be amenable to ultrathin sectioning. Ultrathin sections contained far fewer cells than an SEM specimen, even if sectioned

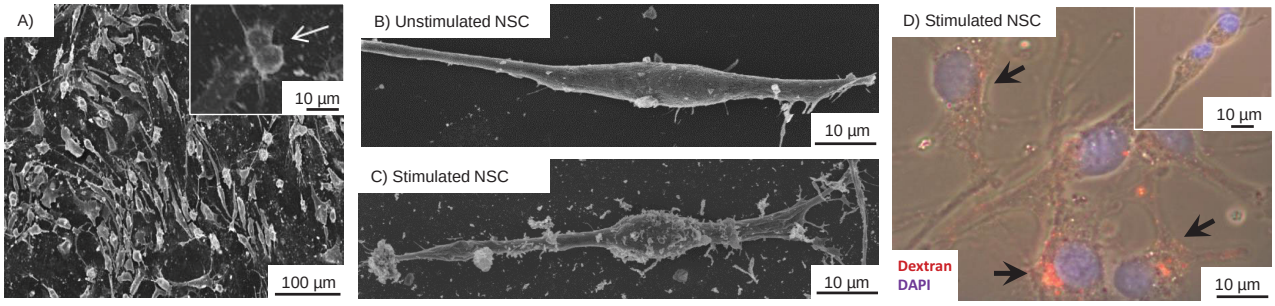

Figure 2. MP-induced responses in NSCs. A) Low-magnification view showing large numbers of viable cells available for morphological analysis, including identification of mitotic profiles (inset). Differences in membrane activity were apparent between B) unstimulated and C) MP-stimulated cells. Dextran (macropinocytosis marker) uptake was higher in D) stimulated cells compared to controls (inset).

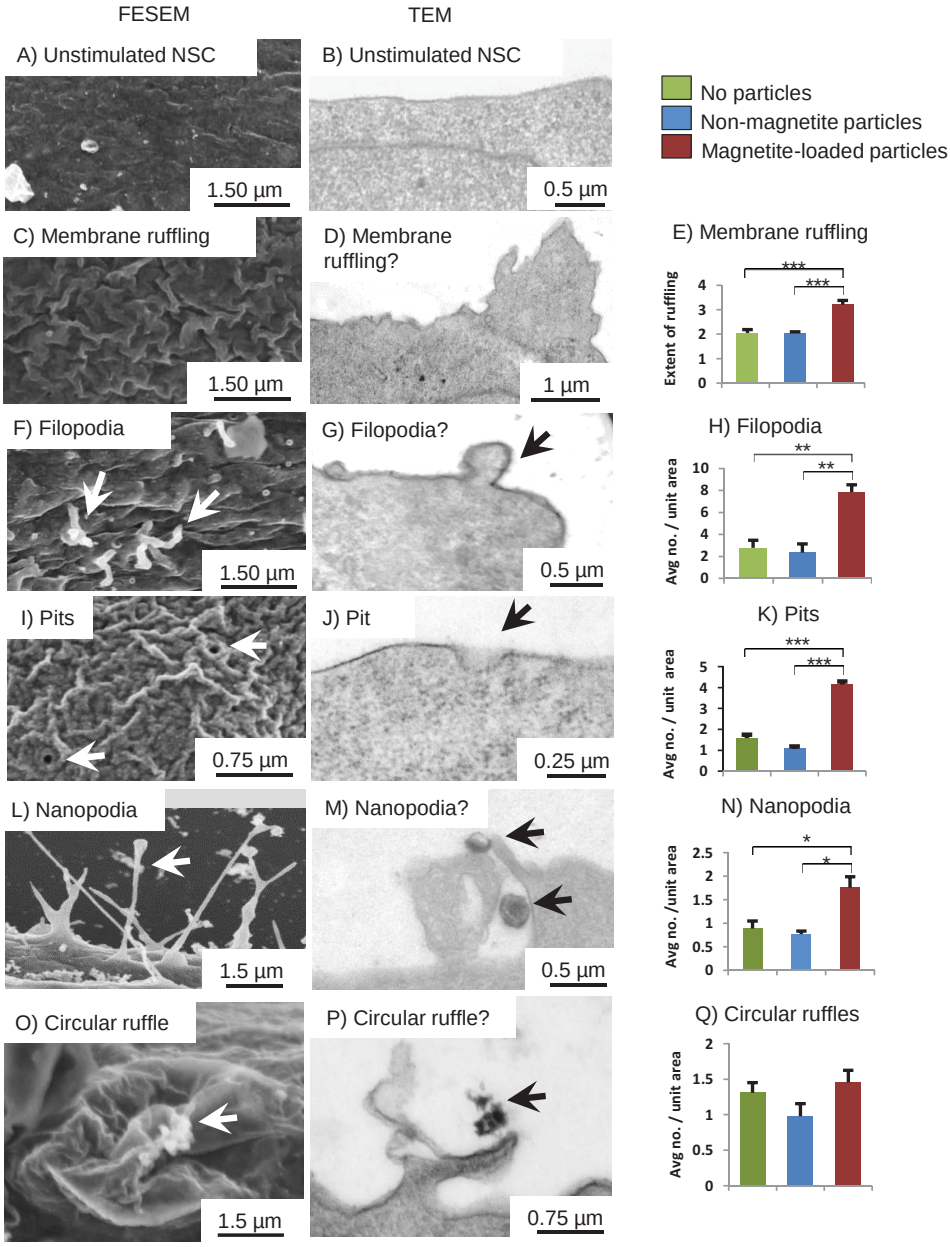

Figure 3. Membrane activity in NSCs. FESEM, TEM images and analyses of extent of A–E) membrane ruffling, F–H) numbers of filopodia, I–K) pits, L–N) nanopodia, and O–Q) circular ruffles following MP addition. Statistical differences are $*p < 0.05$, $**p < 0.01$, $***p < 0.001$, $n = 3$. Arrows indicate each respective feature; arrows in O and P also indicate particle clusters (see Figure 1).

parallel to the original cell monolayer, a more difficult technique than sectioning perpendicular to the monolayer. Finally, TEM sections had to undergo a further staining process (uranyl acetate and lead citrate) individually. It should also be noted that only a small number of ultrathin sections could be studied by TEM at a time, and these were commonly all obtained from a single face of a single fragment of the original resin-embedded sample. These considerations make TEM analyses more expensive and time consuming than OTOTO–FESEM, particularly when trying to generate a 3D reconstruction of the cell membrane surface.[17]

2.3. Comparison of Membrane Responses to Particles Using OTOTO–SEM Versus TEM: A Five-Point Classification System

At higher magnification, membranes of unstimulated NSCs appeared relatively smooth (i.e., fewer endocytotic features, less membrane infoldings) in OTOTO–FESEM (**Figure 3**A) and TEM (Figure 3B). By contrast, the membranes of magnetite-loaded particle stimulated NSCs appeared more activated, with several types of surface responses evident. Five membrane features were quantified: i) pits, which could be distinguished as depressions possessing a diameter of approximately

150–200 nm; ii) filopodia, identified as fine, finger-like projections (ca. 200–250 nm in diameter) extending from the cell surface; iii) nanopodia, identified as finger-like projections similar to filopodia but extending on the cell substrate and possessing a relatively narrow diameter versus filopodia (75–100 nm); iv) membrane ruffling, defined as regular infoldings/undulations over the entire membrane surface; and v) circular ruffles, identified as highly distinctive rounded, cup-like projections with a translucent, parachute-like appearance. The quantitative analysis revealed a significantly greater extent of membrane ruffling ($p < 0.001$; Figure 3C-E), filopodia ($p < 0.01$; Figure 3F-H), pits ($p < 0.001$; Figure 3I-K) and nanopodia ($p < 0.05$; Figure 3L-N) but not circular ruffles ($p = 0.184$ Figure 3O-Q), after MP stimulation.

Membrane features showing similarity to those seen with SEM, were detected using TEM (Figure 3D,G,J,M, and P). However, an unequivocal classification approach in this regard was possible only for pits, where measured diameters were in a similar range (150–250 nm) as to those identified by OTOTO–FESEM. This observation suggests that FESEM captures identifiable membrane activation events more reliably than TEM. Based on these advantages, the OTOTO protocol described here can provide significantly more quantifiable data than is achievable with TEM analyses, given the same resources in terms of time and expense.

SEM has been used previously to study blebs, ruffling and filopodia in cultured cells,[20] but here we have demonstrated the feasibility of distinguishing additional features, specifically nanopodia, pits, and membrane ruffles, with high resolution. These features have been shown in a range of studies to be related to particle trafficking by cell membranes. For example, membrane pits have been shown to mediate MP uptake and both the morphology and diameter of the structures we identify as pits are consistent with that reported in the literature.[21] Filopodia/nanopodia are likely cellular sensors for extracellular materials[22] and these are known to be highly dynamic structures.[23] Investigations into filopodia biology demonstrate considerable variation in the dynamics, length, and position of these cellular protrusions between various cell types and in differing microenvironments. However, the length and diameter of the structures that we classify as filopodia in our study are also consistent with the published literature.[23] The function of the fifth class of circular dorsal ruffles is somewhat obscure but such structures may be related to macropinocytosis.[24] Supporting this concept, four of the features identified showed a statistically significant increase on stimulation of cells with magnetite-loaded particles (that we have previously proven to show high levels of uptake in NSCs) compared with particles with no magnetite (that show significantly less uptake in the same cell type). This finding suggests that the enhanced levels of membrane surface activity exhibited by the NSCs in response to the magnetite-loaded particles, can act as a reliable and robust predictor of the extent of particle uptake in cells—a finding further borne out by the enhanced levels of dextran uptake in cells stimulated with magnetite-loaded particles.

The OTOTO–FESEM method can be combined with techniques such as backscatter detection of iron oxide particles and stereo image analysis, involving a red/green anaglyph, which produces 3D images and facilitates the measurement of the depth of membrane depressions/pits.[25] Such data can enable the identification of the mechanisms responsible for cellular uptake of particles, and reveal which particular mechanisms a particular cell type employs for particle uptake. Therefore, there is the potential in the future to develop a high-throughput assay for counting "particle uptake events" by cells, by identifying and scoring instances of endocytosis.

3. Conclusion

As far as we are aware, this is the first report studying membrane responses of primary NSCs following challenge with MPs. The field of neuro-nanotechnology is heavily reliant on the use of a range of cell lines for nanoparticle activation and uptake studies. However, cells lines are associated with a range of drawbacks such as abnormal physiology, clonal behaviors, and high resistance to cell death.[4] As such, we consider it essential to develop imaging methods consistent with the use of primary cells for translational applications. To our knowledge, we are also the first to develop a detailed classification system by which such membrane responses can be robustly quantified following particle challenge, in order to correlate early membrane responses with particle uptake. We consider that the predictive utility of this approach is therefore of value for cellular studies of particle uptake. The OTOTO procedure results in an electron-conductive cellular membrane,[26,27] allowing for observation of fine ultrastructural detail comparable to the resolution of TEM, and far exceeding that possible through standard fluorescence microscopy methods. We consider therefore that OTOTO–FESEM offers a means to bridge the gap between fluorescence imaging and TEM, particularly given the ready access of many researchers to SEM facilities, and greatly enhances the analytical power of microscopy for evaluating cell surface activity and safety profiles in response to nanoparticle activation. We conclude that this versatile methodology can be exploited for several applications in nanomedicine (**Figure 4**), particularly as a tool to identify novel, neurocompatible materials for neural cell therapy.

4. Experimental Section

The care and use of animals was in accordance with the Animals (Scientific Procedures) Act of 1986 (United Kingdom) with approval by the local ethics committee.

Materials/Equipment: Cell culture reagents were from Life Technologies (Paisley, Scotland, UK; including Alexa Fluor555-conjugated Dextran particles (10 kDa)) and Sigma (Poole, Dorset, UK; including FITC-conjugated Phalloidin). Human recombinant epidermal growth factor (EGF) was from R&D Systems Europe Ltd. (Abingdon, UK). Human recombinant basic fibroblast growth factor (bFGF) was from Peprotech (Rocky Hill, NJ, USA). Thermo Scientific Nunc culture dishes (nontreated surface) and tissue culture-grade plastics were from Fisher Scientific UK (Loughborough, UK). Mouse anti-nestin was from BD Biosciences (Oxford, UK) and FITC-conjugated secondary antibodies were from Jackson Immunoresearch Laboratories Ltd (Westgrove, PA, USA).

BODIPY 564/570 (Life Technologies)-tagged, polylactide-based non-magnetite and magnetite-loaded polymeric particles were a kind gift from Dr. Boris Polyak (Drexel University, Philadelphia). Vectashield mounting medium with 4′,6-diamidino-2-phenylindole (DAPI, nuclear marker) was from Vector Laboratories (Peterborough, UK). The magnefect-nano

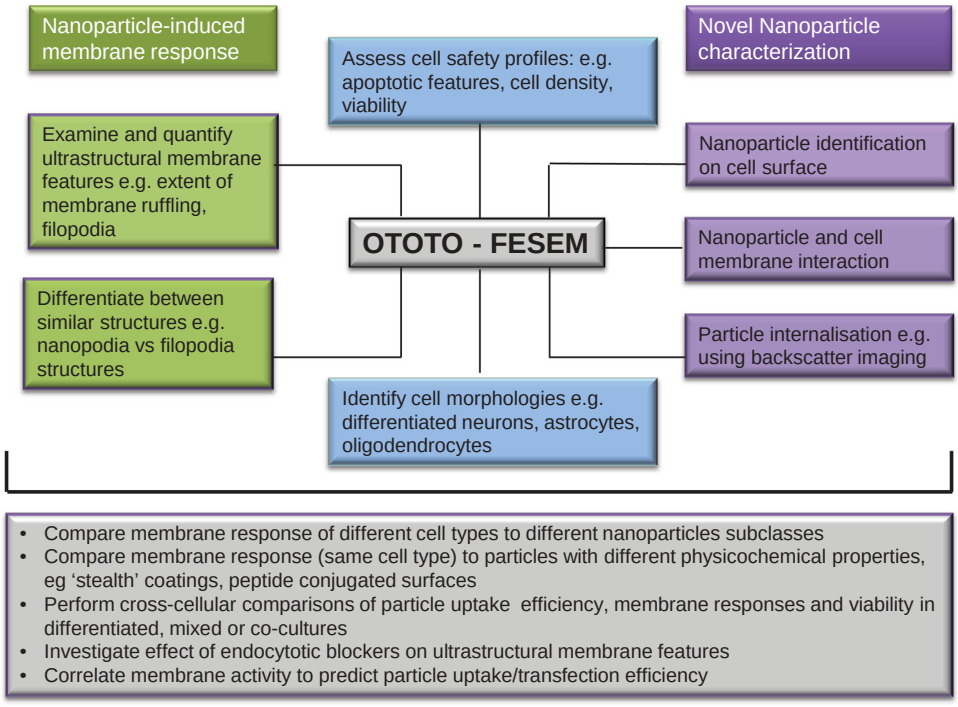

Figure 4. Schematic diagram showing the potential uses of OTOTO–FESEM for nanomedicine applications.

24-magnet array system was purchased from nanoTherics Ltd. (Stoke-on-Trent, UK) and comprises horizontal arrays of NdFeB magnets (grade N42), which correspond with 24-well cell culture plates.

Magnetic Particle Details: Detailed particle formulation and characterization of non-magnetite and magnetite-loaded particles are described in Adams et al.[9] Briefly, DLS measurements indicated similar particle hydrodynamic diameters ranging between 262 and 278 nm with a polydispersity index of 0.15–0.23. Magnetite-loaded particles (referred to as "MP-5×" previously) are composed of a polymeric matrix and have a magnetization at 5 kOe of 24.6 ± 1.2 emu g^{-1} composite.[9]

Neurosphere and NSC Monolayer Culture: Primary NSC cultures were derived from the subventricular zone of CD1 mice (postnatal day 0–3), then maintained and expanded under growth factor stimulation in neurosphere culture medium (DMEM:F12 (3:1 mix) containing B-27 supplement (2%), penicillin (50 U mL^{-1}), streptomycin (50 mg mL^{-1}), heparin (4 ng mL^{-1}), bFGF (20 ng mL^{-1}), and EGF (20 ng mL^{-1})) according to the well characterized "neurosphere" culture method.[6] Cultures were fed every 2–3 d and neurospheres were passaged weekly by dissociation with a mix of accutase-DNase I. For all experiments, NSCs (passages 1–3) were dissociated and plated as 2D monolayers (i.e., a single layer of cells) on coverslips (sequentially coated with polyornithine and laminin) in 24-well plates. Cells were maintained in monolayer maintenance medium composed of a 1:1 mix of DMEM:F12 containing N2 supplement (1%) with the above-mentioned antibiotic, heparin, and growth factor concentrations.

Particle Incubation with NSCs: The day after plating, equal numbers of non-magnetite or magnetite-loaded particles (600 µL $well^{-1}$, corresponding to about 7.8 and 22 µg total weight for each particle, respectively) were added to NSC monolayers. Culture plates were placed on the oscillating magnetic device (magnefect-nano; oscillation frequency (F) = 4 Hz, previously shown to enhance magnetite-loaded particle uptake in NSCs)[28] for 30 min, followed by washing (phosphate buffered saline, PBS) and fixation. For fluorescence microscopy, cells were fixed in paraformaldehyde (PFA; 4%, 20 min; room temperature (RT)). For OTOTO and TEM preparation (see below), cells were fixed in 2.5% (w/v) glutaraldehyde in sodium cacodylate (0.1 M)/calcium chloride buffer (SCB; 2×10^{-3} M, pH 7.2; 2 h; RT). Control cultures were not exposed to particles or magnetic fields.

Phalloidin Labeling of NSCs: To visualize cellular boundaries and cytoskeletal elements, including possible associations with nanoparticles, PFA-fixed cells were stained with FITC-conjugated phalloidin (20 µg mL^{-1}; marker for actin filaments) for 40 min at RT and washed in PBS three times before mounting with DAPI.

Dextran as an Indicator of Macropinocytosis: Fluorescently labeled dextran was used to confirm the presence of macropinocytotic activity. Alexa Fluor 555-conjugated dextran (0.025 mg mL^{-1}) was added to cells along with non-magnetite or magnetite-loaded particles before placing on the magnefect-nano for 30 min (4 Hz). Control cultures were incubated with dextran for 30 min, but without particles or exposure to a magnetic field. Samples were fixed in PFA (4%) and washed with PBS.

Fluorescence Microscopy: Fluorescence- and phase-contrast images were captured using an Axio Scope A1 fluorescence microscope and an Axio Cam ICc1 digital camera (Carl Zeiss MicroImaging GmbH, Goettingen, Germany). Images were merged using AxioVision Software.

OTOTO Processing for FESEM: Glutaraldehyde fixation of samples was followed by OTOTO conductivity staining (OsO_4/thiocarbohydrazide/OsO_4/thiocarbohydrazide/OsO_4): OsO_4 (1%) was applied first for 1 h followed by thorough washing in distilled water, then saturated filtered aqueous thiocarbohydrazide for 20 min, and then a further O (2 h), T (20 min), and O (2 h), with washing between each step. Finally, samples were dehydrated in a graded series of ethanols, critical point dried with CO_2 as the transitional fluid, and mounted onto carbon pads on aluminum stubs. To improve electron conductivity, silver conducting paint (Agar Scientific) was used to coat the sample edges.

FESEM: Non-magnetite- and magnetite-loaded particles (air-dried on aluminum stubs) were visualized using a Hitachi S4500 FESEM (15 kV accelerating voltage). Membrane morphologies (see Results) were examined using a Hitachi S4500 FESEM (5 kV accelerating voltage) after OTOTO preparation. Analyses were carried out on 30 cells from three replicates (n = 3) each generated from a different litter, by an observer blind to the conditions. Pits, filopodia, and nanopodia were expressed per unit area (area of measurement = 25 μm^2) and circular ruffles per cell. For membrane ruffling, a semiquantitative score was assigned from 1–5.

TEM Preparation and Imaging: Glutaraldehyde-fixed samples were postfixed with osmium tetroxide (1%) in SCB for 1 h, washed, and

then dehydrated in a graded series of ethanols, before infiltration and embedding in Spurr resin. After polymerization of the resin at 60 °C for 16 h, ultrathin sections were cut on a Reichert Ultracut E microtome. Sections were collected on 2000 μm hole, 3.05 mm copper grids coated with formvar, which provides a completely electron permeable surface for section mounting (without interruption from grid bars). The mounted sections were then stained with uranyl acetate (2%) in ethanol (70%) and Reynold's lead citrate (2%) in distilled water. Sections were examined in a JEOL 100CX TEMSCAN (Tokyo, Japan) operated in TEM mode at 100 kV and images captured using a SIS systems Megaview III digital camera (Olympus, Tokyo, Japan).

EDX Microanalysis: To identify particles on the cell surface, X-ray microanalysis was carried out on OTOTO-treated samples using a JEOL 100CX TEMSCAN operated in in-lens SEM mode at ×30 k magnification (40 kV accelerating voltage; beam current 100 μA, spot size 30 nm), to detect iron within the particle. Dot mapping was performed using a full area raster while individual spectra were acquired using the SEM in spot mode. Processing of the X-ray counts was carried out using NSS Spectral Imaging software (Fisher Scientific, Loughborough, UK).

Statistics: All data were analyzed by one-way ANOVA with Bonferroni's multiple comparison post-tests as appropriate, using Prism software (version 5.00, GraphPad, CA, USA, www.graphpad.com). All data are expressed as mean ± standard error of the mean.

Supporting Information

Supporting Information is available from the Wiley Online Library or from the author.

Acknowledgements

A.R.F. and C.F.A. contributed equally to this study. This work was funded by grants from the British Biotechnology and Biological Sciences Research Council (BBSRC; DMC, ARF) and the Engineering and Physical Sciences Research Council (EPSRC) via the Doctoral Training Centre in Regenerative Medicine (CFA).

Received: November 3, 2014
Revised: December 29, 2014
Published online: January 29, 2015

[1] S. M. Cromer Berman, P. Walczak, J. W. M. Bulte, *Wiley Interdiscip. Rev. Nanomed. Nanobiotechnol.* **2011**, *3*, 343.
[2] C. Liang, C. Wang, Z. Liu, *Part. Part. Syst. Charact.* **2013**, *30*, 1006.
[3] V. Vaněček, V. Zablotskii, S. Forostyak, J. Růžička, V. Herynek, M. Babič, P. Jendelová, Š. Kubinová, A. Dejneka, E. Syková, *Int. J. Nanomed.* **2012**, *7*, 3719.
[4] M. Pickard, D. Chari, *Nanomedicine* **2010**, *5*, 217.
[5] S. I. Jenkins, M. R. Pickard, N. Granger, D. M. Chari, *ACS Nano* **2011**, *5*, 6527.
[6] M. R. Pickard, P. Barraud, D. M. Chari, *Biomaterials* **2011**, *32*, 2274.
[7] A. S. Arbab, G. T. Yocum, L. B. Wilson, A. Parwana, E. K. Jordan, H. Kalish, J. A. Frank, *Mol. Imaging* **2004**, *3*, 24.
[8] S. H. Lee, B. Castagner, J. C. Leroux, *Eur. J. Pharm. Biopharm.* **2013**, *85*, 5.
[9] C. F. Adams, A. Rai, G. Sneddon, H. H. P. Yiu, B. Polyak, D. M. Chari, *Nanomedicine* **2014**, *11*, 19.
[10] A. J. Mothe, C. H. Tator, *Int. J. Dev. Neurosci.* **2013**, *31*, 701.
[11] G. Gincberg, H. Arien-Zakay, P. Lazarovici, P. I. Lelkes, *Br. Med. Bull.* **2012**, *104*, 7.
[12] A. Trounson, R. G. Thakar, G. Lomax, D. Gibbons, *BMC Med.* **2011**, *9*, 52.
[13] S. Mukherjee, R. N. Ghosh, F. R. Maxfield, *Physiol. Rev.* **1997**, *77*, 759.
[14] K. L. Chen, G. D. Bothun, *Environ. Sci. Technol.* **2014**, *48*, 873.
[15] R. A. Vriend, H. D. Geissinger, *J. Microsc.* **1980**, *120*, 53.
[16] A. R. Fernandes, D. M. Chari, *Integr. Biol.* **2014**, *6*, 855.
[17] A. Terry, *Introduction to Electron Microscopy for Biologists,* Elsevier Inc., Burlington, MA, USA **2008**.
[18] B. J. Marquis, S. A. Love, K. L. Braun, C. L. Haynes, *Analyst* **2009**, *134*, 425.
[19] K. Grandfield, H. Engqvist, *Adv.Mater. Sci. Eng.* **2012**, *2012*, 841961.
[20] K. R. Porter, G. J. Todaro, V. Fonte, *J. Cell Biol.* **1973**, *59*, 633.
[21] V. B. Bregar, J. Lojk, V. Suštar, P. Veranič, M. Pavlin, *Int. J. Nanomedicine* **2013**, *8*, 919.
[22] C. A. Heckman, H. K. Plummer, *Cell. Signal.* **2013**, *25*, 2298.
[23] P. K. Mattila, P. Lappalainen, *Nat. Rev. Mol. Cell Biol.* **2008**, *9*, 446.
[24] J.-L. Hoon, W.-K. Wong, C.-G. Koh, *Mol. Cell. Biol.* **2012**, *32*, 4246.
[25] A. Boyde, *J. Anat.* **2003**, *202*, 183.
[26] L. Keeley, *Comp. Biochem. Phys.* **1973**, *46*, 147.
[27] L. E. Malick, R. B. Wilson, *Stain Technol.* **1975**, *50*, 265.
[28] C. F. Adams, M. R. Pickard, D. M. Chari, *Nanomedicine* **2013**, *9*, 737.

References

1. World Health Organisation. Global Health Estimates Summary Tables. *Geneva* (2013).

2. National Spinal Cord Injury Statistical Centre. Spinal Cord Injury Facts and Figures at a Glance. *Univerisity of Alabama* (2013).

3. Bear, M. F., Connors, B. W. & Paradiso, M. A. *Neuroscience: Exploring the Brain*. (Lippincott Williams & Wilkins, 2007).

4. Verkhratsky, A. & Butt, A. *Glial Neurobiology: A Textbook*. (John Wiley & Sons, Ltd, 2008).

5. Brosius Lutz, A. & Barres, B. a. Contrasting the glial response to axon injury in the central and peripheral nervous systems. *Dev. Cell* **28,** 7–17 (2014).

6. Burda, J. E. & Sofroniew, M. V. Reactive gliosis and the multicellular response to CNS damage and disease. *Neuron* **81,** 229–48 (2014).

7. Kang, S. H., Fukaya, M., Yang, J. K., Rothstein, J. D. & Bergles, D. E. NG2+ CNS glial progenitors remain committed to the oligodendrocyte lineage in postnatal life and following neurodegeneration. *Neuron* **68,** 668–81 (2010).

8. Kyritsis, N., Kizil, C. & Brand, M. Neuroinflammation and central nervous system regeneration in vertebrates. *Trends Cell Biol.* **24,** 128–35 (2014).

9. Lagace, D. C. Does the endogenous neurogenic response alter behavioral recovery following stroke? *Behav. Brain Res.* **227,** 426–32 (2012).

10. Plemel, J. R., Wee Yong, V. & Stirling, D. P. Immune modulatory therapies for spinal cord injury--past, present and future. *Exp. Neurol.* **258,** 91–104 (2014).

11. Frank, B. *et al.* Thrombolysis in stroke despite contraindications or warnings? *Stroke.* **44,** 727–33 (2013).

12. Reinkensmeyer, D., Lum, P. & Winters, J. Emerging technologies for improving access to movement therapy following neurologic injury. *Emerg. Access. Telecommun. Inf. Healthc. Technol. Eng. Challenges Enabling Univers. Access* 136–150 (2002).

13. Fitch, M. T. & Silver, J. CNS injury, glial scars, and inflammation: Inhibitory extracellular matrices and regeneration failure. *Exp. Neurol.* **209,** 294–301 (2008).

14. Rowland, J. W., Hawryluk, G. W. J., Kwon, B. & Fehlings, M. G. Current status of acute spinal cord injury pathophysiology and emerging therapies: promise on the horizon. *Neurosurg. Focus* **25,** E2 (2008).

15. Ali, F., Stott, S. R. W. & Barker, R. a. Stem cells and the treatment of Parkinson's disease. *Exp. Neurol.* **260,** 3–11 (2014).

16. Joyce, N. *et al.* Mesenchymal stem cells for the treatment of neurodegenerative disease. *Regen. Med.* **5,** 933–46 (2010).

17. Trounson, A., Thakar, R. G., Lomax, G. & Gibbons, D. Clinical trials for stem cell therapies. *BMC Med.* **9,** 52 (2011).

18. Ahmed, R. P. H., Ashraf, M., Buccini, S., Shujia, J. & Haider, H. K. Cardiac tumorigenic potential of induced pluripotent stem cells in an immunocompetent host with myocardial infarction. *Regen. Med.* **6,** 171–8 (2011).

19. Okano, H. *et al.* Steps toward safe cell therapy using induced pluripotent stem cells. *Circ. Res.* **112,** 523–33 (2013).

20. Ibrahim, A., Li, Y., Li, D., Raisman, G. & El Masry, W. S. Olfactory ensheathing cells: ripples of an incoming tide? *Lancet. Neurol.* **5,** 453–7 (2006).

21. Gage, F. H. Mammalian neural stem cells. *Science* **287,** 1433–1438 (2000).

22. Kazanis, I., Lathia, J., Moss, L. & ffrench-Constant, C. *The neural stem cell microenvironment*. (Stembook, 2008).

23. Shihabuddin, L. S., Horner, P. J., Ray, J. & Gage, F. H. Adult spinal cord stem cells generate neurons after transplantation in the adult dentate gyrus. *J. Neurosci.* **20,** 8727–35 (2000).

24. Mothe, A. J. & Tator, C. H. Review of transplantation of neural stem/progenitor cells for spinal cord injury. *Int. J. Dev. Neurosci.* **31,** 701–13 (2013).

25. Conti, L., Reitano, E. & Cattaneo, E. Neural stem cell systems: diversities and properties after transplantation in animal models of diseases. *Brain Pathol.* **16,** 143–54 (2006).

26. Drago, D. *et al.* The stem cell secretome and its role in brain repair. *Biochimie* **95,** 2271–85 (2013).

27. Ourednik, J., Ourednik, V., Lynch, W. P., Schachner, M. & Snyder, E. Y. Neural stem cells display an inherent mechanism for rescuing dysfunctional neurons. *Nat. Biotechnol.* **20,** 1103–10 (2002).

28. Pluchino, S. *et al.* Injection of adult neurospheres induces recovery in a chronic model of multiple sclerosis. *Nature* **422,** 688–694 (2003).

29. Aboody, K. S. *et al.* Neural stem cells display extensive tropism for pathology in adult brain: evidence from intracranial gliomas. *Proc Natl Acad Sci U S A* **97,** 12846–12851 (2000).

30. Pickard, M. R., Barraud, P. & Chari, D. M. The transfection of multipotent neural precursor/stem cell transplant populations with magnetic nanoparticles. *Biomaterials* **32,** 2274–2284 (2011).

31. Cummings, B. J. *et al.* Human neural stem cells differentiate and promote locomotor recovery in spinal cord-injured mice. *Proc. Natl. Acad. Sci. U. S. A.* **102,** 14069–14074 (2005).

32. Müller, F.-J., Snyder, E. Y. & Loring, J. F. Gene therapy: can neural stem cells deliver? *Nat. Rev. Neurosci.* **7,** 75–84 (2006).

33. Schwarz, S. C. & Schwarz, J. Translation of stem cell therapy for neurological diseases. *Transl. Res.* **156,** 155–160 (2010).

34. Glass, J. D. *et al.* Lumbar intraspinal injection of neural stem cells in patients with amyotrophic lateral sclerosis: results of a phase I trial in 12 patients. *Stem Cells* **30,** 1144–51 (2012).

35. Selden, N. R. *et al.* Central nervous system stem cell transplantation for children with neuronal ceroid lipofuscinosis. *J. Neurosurg. Pediatr.* **11,** 643–52 (2013).

36. Lee, H. J., Kim, M. K., Kim, H. J. & Kim, S. U. Human neural stem cells genetically modified to overexpress Akt1 provide neuroprotection and functional improvement in mouse stroke model. *PLoS One* **4,** e5586 (2009).

37. Maurer, M. H., Thomas, C., Bürgers, H. F. & Kuschinsky, W. Transplantation of adult neural progenitor cells transfected with vascular endothelial growth factor rescues grafted cells in the rat brain. *Int. J. Biol. Sci.* **4,** 1–7 (2008).

38. Hughes, P., Marshall, D., Reid, Y., Parkes, H. & Gelber, C. The costs of using unauthenticated, over-passaged cell lines: how much more data do we need? *Biotechniques* **43,** 575–586 (2007).

39. Pollock, K. *et al.* A conditionally immortal clonal stem cell line from human cortical neuroepithelium for the treatment of ischemic stroke. *Exp. Neurol.* **199,** 143–55 (2006).

40. Lu, P., Jones, L. ., Snyder, E. . & Tuszynski, M. . Neural stem cells constitutively secrete neurotrophic factors and promote extensive host axonal growth after spinal cord injury. *Exp. Neurol.* **181,** 115–129 (2003).

41. Zhu, W. *et al.* Transplantation of vascular endothelial growth factor-transfected neural stem cells into the rat brain provides neuroprotection after transient focal cerebral ischemia. *Neurosurgery* **57,** 325–33; discussion 325–33 (2005).

42. Park, K. I. *et al.* Neural stem cells may be uniquely suited for combined gene therapy and cell replacement: Evidence from engraftment of Neurotrophin-3-expressing stem cells in hypoxic-ischemic brain injury. *Exp. Neurol.* **199,** 179–190 (2006).

43. Kameda, M. *et al.* Adult neural stem and progenitor cells modified to secrete GDNF can protect, migrate and integrate after intracerebral transplantation in rats with transient forebrain ischemia. *Eur. J. Neurosci.* **26,** 1462–1478 (2007).

44. Blurton-Jones, M. *et al.* Neural stem cells genetically-modified to express neprilysin reduce pathology in Alzheimer transgenic models. *Stem Cell Res. Ther.* **5,** 46 (2014).

45. Neri, M. *et al.* Neural stem cell gene therapy ameliorates pathology and function in a mouse model of globoid cell leukodystrophy. *Stem Cells* **29,** 1559–71 (2011).

46. Setoguchi, T. *et al.* Treatment of spinal cord injury by transplantation of fetal neural precursor cells engineered to express BMP inhibitor. *Exp Neurol* **189,** 33–44 (2004).

47. Yamane, J. *et al.* Transplantation of galectin-1-expressing human neural stem cells into the injured spinal cord of adult common marmosets. *J. Neurosci. Res.* **88,** 1394–405 (2010).

48. Shihabuddin, L. S. *et al.* Intracerebral transplantation of adult mouse neural progenitor cells into the Niemann-Pick-A mouse leads to a marked decrease in lysosomal storage pathology. *J. Neurosci.* **24,** 10642–51 (2004).

49. Lentz, T. B., Gray, S. J. & Samulski, R. J. Viral vectors for gene delivery to the central nervous system. *Neurobiol dis* **48,** 179–88 (2012).

50. Rogers, M.-L. & Rush, R. a. Non-viral gene therapy for neurological diseases, with an emphasis on targeted gene delivery. *J Control Release* **157,** 183–9 (2012).

51. Palmer, T. Genetically modified skin fibroblasts persist long after transplantation but gradually inactivate introduced genes. *Proc. …* **88,** 1330–1334 (1991).

52. Tinsley, R. B., Faijerson, J. & Eriksson, P. S. Efficient non-viral transfection of adult neural stem/progenitor cells, without affecting viability, proliferation or differentiation. *J. Gene Med.* **8,** 72–81 (2006).

53. Cesnulevicius, K. *et al.* Nucleofection is the most efficient nonviral transfection method for neuronal stem cells derived from ventral mesencephali with no changes in cell composition or dopaminergic fate. *Stem Cells* **24,** 2776–91 (2006).

54. Li, L. *et al.* Effects of administration route on migration and distribution of neural progenitor cells transplanted into rats with focal cerebral ischemia, an MRI study. *J. Cereb. Blood Flow Metab.* **30,** 653–62 (2010).

55. Hauger, O. *et al.* MR evaluation of the glomerular homing of magnetically labeled mesenchymal stem cells in a rat model of nephropathy. *Radiology* **238,** 200–10 (2006).

56. Kraitchman, D. L. *et al.* Dynamic imaging of allogeneic mesenchymal stem cells trafficking to myocardial infarction. *Circulation* **112,** 1451–61 (2005).

57. Pearse, D. D. *et al.* Transplantation of Schwann cells and/or olfactory ensheathing glia into the contused spinal cord: Survival, migration, axon association, and functional recovery. *Glia* **55,** 976–1000 (2007).

58. Hong, H., Yang, Y., Zhang, Y. & Cai, W. Non-invasive cell tracking in cancer and cancer therapy. *Curr. Top. Med. Chem.* **10,** 1237–1248 (2010).

59. Hong, H., Yang, Y., Zhang, Y. & Cai, W. Non-invasive imaging of human embryonic stem cells. *Curr. Pharm. Biotechnol.* **11,** 685–692 (2010).

60. Lu, H.-X. *et al.* Neurotrophin-3 gene transduction of mouse neural stem cells promotes proliferation and neuronal differentiation in organotypic hippocampal slice cultures. *Med. Sci. Monit. Int. Med. J. Exp. Clin. Res.* **17,** BR305–311 (2011).

61. Lepore, A. C., Walczak, P., Rao, M. S., Fischer, I. & Bulte, J. W. M. MR imaging of lineage-restricted neural precursors following transplantation into the adult spinal cord. *Exp. Neurol.* **201,** 49–59 (2006).

62. Pickard, M. & Chari, D. Enhancement of magnetic nanoparticle-mediated gene transfer to astrocytes by "magnetofection": effects of static and oscillating fields. *Nanomedicine (Lond)* **5,** 217–232 (2010).

63. Jenkins, S. I., Pickard, M. R., Granger, N. & Chari, D. M. Magnetic nanoparticle-mediated gene transfer to oligodendrocyte precursor cell transplant populations is enhanced by magnetofection strategies. *ACS Nano* **5,** 6527–6538 (2011).

64. Song, M. *et al.* Using a neodymium magnet to target delivery of ferumoxide-labeled human neural stem cells in a rat model of focal cerebral ischemia. *Hum. Gene Ther.* **21,** 603–10 (2010).

65. Polyak, B. *et al.* High field gradient targeting of magnetic nanoparticle-loaded endothelial cells to the surfaces of steel stents. *Proc Natl Acad Sci U S A* **105,** 698–703 (2008).

66. Cohen, M. E., Muja, N., Fainstein, N., Bulte, J. W. M. & Ben-Hur, T. Conserved fate and function of ferumoxides-labeled neural precursor cells in vitro and in vivo. *J Neurosci Res* **88,** 936–944 (2010).

67. Cromer Berman, S. M., Walczak, P. & Bulte, J. W. M. Tracking stem cells using magnetic nanoparticles. *Wiley Interdiscip Rev Nanomed Nanobiotechnol* **3,** 343–355 (2011).

68. McBain, S. C., Yiu, H. H. & Dobson, J. Magnetic nanoparticles for gene and drug delivery. *Int. J. Nanomedicine* **3,** 169–180 (2008).

69. Grützkau, A. & Radbruch, A. Small but mighty: how the MACS-technology based on nanosized superparamagnetic particles has helped to analyze the immune system within the last 20 years. *Cytometry. A* **77,** 643–7 (2010).

70. Fang, C. & Zhang, M. Multifunctional Magnetic Nanoparticles for Medical Imaging Applications. *J. Mater. Chem.* **19,** 6258–6266 (2009).

71. Yiu, H. H. P. Engineering the multifunctional surface on magnetic nanoparticles for targeted biomedical applications : a chemical approach R eview. *Nanomedicine (Lond)* **6,** 1429–46 (2011).

72. Laurent, S. *et al.* Magnetic iron oxide nanoparticles: Synthesis, stabilization, vectorization, physicochemical characterizations, and biological applications. *Society* **108,** 2064–2110 (2008).

73. Bulte, J. W. In vivo MRI cell tracking: clinical studies. *AJR.American J. Roentgenol.* **193,** 314–325 (2009).

74. Ferrucci, J. & Stark, D. Iron oxide-enhanced MR imaging of the liver and spleen: review of the first 5 years. *Am. J. Roentgenol.* **155,** 943–950 (1990).

75. Hofmann-Amtenbrink, M., Hofmann, H. & Montet, X. Superparamagnetic nanoparticles - a tool for early diagnostics. *Swiss Med. Wkly.* **140,** w13081 (2010).

76. Wang, Y. X., Hussain, S. M. & Krestin, G. P. Superparamagnetic iron oxide contrast agents: physicochemical characteristics and applications in MR imaging. *Eur. Radiol.* **11,** 2319–2331 (2001).

77. Dunning, M. D. *et al.* Superparamagnetic iron oxide-labeled Schwann cells and olfactory ensheathing cells can be traced in vivo by magnetic resonance imaging and retain functional properties after transplantation into the CNS. *J. Neurosci.* **24,** 9799–9810 (2004).

78. Mykhaylyk, O., Antequera, Y. S., Vlaskou, D. & Plank, C. Generation of magnetic nonviral gene transfer agents and magnetofection in vitro. *Nat. Protoc.* **2,** 2391–2411 (2007).

79. Rachakatla, R. S. *et al.* Attenuation of Mouse Melanoma by A/C Magnetic Field after Delivery of Bi-Magnetic Nanoparticles by Neural Progenitor Cells. *ACS Nano* (2010).

80. Hamasaki, T. *et al.* Magnetically labeled neural progenitor cells, which are localized by magnetic force, promote axon growth in organotypic cocultures. *Spine (Philadelphia)* **32,** 2300–2305 (2007).

81. Pickard, M., Jenkins, S., Koller, C., Furness, D. & Chari, D. Magnetic nanoparticle labeling of astrocytes derived for neural transplantation. *Tissue Eng Part C Methods* **17,** 89–99 (2010).

82. Lee, H.-Y. *et al.* PET/MRI dual-modality tumor imaging using arginine-glycine-aspartic (RGD)-conjugated radiolabeled iron oxide nanoparticles. *J. Nucl. Med. Off. Publ. Soc. Nucl. Med.* **49,** 1371–1379 (2008).

83. Yiu, H. H. P. *et al.* Fe(3)O (4)-PEI-RITC Magnetic Nanoparticles with Imaging and Gene Transfer Capability: Development of a Tool for Neural Cell Transplantation Therapies. *Pharm Res* **29,** 1328–1343 (2011).

84. Xie, J. *et al.* PET/NIRF/MRI triple functional iron oxide nanoparticles. *Biomaterials* **31,** 3016–3022 (2010).

85. Lin, J.-J. *et al.* Folic acid-Pluronic F127 magnetic nanoparticle clusters for combined targeting, diagnosis, and therapy applications. *Biomaterials* **30,** 5114–5124 (2009).

86. Plank, C., Zelphati, O. & Mykhaylyk, O. Magnetically enhanced nucleic acid delivery. *Adv Drug Deliv Rev* **63,** 1300–1331 (2011).

87. Godbey, W. T., Wu, K. K. & Mikos, A. G. Size matters: molecular weight affects the efficiency of poly(ethylenimine) as a gene delivery vehicle. *J. Biomed. Mater. Res.* **45,** 268–275 (1999).

88. Thomas, M. & Klibanov, A. M. Enhancing polyethylenimine's delivery of plasmid DNA into mammalian cells. *Proc. Natl. Acad. Sci. U. S. A.* **99,** 14640–14645 (2002).

89. Cheong, S.-J. *et al.* Superparamagnetic iron oxide nanoparticles-loaded chitosan-linoleic acid nanoparticles as an effective hepatocyte-targeted gene delivery system. *Int. J. Pharm.* **372,** 169–176 (2009).

90. Kievit, F. M. *et al.* PEI-PEG-Chitosan Copolymer Coated Iron Oxide Nanoparticles for Safe Gene Delivery: synthesis, complexation, and transfection. *Adv. Funct. Mater.* **19,** 2244–2251 (2009).

91. Duan, H. *et al.* Reexamining the Effects of Particle Size and Surface Chemistry on the Magnetic Properties of Iron Oxide Nanocrystals: New Insights into Spin Disorder and Proton Relaxivity. *J. Phys. Chem. C* **112,** 8127–8131 (2008).

92. Huth, S. *et al.* Insights into the mechanism of magnetofection using PEI-based magnetofectins for gene transfer. *J. Gene Med.* **6,** 923–36 (2004).

93. McBain, S. C. *et al.* Magnetic nanoparticles as gene delivery agents: enhanced transfection in the presence of oscillating magnet arrays. *Nanotechnology* **19,** 405102 (2008).

94. Walton, R. M., Magnitsky, S. G., Seiler, G. S., Poptani, H. & Wolfe, J. H. Transplantation and magnetic resonance imaging of canine neural progenitor cell grafts in the postnatal dog brain. *J. Neuropathol. Exp. Neurol.* **67,** 954–962 (2008).

95. Zhu, J., Zhou, L. & XingWu, F. *Tracking neural stem cells in patients with brain trauma. The New England Journal of Medicine* **355,** 2376–2378 (2006).

96. Obenaus, A. *et al.* Long-term magnetic resonance imaging of stem cells in neonatal ischemic injury. *Ann. Neurol.* **69,** 282–291 (2011).

97. Berman, S. C., Galpoththawela, C., Gilad, A. A., Bulte, J. W. M. & Walczak, P. Long-term MR cell tracking of neural stem cells grafted in immunocompetent versus immunodeficient mice reveals distinct differences in contrast between live and dead cells. *Magn. Reson. Med.* **65,** 564–574 (2011).

98. Srinivas, M. *et al.* Imaging of cellular therapies. *Adv. Drug Deliv. Rev.* **62,** 1080–1093 (2010).

99. Pardridge, W. M. Drug delivery to the brain. *J. Cereb. Blood Flow Metab.* **17,** 713–31 (1997).

100. Sasaki, H. *et al.* Therapeutic effects with magnetic targeting of bone marrow stromal cells in a rat spinal cord injury model. *Spine (Phila. Pa. 1976).* **36,** 933–8 (2011).

101. Carenza, E. *et al.* In vitro angiogenic performance and in vivo brain targeting of magnetized endothelial progenitor cells for neurorepair therapies. *Nanomedicine* **10,** 225–34 (2014).

102. Vaněček, V. *et al.* Highly efficient magnetic targeting of mesenchymal stem cells in spinal cord injury. *Int. J. Nanomedicine* **7,** 3719–30 (2012).

103. Li, Y., Rodrigues, J. & Tomás, H. Injectable and biodegradable hydrogels: gelation, biodegradation and biomedical applications. *Chem. Soc. Rev.* **41,** 2193–221 (2012).

104. Burdick, J. A. & Prestwich, G. D. Hyaluronic acid hydrogels for biomedical applications. *Adv. Mater.* **23,** H41–56 (2011).

105. Macaya, D. & Spector, M. Injectable hydrogel materials for spinal cord regeneration: a review. *Biomed. Mater.* **7,** 012001 (2012).

106. Skop, N. B., Calderon, F., Cho, C. H., Gandhi, C. D. & Levison, S. W. Improvements in biomaterial matrices for neural precursor cell transplantation. *Mol. Cell. Ther.* **2,** 19 (2014).

107. Jin, K. *et al.* Transplantation of human neural precursor cells in Matrigel scaffolding improves outcome from focal cerebral ischemia after delayed postischemic treatment in rats. *J. Cereb. Blood Flow Metab.* **30,** 534–44 (2010).

108. Ballios, B. G., Cooke, M. J., van der Kooy, D. & Shoichet, M. S. A hydrogel-based stem cell delivery system to treat retinal degenerative diseases. *Biomaterials* **31,** 2555–64 (2010).

109. Mahoney, M. J. & Anseth, K. S. Three-dimensional growth and function of neural tissue in degradable polyethylene glycol hydrogels. *Biomaterials* **27,** 2265–74 (2006).

110. Aurand, E. R., Wagner, J. L., Shandas, R. & Bjugstad, K. B. Hydrogel formulation determines cell fate of fetal and adult neural progenitor cells. *Stem Cell Res.* **12,** 11–23 (2014).

111. Banerjee, A. *et al.* The influence of hydrogel modulus on the proliferation and differentiation of encapsulated neural stem cells. *Biomaterials* **30,** 4695–9 (2009).

112. East, E., de Oliveira, D. B., Golding, J. P. & Phillips, J. B. Alignment of astrocytes increases neuronal growth in three-dimensional collagen gels and is maintained following plastic compression to form a spinal cord repair conduit. *Tissue Eng. Part A* **16,** 3173–84 (2010).

113. Weightman, A., Jenkins, S., Pickard, M., Chari, D. & Yang, Y. Alignment of multiple glial cell populations in 3D nanofiber scaffolds: toward the development of multicellular implantable scaffolds for repair of neural injury. *Nanomedicine* **10,** 291–5 (2014).

114. Freshney, R. I. Cell line provenance. *Cytotechnology* **39,** 55–67 (2002).

115. Pinkernelle, J., Calatayud, P., Goya, G. F., Fansa, H. & Keilhoff, G. Magnetic nanoparticles in primary neural cell cultures are mainly taken up by microglia. *BMC Neurosci.* **13,** 32 (2012).

116. Conti, L. & Cattaneo, E. Neural stem cell systems: physiological players or in vitro entities? *Nat. Rev. Neurosci.* **11,** 176–87 (2010).

117. Russell, W. & Burch, R. *Principles of Humane Experimental Technique*. (Methuen & Co. Ltd: London, 1959).

118. Stoppini, L., Buchs, P. a & Muller, D. A simple method for organotypic cultures of nervous tissue. *J. Neurosci. Methods* **37,** 173–82 (1991).

119. Crain, S. M. & Peterson, E. R. Bioelectric activity in long-term cultures of spinal cord tissues. *Science* **141,** 427–9 (1963).

120. Weightman, A. P., Pickard, M. R., Yang, Y. & Chari, D. M. An in vitro spinal cord injury model to screen neuroregenerative materials. *Biomaterials* **35,** 3756–65 (2014).

121. Meng, X. *et al.* Magnetic CoPt nanoparticles as MRI contrast agent for transplanted neural stem cells detection. *Nanoscale* **3,** 977–984 (2011).

122. Buerli, T. *et al.* Efficient transfection of DNA or shRNA vectors into neurons using magnetofection. *Nat. Protoc.* **2,** 3090–101 (2007).

123. Sapet, C. *et al.* High transfection efficiency of neural stem cells with magnetofection. *Biotechniques* **50,** 187–9 (2011).

124. Jenkins, S., Pickard, M., Furness, D., Yiu, H. & Chari, D. Differences in magnetic particle uptake by CNS neuroglial subclasses: implications for neural tissue engineering. *Nanomedicine (Lond)* **8,** 951–968 (2013).

125. Jensen, J. & Parmar, M. Strengths and limitations of the neurosphere culture system. *Mol. Neurobiol.* **34,** 153–161 (2006).

126. Lévesque, M. F., Neuman, T. & Rezak, M. Therapeutic microinjection of autologous adult human neural stem cells and differentiated neurons for Parkinson's disease: five-year post-operative outcome. *Stem Cells* **16,** 19 (2009).

127. Lu, P. *et al.* Long-distance growth and connectivity of neural stem cells after severe spinal cord injury. *Cell* **150,** 1264–73 (2012).

128. Xu, L., Ryugo, D. K., Pongstaporn, T., Johe, K. & Koliatsos, V. E. Human neural stem cell grafts in the spinal cord of SOD1 transgenic rats: differentiation and structural integration into the segmental motor circuitry. *J. Comp. Neurol.* **514,** 297–309 (2009).

129. Mothe, A. J., Kulbatski, I., Parr, A., Mohareb, M. & Tator, C. H. Adult spinal cord stem/progenitor cells transplanted as neurospheres preferentially differentiate into oligodendrocytes in the adult rat spinal cord. *Cell Transplant.* **17,** 735–751 (2008).

130. Campos, L. S. Neurospheres: insights into neural stem cell biology. *J Neurosci Res* **78,** 761–9 (2004).

131. Abraham, E., Campbell, A., Brandwein, H. & Oh, S. Meeting Lot-Size Challenges of Manufacturing Adherent Cells for Therapy. *BioProcess Int. Suppl.* **10,** (2012).

132. Thomas, R. J. *et al.* Automated, serum-free production of CTX0E03: a therapeutic clinical grade human neural stem cell line. *Biotechnol Lett* **31,** 1167–72 (2009).

133. Narkilahti, S. *et al.* Monitoring and analysis of dynamic growth of human embryonic stem cells: comparison of automated instrumentation and conventional culturing methods. *Biomed. Eng. Online* **6,** 11 (2007).

134. Maynard, A. D., Warheit, D. B. & Philbert, M. a. The new toxicology of sophisticated materials: nanotoxicology and beyond. *Toxicol. Sci.* **120 Suppl ,** S109–29 (2011).

135. Arora, S., Rajwade, J. M. & Paknikar, K. M. Nanotoxicology and in vitro studies: the need of the hour. *Toxicol. Appl. Pharmacol.* **258,** 151–65 (2012).

136. Nel, A., Xia, T., Mädler, L. & Li, N. Toxic potential of materials at the nanolevel. *Science* **311,** 622–7 (2006).

137. Haniu, H. *et al.* Proteomics-based safety evaluation of multi-walled carbon nanotubes. *Toxicol. Appl. Pharmacol.* **242,** 256–62 (2010).

138. Triboulet, S. *et al.* Molecular responses of mouse macrophages to copper and copper oxide nanoparticles inferred from proteomic analyses. *Mol. Cell. Proteomics* **12,** 3108–22 (2013).

139. Xiao, G. G., Wang, M., Li, N., Loo, J. a & Nel, A. E. Use of proteomics to demonstrate a hierarchical oxidative stress response to diesel exhaust particle chemicals in a macrophage cell line. *J. Biol. Chem.* **278,** 50781–90 (2003).

140. Kedziorek, D. a *et al.* Gene expression profiling reveals early cellular responses to intracellular magnetic labeling with superparamagnetic iron oxide nanoparticles. *Magn. Reson. Med.* **63,** 1031–43 (2010).

141. Pawelczyk, E., Arbab, A. S., Pandit, S., Hu, E. & Frank, J. a. Expression of transferrin receptor and ferritin following ferumoxides-protamine sulfate labeling of cells: implications for cellular magnetic resonance imaging. *NMR Biomed.* **19,** 581–92 (2006).

142. Vogel, C. & Marcotte, E. M. Insights into the regulation of protein abundance from proteomic and transcriptomic analyses. *Nat. Rev. Genet.* **13,** 227–32 (2012).

143. Jenkins, S. I. PhD Thesis: Applications of magnetic particles for oligodendrocyte precursor cell transplantation therapies. (Keele University, 2012).

144. Tickle, J. A., Jenkins, S. I., Pickard, M. R. & Chari, D. M. Influence of Amplitude of Oscillating Magnetic Fields on Magnetic Nanoparticle-Mediated Gene Transfer to Astrocytes. *Nano Life* 1450006 (2014). doi:10.1142/S1793984414500068

145. Strack, R. L. *et al.* A noncytotoxic DsRed variant for whole-cell labeling. *Nat. Methods* **5,** 955–7 (2008).

146. Campos, L. S. *et al.* Beta1 integrins activate a MAPK signalling pathway in neural stem cells that contributes to their maintenance. *Development* **131,** 3433–44 (2004).

147. Tiscornia, G., Singer, O. & Verma, I. M. Production and purification of lentiviral vectors. *Nat. Protoc.* **1,** 241–5 (2006).

148. Pike-Overzet, K., van der Burg, M., Wagemaker, G., van Dongen, J. J. M. & Staal, F. J. T. New insights and unresolved issues regarding insertional mutagenesis in X-linked SCID gene therapy. *Mol. Ther.* **15,** 1910–6 (2007).

149. Keravala, A., Ormerod, B. K., Palmer, T. D. & Calos, M. P. Long-term transgene expression in mouse neural progenitor cells modified with phiC31 integrase. *J. Neurosci. Methods* **173,** 299–305 (2008).

150. Williams, P. D. & Kingston, P. a. Plasmid-mediated gene therapy for cardiovascular disease. *Cardiovasc. Res.* **91,** 565–76 (2011).

151. Zhao, Y. *et al.* Automation of large scale transient protein expression in mammalian cells. *J. Struct. Biol.* **175,** 209–15 (2011).

152. Macaya, D. J., Hayakawa, K., Arai, K. & Spector, M. Astrocyte infiltration into injectable collagen-based hydrogels containing FGF-2 to treat spinal cord injury. *Biomaterials* **34,** 3591–602 (2013).

153. Chorny, M. *et al.* Magnetically driven plasmid DNA delivery with biodegradable polymeric nanoparticles. *FASEB J* **21,** 2510–2519 (2007).

154. Taylor, A., Wilson, K. M., Murray, P., Fernig, D. G. & Lévy, R. Long-term tracking of cells using inorganic nanoparticles as contrast agents: are we there yet? *Chem Soc Rev* **41,** 2707–2717 (2012).

155. Lu, H. *et al.* Retrovirus delivered neurotrophin-3 promotes survival, proliferation and neuronal differentiation of human fetal neural stem cells in vitro. *Brain Res. Bull.* **77,** 158–64 (2008).

156. Mátrai, J., Chuah, M. K. L. & VandenDriessche, T. Recent advances in lentiviral vector development and applications. *Mol. Ther.* **18,** 477–90 (2010).

157. Kim, E., Oh, J.-S., Ahn, I.-S., Park, K. I. & Jang, J.-H. Magnetically enhanced adeno-associated viral vector delivery for human neural stem cell infection. *Biomaterials* **32,** 8654–62 (2011).

158. Epstein, A. L. HSV-1-derived amplicon vectors: recent technological improvements and remaining difficulties--a review. *Mem. Inst. Oswaldo Cruz* **104,** 399–410 (2009).

159. Sehgal, K., Ragheb, R., Fahmy, T. M., Dhodapkar, M. V & Dhodapkar, K. M. Nanoparticle-mediated combinatorial targeting of multiple human dendritic cell (DC) subsets leads to enhanced T cell activation via IL-15-dependent DC crosstalk. *J. Immunol.* **193,** 2297–305 (2014).

160. Weissleder, R., Kelly, K., Sun, E. Y., Shtatland, T. & Josephson, L. Cell-specific targeting of nanoparticles by multivalent attachment of small molecules. *Nat. Biotechnol.* **23,** 1418–23 (2005).

161. Riegler, J. *et al.* Targeted magnetic delivery and tracking of cells using a magnetic resonance imaging system. *Biomaterials* **31,** 5366–71 (2010).

162. MacDonald, C., Barbee, K. & Polyak, B. Force dependent internalization of magnetic nanoparticles results in highly loaded endothelial cells for use as potential therapy delivery vectors. *Pharm Res* **29,** 1270–1281 (2012).

163. Cheng, K. *et al.* Magnetic targeting enhances engraftment and functional benefit of iron-labeled cardiosphere-derived cells in myocardial infarction. *Circ. Res.* **106,** 1570–81 (2010).

164. Pislaru, S. V *et al.* Magnetically targeted endothelial cell localization in stented vessels. *J. Am. Coll. Cardiol.* **48,** 1839–1845 (2006).

165. Arbab, A. S. *et al.* Comparison of transfection agents in forming complexes with ferumoxides, cell labeling efficiency, and cellular viability. *Mol. Imaging* **3,** 24–32 (2004).

166. Frank, J. A. *et al.* Clinically applicable labeling of mammalian and stem cells by combining superparamagnetic iron oxides and transfection agents. *Radiology* **228,** 480–7 (2003).

167. Neri, M. *et al.* Efficient in vitro labeling of human neural precursor cells with superparamagnetic iron oxide particles: relevance for in vivo cell tracking. *Stem Cells* **26,** 505–516 (2008).

168. Fernandes, a R. & Chari, D. M. A multicellular, neuro-mimetic model to study nanoparticle uptake in cells of the central nervous system. *Integr. Biol. (Camb).* **6,** 855–61 (2014).

169. Montet-Abou, K., Montet, X., Weissleder, R. & Josephson, L. Transfection agent induced nanoparticle cell loading. *Mol. Imaging* **4,** 165–71 (2005).

170. Bakhru, S. H. *et al.* Enhanced cellular uptake and long-term retention of chitosan-modified iron-oxide nanoparticles for MRI-based cell tracking. *Int J Nanomedicine* **7,** 4613–23 (2012).

171. Zhang, L. *et al.* High MRI performance fluorescent mesoporous silica-coated magnetic nanoparticles for tracking neural progenitor cells in an ischemic mouse model. *Nanoscale* **5,** 4506–16 (2013).

172. Guzman, R. *et al.* Long-term monitoring of transplanted human neural stem cells in developmental and pathological contexts with MRI. *Proc. Natl. Acad. Sci. U. S. A.* **104,** 10211–10216 (2007).

173. Miyoshi, S. *et al.* Transfection of neuroprogenitor cells with iron nanoparticles for magnetic resonance imaging tracking: cell viability, differentiation, and intracellular localization. *Mol Imaging Biol* **7,** 286–295 (2005).

174. Zhang, Y. *et al.* Ligand-mediated endocytosis of nanoparticles in neural stem cells: implications for cellular magnetic resonance imaging. *Biotechnol. Lett.* **35,** 1997–2004 (2013).

175. Politi, L. S. *et al.* Magnetic-resonance-based tracking and quantification of intravenously injected neural stem cell accumulation in the brains of mice with experimental multiple sclerosis. *Stem Cells* **25,** 2583–2592 (2007).

176. Chen, C.-C. V *et al.* Simple SPION incubation as an efficient intracellular labeling method for tracking neural progenitor cells using MRI. *PLoS One* **8,** e56125 (2013).

177. Farkhani, S. M. *et al.* Cell penetrating peptides: efficient vectors for delivery of nanoparticles, nanocarriers, therapeutic and diagnostic molecules. *Peptides* **57,** 78–94 (2014).

178. Song, H. P. *et al.* Gene transfer using self-assembled ternary complexes of cationic magnetic nanoparticles, plasmid DNA and cell-penetrating Tat peptide. *Biomaterials* **31,** 769–78 (2010).

179. Krpetić, Z. *et al.* Negotiation of intracellular membrane barriers by TAT-modified gold nanoparticles. *ACS Nano* **5,** 5195–201 (2011).

180. Massart, R. Preparation of aqueous magnetic liquids in alkaline and acidic media. *IEEE Trans Magn* **17,** 1247–1248 (1981).

181. Johnson, B. *et al.* Magnetically responsive paclitaxel-loaded biodegradable nanoparticles for treatment of vascular disease: preparation, characterization and in vitro evaluation of anti-proliferative potential. *Curr Drug Deliv* **7,** 263–273 (2010).

182. Marieb, E. N. in *Human Anatomy and Physiology: International Edition* (ed. Murray, M. A.) 721–739 (Pearson Education, 2004).

183. Song, N.-N. *et al.* Non-monotonic size change of monodisperse Fe3O4 nanoparticles in the scale-up synthesis. *Nanoscale* **5,** 2804–2810 (2013).

184. Gugala, Z. & Gogolewski, S. Protein adsorption, attachment, growth and activity of primary rat osteoblasts on polylactide membranes with defined surface characteristics. *Biomaterials* **25,** 2341–2451 (2004).

185. Fernandes, A., Adams, C. F., Jenkins, S. I., Furness, D. N. & Chari, D. M. Early membrane responses to magnetic particles are predictors of particle uptake in neural stem cells. *Part. Part. Syst. Charact.* **In Press,** (2015).

186. Kohler, N., Fryxell, G. E. & Zhang, M. A bifunctional poly(ethylene glycol) silane immobilized on metallic oxide-based nanoparticles for conjugation with cell targeting agents. *J Am Chem Soc* **126,** 7206–7211 (2004).

187. Gupta, B., Revagade, N. & Hilborn, J. Poly(lactic acid) fiber: An overview. *Prog Polym Sci* **32,** 455–482 (2007).

188. Lin Xiao, M., Wang, B., Yang, G. & Gauthier, M. in *Biomedical Science, Engineering and Technology* (ed. Ghista, D.) 247–282 (InTech, 2012).

189. Grayson, A. C. R. *et al.* Differential degradation rates in vivo and in vitro of biocompatible poly(lactic acid) and poly(glycolic acid) homo- and co-polymers for a polymeric drug-delivery microchip. *J Biomat Sci Polym Ed* **15,** 1281–1304 (2004).

190. Tengood, J. E. *et al.* Real-time analysis of composite magnetic nanoparticle disassembly in vascular cells and biomimetic media. *Proc. Natl. Acad. Sci. U. S. A.* **111,** 4245–50 (2014).

191. Jain, T. K., Reddy, M. K., Morales, M. A., Leslie-Pelecky, D. L. & Labhasetwar, V. Biodistribution, clearance, and biocompatibility of iron oxide magnetic nanoparticles in rats. *Mol Pharm* **5,** 316–327 (2008).

192. Weissleder, R. *et al.* Superparamagnetic iron oxide: pharmacokinetics and toxicity. *AJR Am J Roentgenol* **152,** 167–173 (1989).

193. Tartaj, P. in *Encyclopedia of Nanoscience and Nanotechnology* (ed. Hari Singh, N.) **6,** 823 (American Scientific Publishers, 2003).

194. Worthington-Kirsch, R. L., Siskin, G. P., Hegener, P. & Chesnick, R. Comparison of the efficacy of the embolic agents acrylamido polyvinyl alcohol microspheres and tris-acryl gelatin microspheres for uterine artery embolization for leiomyomas: a prospective randomized controlled trial. *Cardiovasc Interv. Radiol* **34,** 493–501 (2011).

195. Santos, T. *et al.* Polymeric Nanoparticles to Control the Differentiation of Neural Stem Cells in the Subventricular Zone of the Brain. *ACS Nano* **6,** 10463–10474 (2012).

196. Heffernan, C., Sumer, H., Guillemin, G. J., Manuelpillai, U. & Verma, P. J. Design and screening of a glial cell-specific, cell penetrating peptide for therapeutic applications in multiple sclerosis. *PLoS One* **7,** e45501 (2012).

197. Pakulska, M. M., Ballios, B. G. & Shoichet, M. S. Injectable hydrogels for central nervous system therapy. *Biomed. Mater.* **7,** 024101 (2012).

198. Ko, H.-Y., Park, J. H., Shin, Y. B. & Baek, S. Y. Gross quantitative measurements of spinal cord segments in human. *Spinal Cord* **42,** 35–40 (2004).

199. Keung, A. J., de Juan-Pardo, E. M., Schaffer, D. V & Kumar, S. Rho GTPases mediate the mechanosensitive lineage commitment of neural stem cells. *Stem Cells* **29,** 1886–97 (2011).

200. Nomura, H. *et al.* Extramedullary chitosan channels promote survival of transplanted neural stem and progenitor cells and create a tissue bridge after complete spinal cord transection. *Tissue Eng. Part A* **14,** 649–65 (2008).

201. Bible, E. *et al.* The support of neural stem cells transplanted into stroke-induced brain cavities by PLGA particles. *Biomaterials* **30,** 2985–94 (2009).

202. Crang, A. J., Gilson, J. & Blakemore, W. F. The demonstration by transplantation of the very restricted remyelinating potential of post-mitotic oligodendrocytes. *J. Neurocytol.* **27,** 541–53 (1998).

203. Zhang, H., Lee, M. & Hogg, M. Gene delivery in three-dimensional cell cultures by superparamagnetic nanoparticles. *ACS Nano* **4,** 4733–4743 (2010).

204. Teixeira, A. I. *et al.* The promotion of neuronal maturation on soft substrates. *Biomaterials* **30,** 4567–72 (2009).

205. Chevallay, B. & Herbage, D. Collagen-based biomaterials as 3D scaffold for cell cultures: applications for tissue engineering and gene therapy. *Med. Biol. Eng. Comput.* **38,** 211–218 (2000).

206. Mori, H., Takahashi, A., Horimoto, A. & Hara, M. Migration of glial cells differentiated from neurosphere-forming neural stem/progenitor cells depends on the stiffness of the chemically cross-linked collagen gel substrate. *Neurosci. Lett.* **555,** 1–6 (2013).

207. Elias, P. Z. & Spector, M. Viscoelastic characterization of rat cerebral cortex and type I collagen scaffolds for central nervous system tissue engineering. *J. Mech. Behav. Biomed. Mater.* **12,** 63–73 (2012).

208. Gefen, A. & Margulies, S. S. Are in vivo and in situ brain tissues mechanically similar? *J. Biomech.* **37,** 1339–52 (2004).

209. Lu, D. *et al.* Collagen scaffolds populated with human marrow stromal cells reduce lesion volume and improve functional outcome after traumatic brain injury. *Neurosurgery* **61,** 596–602; discussion 602–3 (2007).

210. Subramanian, M., Lim, J. & Dobson, J. Enhanced nanomagnetic gene transfection of human prenatal cardiac progenitor cells and adult cardiomyocytes. *PLoS One* **8,** e69812 (2013).

211. Child, H. W. *et al.* Working together: the combined application of a magnetic field and penetratin for the delivery of magnetic nanoparticles to cells in 3D. *ACS Nano* **5,** 7910–9 (2011).

212. Wang, T.-Y., Forsythe, J. S., Nisbet, D. R. & Parish, C. L. Promoting engraftment of transplanted neural stem cells/progenitors using biofunctionalised electrospun scaffolds. *Biomaterials* **33,** 9188–97 (2012).

213. Mothe, A. J., Tam, R. Y., Zahir, T., Tator, C. H. & Shoichet, M. S. Repair of the injured spinal cord by transplantation of neural stem cells in a hyaluronan-based hydrogel. *Biomaterials* **34,** 3775–83 (2013).

214. Mayrhofer, P., Schleef, M. & Jechlinger, W. Use of minicircle plasmids for gene therapy. *Methods Mol. Biol.* **542,** 87–104 (2009).

215. Yang, W.-H. *et al.* Regulated expression of lentivirus-mediated GDNF in human bone marrow-derived mesenchymal stem cells and its neuroprotection on dopaminergic cells in vitro. *PLoS One* **8,** e64389 (2013).

216. Vigna, E. *et al.* Robust and efficient regulation of transgene expression in vivo by improved tetracycline-dependent lentiviral vectors. *Mol. Ther.* **5,** 252–61 (2002).

217. Van Gaal, E. V. B., Hennink, W. E., Crommelin, D. J. a & Mastrobattista, E. Plasmid engineering for controlled and sustained gene expression for nonviral gene therapy. *Pharm. Res.* **23,** 1053–74 (2006).

218. Aronovich, E. L., McIvor, R. S. & Hackett, P. B. The Sleeping Beauty transposon system: a non-viral vector for gene therapy. *Hum. Mol. Genet.* **20,** R14–20 (2011).

219. Kebriaei, P. *et al.* Infusing CD19-directed T cells to augment disease control in patients undergoing autologous hematopoietic stem-cell transplantation for advanced B-lymphoid malignancies. *Hum. Gene Ther.* **23,** 444–50 (2012).

220. Thomas, R. J. *et al.* Automated, scalable culture of human embryonic stem cells in feeder-free conditions. *Biotechnol. Bioeng.* **102,** 1636–1644 (2009).

221. Zhou, X. & Wong, S. High Content Cellular Imaging for Drug Development. *IEEE Signal Process. Mag.* **23,** 170–174 (2006).

222. Rosner, M. H. & Auerbach, M. Ferumoxytol for the treatment of iron deficiency. *Expert Rev. Hematol.* **4,** 399–406 (2011).

223. Aboody, K., Capela, A., Niazi, N., Stern, J. H. & Temple, S. Translating stem cell studies to the clinic for CNS repair: current state of the art and the need for a Rosetta stone. *Neuron* **70,** 597–613 (2011).